FCCat 4
2025

May 19th-23rd, 2025 – Ronce-les-Bains (France)

Scientific program

FCCat 2025 : French Conference on Catalysis

https://fccat2025.sciencesconf.org/

Platinum Sponsors

TotalEnergies

Ircelyon

IFP Energies nouvelles

Gold Sponsors

Fondation de la Maison de la Chimie

1431 Université de Poitiers

Bronkhorst®

EURECAT

Silver Sponsors

Chemistry Europe
European Chemical Societies Publishing

ROYAL SOCIETY OF CHEMISTRY

MDPI

UCCS
UNITÉ DE CATALYSE ET CHIMIE DU SOLIDE

LCS Laboratoire Catalyse & Spectrochimie
INSTITUT CARNOT ESP

UCEiV
Unité de Chimie Environnementale et Interactions sur le Vivant

ICGM
Institut Charles Gerhardt Montpellier

IC2MP
Institut de Chimie des Milieux et Matériaux de Poitiers

ICPEES
Institut de Chimie et Procédés pour l'Énergie, l'Environnement et la Santé

Silver Sponsors / FCCat 2025 Exhibitors

micromeritics

MICROTRAC
PARTICLE CHARACTERIZATION

TOP INDUSTRIE
High Pressure Technology

SRA INSTRUMENTS
ANALYTICAL SOLUTIONS 25

SISTEC
ANALYSE DE GAZ

magritek

CHEMLYS
Chemical analysis & consulting

Equilabo

CARL ROTH

Daily planning of FCCat2025

Time	Monday, May 19th	Tuesday, May 20th	Wednesday, May 21st	Thursday, May 22nd	Friday, May 23rd
07:30		Breakfast	Breakfast	Breakfast	Breakfast
08:30		**Lecture H. Poelman**	**Lecture L. Liotta**	**Lecture C. Courson**	
09:00					**Lecture A.Rudi**
09:30		Keynote M. Boronat	Keynote K. Kobl	Keynote C. Camp	
10:00		Coffee (10h00-10h30)	Coffee Break (10h00-10h30)	Coffee Break (10h00-10h30)	Coffee Break (10h00-10h30)
10:30		**DRM, MTO, WGS (OC1)** G. Jabotra A.Salichon J.Ren A. Le Ray S. Nouma **VOC, DeNO$_x$, aromatics (OC2)** J. Machinski A. Rokicinska N. Chaouati N. Marchenko A. Ben Attia	**Structure, Simulation, DFT (OC5)** C. Chizallet E. Ikwa J. Kang M. Cotoni S. Batool R. André **Biomass (OC6)** A. Djellali D. Laurenti L. Hervé M. Elhallal T. Onfroy I. Nciri	**Hydrogenat-n, NH$_3$ (OC7)** A. Tomer P. Azimov T. Al Bayeh S. Akrour J.-Ph. Dacquin K. Bakkouche **Adv. char-n, Kinetics, Sorption (OC8)** T. Cabanis E. Vottero K. Thomas N. Nassar M. De Rocco P. Fongarland	Keynote A. Ruppert
11:00					Conclusions
11:30					Lunch boxes, Bus departure to Surgères TGV (12h00)
12:00					
12:30		Lunch (12h10-14h00)	Lunch (12h30-14h00)	Lunch (12h30-14h00)	
14:00		Keynote V. Ordomsky	Free afternoon Available social activities : heated swimming pool, sport-club, petanque, hiking, bikes rental service	Exhibitors - Round table (14h-15h)	
14:30		**HDS, Biomass derivatives (OC3)** S. Chamorro C. Pellegrin S. Gigot A. Beauvois D. Ryaboshapka **H$_2$ act-n, Hyd-n of CO$_2$, propane (OC4)** S. Scott S. Amar Gil N. Cordier O. Liaaychi A. Di Guliano			TGV departure Surgères-Paris (14h08)
15:00				**Photo, electro (OC9)** A. Ranscht V. Theuns C. Tabariés Y. Djerroud **CO$_2$ Methanation (OC10)** P.Hongmanorom L. Castoldi Z. Boukha S. Gupta L. Piccolo	
15:30	TGV arrival - Bus departure from Surgères-TGV (15h20)				
16:00	Exhibition stands intallation possible from 15h till 18h				
16:30	Bus arrival to Azureva (16h20)	Coffee Break (16h30-17h00)		Coffee Break (16h40-17h00)	
17:00					
17:30	Keys and badges distribution	Exhibitors - Round table (17h-18h)		DivCat Prizes + Lectures (17h-19h)	
18:00	Opening (18h00) **Lecture N. Bion**	**Posters Session**	**Posters Session**		
19:00	Welcome party	Mouclade (Traditional mussels preparation)	Oysters tasting	Free time Exhibition stands removal	
20:00	Diner (20h-22h, last entry at 20h30)	Diner (20h-22h, last entry at 20h30)	Diner (20h-22h, last entry at 20h30)	Gala Diner (20h00 sharp, bar closing at 01h00, no noise after 02h00)	

* The oral presentations sessions will take place:
on the left (odd sessions) – in the Plenary room,
on the right (even sessions) – in the Marine room.

Monday, May 19th

16h00	**Open desk for keys and badges distribution**
18h00	**Opening of FCCat 2025**
18h15	**Plenary lecture** Nicolas BION *IC2MP, Institut de Chimie des Milieux et Matériaux de Poitiers, Université de Poitiers, Poitiers, France* **Toward NH_3 synthesis in mild conditions**
19h15	**Welcome drink**
20h00	**Diner**

Tuesday, May 20th

08h30 **Plenary lecture**

Hilde Poelman

LCT, Laboratory for Chemical Technology, University of Gent, Belgium

How X-Ray spectroscopies help to understand the dry reforming reaction

09h30 **Key-note**

Mercedes Boronat

ITQ, Instituto de Tecnología Química, UPV-CSIC, Valencia, Spain

New developments in the molecular modelling of zeolites for heterogeneous catalysis

10h00 **Coffee break (10h00-10h30)**

Oral conferences (OC1), Plenary room
DRM, MTO, WGS

10h30 **On the role of Cu (II) insertion in $LaFeO_3$ for H_2 production in Chemical Looping Dry Reforming of CH_4 (CL-DRM)**

G. Jabotra[1], A. Sfeir[1], L.Stievano[4], A. Löfberg[1], S. Royer[1,3], S. Sharma[2], J.-P. Dacquin[1]

[1] *Unité de Catalyse et Chimie du Solide (UCCS), Université de Lille, France*

[2] *Indian Institute of Technology Gandhinagar (IITGN), Palaj, India*

[3] *Unité de Chimie Environnementale et Interactions sur le Vivant (UCEiV), Université du Littoral Côte d'Opale, France*

[4] *Institut Charles Gerhardt Montpellier (ICGM), University of Montpellier, CNRS, ENSCM, France*

10h50 **Fundamental insights into a highly efficient $GaZrO_x$/SAPO-34 bifunctional catalyst for the methanol-mediated syngas to light olefins conversion**

A. Salichon[1], R. Checa[1], P. Afanasiev[1], S. Loridant[1]

[1] *Institut de Recherches sur la Catalyse et l'Environnement de Lyon, CNRS – Université Lyon 1, Villeurbanne, France*

11h10 **Co-immobilization of polyoxometalates and organic cations onto (mesoporous) silica for supported oxidative carboxylation of alkenes**

J. Ren[1], R. Villanneau[1]

[1] *Institut Parisien de Chimie Moléculaire, Sorbonne Université, Paris, France*

11h30 **Higher alcohols synthesis from syngas over sulfide-based catalysts**

A. Le Ray[1], A. T. F. Batista[2], C. Geantet[1], P. Raybaud[2], P. Afanasiev[1],

[1] *Institut de Recherches sur la Catalyse et l'Environnement de Lyon, CNRS – Université Lyon 1, Villeurbanne, France*

[2] *IFP Energies nouvelles, Solaize, France*

11h50 **Water-Gas-Shift WGS reaction mechanisms over SiO2 and TiO2 supported MoS2 catalysts**

S. Nouma[1], X.Portier[1], L. Oliviero [2]

[1] *CIMAP, Université de Caen Normandie, CEA, ENSICAEN, CNRS, Caen, France*

[2] *Laboratoire Catalyse et Spectrochimie, ENSICAEN, Caen, France*

Oral conferences (OC2), Marine room
VOC, DeNOx, aromatics

10h30 **The role of Cu/Mn ratio in mixed oxides for total oxidation of air pollutants**

J. Machinski[1], E. Genty[1], C. Eddine Bounoukta[1], C. Poupin[1], V. La Parola[2], S. Siffert[1], E. Berrier[3], L. F. Liotta[2], R. Cousin[1]

[1] *Unité de Chimie Environnementale et Interactions sur le Vivant (UCEiV), Université du Littoral Côte d'Opale, France*

[2] *Institute for the Study of Nanostructured Materials (ISMN)-CNR, ,Palermo, Italy*

[3] *Unité de Catalyse et Chimie du Solide (UCCS), Université de Lille, France*

10h50 **Role of hollow @SiO_2 and @TiO_2 supports in catalytic activity of CuO and Co_3O_4 phases in total oxidation of toluene**

A. Rokicinska[1], M. Żurowska[1,2], R. Sadowski[1], Marek Dębosz[1], P. Kuśtrowski[1]

[1] *Faculty of Chemistry, Jagiellonian University, Kraków, Poland*

[2]*Doctoral School of Exact and Natural Sciences, Jagiellonian University, Krakow, Poland*

11h10 **Exploring the Catalytic Properties of Extra-Large Pores ZEO-1 Zeolite**

N. Chaouati[1], M. Fahda[1], S. Mintova[1], L. Pinard[1] ,V. Valtchev[1]

[1] *Laboratoire Catalyse et Spectrochimie, ENSICAEN, Caen, France*

11h30 **Designing Pt/TiO_2 catalysts for efficient dehydrogenation of perhydrobenzyltoluene**

N. Marchenko[1], M. Kharma[1], F. Morfin[1], L. Piccolo[1], N. Rocha Batalha[1], V. Meille[1]

[1] *Institut de Recherches sur la Catalyse et l'Environnement de Lyon, CNRS – Université Lyon 1, Villeurbanne, France*

11h50 **Investigations in the H_2-SCR pathways over a Pt/SiO_2-Al_2O_3 catalyst**

A. Ben Attia[1], F. Can[1], X. Courtois[1]

[1] *Institut de Chimie des Milieux et Matériaux de Poitiers, Université de Poitiers, France*

Lunch (12h10-14h00)

14h00 **Key-note**

Vitaly ORDOMSKY

UCCS, Unité de Catalyse et Chimie du Solide, Lille, France

Liquid metals in catalysis

Oral conferences (OC3), Plenary room
HDS, Biomass derivatives

14h30 **Conversion of bio-derived levulinic acid, evaluation of conditions and catalyst performance**

S. Chamorro[1], M.Araque [1], B.Katryniok [1], X.Dominguez-Benetton [2], O.Martinez [2,]

[1] Unité de Catalyse et Chimie du Solide, CNRS – Université de Lille, France;

[2]Separation and Conversion Technologies VITO, Mol, Belgium

14h50 **Catalytic hydroconversion of enzymatic hydrolysis lignin into sustainable aviation fuels**

C. Pellegrin[1], A. Daudin[2], N. Charon[2], C. Geantet[1], D. Laurenti[1],

[1] Institut de Recherches sur la Catalyse et l'Environnement de Lyon, CNRS – Université Lyon 1, Villeurbanne, France

[2] IFP Energies nouvelles, Solaize, France

15h10 **Development of non-noble metal catalysts for the dehydrogenation of formic acid**

S. Gigot[1], É. Charon[2], M. Pinault[2], C. Genre[1], T. Cantat[1]

[1] CEA, Commissariat à l'énergie atomique et aux énergies alternatives, Saclay, France

[2] Laboratoire des Édifices Nanométriques - NIMBE, CEA, CNRS, Université Paris-Saclay, France

15h30 **Local and time-resolved characterization of a bimetallic Fe-Cu catalyst by environmental TEM and hyperspectral in situ Quick-XAS imaging**

A. Beauvois[3], A. Traore[1], O. Ersen[1], E. Marceau[2], V. Briois[3]

[1] IPCMS, Institut de Physique et Chimie des Matériaux de Strasbourg, Strasbourg, France

[2] UCCS, Unité de Catalyse et Chimie du Solide, CNRS – Université de Lille, France3

[3] Synchrotron SOLEIL, Saint-Aubin, France

15h50 **On the catalytic activity and structure of the CoReS phase in reactions involving hydrogen**

D. Ryaboshapka[1], L. Piccolo[1], P. Bargiela[1], P. Afanasiev[1], V. Briois[2]

[1] Institut de Recherches sur la Catalyse et l'Environnement de Lyon, CNRS – Université Lyon 1, Villeurbanne, France

[2] Synchrotron SOLEIL, Saint-Aubin, France;

Oral conferences (OC4), Marine room
H_2 activation, Hydrogenation of CO_2, propane

14h30 **First observation of propylGa(III) active sites during non-oxidative propane dehydrogenation, by X-ray absorption spectroscopy**

J. A. Chalmers[1], A. S. Hoffman[2], F. D. Vila[3], S. R. Bare[2], S. Scott[1,4]
[1] *Department of Chemical Engineering, University of California, Santa Barbara, USA.*
[2] *Stanford Synchrotron Radiation Lightsource, SLAC National Accelerator, USA.*
[3] *Department of Physics, University of Washington, Seattle, USA.*
[4] *Department of Chemistry and Biochemistry, University of California, Santa Barbara, USA*

14h50 **Tuning Ga-Sites and Acidity on Ga/Al_2O_3 Catalysts via H_2 Reduction or Co-Feeding: Insights into Propane Dehydrogenation Performance**

S. Amar Gil[1], C. Especel[1], F. Passamonti[2], V. Benítez[1], F. Epron[1]
[1] *Institut de Chimie des Milieux et Matériaux de Poitiers, Université de Poitiers, France*
[2]*Instituto de Investigaciones en Catálisis y Petroquímica – INCAPE, Santa Fe, Argentina*

15h10 **Pertinence of the assisted plasma catalysis for the valorization of CO_2 by hydrogenation**

N. Cordier[1], N. Choudhary[2], P. Da Costa[2], E. Fourré[1], C. Batiot-Dupeyrat[1]
[1] *Institut de Chimie des Milieux et Matériaux de Poitiers, Université de Poitiers, France*
[2]*Sorbonne University, Institut Jean Le Rond D'Alembert (IJLRA), UMR 7190, St Cyr l'Ecole, France*

15h30 **Insight into MoS_2 structure on the activity for CO_2 hydrogenation into syngas: A step towards H_2 economy**

O. Liaaychi[1,2], A. Sfeir[2], P. Blanchard[2], C. Lancelot[2], C.Lamonier[2], S.Laassiri[1], J.-P. Dacquin[2], S.Royer[2]
[1] *CBS-GPE, Mohammed VI Polytechnic University, 43150 Ben Guerir, Morocco*
[2] *Unité de Catalyse et Chimie du Solide (UCCS), Université de Lille, France*

15h50 **Batch heterogeneous catalytic selective hydrogenation of vegetable oils: regression of kinetic parameters from pseudo-first-order to detailed reaction mechanisms**

A. Di Giuliano[1,2], E. Pellegrino[1], N. Cancrini[1], K. Gallucci[1]
[1] *Università degli Studi dell'Aquila, L'Aquila, Italy*
[2] *Institut de chimie et procédés pour l'énergie, l'environnement et la santé (ICPEES), CNRS UMR 7515 -University of Strasbourg, France*

16h10 **Coffee break (16h10-17h00)**

17h00 **Exhibitors round table**

18h00 **Poster session**

19h00 **Mouclade (Traditional mussels preparation)**
Terrace in front of the swimming-pool

20h00 **Diner (last entry at 20h30)**

Wednesday May 21st

08h30 **Plenary lecture**

Leonarda Francesca LIOTTA

ISMN-CNR, Institute for the Study of Nanostructured Materials, Palermo, Italy

Catalysis by Gold for CO and VOCs oxidation reactions: structure-activity relationship

09h30 **Key-note**

Kilian KOBL

Ypso Facto, Nancy, France

Modelling bioprocesses in chemical engineering

10h00 **Coffee break (10h00-10h30)**

Oral conferences (OC5), Plenary room
Structure, DFT, Simulation

10h30 **Thermodynamic and kinetic origins of platinum single atoms supported on chlorinated γ-Al_2O_3: from calcined to reduced states**

A. Hellier[1], A. T. F. Batista[1], C. Legens[1], A.-S. Gay[1], A. Aguilar Tapia[2], O. Proux[3], J.-L. Hazemann[4],Y. Joly[4], W. Baaziz[5], O. Ersen[5], C. Chizallet[1], P. Raybaud[1,6]

[1] IFP Energies nouvelles, Rond-point de l'échangeur de Solaize, Solaize, France
[2]ICMG, UAR 2607 CNRS Université Grenoble Alpes, Grenoble France
[3] OSUG, UAR 832 CNRS-Université Grenoble Alpes, Grenoble, France
[4] Institut Néel, UPR 2940 CNRS Université Grenoble Alpes, Grenoble, France
[5] IPCMS, CNRS-Université de Strasbourg, Strasbourg, France
[6] ENS Lyon, CNRS, Laboratoire de Chimie UMR 5182, Lyon, France

10h50 **Relationships between Structure, Stability and Size of Pd Nanoparticles Investigated by Ab Initio Models**

E. Ikwa[1,2], M. Rivallan[1], T. Nardin[1], A. Hugon[1], D. Loffreda[1,2]

[1] IFP Energies nouvelles - Etablissement de Lyon, Solaize, France
[2] ENS de Lyon, CNRS, UCB Lyon 1, UMR 5182, Lyon, France

11h10 **Periodate activation by zero valent iron particles embedded into nitrogen rich biochar for bisphenol A degradation: efficiency and mechanism**.

J. Kang[1,2], J.-P.Dacquin[2], S. Royer[3], H. Zhang[1]

[1] Environmental Catalysis Laboratory, Wuhan University, Wuhan, China
[2] Unité de Catalyse et Chimie du Solide (UCCS), Université de Lille, France
3 Unité de Chimie Environnementale et Interactions sur le Vivant (UCEiV), Université du Littoral Côte d'Opale, France

11h30 **Influence of nanocrystals morphology in the stabilization of oxidized Pt single atoms on γ-Al_2O_3**

M. Cotoni[1,2],F. Moreau[1], L. Lemaitre[1], M. De Mello Timm[1], V. Rouchon[1], D. Gioffrè[2], A. Cabiac[1], C. Bouchy[1], C. Copéret[2], C. Chizallet[1]

[1] IFP Energies nouvelles - Etablissement de Lyon, Solaize, France
[2] Swiss Federal Institute of Technology Zurich, Zürich, Switzerland

11h50 **Microkinetic study of acid gas valorization on Na faujasite**

M. Fabbiani, S. R. Batool[1], L.Pinard[1], R.Ghassemi[2], S. Zare Ghorbaei[2], J. Lauwaert[2], J. Thybaut[2], V. Valtchev[1]

[1] Laboratoire Catalyse et Spectrochimie, ENSICAEN, Caen, France

[2]Laboratory for Chemical Technology (LCT), Ghent university, Ghent, Belgium

12h10 **News from CeO_2 catalysts : an unreported cerium oxyhydroxide phase and operando monitoring of H_2 activation as surface hydrides**

R. André[1], G. Rousse[2], J.-J. Gallet[3], F. Bournel[3], S. Carenco[1]

[1]Laboratoire de Chimie de la Matière Condensée de Paris (LCMCP), Sorbonne Université

[2]Chimie du Solide-Energie, UMR 8260, Collège de France & Sorbonne Université

[3]Laboratoire de Chimie Physique Matière et Rayonnement (LCPMR), Sorbonne Université

Oral conferences (OC6), Marine room
Biomass

10h30 **Carbon supported metal oxides nanoparticles and their applications in biomass valorization**

A. Djellali[1], J. Blanchard[1]

[1] Laboratoire de Réactivité de Surface, Sorbonne Université, Paris, France

10h50 **Functionalization of lignocellulosic biomass for the production of bio-binders**

N. Daridon[1], C. Geantet[1], D. Laurenti[1]

[1] Institut de Recherches sur la Catalyse et l'Environnement de Lyon, CNRS – Université Lyon 1, Villeurbanne, France

11h10 **A bottom-up approach to design new catalytic systems for the mild oxidation of furan derivatives**

L. Hervé[1], F. Rataboul[1], C. Pinel[1], A. Cabiac[2], M. Fernandez Espada Pastor[2], L. Djakovitch[1]

[1] Institut de Recherches sur la Catalyse et l'Environnement de Lyon, CNRS – Université Lyon 1, Villeurbanne, France;

[2] IFP Energies nouvelles - Etablissement de Lyon, Solaize, France

11h30 **Unlocking the Potential of Au-Pt Core-Shell Catalysts: A Microemulsion Approach for Enhanced Glucose Oxidation to Glucuronic Acid in base free media**

M. Elhallal[1], V. Ordomski[1], M. Capron[1]

[1] UCCS, Unité de Catalyse et Chimie du Solide, CNRS – Université de Lille, France

11h50 **Effect of the replacement of Mg^{2+} by Zn^{2+} in metallic silicates on acid-base properties and on their activity in g-valerolactone ring opening reaction**

A. Issa[1,2], T. Onfroy[1], G. Laugel[1], J. Hochepied[2], H. Lauron-Pernot[1]

[1] Laboratoire de Réactivité de Surface, Sorbonne Université, Paris, France

[2]ENSTA UCP, IP Paris, Palaiseau, France

12h10 **Investigation of Liquid Organic Hydrogen Carriers (LOHC) Issued from Biomass Resources**

I. Nciri[1], C. Coutanceau[1], K. De Oliveira Vigier[1]

[1] Institut de Chimie des Milieux et Matériaux de Poitiers, Université de Poitiers, France

	Lunch (12h30-14h00)
14h00	**Free afternoon (14h00-18h00)**
18h00	**Poster session**
19h00	**Oysters tasting** Terrace in front of the plenary room
20h00	**Diner (last entry at 20h30)**

Thursday, May 22nd

08h30 **Plenary lecture**

Claire COURSON

ICPEES, Strasbourg, France

Over the hydrogen rainbow : the uses of catalysis for production of hydrogen

09h30 **Key-note**

Clément CAMP

CP2M, Lyon, France

Catalysis by heterobimetallic molecular systems

10h00 **Coffee break (10h00-10h30)**

Oral conferences (OC7), Plenary room
Hydrogenation, NH_3

10h30 **Heterogeneous noble-metal-free catalysts for the semi-hydrogenation of alkynols under mild conditions**

A. Tomer[1], L. Djakovitch[1], N. Perret[1]

[1] *Institut de Recherches sur la Catalyse et l'Environnement de Lyon, CNRS – Université Lyon 1, Villeurbanne, France*

10h50 **Tuning the hydrogenation selectivity by playing with the carbide speciation in Mo-W mixed carbides**

P. Azimov[1], C. Guibert[1], C. Sayag[1], X. Carrier[1]

[1] *Laboratoire de Réactivité de Surface, Sorbonne Université, Paris, France*

11h10 **Selective C–O hydrogenolysis of erythritol over rhenium-based catalyst: effect of the support and nature of alcohols**

T. Al-Bayeh[1], A. Pinel[1], F. Ratabouil[1], N. Perret[1]

[1] *Institut de Recherches sur la Catalyse et l'Environnement de Lyon, CNRS – Université Lyon 1, Villeurbanne, France*

11h30 **Promoting Ru Electron Density by basic Hydroxyls of Metal Oxide Support toward Efficient Ammonia Synthesis**

S. Akrour[1], A. Vimont[2], S. Casale[1], G. Costentin[1], C. Thomas[1]

[1] *LRS, Sorbonne Université – CNRS, Paris, France*

[2] *Laboratoire Catalyse et Spectrochimie, ENSICAEN, Caen, France*

11h50 **Straightforward synthesis of highly active inorganic electride composites for green ammonia synthesis**

A. Addou[1,2], A. Sfeir[2], J.-P. Dacquin[2], S. Royer[2,3], S. Laassiri[1]

[1] *CBS-GPE, Mohammed VI Polytechnic University, Ben Guerir, Morocco*

[2] *Unité de Catalyse et Chimie du Solide (UCCS), Université de Lille, France*

[3] *Unité de Chimie Environnementale et Interactions sur le Vivant (UCEiV), Université du Littoral Côte d'Opale, France*

12h10 **H_2-Assisted Synthesis of $Ni_2P/Ni_{12}P_5$ Nanocatalysts for Low Temperature Phenylacetylene Hydrogenation**

K. Bakkouche[1], S. Carenco[1]

[1] *Laboratoire de Chimie de la Matière Condensée de Paris, Sorbonne Université, Paris, France*

Oral conferences (OC8), Marine room
Adv. characterization, Kinetics, Sorption

10h30 **Probing surface reaction dynamics using calorimetry vs gas chromatography: The case of isopropanol dehydration**

T. Cabanis[1], A. Auroux[1], J. Dubois2, N. Sbirrazzuoli[3], G. Postole[1]

[1] *Institut de Recherches sur la Catalyse et l'Environnement de Lyon, CNRS – Université Lyon 1, Villeurbanne, France*

[2] *Trinseo Netherlands B.V., Innovatieweg 14, Hoek, The Netherlands*

[3] *Institut de Chimie de Nice (ICN) – UMR CNRS 7272, Université Côte d'Azur (UCA), Nice, France*

10h50 **Isobutanol dehydration catalyzed by HFER: mechanism insights from FT-IR and kinetic modelling**

E. Vottero[1], R. Aboulayt[1], A. Vimont[1], P. Bazin[1], K. Thomas[1], S. Maury[2], C. Chizallet[2], A. Travert[1]

[1] *Laboratoire Catalyse et Spectrochimie, ENSICAEN, Caen, France;*

[2] *IFP Energies nouvelles - Etablissement de Lyon, Solaize, France*

11h10 **Highlighting the Positive Impact of Zeolite on Platinum-Catalyzed Hydrogenation through a High-Throughput Infrared Study**

K. Thomas[1], M. El Zayed[1], P. Bazin[1], L. Pinard[1]

[1] *Laboratoire Catalyse et Spectrochimie, ENSICAEN, Caen, France*

11h30 **ME-PSD IR Spectroscopy to study CO oxidation reaction under Pt/Al_2O_3 catalyst**

N. Nassar[1], A. Djaafri[1], M.Richard[1], C.Dujardin[1], A.Tougerti[1], S.Cristol[1]

[1] *Unité de Catalyse et Chimie du Solide, CNRS – Université de Lille, France*

11h50 **Cu_2O Nanocatalysts: Morphology-Dependent Reactivity and Operando Insights from NAP-XPS**

M. De Rocco[1], A. Capitaine[2], A. Dabbous[2], B. Sciacca[2], J. Gallet[3,4], F. Bournel[3,4], D. Pierucci[5,6], S. Cristol[1], P. Simon[1], H. Tissot[1]

[1] *Unité de Catalyse et Chimie du Solide (UCCS), Université de Lille, France*

[2] *Aix-Marseille Université, CNRS, CINaM, Marseille, France*

[3] *Sorbonne Université, LCPMR, F-75005, Paris, France*

[4] *Synchrotron SOLEIL, L'Orme des Merisiers, Saint-Aubin, Gif-sur-Yvette, France*

[5] *Sorbonne Université, UPMC Univ. Paris 06, UMR 7588, INSP, , Paris, France*

[6] *CNRS, UMR 7588, Institut de NanoSciences de Paris, Paris, France*

12h10 **Sorption-Enhancement Reaction Process (SERP) with in-situ water removal for an Intensified Methanol Production from CO_2: from experiment to modelling**

E. Antonuccio[1], D. Edouard[1], G. Aubert[1], L. Vanoye[1], P. Fongarland[1]

[1] *CP2M, University of Lyon1-CPE-Villeurbanne, France*

Lunch (12h30-14h00)

14h00 **Exhibitors round table**

Oral conferences (OC9), Plenary room
Photo, electro

14h30 **Molecular Understanding of Heterogeneous Organometallic Photocatalysts**
R. Jabbour[1], Q. Perrinet[2], T. Robinson[1], A. Ranscht[3], A. Solé-Daura[4], A. Ghosh[3], J. Canivet[3], V. de Waele[2], C. Mellot-Draznieks[4], A. Lesage[1], F. M. Wisser[3,5]
[1]Centre de RMN à Très Hauts Champs, Université de Lyon, Villeurbanne, France
[2]LASIRE, Université de Lille, Lille, France
[3] Institut de Recherches sur la Catalyse et l'Environnement de Lyon, CNRS – Université Lyon 1, Villeurbanne, France
[4] Collège de France, Paris, France
[5] Erlangen Center for Interface Research and Catalysis (ECRC), Friedrich-Alexander-Universität Erlangen-Nürnberg, Erlangen, Germany

14h50 **Exploring $BaTiO_3$-Derived Materials for Advancing SOFC Electrode Performance**
V. Theuns[1], D. Ledru[2], M.H. Chambrier[2], A. Rolle[1], A.-S. Mamede[1], H. Tissot[1], E. Berrier[1]
[1] UCCS, Unité de Catalyse et Chimie du Solide, CNRS – Université de Lille, France
[2] Université de Artois, Lens, France

15h10 **Catalytic electroreduction of CO_2 to methanol on cobalt phthalocyanines: effect of macrocycle functionalization**
C. Tabariés[1], J. Capitolis[1], M. Prévot[1], L. Piccolo[1], A. Khodadadi[2], G. Zanotti[2], R. Flammini[2], Contini G.[1]
[1] Institut de Recherches sur la Catalyse et l'Environnement de Lyon, CNRS – Université Lyon 1, Villeurbanne, France
[2] Istituto di Struttura della Materia, CNR, Roma, Italy

15h30 **Zinc oxide photoanodes convert glycerol waste into valuable chemicals and hydrogen, providing a sustainable solution to reduce waste and address energy challenges**.
Y. Djerroud[1], Jie Yu[1], Frederic Dappozze[1]
[1] Institut de Recherches sur la Catalyse et l'Environnement de Lyon, CNRS – Université Lyon 1, Villeurbanne, France

Oral conferences (OC10), Marine room
CO_2 Methanation, Dehydrogenation

14h30 **Powdery metal nanoparticle-based catalysts prepared by spark ablation for CO_2 methanation**
P. Hongmanorom[1], D. Debecker[1]
[1] Institute of Condensed Matter and Nanoscience, Université Catholique de Louvain, Louvain-la-Neuve, Belgium

14h50 **Silica-supported DFM catalysts for CO_2 methanation: Comparative study with Al_2O_3-based catalysts**

L. Castoldi[1], G. Nava[1], S. Molina-Ramírez[2], C. Cristiani[2], B. Di Credico[3], E. Finocchio[4], L. Lietti[1], R. Scotti[1]

[1] Dipartimento di Energia (Laboratory of Catalysis and Catalytic Processes), Politecnico di Milano, Milano, Italy.

[2]Dipartimento di Chimica, Materiali e Ingegneria Chimica Giulio Natta, Politecnico di Milano, Milano, Italy.

[3]Dipartimento di Scienza dei Materiali, Università Milano-Bicocca, Milano, Italy.

[4]Dipartimento di Ingegneria Civile, Chimica e Ambientale, Università di Genova, Genova, Italy Politecnico di Milano, Milan, Italy

15h10 **The promoter effect of MgO on the performance of $Ni(acac)_2$-grafted hydroxyapatite in the Sabatier reaction**

N. Berroug[1], M.A. Gutiérrez-Ortiz[1], J. R. González-Velasco[1], Z. Boukha[1]

[1] Chemical Technologies for Environmental Sustainability Group, University of the Basque Country, Bilbao, Spain

15h30 **CO_2 methanation catalysts derived from Ni-alkaline earth metal carbonates**

S. Gupta[1], C. Poupin[1], S. Royer[1], E. Abi-Aad[1]

[1] Unité de Chimie Environnementale et Interactions sur le Vivant (UCEiV), Université du Littoral Côte d'Opale, France

15h50 **Rhenium-based materials for integrated carbon capture and utilization**

S. Scognamiglio[1,2,3], F. Morfin[1], R. Checa[1], J. Ivañez[1], G. Landi[2], L. Piccolo[1]

[1] Institut de Recherches sur la Catalyse et l'Environnement de Lyon, CNRS – Université Lyon 1, Villeurbanne, France

[2] Institute of Science and Technology for Sustainable Energy and Mobility – CNR, Naples, Italy

[3] Dipartimento di Scienza Applicata e Tecnologia (DISAT), Politecnico di Torino, Italy

16h10 **Coffee break (16h10-17h00)**

17h00 **DivCat Prizes and Lectures (17h00-19h00)**

19h00 **Free time, exposition stand removal**

20h00 **Gala Diner**
Ceremony for « Best oral presentation » and « Best poster » Prizes

Friday, May 23rd

09h00 **Plenary lecture**

Andreas RUDI

KIT-IIP, Karlsruhe Institute of Technology, Institute for Industrial Production, Karlsruhe, Germany

From catalyst to product: multi-dimensional assessment of chemical processes

10h00 **Coffee break**

10h30 **Key-note**

Agnieszka RUPPERT

LUT, Łódź University of Technology, Poland

Catalytic conversion of gamma valerolactone

11h00 **Conclusions**

11h30 **Lunch boxes distribution and bus departure at 12h00**

Poster Session (Tuesday 20th)

P-1 CO_2 purification of industrial flue gas: effect of physico-chemical properties obtained by different preparation methods on CoCuAl oxide for the Selective Catalytic Reduction process

A. Rahhal[1], E. Genty[1], R. Cousin[1], A. Ponchel[2], S. Noel[2], C. Poupin[1], S. Siffert[1]

[1] Univ. Littoral Côte d'Opale, UR 4492, UCEIV, Unité de Chimie Environnementale et Interactions sur le Vivant, F-59140, Dunkerque, France

[2] Univ. Artois, CNRS, Centrale Lille, Univ. Lille, UMR 8181, Unité de Catalyse et de Chimie du Solide (UCCS), rue Jean Souvraz, SP 18, 62300 Lens, France

P-2 Catalytic oxidative desulfurization of Marine fuel oil: investigating catalyst deactivation

J. Alakari[1], T. Roy[1], L. Poinel[1], C. Lancelot[2], P. Blanchard[2], C. Lamonier[2]

[1] SEGULA Technologies, 44550 Montoir De Bretagne, France

[2] Univ. Lille, CNRS, Centrale Lille, ENSCL, Univ. Artois, UMR 8181 – UCCS – Unité de Catalyse et Chimie du Solide, 59000 Lille, France

P-3 Influence of Water Vapor Treatment for NH_3-TPD on Zeolites

B. Amoury[1], J. Adolphs[2], S. Gökpinar[2], Y. Konishi[3]

[1] Microtrac Formulaction, 3 Paule Raymondis Street, 31200 Toulouse, France

[2] Microtrac Retsch GmbH, Retsch-Allee 1-5, 42781 Haan, Germany

[3] Microtrac BEL Corp., Tokyo, Japan

P-4 Valorization of Greenhouse and Acid Gas by Low-Silica Zeolite Catalyst

S.R. Batool[1], M. Fabbiani[1], L. Pinard[1], A. Novikov[2] , H. Retot[2] , V. Valtchev[1]

[1] LCS, CNRS-ENSICaen-UniCaen, 14000 Caen, France

[2] Saint Gobain Research Provence and NORPRO, Cavaillon, France

P-5 Versatile Macroligand Strategy for the Heterogenized Ni-Catalyzed Direct C-H Arylation of Benzothiophenes

J. Canivet[1], E. Chaigne-Tarlotin[1], E.A. Quadrelli[1]

[1] IRCELYON, Univ. Lyon 1, CNRS UMR 5256, Villeurbanne, France

P-6 Porous Organic Polymers for Heterogeneous CO_2-to-HCO_2H Photoreduction

E. Chaigne-Tarlotin[1], J. Canivet[1], E.A. Quadrelli[1]

[1] IRCELYON, Univ. Lyon 1, CNRS UMR 5256, Villeurbanne, France

P-7 An Old Yet Indispensable Method: n-Hexane Cracking for Composite Zeolite Characterization

R. Zhang[1,2], N. Chaouati[2] , B. Wang[1] , J. Xu[1,3], H. Liu[4] , H. Zhao[4] , J. Wang[4], S. Xu[3] , F. Dalena[2] , Z. Qin[1] , X. Gao[4], S. Mintova[1,2], L. Pinard[2]

[1] China University of Petroleum (East China), Qingdao, China

[2] LCS, UMR 6506, ENSICAEN, France

[3] Institute of Chemical Physics, Chinese Academy of Sciences, Dalian, Liaoning

[4] PetroChina Company Limited, Beijing, P. R. China; e ICPEES, UMR 7515,

P-8 A variety of environments of Lewis acid sites and hydroxyl groups of USY zeolites deciphered by DFT and high-resolution ^1H Solid-State NMR

T. Jarrin[1], Z. Wang[2], T. de Bruin[3], G. Pirngruber[1], M. Rivallan[1], A. Lesage[2], C. Chizallet[1]

[1] IFP Energies nouvelles, Rond-point de l'échangeur de Solaize, 69360 Solaize, France

[2] Centre de RMN à Très Hauts Champs, Université de Lyon, 69100 Villeurbanne, France

[3] IFP Energies nouvelles, 1 et 4 Avenue de Bois Préau, 92852, Rueil-Malmaison, France

P-9 Impact of Limonene on the Products of Catalytic Pyrolysis of Polyethylene

S. Denguezli[1], Sophie Duquesne[2], A. Dufour[3], J.-F. Lamonier[1]

[1] Univ. Lille, CNRS, Centrale Lille, Univ. Artois, UMR 8181, Unité de Catalyse et Chimie du Solide (UCCS), Lille, 59000 (France)

[2] Univ. Lille, CNRS, Centrale Lille, INRAE, UMR 8207, Unité Matériaux et Transformations (UMET), Lille, 59000 (France)

[3] Univ. Lorraine, CNRS, UMR 7274, Laboratoire Réactions et Génie des Procédés (LRGP), Nancy, 54000 (France)

P-10 Porosity control of hierarchical zeolites provides effective catalyst for continuous-flow methyl oleate skeletal isomerization

J.F. Sierra-Cantor[1], O. Gimello[1], A. Aubert-Pouëssel[1], C.-A. Guerrero Fajardo[2], F. Di Renzo[1], C. Gérardin[1], N. Tanchoux[1]

[1] ICGM, Université de Montpellier-CNRS-ENSCM, Montpellier, France,

[2] Departamento de Quimica, Universidad Nacional de Colombia, Bogotá, Colombia

P-11 Novel time-resolved IR/isotopic exchange methodology for the mechanistic investigation of CO_2 hydrogenation to methanol

A. Djaafri[1], M. Richard[1], C. Dujardin[1], I. De Waele[2]

[1] Univ. Lille, CNRS, Centrale Lille, Univ. Artois, UMR 8181 – UCCS – Unité de Catalyse et Chimie du Solide, F-59000 Lille, France.

[2] Univ. Lille, CNRS, UMR 8516, LASIRE, Laboratoire de Spectroscopie pour les interactions, la Réactivité et l'Environnement, F59 000, Lille, France

P-12 Polyolefins recycling: Mechanism of the polyolefin bifunctional hydrocracking from a polymer approach

J. Florez[1], S. Maury[1], R. Martinez-Franco[1], J. Fernandes[1], V. Monteil[2]

[1] IFP Energies nouvelles, Rond-point de l'échangeur de Solaize, 69360 Solaize, France

2 Catalysis, Polymerization, Processes and Materials laboratory CP2M, 69616 Villeurbanne, France

P-13 Influence of preparation method of CuAl mixed oxide issued from LDH catalytic total oxidation of model fumes issued from biomass combustion

E. Genty[1], P.-E. Danjou[1], C. Poupin[1], S. Siffert[1], R. Cousin[1]

[1] Université du Littoral Côte d'Opale, Unité de Chimie environnementale et Interactions sur le Vivant (UCEIV), 145 avenue Maurice Schumann, 59140 Dunkerque, France

P-14 Electrochemistry Unlocks New Possibilities in Difluoromethylation of Alkenes

H. Kim[1]

[1] Department of Chemistry, Pohang University of Science and Technology, 37673 Pohang, South Korea

P-15 Catalytic activity of MoO_x@SiO_2 yolk-shell structures in propane dehydrogenation and subsequent propylene metathesis

A. Rokicińska[1], M. Myradova[2], M. Mandrela[1], D. Waśniowska[1], M. Dębosz[1], P. Michorczyk[2], P. Kuśtrowski[1]

[1] Faculty of Chemistry, Jagiellonian University, Gronostajowa 2, 30-387 Krakow, Poland

[2] Department of Organic Chemistry and Technology, Cracow University of Technology, Warszawska 24, 31-155 Krakow, Poland

P-16 Methane Pyrolysis into Hydrogen and Carbon material: A comparative study between Microwave vs. Conventional heating methods

V. L'hospital[1], L. Goulart de Araujo[1], E. Landrivon[1], A. Mello[2], M. Radoiu[2], Y. Schuurman[1], N. Guilhaume[1], D. Farrusseng[1]

[1] IRCELYON, CNRS-Université de Lyon, 69626 Villeurbanne, France

[2] Microwave Technologies Consulting, 69100 Villeurbanne, France

P-17 Innovative approach for highly contaminated PET recycling

M. Lorenzi[1], L. Castoldi[2]

[1] *Greenchemicals S.R.L.*

[2] *Politecnico di Milano, Department of Energy, LCCP group, via La Masa 34, 20156 Milano, Italy*

Poster Session (Wednesday 21st)

P-18 Plasma-catalytic hybrid process for CO_2 valorization into liquid fuels

N. Merino[1,3], S. Ognier[1], X. Duten[2], M. Mikhail[3], M. Tatoulian[1]

[1] *Institut de Recherche de Chimie Paris, UMR 8247 (CNRS – Chimie ParisTech), Équipe 2PM, 75005 Paris, France*

[2] *LSPM – CNRS UPR 3407 – Université Sorbonne Paris Nord, 93430 Villetaneuse, France*

[3] *ENERGO, 59120 Loos – Lille, France*

P-19 Shaping of Ni-Co catalyst for up-scale biogas dry reforming

M. Mohamad Ali[1], M. Chaghouri.[1], L. Tidahy[1], M. Marinova[2], S. Royer[1,3], E. Abi-Aad[1], C. Ciotonea[1], C. Gennequin[1]

[1] *Université du Littoral Côte d'Opale, UCEIV, 59140 Dunkerque, France*

[2] *Université de Lille, Institut Michel-Eugène Chevreul (IMEC), 59000 Lille, France*

[3] *Université de Lille, Unité de Catalyse et de Chimie du Solide (UCCS), 59000 Lille, France*

P-20 Tailoring of the properties of sepiolite clays active in isopropanol dehydration to propylene

T.H. Nguyen[1], J.-L. Dubois[2], T. Caillot[1], A. Auroux[1], G. Postole[1]

[1] Université Claude Bernard Lyon 1, CNRS, IRCELYON, UMR 5256, Villeurbanne, F-69100
[2] Trinseo Netherlands B.V., Innovatieweg 14, 4542 NH Hoek, The Netherland

P-21 Lab-Scale Evaluation of Functional Materials for Ammonia Production from Steel Industry Residual Gases

S. Palencia Ruiz[1], L. Lukashuk[1], H.A.J. van Dijk[2]

[1] Johnson Matthey, Billingham, UK
[2] TNO, Petten, the Netherlands

P-22 Anode catalytic materials for the oxidative coupling of methane (OCM)

M. Guillon[1], K. Parkhomenko[1], A.-C. Roger[1]

[1] ICPEES, University of Strasbourg, 67087 Strasbourg, France

P-23 Greenhouse and acid gas conversion by electrothermal catalysis

H. Poelman[1], G. Veryasov[2], H. Retot[3] , I. Shlyapnikov[4] , J. Lauwaert[5], A. Delparish[6], M. Grilc[7], V. Valtchev[8], H. Dura[9], B. Raa[10] and J. Thybaut[1]

[1] Laboratory for Chemical Technology, Technologiepark 125, 9052 Ghent, Belgium
[2] Total Energies One Tech Belgium, Zone industrielle C, 7181 Seneffe, Belgium
[3] Saint Gobain Research Provence and NORPRO, Cavaillon, France
[4] Center of Excellence Low Carbon Technologies, 1000 Ljubljana, Slovenia
[5] Industrial Catalysis and Adsorption Technology, V. Vaerwyckweg 1-C, 9000 Ghent, Belgium
[6] PDC Research Foundation, Paardeweide 7, NL-4824EH Breda, The Netherlands
[7] Catalysis and Chemical Reaction Engineering, NIC, Hajdrihova 19, 1000 Ljubljana, Slovenia
[8] Laboratory of Catalysis and Spectrochemistry, CNRS-ENSICaen-UniCaen, 14000 Caen, France
[9] DECHEMA Energie und Klima, Theodor-Heuss-Allee 25, 60486 Frankfurt, Germany
[10] Industrial Systems Engineering & Product Design, Technologiepark 46, 9052 Ghent, Belgium

P-24 Magnesium hydroxide fluorides as catalysts for the isomerization of glucose to fructose

C. Sa[1], B. Yeskendir[1], J. Sierra[2], T. Onfroy[1], G. Laugel[1], F. Richard[2], S. Célérier[2], H. Lauron-Pernot[1]

[1] Laboratoire de Réactivité de Surface, Sorbonne Université, 75005 Paris, France
[2] IC2MP, 86000 Poitiers, France

P-25 Cu and ZnO nanoparticles supported on MWCNTs as nanocatalysts for selective N-formylation using CO_2 and H_2

N.-A. Thai[1,2,3], P. Fau[3], D. Mesguich[2], A. Ouali[1]

[1] Institut Charles Gerhardt Montpellier, UMR 5253 Univ Montpellier, CNRS, ENSCM Pôle Chimie Balard Recherche - CC043 1919 route de Mende, 34293 Montpellier, France
[2] CIRIMAT, Université de Toulouse, CNRS, Université de Toulouse 3 - Paul Sabatier, 118 route de Narbonne, 31062 Toulouse, France

P-26 Integrated thermochemical CO_2 valorization to middle-range olefins

J. Vachaud[1], S. Jambur[2], A. Roussey[1], J. Boon[2], A.L. Alvarenga Marinho[1], A.-C. Roger[3], S. Thomas[3], L. Lücking[2]

[1] CEA, LITEN, DTNM, Univ. Grenoble Alpes, Grenoble, 38000, France
[2] TNO Energy Transition, Westerduinweg 3, 1755 LE Petten, the Netherlands
[3] Institute of Chemistry and Processes for Energy, Environment and Health (ICPEES), UMR 7515 CNRS-University of Strasbourg, Strasbourg 67087 Cedex 02, France

P-27 Stoichiometric selective carbonylation of methane to acetic acid by chemical looping

Y. Wang[1], C. Dong[1,2], M. Shamzhy[3], Y.G. Kolyagin[1], J. Zaffran[1] *, A.Y. Khodakov[1] * and V.V. Ordomsky[1]

[1] UCCS–Unité de Catalyse et Chimie du Solide, Université de Lille, CNRS, Centrale Lille, ENSCL, Université d'Artois, UMR 8181, Lille, France

[2] *Department of Chemistry, The University of Hong Kong, Hong Kong, China*
[3] *Department of Physical and Macromolecular Chemistry, Faculty of Science, Charles University, Hlavova 2030/8, 12843 Prague, Czech Republic*

P-28 Study of catalysts Ni-Ce-Mg-Al , Ni-Co-Mg-Al and Ni-Mg-Al obtained via hydrotalcites for the dry reforming of the methane

A. Zazi[1,2], V.M. Gonzalez de la Cruz[3], D. Halliche[1], J.P. Holgado[3], A. Caballero[3], O. Cherifi[1]

[1] *Laboratoire de chimie du gaz naturel, Faculté de chimie, USTHB, BP 32 El Alia, Algérie*
[2] *Département de chimie, Faculté des sciences, UMMTO, Tizi Ouzou, Algérie*
[3] *Instituto de Ciencia de Materiales de Sevilla (CSIC-University of Seville) and Departamento de Quimica Inorganica, University of Seville, Avda. Americo Vespucio, 49, 41092 Seville, Spain*

P-29 Synthesis and comparison of Pt and Pt_3Sn supported catalysts for transfer hydrogenation from perhydro-dibenzyltoluene to acetone

S. Smitkriti[1,2], X. Ji[2,3], L. Veyre[1], V. Meille[2], C. Thieuleux[1]

[1] *Catalysis, Polymerization, Processes and Materials laboratory CP2M, 69616 Villeurbanne, France*
[2] *IRCELYON, CNRS, Université Claude Bernard Lyon 1, 2 avenue A. Einstein, 69626 Villeurbanne, France*
[3] *LAGEPP, Université Claude Bernard Lyon 1, 69100 Villeurbanne, France*

P-30 Reduced cobalt oxide catalysts for catalytic ozonation of toluene

H. Zhang[1], V. Meille[1], S. Gil[1]

[1] *IRCELYON, CNRS, Université Claude Bernard Lyon 1, 2 avenue A. Einstein, 69626 Villeurbanne, France*

P-31 Ni-Based cermets and high entropy alloys for efficient ammonia decomposition

D. Milas[1], T. Belin[1], N. Bion[1], F. Can[1], C. Comminges[1], X. Courtois[1], A. Meunier[1], J. Boissadie[2], G. Taillades[2]

[1] *Institut de Chimie des Milieux et Matériaux de Poitiers (IC2MP), CNRS, Université de Poitiers, 86000 Poitiers, France*
[2] *Institut Charles Gerhardt Montpellier (ICGM, UMR 5253), CNRS, Université de Montpellier, 34293 Montpellier, France*

P-32 Proving photoactive Polyoxometalates as potent prosthetic groups for a novel class of artificial metalloenzymes

A. Ranscht[1], D. Murillo Ilbay[1], N. Savic[1], T. N. Parac-Vogt[1]

[1] *Laboratory of Bioinorganic Chemistry, KU Leuven, 3001 Leuven, Belgium*

P-33 Biochar-based catalysts for reforming reactions

A. Jabbarova[1], K.Parkhomenko[1], A. Beuchat[1], M. Malikzade[1], M. Guillmont[2], B. Rety[2], Z. Nadif[2], C. Courson[1], D. Begin[1], R. Gadiou[2], N. Thevenin[3], L. Ruidavets[3]

[1] *Institut de Chimie et Procédés pour l'Energie, l'Environnement et la Santé (ICPEES), CNRS, Université de Strasbourg, Strasbourg, France.*
[2] *Institut de Science des Matériaux de Mulhouse (IS2M), CNRS, Université Haute-Alsace, Mulhouse, France*
[3] *RITTMO Agroenvironnement®, Colmar, France*

P-34 One-pot Lignin Catalytic Depolymerization and Demethylation

H. Lilti[1], C. Geantet[1], D. Laurenti[1]

[1] *Institut de Recherches sur la Catalyse et l'Environnement de Lyon, UMR 5256 – CNRS / Université Lyon 1*

https://fccat2025.sciencesconf.org/

Plenary Lectures

Towards NH_3 synthesis in mild conditions

Nicolas Bion[1]*
[1]*Institut de Chimie des Milieux et Matériaux de Poitiers (IC2MP), CNRS, University of Poitiers, 86000 Poitiers, France*
*nicolas.bion@univ-poitiers.fr

The well-known Haber-Bosch industrial process (H-B) for ammonia synthesis has been optimized using H_2 produced by steam reforming of natural gas or coal. It operates at high temperatures (up to 873 K) and high pressures (15-40 MPa) in very large-scale, centralised production plants (>1000 tNH_3/day) to ensure economic viability. After more than a century of industrialization, the energy efficiency of this process has been considerably improved. However, ammonia production is still extremely CO_2-intensive, and needs to be decarbonized like many other industrial processes. This challenge is particularly important given that beyond the current uses of ammonia (fertilizers, explosives), new applications could emerge over the next few decades. In the event of the development of a hydrogen economy, the use of ammonia as a liquid hydrogen carrier is a considered option for long-distance transport and/or long-term storage [1]. Indeed, ammonia exhibits a high gravimetric (17.8 wt%) and volumetric (121 kg m^{-3}) hydrogen densities and liquefies at modest pressures (10 bar at 25°C) or moderate temperature (-33 °C at 1 bar). Ammonia is also studied as an alternative shipping fuel despite safety issues and its potential impact on the global nitrogen cycle [2].

Among the solutions for developing low-carbon ammonia production, replacing steam reforming of natural gas with water electrolysis for hydrogen production is a promising route. Substituting green hydrogen for grey hydrogen can lead to a radical change in the process, as the conversion of green hydrogen to ammonia seems better suited to small, flexible, and decentralized units capable of supporting the intermittent nature of renewable energies. These small units will be economically viable provided that the ammonia synthesis reaction can be carried out under much milder temperature and pressure conditions (573 to 623 K and 1 to 5 MPa) [3]. The competition is therefore on to design the catalysts that will achieve this goal.

In this contribution, the most promising reported families of catalysts capable of generating ammonia at low pressure and mild temperatures will be discussed. A focus will be made on the strategies followed to overcome the bottleneck related to N_2 dissociation at low temperatures. Supported ruthenium catalysts have been particularly investigated to facilitate this rate-determining step. The electronic enrichment of the metal nanoparticles is a reported solution. It can be achieved by using additional electron-donating oxides at the interface between the active nanoparticle and the support, or by depositing Ru directly on electride-type supports (Figure 1a) [4]. In the latter case, a challenge consists in accurately determining the number of accessible active sites.

Among the alternative pathways to Ru catalysts, highly active catalytic formulations have been developed based on Li-N-H nitride hydrides and doped CoMoN solids. In the first case, activity at very low temperatures has been reported, but the sensitivity to air of this family of Li-containing compounds complicates technology transfer to industrial application. In the second case, the Mars van Krevelen mechanism, involving lattice N atoms in ammonia generation, has been proposed on the basis of isotopic exchange experiments and DFT calculations [5]. This paved the way for the use of these materials in a 2-step chemical looping concept. Very recently, mixed formulations oxynitride-hydride have shown very high activity with Ru nanoparticles, where Ru acts not as a direct active site but as a promoter of the generation of anionic vacancies (Figure 1b) [6].

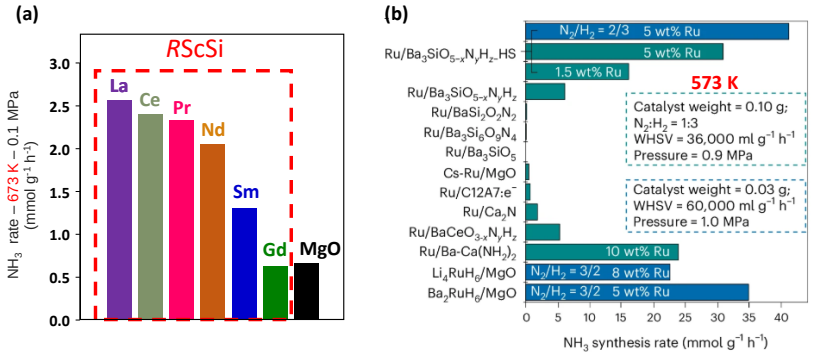

Figure 1. NH_3 synthesis rate obtained (a) at 673 K and 0.1 MPa on a series of Ru(2.5wt%) supported on *R*ScSi intermetallic phase with various R elements [4]; (b) at 573 K and P= 0.9 or 1 MPa on Ru supported on various hydrides, nitrides and oxynitride-hydride (extracted from [6]). Both series are compared with classical Ru/MgO or Cs-Ru/MgO catalysts.

In addition to thermocatalytic ammonia synthesis, alternative technologies are being explored and will be discussed, with particular emphasis on electrocatalytic studies which are showing promising results. In this field, attention will also be drawn to the many false positive works, particularly in the low-temperature electrosynthesis mode.

References

1. M. Aziz, A. T. Wijayanta, A. B. D. Nandiyanto, *Energies.* **2020**, *13*, 3062
2. P. Wolfram, P. Kyle, X. Zhang, *et al.*, *Nat Energy.* **2022**, *7*, 1112
3. J. A. Faria, *Curr. Opin. Green Sustain. Chem.* **2021**, *29*, 100466
4. C. Croisé, K. Alabd, S. Tencé, *et al.*, *ChemCatChem*. **2023**, *15*, e20220117
5. S. Laassiri, C. D. Zeinalipour-Yazdi, N. Bion, *et al.*, *Faraday Discuss.* **2021**, *229*, 281
6. Z. Zhang, K. Miyashita, T. Wu, *et al.*, *Nat. Chem.* **2025**, *in press*

How X-ray spectroscopies help to understand the dry reforming reaction

H. Poelman
Laboratory for Chemical Technology, Tech Lane Science Park 125, 9052 Ghent, Belgium
hilde.poelman@UGent.be

Introduction

Catalysts take up a crucial role in chemical industry, promoting a wide range of chemical reactions. Improving the design of catalysts requires knowledge on their structure-activity relationship. To obtain the latter, one needs to examine the catalyst, not only before and after use – as prepared and *post mortem* – but rather during its activity, i.e. *operando* (Latin: while working). The latter term implies measuring its performance online as a function of time, while simultaneously tracking the material characteristics, as it is enabling the reaction. This in particular makes characterisation quite challenging, as the chosen technique needs to be able to withstand high temperature and pass through reaction environments.

Based on their high penetration power, X-rays offer many options to probe solid materials *operando*[1]. X-ray diffraction (XRD) is well-established as lab-scale technique, including *operando* application. In addition, X-ray absorption (XAS), emission (XES), Raman scattering (XRS), as well as modulation-excitation absorption (MEXAS) spectroscopies of X-rays can bring valuable information, not only about the cations, but also on the lighter elements. To showcase the power of X-ray spectroscopies, we delve into the dry reforming of methane (DRM, $CH_4+CO_2 \leftrightarrow 2H_2+2CO$, $\Delta H_0^{298K}=247kJ/mol$) as reaction of interest,[2] with supported Ni as designated catalyst. The use of plain Ni however entails several challenges, such as phase transformations, sintering, carbon accumulation, leading to rapid deactivation. In the past decade, several modifications have been proposed to tackle these issues: a more stable or even active support, Fe promotion for Ni stabilization and carbon control. To unravel how exactly these modifications work, X-rays have proved immensely important.

Materials and Methods

Ni-Fe/$MgAl_2O_4$ and Ni/$MgFeAlO_x$ were used in this study (Figure 1). Next to regular lab characterization (physisorption, temperature programmed reduction/oxidation, normal and *in situ* XRD), *operando* characterization of Ni, Fe, Al, Mg, O and C was performed using X-ray techniques at synchrotron beamlines (DUBBLE and ID20 at ESRF, SuperXAS at SLS and ROCK at SOLEIL). Data analysis was performed using IFEFFIT, principal component analysis (PCA), Multivariate Curve Resolution-Alternating Least Squares (MCR-ALS), Finite Difference Method Near Edge Structure (FDMNES) modelling and phase-sensitive detection (PSD).

Results and Discussion

To avoid interaction of Ni with an Al_2O_3 support, the use of spinel $MgAl_2O_4$ has been proposed. Iron promotion can then be introduced in two ways: co-impregnation of both metals or by modifying the spinel support with Fe. In the latter case, catalyst activation by reduction extracts part of Fe from the support, to form alloy with Ni, while the remainder Fe fraction in the support gets partially reduced from 3+ to 2+.[3,4] The Fe-modified support proved active itself, showing redox functionality and high thermal stability, while mitigating carbon under dry reforming conditions.[5]

The evolution of light elements can be assessed by *in situ* XRS. Upon reducing the Fe-modified support, the Al $L_{2,3}$ and O K XRS signals showed enhanced distortion, resulting from the partial Fe segregation from the $MgFeAlO_x$ lattice. This however facilitated the lattice oxygen mobility and hence its catalytic activity.[3] Next, the Ni/$MgFeAlO_x$ catalyst was examined by combining XRS-XES *in situ*. The structural modifications of the catalyst during redox and DRM treatments not only involved the main catalytic players Ni and Fe, tracked by XES, but also entailed a role for the low Z elements O, Al and related Mg, adequately probed by XRS.[6]

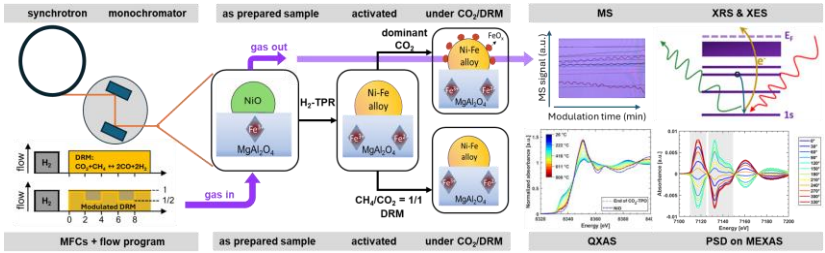

Figure 1. Synchrotron X-rays for *operando* investigation of a Ni-Fe/$MgFeAlO_x$ DRM catalyst.

Since transmission XAS is a bulk technique, gaining information on the active sites only is not straightforward. This limitation can be circumvented by applying modulated gas concentrations for MEXAS, providing a periodic stimulus that only induces a response from the active part of the catalyst. Application to the Ni-Fe/$MgFeAlO_x$ DRM catalyst at both Fe and Ni K edges, allowed to kinetically differentiate between the two by means of bi-element PSD.[7]

A very recent application of EXAFS uses the Debye-Waller factor to determine the dynamic temperature variations within active Ni nanoparticles during catalytic reaction. This selective nanothermometry allows to monitor the actual temperature of particles, which can be quite different from the set temperature, owing to the nature of the reaction. As such, for dry reforming of methane, the reaction's endothermicity causes Ni nanoparticles to become local heat sinks with their temperature deviating by 90 °C from the reactor temperature.[8]

Significance

Next to the fundamental relevance for understanding and improvement of DRM catalysts, the discussed material modifications are already being implemented for pilot scale-up (TRL ~5).

References

1. M. Filez et al., *Angew. Chem. Int. Ed.* **2019**, 58, 13220
2. D.L.T. Nguyen et al., *J. Ind. Eng. Chem.* **2024**, 25, 169
3. A. Longo et al., *ACS Catal.* **2020**, 10, 6613
4. A. Dharanipragada et al., *AIChE J.* **2018**, 64, 1339
5. S. Theofanidis et al., *ACS Catal.* **2018**, 8, 5983
6. S.K. Das et al., *ACS Catal.* **2024**, 14, 1311
7. V. De Coster et al. *ACS Catal.* **2023**, 13, 12445
8. M. Filez et al. *Nature Catal.* **2025**

Catalysis by Gold for CO and VOCs oxidation reactions: structure-activity relationship

Leonarda F. Liotta *
[1]*Institute for the Study of Nanostructured Materials (ISMN)-CNR*
Via Ugo La Malfa, 153, 90146, Palermo, Itay
*leonardafrancesca.liotta@cnr.it

Introduction

The catalytic oxidation of carbon monoxide (CO) and volatile organic compounds (VOCs) is a critical process in air pollution control, with significant environmental and health implications. Au-based catalysts, particularly those supported on reducible oxides have emerged as promising candidates for oxidation reactions due to their exceptional activity at low temperatures[1]. CO, primarily emitted from vehicle exhaust and industrial processes, is a toxic gas that poses serious health risks. Likewise, VOCs, including toluene, propene, benzene, and formaldehyde, are major contributors to smog formation and indoor air pollution, necessitating efficient removal strategies.

Among various support oxides, CeO_2 plays a crucial role in enhancing the performance of Au catalysts. Its high oxygen storage capacity, redox properties, and strong metal-support interactions promote efficient oxidation pathways[2,3]. The introduction of Y^{3+} into CeO_2 promotes the formation of active oxygen species, enhancing the catalytic activity at low temperature of Au supported catalysts[4].

The unique catalytic behavior of Au-supported catalysts that is influenced by factors such as preparation methods, nature of the support, particle size, pre-treatment and reaction conditions, has led to extensive research efforts in optimizing their performance. This study explores the significance of Au supported catalysts for CO and VOC oxidation, focusing on key properties and advancements in catalyst design[5,6].

Materials and Methods

Au catalysts with low metal loading, such as 1, 1.5, 3wt% were prepared by deposition–precipitation (DP) method using an aqueous solution of $HAuCl_4 \cdot 3H_2O$. The supports were CoAl mixed oxide, ceria, Y-doped ceria, Co-promoted ceria. Characterizations were carried out by XRD, surface area and pore size distribution analysis, TPR, HR-TEM, XPS, Raman. CO and VOCs catalytic oxidation tests were performed in flow fixed-bed reactors at atmospheric pressure, in a range of temperature between 25-350 °C, depending on the probe molecule, at gas hourly space velocity (GHSV) typically of 30,000 h^{-1}.

Results and Discussion

The high dispersion of Au particles on the ceria and the formation of oxygen vacancies directly connected to Ce^{3+} amount were proven play a key role in enhancing the VOCs oxidation activity. Ce^{3+} ions represent nucleation centers for the stabilization of the active Au ionic species, and, at the same time, gaseous oxygen is easily activated over these centers, enhancing catalytic activity. It was demonstrated that Au/Co (9,12mol%)-promoted ceria catalysts performed better than Au/ceria and exhibited almost full HCHO oxidation into CO_2 at 25 °C with great stability for the time on stream (40 h), as shown in Fig. 1[3].

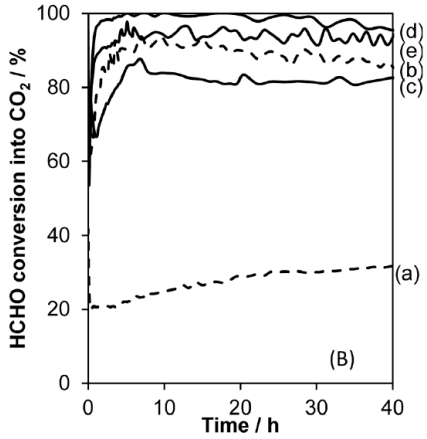

Fig. 1. HCHO conversion into CO2 for the: (a) 1.5Au/Ce; (b) 1.5Au/CeCo9; (c) 3Au/Ce; (d) 3Au/CeCo12 and (e) 3Au/CeCo9 catalysts at 25 °C for 40 h.

Metallic Au particles over an inert oxide show poor catalytic activity and tendency to sinter. The main requisite to attain high activity in VOC oxidation, such as propene oxidation, has been proved to be the occurrence of metal–support interaction leading to both, nucleation of small gold particles at the surface defects of the support and stabilization of ionic gold species at the interface with a reducible oxide[6].

Significance

The design of Au catalysts with tailored properties optimized particle size, support interactions, and oxygen mobility enables sustainable and cost-effective pollution control solutions.

References

1. S. Sciré, L.F. Liotta, Appl. Catal. B **2012**, *125*,222
2. E.I. García-López, Z. Abbasi, F. Parrino, V. La Parola, L.F. Liotta, G. Marcì, Catalysts **2021**, *11*, 1467
3. G. Rochard, J.-M. Giraudon, L.F. Liotta, V. La Parola, J.-F. Lamonier, Catalysis Science and Technology, **2019**, *9*, 3203
4. L. Ilieva, P.Petrova, L.F. Liotta, J.W. Sobczak, W. Lisowski, Z. Kaszkur, G. Munteanu, T. Tabakova, Catalysts **2016**, *6*, 99
5. G. Rochard, E. Genty, J.-M. Giraudon, C. Poupin, J.-F. Lamonier, S. Siffert, V. La Parola, L. F. Liotta, R. Cousin, Molecules **2024**, *29*, 2285
6. M. Ousmane, L.F. Liotta, G. Pantaleo, A.M. Venezia, G. Di Carlo, M. Aouine, L. Retailleau, A. Giroir-Fendler, Catalysis Today, **2011**, *176*, 7

Over the hydrogen rainbow: the uses of catalysis for the production of H_2

Claire COURSON
ICPEES-UMR 7515, University of Strasbourg, 67087 Strasbourg, France
Claire.courson@unitra.fr

Introduction

In the context of unavoidable climate change prevention, a carbon-neutral energy carrier such as hydrogen seems to be the best solution. In fact, its use does not contribute to increasing CO_2 levels in the atmosphere. However, in order to meet growing energy demand while respecting carbon neutrality, hydrogen production must follow clean and efficient methods. There are various production routes with varying carbon footprints, classified according to a gradation of colours known as the hydrogen rainbow.

Today, 90% of the hydrogen production uses thermal conversion of fossil fuel with a strong impact on CO_2 production. These include technologies such as steam reforming of natural gas and light hydrocarbons, partial oxidation of heavy hydrocarbons, and gasification of coal.

Other processes such as water electrolysis or biomass pyrogasification are solutions for the production of low-carbon, renewable hydrogen. However, their costs must fall sharply to make them competitive. In this area, catalysis has the means to meet this immense challenge.

After a presentation of the different shades of the hydrogen rainbow (Fig. 1), this conference will look at the different actual ways of hydrogen production. It will highlight the role that catalysis can play in these processes. It will then focus on future developments trend and specify the points of action of catalysis in new processes for greening hydrogen production.

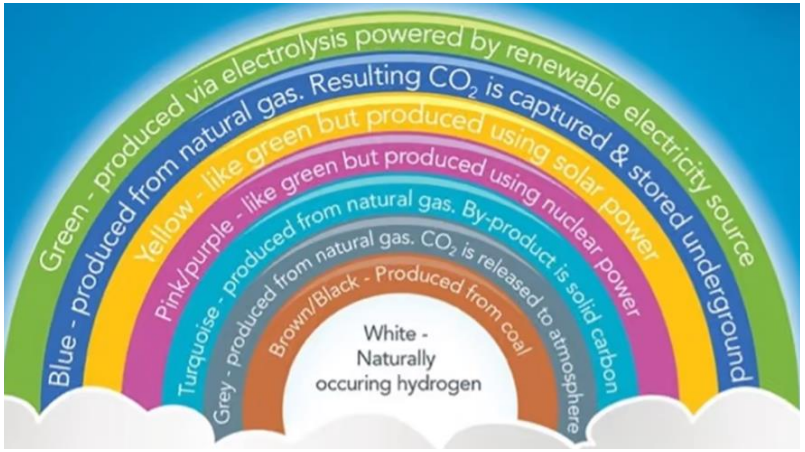

Figure 1. The hydrogen rainbow [1].

References

1. Costain. (2021). Blue or Green hydrogen? What colour will the fuel of the future be? https://www.costain.com/news/insights/blue-or-green-hydrogen-what-colour-will-the-fuel-of-the-future-be/

From catalyst to product: Multi-dimensional assessment of chemical processes

Andreas Rudi*, Paul Heinzmann, Uwe Langenmayr, Alexander Schneider, Frank Schultmann
Karlsruhe Institute of Technology (KIT), Institute for Industrial production (IIP), 76817 Karlsruhe
*andreas.rudi@kit.edu (corresponding author)

Introduction

Catalysts play a pivotal role in industrial chemistry, enabling efficient chemical transformations with reduced energy consumption and environmental impact. However, the transition from catalyst development to industrial application involves complex, multi-dimensional evaluations. This keynote will discuss the systematic assessment of chemical processes from early-stage discovery to commercialization. A Techno-Economic-Environmental Analysis (TEEA) serves as a guiding framework, ensuring feasibility and sustainability at each development stage. Recent studies have demonstrated the value of TEEA in early-stage assessments of Power-to-X and synthetic fuel pathways, highlighting trade-offs between emission reductions and economic viability[1,2].

As illustrated in Figure 1, the transition from academic research to industrial application follows a structured trajectory. Initial concept development involves fundamental and applied research, leading to proof-of-concept validation. The process then moves into scale-up, incorporating technology transfer and development efforts. Finally, the product reaches the market, where economic success is determined by profitability and sustainability metrics.

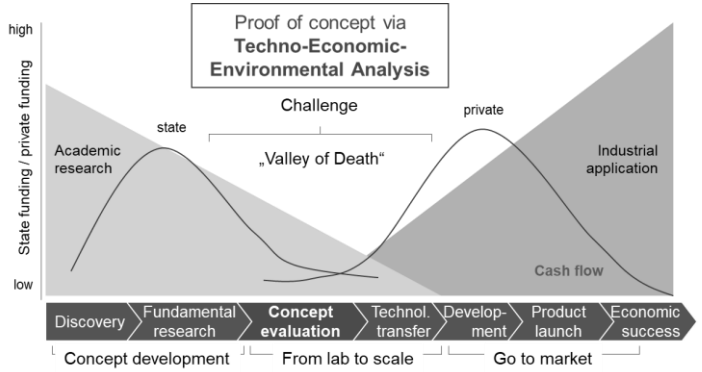

Figure 1. Bridging the "Valley of Death" with Techno-Economic-Environmental Analysis

Materials and Methods

A comprehensive assessment of catalytic processes requires the integration of experimental evaluation, system analysis, and sustainability assessment to guide development from laboratory research to industrial application. Technical performance is determined by key indicators such as turnover frequency, selectivity, and stability, supported by kinetic modeling and reactor simulations to optimize operating conditions and predict scalability.

To ensure holistic viability, a TEEA framework is employed. This approach combines economic analysis—covering production costs, resource efficiency, and process scalability—with environmental and social assessments. This has been successfully applied in various contexts, such as hydrogen-based fuel production[3] and biomass upgrading processes[4], to evaluate sustainability across entire value chains. Together, these methods provide a robust basis for evaluating sustainability across the full value chain.

Complementing this, system analysis is used to capture interdependencies within the broader chemical and energy systems, enabling the identification of infrastructure constraints, resource flows, and cross-sectoral impacts. To reconcile the multiple dimensions of sustainability, multi-criteria decision analysis is applied, allowing for transparent integration and prioritization of diverse indicators based on stakeholder values and strategic objectives. This structured methodology ensures that catalytic processes are not only technologically sound and economically feasible but also system-compatible and aligned with sustainability targets.

Results and Discussion

Key insights from TEEA evaluations highlight the importance of early-stage integration of economic and environmental factors in catalyst development. Case studies demonstrate how decision-making at the lab scale impacts long-term feasibility. The evaluation of process parameters such as reactor design, feedstock availability, and regulatory constraints further refines industrial viability. For instance, this is evidenced by comparative studies of Methanol-to-Gasoline versus Fischer-Tropsch pathways, where process design choices substantially impact both economic competitiveness and environmental footprints[2].

Significance

This systematic approach enhances innovation efficiency in catalysis research, ensuring that novel catalysts transition smoothly from the lab to commercial scale. By adopting a multi-dimensional assessment, industries can optimize chemical processes towards sustainability.

References

1. U. Langenmayr, P. Heinzmann, A. Schneider, M. Ruppert, A. Rudi, W. Fichtner **2025** A Multi-Method Approach for the Analysis of Stand-alone Power-to-X Production Dynamics - Quantifying the Trade-off Between Emission and Cost Reduction. *In press*.
2. A. Schneider; M. Harnischmacher; A. Rudi; F. Schultmann **2025** Comparative economic and environmental assessment of Hydrogen and its Derivatives Supply Chains: Renewable Energy Integration for Methanol-to-Gasoline and Fischer-Tropsch Processes. *In press*.
3. S. Glöser-Chahoud, P. Heinzmann, U. Langenmayr, F. Schultmann **2025** Production of Alternative Fuels and Chemicals from Green Hydrogen and Various Carbon Sources. In: Braun, Espinosa Gutiérrez, Tröger, Hirth (eds) Eco-Industrial Development as an Industrial Strategy. Green Energy and Technology. Springer, Cham. https://doi.org/10.1007/978-3-031-73576-9_15
4. M. Götz, A. Rudi, R. Heck, F. Schultmann, A. Kruse **2022** Processing Miscanthus to high-value chemicals: A techno-economic analysis based on process simulation. *GCB Bioenergy*. doi: 10.1111/gcbb.12923

Keynote Lectures

New developments in the molecular modelling of zeolites for heterogeneous catalysis

Mercedes Boronat[1]*
[1]*Instituto de Tecnología Química, Universitat Politècnica de València – Consejo Superiror de Investigaciones Científicas, 46022 València, Spain*
*boronat@itq.upv.es

Introduction

Zeolites are microporous aluminosilicates largely employed in industry as efficient heterogeneous catalysts, because they can host different types of active sites including Brønsted acid sites, Lewis acid sites and redox active sites.[1] Computational modelling has traditionally assisted in the design of improved zeolites for target applications, and I will show two recent examples where we apply high-throughput and machine learning techniques to investigate the confinement effect of zeolites and the mobility of redox active sites under reaction conditions.

Results and Discussion

Acid zeolites find broad application in petrochemistry and chemical industry. The stabilization of organic reaction intermediates and transition states inside the zeolite microporous voids by weak Van der Waals interactions is very sensitive to the fit of the adsorbed species with the surrounding environment, but approaching the level of molecular recognition of enzymes with solid catalysts is a challenging goal.[2] In the first example, we focus on the competing transalkylation and disproportionation of diethylbenzene (Figure 1), where the key diaryl intermediates for the two competing reactions only differ in the number of ethyl substituents in the aromatic rings. By combining a fast high-throughput screeening of all zeolite structures able to stabilize the key intermediates with a more computationally demanding periodic DFT study of the mechanism on the most promising candidates, a series of potentially selective zeolite structures were theoretically proposed and experimentally synthesized and tested. The results presented demonstrate that subtle changes in the zeolite architecture can modulate the preferred reaction pathways, leading to a precise control of the host-guest interactions and the selectivity of the proces.[3]

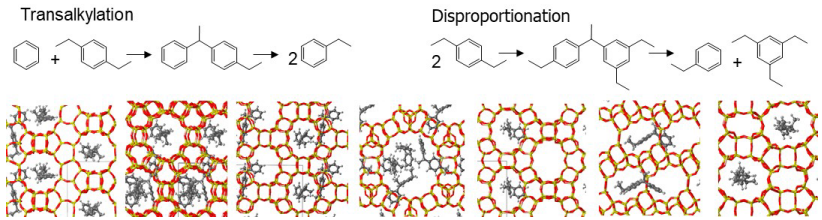

Figure 1. Reactions considered and key intermediates confined in selected zeolites.

Cu-exchanged zeolites play a crucial role as redox catalyst for the removal of greenhouse gases. Cu-CHA with the chabazite crystallographic structure, is the commercial catalyst used for the abatement of NOx emissions from diesel vehicles through the selective catalytic reduction reaction (NH_3-SCR-NOx), and it is also being applied in the partial oxidation of methane to methanol with O_2 and H_2O (MTM reaction).[1] The catalytic activity of Cu-CHA for these two reactions relies on the mobility of solvated Cu^+ cations that act as dynamic active sites, and on the probability of finding two solvated Cu^+ cations simultaneously in the same cavity of the zeolite microporous structure. *Ab initio* molecular dynamics (MD) simulations can provide quantitative atomistic insight on Cu^+ mobility,[4] but they are too computationally expensive to explore large length and time scales or diverse catalyst compositions. In the second example we report a machine learning (ML) interatomic potential that accurately reproduces DFT results allowing multi-nanosecond simulations and diverse chemical compositions of the Cu-CHA catalyst.[5] Simulations at several temperatures in the NVT ensemble show that two NH_3 molecules are enough to mobilize Cu^+, but a higher H_2O loading is needed to detach Cu^+ from the framework. In addition, the diffusion of H_2O-solvated Cu^+ cations through the windows connecting adjacent cavities is easier than that of NH_3-solvated Cu^+, which is reflected in a higher mobility. These results demonstrate the power of combining ML and MD simulations to study cation transport in microporous solids.

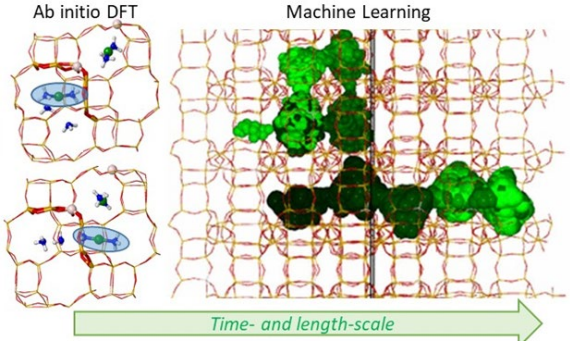

Figure 2. Representation of representation of the increased time- and length scales of machine-learning accelerated molecular dynamics simulations.

References

1. P. del Campo, C. Martínez, A. Corma. *Chem. Soc. Rev.* **2021**, *50*, 8511.
2. M. Moliner, M. Boronat, *Microporous Mesoporous Mater.* **2022**, *358*, 112354.
3. P. Ferri, Ch. Li, D. Schwalbe-Koda, M. Xie, M. Moliner, R. Gómez-Bombarelli, M. Boronat, A. Corma, *Nature Commun.* **2023**, 14, 2878.
4. R. Millán, P. Cnudde, V. van Speybroeck, M. Boronat. *JACS Au* **2021**, *1*, 1778.
5. R. Millán, E. Bello-Jurado, M. Moliner, M. Boronat, R. Gomez-Bombarelli. *ACS Central Sci.* ***2023****, 9*, 2040.

Liquid metals in catalysis

Vitaly Ordomsky*
[1]*Univ. Lille, CNRS, Centrale Lille, ENSCL, Univ. Artois, UMR 8181 – UCCS – Unité de Catalyse et Chimie du Solide, F-59000, Lille, France*
*vitaly.ordomsky@univ-lille.fr

Introduction

Liquid metals (LMs) are metals with low melting points, such as gallium (Ga), indium (In), bismuth (Bi), and tin (Sn), as well as their alloys. These materials exhibit unique properties, including high electrical and thermal conductivities combined with liquid-phase mobility. These characteristics have driven rapid advancements in various fields, such as flexible electronics, soft robotics, and biomedicine. More recently, significant efforts have been directed toward utilizing LMs in catalysis[1]. One of the key advantages of LMs in catalysis is their ability to act as solvents with distinct properties compared to conventional organic or aqueous phases. They can mix with reactants while remaining easily separable after the reaction, effectively combining the benefits of both homogeneous and heterogeneous catalysts. This helps address challenges such as catalyst separation in homogeneous catalysis and deactivation due to coking or sintering in heterogeneous systems. A major application of LM in catalysis involves the dissolution of noble metals (e.g., Pt, Pd) or transition metals (e.g., Ni, Co) in small quantities. This results in exceptional catalytic activity and coke resistance, particularly in reactions like propane and butane dehydrogenation[2], as well as methane pyrolysis for hydrogen and carbon production[3]. The liquid metal environment modifies the properties of the dissolved metal, stabilizing it in a single-atom state with delocalized electrons. This unique electronic structure enhances catalytic performance. Additionally, it has been demonstrated that the appropriate selection of low-melting-point metals can not only maximize metal dispersibility but also fine-tune the electronic structure of active sites. This leads to improved catalytic activity and long-term stability in applications such as Fischer-Tropsch synthesis[4] and alcohol amination[5].

Another promising application involves CO_2 conversion, where LM oxidation by CO_2 can facilitate carbon production[6]. Moreover, LMs have recently been explored for enhancing non-metallic catalysts, such as zeolites[7-8]. In methanol-to-hydrocarbon (MTH) conversion, commonly used zeolite catalysts suffer from rapid deactivation due to coke deposition, necessitating frequent regeneration. We have demonstrated that low-melting-point metals like Ga can significantly improve methanol conversion stability[7] by reducing coke formation and aiding carbonaceous species desorption from the zeolite to the intercrystallite zone. Beyond thermocatalysis, LM also hold great potential in photocatalysis and electrocatalysis[9]. Their high mobility allows for dynamic surface tension modulation in response to electric charges, offering flexibility in catalyst design. Looking ahead, the exceptional properties of LM present numerous advantages and exciting opportunities for catalytic applications, paving the way for further innovations in this field.

Materials and Methods

The catalysts have been prepared by mixing liquid metals (Ga, In, Bi, Sn) and their alloys with the catalysts (e.g. HZSM-5) to provide the required concentration of metal in the material with subsequent thermal treatment of the material. The catalytic tests have been performed in fixed bed or batch reactor in the reactions of hydrogenation of CO, CO_2, methanol to hydrocarbons conversion, partial oxidation of methane etc.

Results and Discussion

Our catalytic results demonstrate that LM can have a strong influence on the activity, selectivity, and stability of catalysts (**Figure 1**). For example, the formation of an LM film over Fe increases activity by up to 10 times by enhancing C–O dissociation during Fischer-Tropsch synthesis[4]. Selectivity can also be significantly improved in the presence of LM through its interaction with active sites on both metallic and non-metallic catalysts[8,9]. Additionally, incorporating LM into ZSM-5 enhances catalyst stability by up to 14 times by slowing coke deposition and facilitating the desorption of carbonaceous species from the zeolite. Thus, LM affects catalysts in multiple ways. Our goal is to understand how introducing mobility to the catalyst can improve its performance.

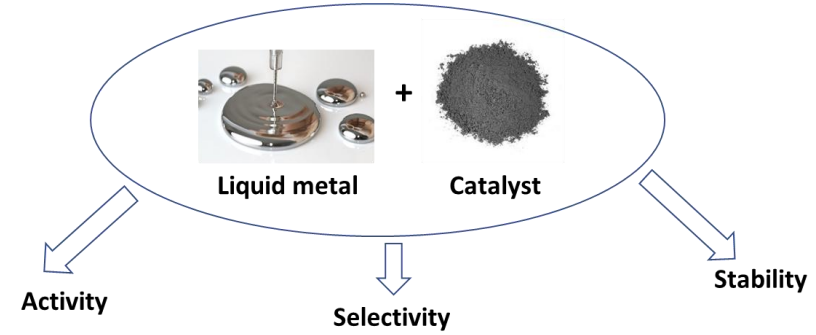

Figure 1. The effect of Liquid Metal on the catalytic performance.

Significance

The LM system can provide active, selective and stable catalytic performance by combining the properties of homogeneous and heterogeneous catalysis from both industrial and fundamental perspectives.

References

1. T. Daeneke, et al., *Chemical Society Reviews* **2018**, *47 (11)*, 4073.
2. N. Taccardi, et al., *Nat. Chem.* **2017**, *9*, 862.
3. D.C. Upham, et al. *Science* **2017**, 358, 917.
4. V.V. Ordomsky, et al. *ACS Catalysis* **2017**, *7 (10)*, 6445.
5. F. Niu, et al. *Green Chemistry* **2020**, *22 (13)*, 4270.
6. K. Zuraiqi, et al., *Energy Environ. Sci.* **2022**,*15*, 595.
7. Y. Zhou, et al., *Nature Communications* **2024**, *15 (1)*, 2228.
8. Y. Zhou, et al., *ACS Catalysis* **2024**, *14 (10)*, 7806.
9. M.N. Tran, et al., Applied Catalysis B **2025**, *363*, 124834

Modelling bioprocesses in chemical engineering

Kilian Kobl[1]*, Yohann Le Guennec[1], Airy Tilland[1]
[1]*Ypso-Facto, 19 Avenue Foch, 54000 Nancy, France*
*kilian.kobl@ypso-facto.com

Introduction

Mechanistic modeling is a powerful tool for understanding, optimizing, and innovating biochemical and biopharmaceutical processes [1]. It provides a predictive framework based on fundamental physical and chemical principles [2]. While traditional development approaches rely on expert intuition and extensive experimental work, which can be time-consuming and costly, mechanistic models improve process understanding and reduce experimental requirements [3]. This work outlines a structured approach to mechanistic model development, by presenting a step-by-step methodology for building such models, with a focus on enzymatic reactions. It is illustrated with two case studies: enzymatic isomerization of glucose to fructose [4] and enzymatic conversion of phosphatidylcholine (PC) to lysophosphatidylcholine (LPC) and glycerophosphatidylcholine (GPC).

Materials and methods

A structured methodology was used for model development in both case studies, consisting of defining process objectives, collecting and analyzing data, identifying key process phenomena, building representative models, calibrating parameters, and using the model for optimization. A trends study was first performed to establish qualitative relationships between key process parameters, such as for example temperature and enzyme concentration, and key performance indicators, such as yield. A quantitative mechanistic model was then built, using thermodynamic, kinetic, mass/heat transfer and hydrodynamic blocks. Experimental data were used for model calibration, ensuring accurate process predictions.

Results and discussion

The first case study on enzymatic isomerization of glucose to fructose illustrates the modeling methodology. Based on key process parameters identified in the trend study, the mechanistic model for the glucose/fructose case was built, and the final model was calibrated using the experimental data. The case study showcases the advantage of a mechanistic model for the transition from batch to continuous processing. The ability to modify the model's hydrodynamic component while keeping thermodynamic and kinetic parameters unchanged is possible thanks to the flexibility of mechanistic modeling. The performance of switching to a continuous stirred-tank reactor (CSTR), was evaluated by simulation, predicting the variations in fructose purity and reactor productivity based on reactor volume. Such simulations guide process design without requiring extensive additional experiments, significantly reducing development time and costs.

A second case study on PC-to-LPC conversion further illustrates the benefits of mechanistic modeling. A trends study first assessed the impact of key parameters on LPC production. The model was then calibrated with batch experimental data (Figure 1). Subsequently, the model was used for process optimization. One challenge that was encountered in this process was enzyme deactivation, which impacts reaction kinetics over time. By adding the deactivation reaction, the model successfully predicted this behavior and helped identifying process conditions to obtain an optimal product yield. Finally, continuous enzyme injection was explored as a potential solution, with simulations showing increased LPC yield and improved process robustness, though with longer reaction times.

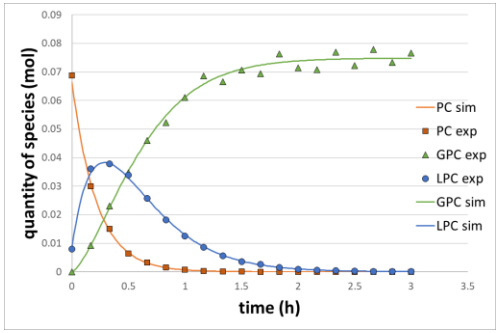

Figure 1. Quantities of species during the enzymatic transformation of PC to LPC and GPC (Dots – experimental data, lines – simulations).

Significance

Mechanistic modeling is a critical tool for modern biochemical and pharmaceutical process development. By leveraging first-principle knowledge, these models provide a systematic understanding of complex processes, enabling predictions for untested operating conditions and process configurations. This facilitates efficient data-driven decision-making across industrial applications.

References

1. D. Pfister, L. Nicoud, M. Morbidelli, Continuous Biopharmaceutical Processes, Cambridge University Press, Cambridge, 2018
2. R.-M. Nicoud, Chromatographic processes, Cambridge University Press, Cambridge, 2015
3. Kilian Kobl et al., Org. Process Res. Dev. 2024, 28, 2569
4. R. D. Sproull, H. C. Lim, D. R. Schneider, *Biotechnol. Bioeng.*, 1976, 18, 633

Heterobimetallic catalysis: from molecules to dual-atom supported catalysts

Clément Camp*

[1] *Laboratory of Catalysis, Polymerization, Processes and Materials, CP2M UMR 5128, CNRS, Universite Claude Bernard Lyon 1, CPE Lyon, 43 Bd du 11 Novembre 1918, F-69616 Villeurbanne, France*

*clement.camp@univ-lyon1.fr

Introduction

One of the current frontiers in organometallic catalysis is to study the combined action of two metal centers to promote novel modes of reactivity, where the two metal centers act in synergy, in order to access a chemistry not possible with monometallic species. The association of late transition metal centers (eg. Ir, Os, Co, Au) with Lewis acidic metals (such as Al, Hf, Ta, Mo) is particularly interesting to create polarized metal-metal pairs presenting original electronic structures, and thus potentially novel reactivity. Recently, we have shown that these heterobimetallic complexes are able to activate carbon dioxide[1-3] as well as C-H bonds (Fig. 1b)[4-7] in a concerted way on both metal centers.

Materials and Methods

Protonolysis or salt-metathesis synthetic methodologies are developed to prepare, in solution, well-defined heterobimetallic complexes, featuring both metal centers at close proximity due to metal-metal bonding or bridging hydrides or alkyl moieties. Using a Surface OrganoMetallic Chemistry (SOMC) approach, these heterobimetallic complexes are used to prepare original heterogeneized catalysts featuring well-defined dual-atom active sites (Fig. 1a).[5,6] The SOMC methodology prevents undesired dimerization/agglomeration as seen in solution and therefore allows to access unique low-coordinate surface species not attainable in solution. The latter can be activated through hydrogen treatment under mild conditions.

Results and Discussion

These original supported M/M' (M = Hf, Ta, Mo ; M' = Ir, Co) species exhibit drastically enhanced catalytic performances in H/D exchange reactions with respect to (i) monometallic analogues as well as (ii) homogeneous systems (Fig. 1c). In particular, deuteration of $C(sp^2)$–H[5,7] and challenging $C(sp^3)$–H[6] bonds is achieved with excellent productivity under mild conditions without any additives. In this presentation we will describe our latest results in this area of research, in particular recent efforts to replace iridium by more sustainable metals.

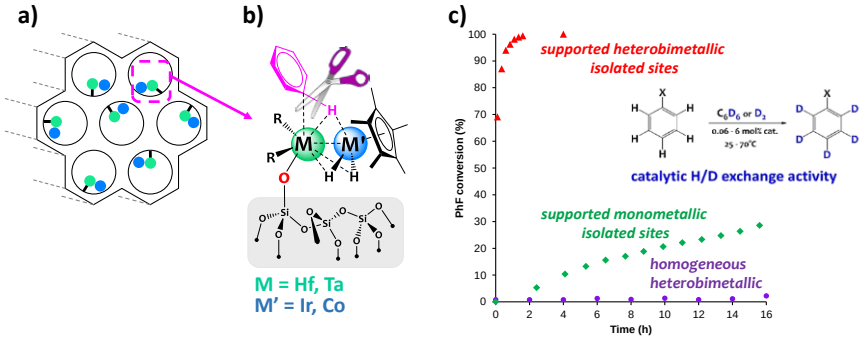

Figure 1. a) Schematic representation of dual-atom heterobimetallic active sites supported at the surface of a mesoporous silica; b) structure of the surface active species and concerted C-H activation mechanism across the two metals c) Conversion vs. time for three catalysts tested in the H/D exchange between fluorobenzene and D_2 or C_6D_6 as deuterium source (red triangle) supported heterobimetallic, (green diamond) supported monometallic, (purple circle) homogeneous heterobimetallic catalysts.

References

1. L. Escomel, I. Del Rosal, L. Maron, E. Jeanneau, L. Veyre, C. Thieuleux, C. Camp, *J. Am. Chem. Soc.* **2021**, *143*, 4844–4856.
2. A. Lachguar, I. Del Rosal, L. Maron, E. Jeanneau, L. Veyre, C. Thieuleux, C. Camp, *J. Am. Chem. Soc.* **2024**, *146*, 18306–18319.
3. A. Lachguar, C. Z. Ye, S. N. Kelly, E. Jeanneau, I. Del Rosal, L. Maron, L. Veyre, C. Thieuleux, J. Arnold, C. Camp, *Chem. Commun.* **2024**, *60*, 7878-7881.
4. A. Lachguar, A. V. Pichugov, T. Neumann, Z. Dubrawski, C. Camp, *Dalton Trans.* **2024**, *53*, 1393-1409.
5. S. Lassalle, R. Jabbour, P. Schiltz, P. Berruyer, T. Todorova, L. Veyre, D. Gajan, A. Lesage, T. Thieuleux, C. Camp, *J. Am. Chem. Soc.* **2019**, *141*, 19321–19335.
6. A. V. Pichugov, L. Escomel, S. Lassalle, J. Petit, R. Jabbour, D. Gajan, L. Veyre, E. Fonda, A. Lesage, C. Thieuleux, C. Camp, *Angew. Chem. Int. Ed.* **2024**, *136*, e202400992.
7. A. Lachguar, T. Neumann, A. V. Pichugov, E. Jeanneau, L. Veyre, C. Thieuleux, C. Camp, *Dalton Trans.* **2025**, advance article, https://doi.org/10.1039/D4DT03171G

From biomass to added-value chemicals and fuels: how tailored catalysts and reaction conditions shape the path

Agnieszka Ruppert *

Institute of General and Ecological Chemistry, Faculty of Chemistry, Lodz University of Technology ul. Zeromskiego 116 90-924 Łodz, Poland

*agnieszka.ruppert@p.lodz.pl.

Introduction

The valorization of versatile platform molecules such as hydroxymethylfurfural (HMF) derived from lignocellulosic biomass is considered a highly valuable way to obtain high value-added chemicals and fuels. Among them, 2,5-dimethylfuran (DMF) and 2,5-dimethyltetrahydrofuran (DMTHF) are pivotal molecules of high value, with applications as biofuels or biofuel additives. Additionally, both ring reduction products like 2,5-bis(hydroxymethyl) tetrahydrofuran (BHMTHF) or ring opening products like 1-Hydroxyhexane-2,5-dione (HHD) can be favorably applied as high-prospect biofuel or bio-polymer precursor (scheme 1).

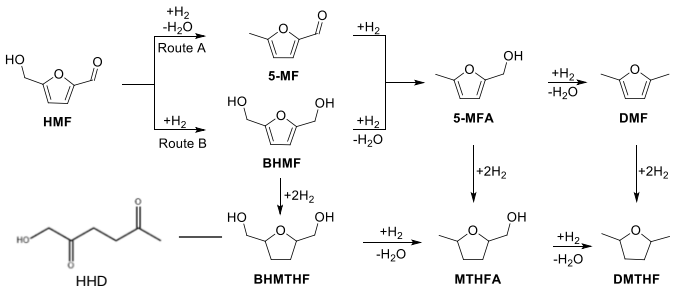

Scheme 1. Hydrogenation of HMF towards chosen platform molecules.

Materials and Methods

Both noble metal and non-noble metal-based catalysts (e.g. Ru, Ni) were studied, and various preparation methodologies will be discussed, highlighting their role in obtaining either ultra-small, uniform nanometer-sized particles or larger particles. The role of active sites will be evaluated by discussing the results of surface and bulk techniques including HRTEM, ToF-SIMS, XPS, XRD, TPR, CO-FTIR. The catalysts were tested in the liquid phase HMF hydrodeoxygenation under a broad range of reaction conditions and in various solvents.

Results and Discussion

We identified several key-factors with a strong influence on the reaction course. Firstly, by changing the solvent nature, we can tune the reaction pathway of HMF hydrogenation towards ring reduction like BHMTHF (in a 100% 1,4-dioxane solvent) or towards ring opening products like HHD (in a 100% water solvent). Additional tuning can be achieved by adjusting the reaction temperature or the hydrogen pressure. For example, lower temperatures and high pressure favor high yields to BHMF, BHMTHF and HHD, whereas higher temperatures and low pressure change the reaction pathway, leading to a high DMF yield. In all cases the yield to those products can be further significantly boosted by modifying the properties of the catalysts.

There are however several challenges associated with the design of sustainable and efficient processes for the catalytic conversion of biomass. In particular, challenges associated to the catalyst design, including notably the development and application of more robust non-noble metal-based catalysts and of more active catalysts operating under milder reaction conditions. To address such challenges, various new strategies have been developed and rely on the synthesis of fine-tuned nanomaterials. Among them, a particularly interesting approach involves the use of solar light to precisely control the formation of supported nanoparticles [1-2]. Secondly the influence of the process conditions is being investigated as a mean to orientate the selectivity of the reaction.

These challenges will be discussed, with a primary focus on the understanding of the relationship between the catalytic activity and the bulk and surface physico-chemical properties of the catalysts. This understanding is a key-step toward developing more sustainable processes for converting biomass-derived substrates into platform molecules.

Significance

Key factors allowing high reaction performances with limited over-hydrogenation products have been identified. Both the importance of optimal reaction conditions and the role of active sites will be discussed in the synthesis of added value molecules with high yield.

Acknowledgement

The authors gratefully acknowledge the National Center of Science (NCN) Krakow, Poland, grant OPUS-LAP (2020/39/I/ST4/02039) for financially support.

References

1. P. Kashyap, M. Jędrzejczyk, M. Akhgar, N. Keller, A.M. Ruppert, *ChemCatChem* **2025,** 17(2), e202401433
2. A.M Ruppert, M. Brzezińska, N. Keller, *Catalysis Today*, **2024,** 433, 114651
3. M. Przydacz, M. Jędrzejczyk, J. Rogowski, D. Ihiawakrim, N.Keller, A.M.Ruppert, *Fuel*, **2024**, 356, 129606

OC1: DRM, MTO, WGS

On the role of Cu (II) insertion in $LaFeO_3$ for H_2 production in Chemical Looping Dry Reforming of CH_4 (CL-DRM)

Ganesh JABOTRA[1,2], Amanda Sfeir[1], Lorenzo Stievano[4], Axel Löfberg[1], Sébastien Royer[1,3], Sudhanshu Sharma[2], Jean-Philippe Dacquin[1]

[1] *Unité de Catalyse et Chimie du Solide, UMR 8181, Université de Lille, CNRS, Centrale Lille, ENSCL, Université d'Artois, F-59000 Lille, France*

[2] *Indian Institute of Technology Gandhinagar (IITGN), Gujarat, 382355, Palaj, India*

[3] *Université Littoral Côte d'Opale, UR 4492, UCEIV, Unité de Chimie Environnementale et Interactions sur le Vivant, Dunkerque, F-59140 France*

[4] *Institut Charles Gerhardt Montpellier (ICGM), Univ. Montpellier, CNRS, ENSCM, Montpellier, France*

*Corresponding author email: ganesh.jabotra@univ-lille.fr

Introduction: CL-DRM offers a promising alternative to address the thermodynamic limitations associated with conventional catalytic dry reforming of methane (DRM)[1]. In this cyclic process, the reforming reaction (CH_4 conversion into CO and H_2) occurs over an oxygen carrier. This reaction operates separately from the further reoxidation of the oxygen carrier, using CO_2 in our study. As illustrated in Figure 1, the two-step reaction allows for obtaining pure products, overcoming thermodynamic limitations associated with conventional DRM[2]. Another advantage of CL over conventional reforming is that deposited carbon (deactivating catalyst) can be eliminated during the reoxidation step[1]. Our objective here is to show how an ideal H_2/CO ratio of 2, adapted to Fischer-Tropsch synthesis, can be obtained using CL-DRM using simple Fe-Cu-based perovskite composition while mitigating the carbon accumulation in the oxygen carrier (the active solid/catalyst). $LaFeO_3$ is first selected thanks to favorable thermodynamic properties for CL-DRM[2].

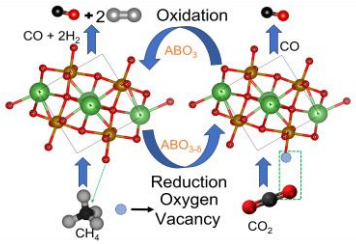

Figure 1 Schematic illustration of CL-DRM

Materials and Methods: Catalyst synthesis is done using a complexation method, using citric acid as a complexing agent. Material characterization includes XRD, N_2 physisorption, XPS, Raman spectroscopy, SEM, HRTEM-HAADF-EELS, Mössbauer and EPR spectroscopies. The reducibility of perovskites is evaluated by using H_2-TPR (usual) and CH_4-TPR (to evaluate surface reactivity toward CL-DRM reductant). Subsequently, oxygen carrier performances are evaluated in a fixed-bed reactor configured for the chemical looping dry reforming of CH_4 (CL-DRM), functioning in a dynamic regime.

Results and Discussion: XRD confirms phase purity, while Raman spectroscopy, Figure 2(b), indicates reduced Fe-O bond strength when Cu partially substitutes Fe in the structure (shift to the lower wavenumber of Fe-O stretching band), suggesting enhanced lattice oxygen mobility[3]. HAADF and EDS images, Figure 2(c-d), confirm the materials' high crystallinity and elemental uniformity. Table 1 provides H_2/CH_4 consumptions during TPR tests and copper reducibility quantification. Mössbauer analysis evidenced an isomer shift between (0.35-0.44) consistent with Fe^{3+} in a high-spin[3]. The increase in O_{ads}/O_L ratio obtained from O 1s XPS signals suggests the presence of oxygen vacancies in doped samples[3]. All trends are in favour of higher lattice oxygen mobility for Cu-perovskites.

Table 1 Chemical states and redox properties of $LaFe_{1-x}Cu_xO_3$

Sample	H_2-TPR		CH_4-TPR	O_2-TPD	Mössbauer	XPS
	H_2-uptake (mmol/g)	Degree of reducibility (%)	CH_4 uptake (mmol/g)	O_2 desorbed (µmol/g)	IS (mms^{-1})	(O_{ads}/O_L)
X = 0	-	-	214.97	-	0.37(1)	1.18
X = 0.05	0.18	87.5	70.36	-	0.35(7)/0.38(7)	1.21
X = 0.1	0.33	80.4	70.54	0.14	0.44(2)	1.04
X = 0.15	0.53	86.2	69.30	0.26	0.36(1)/0.35(1)	1.44

*O_L = Lattice oxygen, O_{ads} = Surface adsorbed oxygen species, IS = Isomer Shift

CL-DRM test is conducted over 10 cycles at 900°C, with CH_4 and CO_2 exposure times set to 2 min, followed by a 1 min argon purge between oxidant and reductant steps. Product gases are quantified at each step. $LaFeO_3$ (Figure 3(a)) achieves excellent CH_4 conversion (75%) during the reduction step, although it exhibits an H_2/CO ratio of 2.5> 2 and significant carbon deposition (70% of carbon balance, Figure 3(c)). The H_2/CO ratio in doped samples aligns with the ideal value of 2 (Figure 3(b)). Among these, $LaFe_{0.85}Cu_{0.15}O_3$ shows the highest CH_4 conversion (~50%) and 90% carbon balance. Thus, Cu substitution in $LaFeO_3$ reduces CH_4 conversion, reduces coke deposition and achieves the ideal H_2/CO ratio of 2. In the oxidant step, $LaFeO_3$ displays the highest CO_2 conversion (Figure 3(d)), consistent with its more significant carbon deposition, which is removed via $CO_2(g) + C(s) \rightarrow 2CO(g)$ reverse Boudouard reaction. Very promisingly, no deactivation occurs during the 10 cycles (on the contrary, Cu-containing formulations progressively activated), demonstrating a complete C(s) gasification at the oxidation step at 900°C.

Significance: Enhanced oxygen mobility via Cu (II) insertion enables low coke deposition and high-quality syngas (H_2/CO = 2), ideal for methanol, Fischer-Tropsch synthesis and H_2 production, emphasizing the industrial significance of our work.

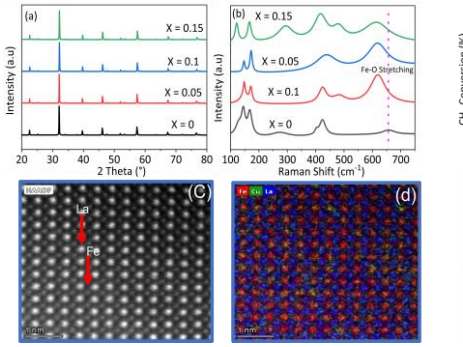

Figure 2 (a) XRD (b) Raman (c-d) STEM-EDS of $LaFe_{1-x}Cu_xO_3$

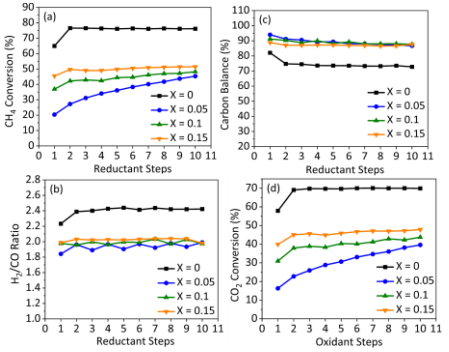

Figure 3 CL-DRM test

References: 1. Löfberg et al, *Appl Catal B*, 2017, **212**, 159–174

2. Dai et al, J. Phys. Chem. B 2006, **110**, 22525–22531

3. Rao et al, J. Chem. Eng, 2022, **435**, 13488

Fundamental insights into a highly efficient $GaZrO_x$/SAPO-34 bifunctional catalyst for the methanol-mediated syngas to light olefins conversion

Antoine Salichon[1,*], Ruben Checa[1], Pavel Afanasiev[1], Stéphane Loridant[1]
[1]*Université Claude Bernard Lyon 1, CNRS, IRCELYON, UMR 5256, Villeurbanne, F-69100, France*
**antoine.salichon@ircelyon.univ-lyon1.fr*

Introduction

Light olefins ($C_2^=$-$C_4^=$) are key chemicals in the polymer industry. Such compounds are currently mainly synthetized by cracking of hydrocarbons. A sustainable alternative could be the use of syngas (CO+H_2). An original bifunctional OX/ZEO catalyst composed of a hydrogenating oxide and an acidic zeotype was discovered to both hydrogenate CO to methanol and transform the latter to light olefins with a high yield.[1] However, the selectivity at high conversion of OX/ZEO process needs to be improved.[2] Recently, a $GaZrO_x$ solid solution showed superior performance in combination with SAPO-34 zeolite.[3] However, to understand the precise reaction mechanism occurring on such material, a fundamental study is necessary.

Materials and Methods

GaZr mixed oxides were synthetized by co-precipitation method. Other Ga-based catalysts including α, β and γ Ga_2O_3 polymorphs and a zirconia supported Ga_2O_3 (Ga/m-ZrO_2)catalyst were prepared by controlled precipitation, and incipient wetness impregnation, respectively, followed by thermal treatments. SAPO-34 zeotypes with modulated acidity (i.e. Si/Al ratio) were prepared hydrothermally. OX/ZEO bifunctional catalysts were tested in a fixed bed reactor from 1 to 25 bar, from 300 to 475 °C and under a H_2/CO/N_2=60/30/10 feed. Products analysis was performed using a microGC equipped with a TCD detector. Structural, textural, redox, and acidic properties were determined before and after reaction by crossing numerous techniques including XRD, TEM, N_2 adsorption-desorption isotherms and NH_3-TPD. Surface species formed on $GaZrO_x$ under CO and/or H_2 were thoroughly studied by H_2-TPD and *in situ*/*operando* DRIFTS and XPS.

Results and Discussion

$GaZr_{5.0}O_{11.5}$ solid solution proves to be a highly effective catalyst for the conversion of syngas to light olefins through methanol intermediate. In mechanical mixture with a moderately acidic SAPO-34 zeotype, it led to CO conversion up to ca. 61% and ca. 76% light olefins selectivity (among hydrocarbons), after optimization of various parameters including temperature, pressure, contact time and OX/ZEO mass balance. Interestingly, similar performance was obtained with Ga/m-ZrO_2 catalyst (Figure 1a.) suggesting that Ga incorporation into the ZrO_2 lattice is not mandatory to reach high conversion and selectivity. However, the Ga mass content noticeably influences the $C_2^=C_4^=$ selectivity. Indeed, during ethylene hydrogenation probe reaction testing, a $GaZr_{5.6}$ oxide led to a low C_2H_4 conversion to ethane of 6.5% whereas it was at least 40% for α, β and γ Ga_2O_3 polymorphs. Such elevated values were also found for $ZnZrO_x$ and Cu-ZnO-Al_2O_3 which are also highly active for the synthesis of methanol. $GaZrO_x$ material thus provides an optimal combination of activity and selectivity in the conversion of syngas to light olefins. To gain insights on the high performance of the mixed oxide, H_2-TPD tests were carried out. A pretreatment under He led to a single desorption peak at ca. 520 °C (attributed to strongly-bonded H-species) while a prior reduction under H_2 was responsible of weakly-bonded H-species generation. These surface intermediates have been identified as Ga-H hydrides and could be formed in an homolytic fashion on Ga_{oct}-V_o-Ga_{oct} sites, thus boosting their amount and reactivity during hydrogenation reactions.[4] Such species were detected under H_2 and CO/H_2 atmospheres by DRIFTS (band at ca. 1985 cm^{-1}).[4] The highly reactive Ga-H species were found to readily hydrogenate HCOO*, which was formed by reaction between CO and remarkably labile surface OH groups, to CH_3O* intermediate (2823, 2931 cm^{-1}) (Figure 1.b), further desorbed as methanol and converted to $C_2^=$-$C_4^=$ species (broad band in 1000-1300 cm^{-1} region at T=300 °C) on the acidic sites of the zeotype, leading to high performance. Concomitantly, water production was evidenced under H_2 by MS suggesting oxygen vacancies formation on the GaZr oxide. Such sites could play a significant role during H_2O dissociative adsorption leading to OH groups regeneration, as well as promoting CO activation and the alleged H_2 homolytic dissociation pathway. Oxygen vacancies located in the neighbourhood of Ga-H hydrides and surface hydroxyls should thus favour the CO hydrogenation to methanol.

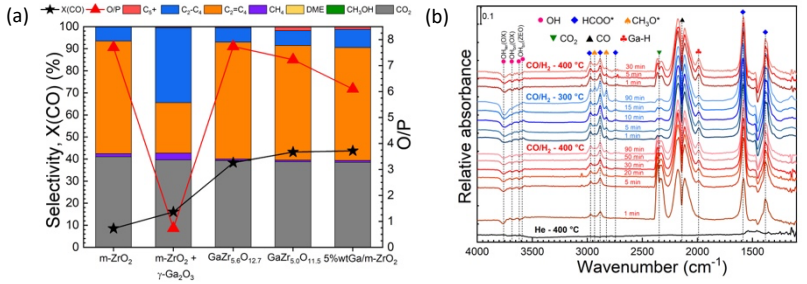

Figure 1. (a) X(CO) conversion, selectivity values and O/P (Olefin/Parrafin) ratio measured during reaction of various catalysts in combination with SAPO-34 (OX/ZEO=70/30wt%) at T=400 °C and P=25 bar and (b) *in situ* DRIFT spectra recorded on $GaZr_{5.0}O_{11.5}$/SAPO-34 (70/30 wt%) bifunctional catalyst under a H_2/CO/He (60/30/10) flow at T=300-400 °C.

Significance

In addition to confirm the high performance of GaZr oxide combined with SAPO-34 for the methanol-mediated syngas to light olefins conversion, this work demonstrates the key role of surface hydroxyl and hydride species, and underlines the probable role of neighboring oxygen vacancies. *Operando* NAP-XPS, ^{69}Ga NMR and ESR experiments are expected to provide further understanding on the electronic and surface structure of $GaZrO_x$ material during carbon monoxide hydrogenation to methanol and thus provide new fundamental insights.

References

1. K. Cheng, B. Gu, X. Liu, J. Kang, Q. Zhang, Y. Wang, *Angew. Chem. Int. Ed.* **2016**, *55*, 4725
2. A. Salichon, P. Afanasiev, S. Loridant, *ACS Catal.* **2024**, *14*, 243
3. F. Meng, P. Zhang, L. Ma, G. Yang, R. Zhang, B. Wang, Y. Hu, Z. Li, *Chem. Eng. J.* **2023**, 467
4. C. Yang, S. Ma, Y. Liu, L. Wang, D. Yuan, W-P Shao, L. Zhang, F. Yang, T. Lin T, H. Ding, H. He, Z-P. Liu, Y. Cao, Y. Zhu, X. Bao, *Nat Commun.* **2024**, *15(540)*

Co-immobilization of polyoxometalates and organic cations onto (mesoporous) silica for supported oxidative carboxylation of alkenes

Jingjing REN,[1] Richard VILLANNEAU[1]*
[1] *Institut Parisien de Chimie Moléculaire, Sorbonne Université, 75005 Paris, France*
*richard.villanneau@sorbonne-universite.fr

Introduction

Cyclic carbonates are key compounds with a large scope of applications, such as plastics (including polycarbonates) or solvents in paints and batteries.[1] However, their industrial production still uses extremely toxic C(IV) sources such as phosgene and gives rise to HCl.[2] At the same time, CO_2 is the most abundant greenhouse gas in the atmosphere[3] and its mitigation remains one of the greatest environmental challenges of our time. Using this widely available, cheap and non-toxic resource as a carbonaceous feedstock in Carbon Capture and Utilization processes looks like an exciting opportunity.[4] In this context, the one-pot synthesis of cyclic carbonates from alkenes, using an oxidant and CO_2 is of obvious interest. This strategy, referred as oxidative carboxylation cascade reaction, requires the successive use of oxidation (OxCat) and CO_2 cycloaddition catalysts (CyCat).[5] Of all OxCat and CyCat catalysts described so far, we recently showed that first-row transition metal-substituted polyoxometalates $[PW_{11}O_{39}M(H_2O)]^{n-}$ (TMS-POMs; M = Cr, Mn, Fe, Co, Ni, Zn) proved effective for each individual step,[6] ideally leading to auto-tandem catalysis processes. The aim of this work is i) to present the results of the individual steps with TMS-POMs, ii) to show the optimization of the experimental conditions for improving the one-pot reaction and iii) to show that immobilizing TMS-POMs onto alkylammonium-functionalized mesoporous silica improve the global efficiency of the process. Remarkably, this reaction was studied in the absence of halides, leading to milder reaction conditions of temperature or pressure.

Materials and Methods

All TMS-POMs catalysts were characterized by ATR-IR, multinuclear NMR, Raman and UV-visible spectroscopies. Supported TMS-POMs catalysts were characterized by thermogravimetric analyses (TGA/DSC), UV-visible and Raman spectroscopies, HR-TEM, X-EDS and X-Ray diffraction. The specific surface areas were evaluated using the Brunauer–Emmett–Teller (BET) method. Pore size distribution curves were calculated from the N_2 isotherms using the Barrett–Joyner–Halenda (BJH) method. All catalysis results were obtained by ^{1}H NMR and GC-MS. For the catalytic experiments in homogeneous conditions: NR_4^+ salts of TMS-POMs used as Cy-Cat catalyst (0.1 mmol) were dissolved in a mixture of 0.7 mL of benzonitrile and 12.2 mmol of epoxide in an autoclave. The final P(CO_2) was fixed at the desired pressure at room temperature then set at the desired temperature (usually 30 to 120°C). For the oxidation experiments using H_2O_2, NR_4^+ salt of TMS-POMs used as OxCat catalyst (0.024 mmol) was dissolved in a mixture of 0.6 mL of aqueous hydrogen peroxide (H_2O_2, 6 mmol), alkene (6 mmol) and 13 mL of solvents (PhCN or CH_3CN).

Results and Discussion

In this study, we have shown that TMS-POMs were efficient homogeneous catalysts for the formation of cyclic carbonate from epoxides, even in the absence of Lewis bases such as halides, which are incompatible with oxidation processes involving H_2O_2. In particular, the epoxide conversion as well as the corresponding carbonate selectivity were quantitative at relatively low temperature (80°C) and CO_2 pressure using $NR4^+$ salts of $[PW_{11}O_{39}M^{II}(H_2O)]^{5-}$ (with M = Co, Ni, Zn). In addition, DFT calculations have suggested that an unexpected carbonic anhydrase-like mechanism occurred in the absence of halides. In the case of oxidation experiments, the same $[PW_{11}O_{39}M^{II}(H_2O)]^{5-}$ (with M = Co, Ni, Zn) complexes were used as OxCat either in the presence of H_2O_2 with moderate yield or in the presence of O_2 with a complete conversion of the alkene using a Mukaiyama-type process. In the whole sequence of reactions, we have also found that the catalytic efficiency was also increased by using quaternary ammonium counter-ion with long chains. While this behavior was known in the case of CyCat (see fig. 1 left), this was a more unexpected result for epoxidation reactions. This trend was also confirmed after immobilization of the catalysts on mesoporous silica. The catalytic materials with the highest turnover frequency were obtained using both NR_4^+ cations from TMS-POMs and alkylammonium grafted onto silicas with the longest chains (fig.1 right).

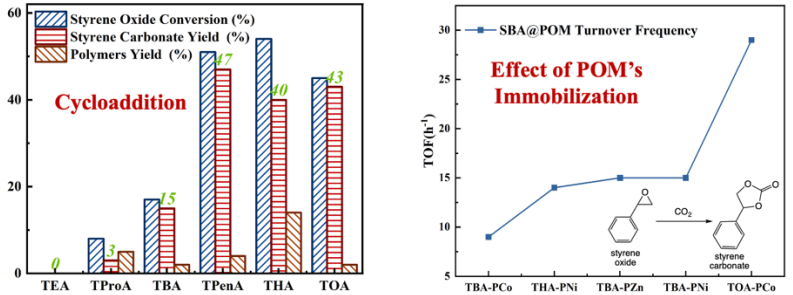

Figure 1. CO_2 cycloaddition on styrene oxide with $[PW_{11}O_{39}Co(H_2O)]^{5-}$ in homogeneous conditions (left) and supported onto SBA-$CH_2CH_2CH_2NMe_3Cl$ (right) as a function of chain length of the NR_4^+ counter-ion.

Significance

This work is of interest to the broad community of molecular chemists, in the field of both homogeneous catalysis and coordination chemistry, since it provides clues to a better understanding of an important multiparameter reaction such as the alkenes oxidative carboxylation, which combines the use of green oxidants (O_2 or H_2O_2) and activation of CO_2.

References

1. A. J. Kamphuis, F. Picchioni, P. P. Pescarmona, *Green. Chem.* **2019,** *21*, 406.
2. S. Fujita, M. Arai, B.M. Bhanage, Direct Transformation of Carbon Dioxide to Value-Added Products over Heterogeneous Catalysts, in: B.M. Bhanage, M. Arai (Eds.), Transform. Util. Carbon Dioxide, Springer Berlin Heidelberg, 2014, pp. 39–5.
3. EPA. U.S. Environmental Protection Agency. Overview of Greenhouse Gases, (24/02/23).
4. M. Aresta, A. Dibenedetto, A. Angelini, *J. CO2 Util.* **2013**, *3-4*, 65; A.W. Kleij, M. North, A. Urakawa, *Chemsuschem* **2017**, *10*, 1036; M. Aresta, *Coord. Chem. Rev*. **2017**, *334,* 150. d) C. Chauvier, T. Cantat, *ACS Catal*. **2017**, *7*, 2107.
5. X.D. Lang, L.N. He, *Chem. Rec.* **2016**, *16*, 1337; L. Wang, S. Que, Z. Ding, E. Vessally, RSC Adv. 10 (2020) 9103; M. Balas, R. Villanneau, F. Launay, *J. CO2 Util*, **2022**, *65*, 102215.
6. J. Ren, A. Proust, F. Launay, R. Villanneau, *Chem. Commun*. **2024**, *60*, 4549.

Higher alcohols synthesis from syngas over sulfide-based catalysts

Antoine Le Ray[1], Ana T. F. Batista[2], Pascal Raybaud[2], Christophe Geantet[1], Pavel Afanasiev[1*]
[1]*Institut de Recherches sur la Catalyses et l'Environnement de Lyon (IRCELYON, Université Claude Bernard Lyon 1, 69626 Villeurbanne, France)*
[2]*IFP Energies nouvelles, Rond-point de l'échangeur de Solaize, BP 3, 69360 Solaize, France*
*pavel.afanasiev@ircelyon.univ-lyon1.fr

Introduction

Higher alcohols can be defined as alcohols with two or more carbons in their chain. Currently, alcohols such as ethanol and isobutanol are already used as additives in gasoline. They offer a promising way to reduce the carbon footprint of fuel, especially when they are produced from renewable biomass feedstocks. Higher alcohol synthesis (HAS) can be achieved through the conversion of syngas, a reaction that is gaining interest due to the possibility of using syngas produced from biomass gasification. However, traces of a few ppm of contaminants such as H_2S or NH_3 are often reported in these feedstocks. These contaminants could be problematic for the use of catalytic active phases sensitive to them. Hence, among the different HAS catalysts, molybdenum disulfide (MoS_2) based catalysts are naturally sulfur and nitrogen resistant which make them valuable compared to others. To improve HAS activity, MoS_2 are usually promoted with alkali metals[1], doped with VIII metals[2] and supported over an appropriate carrier such as basic metal oxides or carbon[3]. However, many challenging open questions related to the precise role of the promoters as well as to the improvement of their activity and selectivity remain and are addressed in the present work.

Materials and Methods

A series of supported catalysts were synthesized and tested, including MoS_2/C, K_2-MoS_2/C, K_2-($Co_{0.5}$)MoS_2/C, Cs_2-MoS_2/C and Cs_2-($Co_{0.5}$)MoS_2/C. One-step and two-step preparations were carried out : either alkali metal (K or Cs) and cobalt were introduced as oxide precursors (K_2MoO_4, Co nitrate) simultaneously with molybdenum; or they were added onto the pre-sulfided MoS_2/C, respectively. The solids were dried and sulfurized under H_2S/H_2 flow (1:5) for 4h at 400°C. Structural, textural and acidic properties were determined by XRD, TEM, N_2 adsorption-desorption isotherms, H_2 TPR, ICP-OES, NH_3 and CO_2 TPD, XPS, DRIFTS, and Raman spectroscopy. Catalytic tests were conducted in a fixed-bed reactor at temperatures from 260 to 360°C, H_2/CO molar ratios from 1 to 7, feed rates from 400 to 2000 ml.g_{cat}^{-1}.h^{-1} and at 50 bar pressure. Product analysis was performed by online micro-GC equipped with TCD detector.

Results and Discussion

Among the catalysts investigated, alkali-promoted MoS_2 doped with cobalt exhibited the highest activity in higher alcohol synthesis. Increasing temperature and H_2/CO ratio led to an increase in the CO conversion but were detrimental to the higher alcohols selectivity at the profit of hydrocarbons and CO_2 (figure 1.a, 1.b). The highest C_{2+}OH selectivity of 55% was obtained with the $K_2Co_{0.5}MoS_2$/C catalyst at a CO conversion of 7.3% under the conditions of T=300°C, P=50 bar, GHSV=2000ml.g_{cat}^{-1}.h^{-1} and a H_2/CO ratio of 1. $Cs_2Co_{0.5}MoS_2$/C demonstrated remarkable performance with the increase of H_2/CO ratio, reaching a C_{2+}OH selectivity of 24.9% at a CO conversion of 44% enabling the highest yield (10.9%) at T=300°C, P=50bar, GHSV=1160ml.g_{cat}^{-1}.h^{-1} and at H_2/CO=7.

All catalysts exhibited a long activation period (superior to 20 h) during which the catalytic activity is presumably significantly modified. This period might be attributed to the spreading of the alkali metals at various positions over the catalyst (on the support or on the active phase). However, further analysis of this phenomenon is needed. Therefore, the role of the alkali metals will be analyzed in the future using operando investigations of the evolution of active metal species (XAS, Raman) and DFT simulations to better understand the role of the alkali metal on reaction pathways.

Moreover, we plan to explore the effect of alternative sulfide phases and supports to improve C_{2+}OH selectivity.

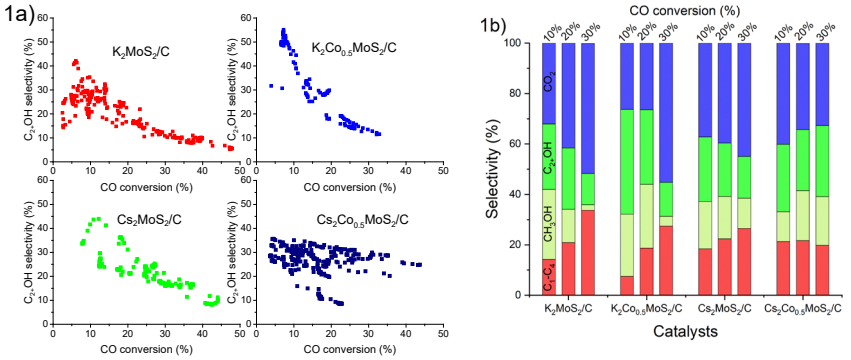

Figure 1. (a) C_{2+}OH selectivity obtained with molybdenum sulfide catalyst promoted with alkali metals and doped with cobalt over carbon support as a function of the CO conversion for various temperatures and GHSV. (b) Selectivities obtained for different catalysts at three levels of CO conversion (10%, 20%, and 30%).

Significance

This work advances current knowledge on the state and location of the alkali promoters in (Co)MoS_2 based HAS catalyst during activation and reaction their impact on catalytic performance, in particular C_{2+}OH selectivity

References

1. F. Zeng, Appl. Catal. B: Env. **2019**, 246, 232
2. X. Xi, Appl. Catal. B: Env. **2020**, *272*, 118950
3. M.E. Osman, ACS omega, **2022**, 7, 21346

Water-Gas-Shift WGS reaction mechanisms over SiO_2 and TiO_2 supported MoS_2 catalysts

S. Nouma[1]*, X.Portier[1], L. Oliviero [2]

[1] *CIMAP, Université de Caen Normandie, CEA, ENSICAEN, CNRS, Normandie Univ, 14000 Caen, France*

[2] *LCS, Université de Caen Normandie, ENSICAEN, CNRS, Normandie Univ, 14000 Caen, France*

** saloua.nouma@ensicaen.fr*

Introduction

As hydrodesulfurization (HDS) reaction, the water gas shift (WGS) activity of the nanolayered MoS_2 catalysts is correlated with the number of coordinatively unsaturated sites located along the slab edges. However, the reaction mechanisms over each type of edge sites and the role of support sites is not totally known yet .[1, 2]

Indeed, based on several studies, the favorable pathways of the WGS on MoS_2 catalysts were much more complicated than a pure redox mechanism. From a recent work in our LCS group, an associative mechanism based on COOH dissociation into CO_2 and H has been suggested for M-edge and a novel one based on COS hydrolysis for S-edge sites; CO + MoS_2 → MoS* + COS *(1)*, COS + H_2O → CO_2 + H_2S *(2)* and H_2S + MoS* → MoS_2 + H_2 *(3)*. [3] These results were obtained on MoS_2 catalysts supported on Al_2O_3 that present both kind of sites and were prepared with chelating agent which complexify the catalyst behavior. Thus**,** we aim in this work to complete the mechanism study on TiO_2 and SiO_2 supports leading to MoS_2 slabs exposing different types of edges in absence of chelating agent: only M-edge sites for TiO_2 and both M- and S- edge sites for SiO_2. Then, we perform IR characterization via CO adsorption and IR operando study of the WGS activity of MoS_2 on TiO_2 and SiO_2 supports. The variation of exposed active sites changes the catalyst activity and stability as well as the reaction mechanism**.**

Materials and Methods

The catalysts supported on SiO_2 (506 m^2/g, Merck) or TiO_2 (anatase/rutile mixture, 65 m^2/g, Degussa) were prepared by wetness impregnation method (3 at.Mo/nm^2) and sulfided in-situ in the IR cell or catalytic reactor at 350°C/2h. Low-temperature CO adsorption followed by IR spectroscopy is used to quantify M- and S- edge sites concentration. Activity in WGS at 300°C and atmospheric pressure was measured in a glass reactor by evaluating the CO conversion. The reaction mechanisms have been revealed by Operando IR experiments in a specific cell called 'Sandwich cell'.

Results and Discussion

Activity tests in WGS show that CO conversion is higher in the case of MoS_2/TiO_2 at the very beginning in accordance with the greater number of edge sites compared with the SiO_2 support. Then, deactivation occurs for both catalysts (Fig 1.A, B) but more marked and continuous over time on TiO_2. In this latter case, it can be explained by the low stability of M-edge sites upon reaction flow. Indeed, IR study shows that these sites that are the only ones exposed on TiO_2, undergo a S-O exchange with H_2O that hinders further CO adsorption (Table 1). On SiO_2, the additional presence of S edge sites explains the higher activity and stability after the initial deactivation, they aren't affected by H_2O.Furthermore, these S-edge sites interact with CO at 300°C and create S vacancies which agrees with the COS mechanism on these sites (Table 1). Accordingly, COS has been only detected during WGS test over MoS_2/SiO_2 (Fig 1.C), its formation being more pronounced at the beginning of reaction. Both the COS profile and the deactivation on SiO_2 can be ascribed to a loss of S during the reaction meaning that the catalytic cycle is not complete. The observation of continuous consumption of H_2O and production of CO_2 is a sign that some COS is indeed hydrolyzed (step 2 of the COS Redox mechanism) so step 3 should be the missing one.

Table 1. Edge sites concentration obtained by CO adsorption: Effect of H_2O and CO treatments at 300°C.

		Edge sites concentration (µmol/g)		
Catalyst	Sites nature	Sulfidation at 350°C	H_2O treatment at 300°C	CO treatment at 300°C
MoS_2/SiO_2	M-edge	26	15 (- 42%)	15
	S-edge	14	14	20 (+ 30%)
MoS_2/TiO_2	M-edge	81	1 (- 98%)	27 (+ 32%)
	S-edge	2	2	2

Accordingly, the quantification of the H_2 produced shows that there is a gap between CO conversion and H_2 production (Fig 1.D). Then the S loss can be limited by working under continuous H_2S flow; this is underlined by the improved catalytic activity and the long-term stability (Fig 1.A'). For TiO_2, introduction of H_2S in the feed, doesn't change the initial activity but decreases the deactivation on the long term that can be explained by a limitation of the S/O exchange. (Fig 1.B'). Finally, the operando tests show no formate species on the catalyst surface for MoS_2/SiO_2 contrary to MoS_2/TiO_2 (fig 1.E) on which bicarbonate (green lines) and formate (orange lines) species have been detected. The absence of COS formation on MoS_2/TiO_2 is confirmed by flowing CO alone in the cell at reaction temperature. However, in this case formation of H_2 is observed in accordance with the contribution of surface OH (not showed).

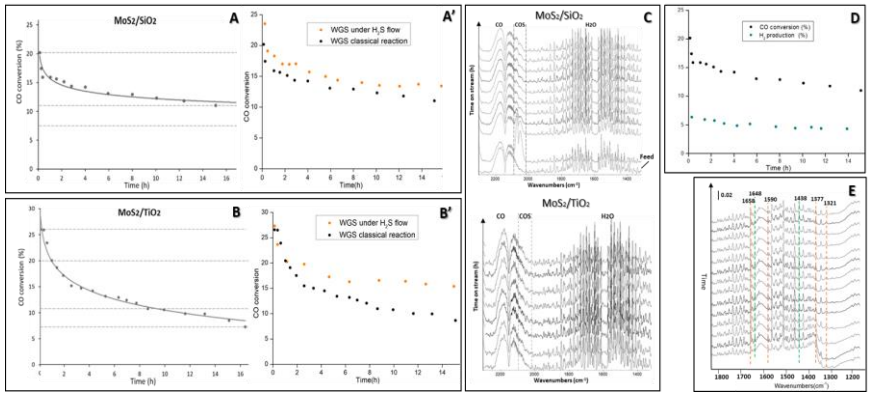

Figure 1. A/B, CO conversion vs. time over MoS_2 catalysts. C, IR spectra of phase-gas during WGS. D, CO conversion and H_2 production for MoS_2/SiO_2.E, IR spectra (operando test) of the MoS_2-TiO_2 catalyst surface during the WGS reaction.

The obtained results agree with the only occurrence of the COS redox mechanism on MoS_2/SiO_2 catalyst. In addition, the accumulation and reactivity of formate species on MoS_2/TiO_2 catalyst surface during reaction confirm this associative WGS pathway on M-edge sites.

Significance

WGS is a very interesting reaction that enables hydrogen to be produced from both renewable biomass and fossil resources. Our interest to Mo based sulfide catalysts is due to its excellent tolerance to S suited to the properties of biomass in contrary to usual WGS catalysts that rapidly deactivate after contact with sulfur-containing compounds. The understanding of the WGS reaction mechanisms is a key factor to optimize H_2 production over these catalysts.

References

1. L. Oliviero, A. Travert, E.Dominguez Garcia, J. Chen, F.Maugé, J. Catal. **2021**, 403, 87–97.
2. S. Yun, V. V. Guliants, *Energy Fuels.* **2019**, *33* (11), 11655–11662.
3. W.Zhao, F. Maugé, J. Chen, L. Oliviero, *J. Chem. Eng.* **2023**, *455*, 140575.

OC2: VOC, DeNOx, aromatics

The role of Cu/Mn ratio in mixed oxides for total oxidation of air pollutants

Julien Machinski[1], Eric Genty[1], Charf Eddine Bounoukta[1], Christophe Poupin[1], Valeria La Parola[2], Stéphane Siffert[1], Elise Berrier[3], Leonarda Francesca Liotta[2], Renaud Cousin[1]*

[1]*Unité de Chimie Environnementale et Interactions sur le Vivant (UCEiV), Université du Littoral Côte d'Opale (ULCO), Dunkerque, 59140, France*
[2]*Institute for the Study of Nanostructured Materials (ISMN)-CNR, Via Ugo La Malfa, 153, Palermo, 90146, Italy*
[3]*Unité de Catalyse et Chimie du Solide (UCCS), UMR 8181, Université de Lille, CNRS, Centrale Lille, Université Artois, Lille, 59000, France*
*renaud.cousin@univ-littoral.fr

Introduction

The global shift towards renewable energy sources is reshaping the landscape of energy production, with biomass playing a pivotal role in this transition [1]. As a renewable and versatile fuel, biomass is increasingly favored; however, its combustion releases various pollutants, including carbon monoxide (CO), Volatile Organic Compounds (VOCs), Polycyclic Aromatic Hydrocarbons (PAHs), and soot particles [2]. These emissions pose significant environmental and health risks, underscoring the urgent need for effective remediation strategies. Transition metal oxides present a cost-effective and efficient alternative to noble metal catalysts traditionally used for oxidation processes. Copper and manganese oxides are particularly promising due to their high activity for CO and VOC total oxidation at relatively low temperatures [3-4]. Among the synthesis techniques, oxalate co-precipitation offers a robust approach to produce mixed-metal oxide materials. This method not only enables co-precipitation of multiple metals into a single oxalate matrix but also results small particle and crystallite sizes for the mixed oxide phases, excellent reproducibility and low synthesis duration [5]. These characteristics are essential for the development of catalytic materials that achieve high oxidation efficiency with structural and performance stability. In this study, the main objectives concern the development of CuMn mixed oxides catalysts for an application in model oxidation reactions representatives to emission of biomass combustion.

Materials and Methods

Copper-manganese oxalate precursors were synthesized as follows: copper nitrate ($Cu(NO_3)_2{\cdot}3H_2O$) and manganese nitrate ($Mn(NO_3)_2{\cdot}4H_2O$) were dissolved in 200 mL of pure acetone. Separately, oxalic acid was also dissolved in 200 mL of acetone. The nitrate solution was then added directly to the oxalic acid solution under vigorous stirring during 30 minutes, allowing for rapid oxalate precipitation. The resulting mixture was filtered, washed with acetone, and dried at 60°C for 48 hours. The dried oxalate precursor was then calcined at 500°C for 4 hours under an air flow. The samples were named based on their Cu:Mn ratios: $Cu_1Mn_4O_x$ (1:4), $Cu_1Mn_1O_x$ (1:1), $Cu_4Mn_1O_x$ (4:1), alongside copper oxide (CuO_x) and manganese oxide (MnO_x) reference samples synthesized under identical conditions. These catalysts were characterized by several physicochemical methods: XRD, H_2-TPR, XPS, N_2 sorption, SEM, Raman, IR, and UV-visible spectroscopy. Carbon black oxidation tests, N330 Degussa was mechanically mixed with the catalyst (10% carbon black, 90% catalyst). This mixture was analyzed using DSC-TGA analysis, coupled with mass spectrometer to quantify the CO_2 produced. For CO and toluene oxidation tests, 100 mg of each catalyst was pre-treated by heating under an air flow at 150°C. The gas mixture for CO oxidation was prepared to obtain 1000 ppm of toluene or CO in air flow 100 mL/min. Outflow gases were analyzed using Agilent 490 Micro gas chromatography and ADEV 4400 IR CO-CO_2 analyzer.

Results and Discussion

Oxalate precipitation method proved advantageous for the preparation of copper-manganese mixed oxides, revealing significant textural and physicochemical differences. XRD analysis of mixed oxides show the presence of spinel phase ($Cu_{1.5}Mn_{1.5}O_4$) formation suggesting an interesting distribution of copper and manganese species, confirmed by microscopy analysis. The presence of mixed oxides allows to reduce the material at low temperature compared to the single oxide issued from oxalate precursors, suggesting good interactions between copper and manganese species.

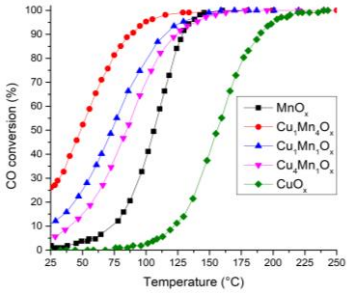

Figure 1. Conversion vs. temperature of CO oxidation over $CuMnO_x$ mixed oxides

For CO total oxidation tests (Figure 1), CuMn mixed oxides show improved performance with higher manganese content. The copresence of Mn_3O_4 and spinel phases enhances the catalytic oxidation at low temperature suggesting a synergetic effect between these two phases for total oxidation of CO. A beneficial influence of presence of Cu and Mn on mixed oxides is observed by a conversion at lower temperature than the single oxides. Similar trends were observed for toluene oxidation, suggesting strong catalytic potential in VOC total oxidation.

Significance

This presentation focuses on the efficiency of the oxalate route to produce highly active copper-manganese oxides. The influence of Cu/Mn ratio is studied through various physicochemical characterization methods, notably revealing the presence by XRD of the spinel phase ($Cu_{1.5}Mn_{1.5}O_4$) and others Mn or Cu oxides are confirmed. Relationships between catalytic activity and physicochemical properties were established, demonstrating that an optimal ratio enhances pollutants oxidation at low temperatures, probably due to a synergistic effect between Mn_3O_4 and the spinel phase. These results confirm the potential of these catalysts for treating emissions from biomass combustion, paving the way for cleaner energy applications and effective pollution control.

References

1. C. Paris, H. Dib, C. E. Bounoukta, E. Genty, C. Poupin, S. Siffert, R. Cousin, *Catalysts*. **2024**, 14(7), 455
2. R. Fan, J. Li, L. Chen, *et al.*, *Environ. Res.* **2014**, *135*, 1–8.
3. M. Li *et al.*, *Colloid Interface Sci.* **2023**, *630*, 301-316
4. S. Dey, G. C. Dhal, D. Mohan, R. Prasad, *Mater. Discov.* **2018**, *12*, 63-71
5. Y. D. G. Edañol *et al.*, *IOP Conf. Ser.: Mater. Sci. Eng.* **2019**, *625*, 012016.

Role of hollow @SiO_2 and @TiO_2 supports in catalytic activity of CuO and Co_3O_4 phases in total oxidation of toluene

Anna Rokicińska[1]*, Magdalena Żurowska[1,2], Radosław Sadowski[1], Marek Dębosz[1], Piotr Kuśtrowski[1]

[1]*Faculty of Chemistry, Jagiellonian University, Gronostajowa 2, 30-387 Krakow, Poland*

[2]*Doctoral School of Exact and Natural Sciences, Jagiellonian University, S. Łojasiewicza 11, 30-387 Krakow, Poland*

*anna.rokicinska@uj.edu.pl

Introduction

It is known that chemical composition, structure, porosity and morphology of a support can have a tremendous influence on catalytic activity of a deposited active phase. Therefore, a key aspect of designing supported systems for catalytic processes, including the total oxidation of volatile organic compounds (VOCs), is finding the most effective combination of support and active phase. In this work, we have tried to explain a real role of interactions between CuO and Co_3O_4 phases, which are considered to be very promising for use in the VOCs combustion,[1] and a support (SiO_2 and TiO_2). In order to exclude the influence of porosity and morphology of the support, both SiO_2 and TiO_2 were synthesized in the form of a hollow structure,[2] selecting the preparation method in a way that ensured obtaining similar textural parameters.

Materials and Methods

The polymer templating method was used for the synthesis of the SiO_2 and TiO_2 supports. Oxide phase precursors were deposited on the surface of spherical particles of polystyrene or resorcinol-formaldehyde resin, respectively. Subsequently, the polymer@oxide composites were modified with Cu^{2+} or Co^{2+} cations using wet impregnation. The amounts of the introduced components were chosen to obtain 5, 10 and 15 wt.% of CuO or Co_3O_4 in the final catalyst. The synthesized materials after removal of the polymer core by high temperature calcination were examined using XRD, XRF, UV-Vis-DR, XPS, SEM/EDX, DRIFT and H_2-TPR. Moreover, their catalytic activity in the total oxidation of toluene was tested.

Results and Discussion

The SiO_2- and TiO_2-based supports with a uniform spherical particle shape (cf. SEM images in Figure 1) and similar porosity (38 m^2/g and 29 m^2/g for @SiO_2 and @TiO_2, respectively) were obtained. Analysis of XRD patterns of these materials revealed the presence of amorphous SiO_2 (for @SiO_2) and anatase phase (for @TiO_2). The active phase was introduced onto the hollow SiO_2 and TiO_2 spheres in the expected amounts as confirmed by XRF measurements. In the Cu-containing catalysts, the CuO phase was formed after calcination, whereas the @SiO_2_Co catalysts showed the presence of the spinel Co_3O_4 phase. However, for the TiO_2-based materials, an additional crystalline phase of $CoTiO_3$ appeared. The XRD results were supplemented by UV-Vis-DR, DRIFT and XPS analyses. The synthesized materials exhibited high catalytic activity in the total oxidation of toluene (Figure 2). The best catalytic performance was achieved for the @TiO_2_Cu and @SiO_2_Co catalysts. The @TiO_2_Cu worked more efficiently at lower temperatures, while the @SiO_2_Co catalysts achieved 100% toluene conversion faster. It was found that the catalytic activity is strongly influenced by the strength of interaction between active phase and support, manifested by observed reducibility. Assuming the Mars-van Krevelen mechanism, involving lattice oxygen determines the catalytic efficiency in the combustion reaction.

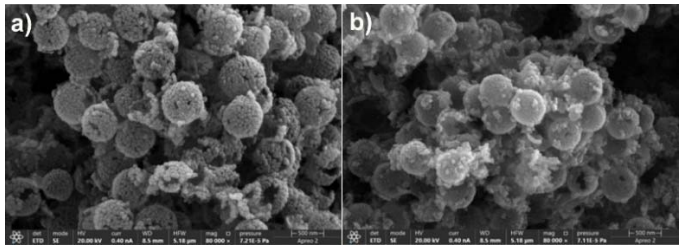

Figure 1. SEM images for (a) hollow SiO_2 and (b) hollow @TiO_2 supports.

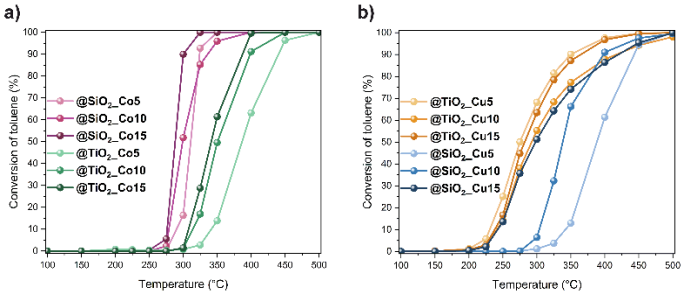

Figure 2. Conversion vs. reaction temperature for (a) Co- and (b) Cu-containing catalysts tested in total oxidation of toluene.

Significance

Understanding the real role of interactions between typical components of a supported catalyst designed for the VOCs combustion, which would be difficult without excluding additional parameters influencing the catalytic behavior of the system (e.g. porosity, morphology), brings us closer to the development of commercial supported oxide catalysts for this process.

Acknowledgement

We thank the National Science Centre of Poland for financial support in the implementation of research (grant no. 2020/39/D/ST5/02703).

References

1. X. Wu, R. Han, Q. Liu, Y. Su, S. Lu, L. Yang, Ch. Song, N. Ji, D. Ma, X. Lu, *Catal. Sci. Technol.,* **2021***, 11,* 5374-5387
2. A. Rokicińska, P. Łątka, B. Olszański, M. Żurowska, M. Dębosz, M. Michalik, P. Kuśtrowski, *Chem. Eng. J.* **2024**, *480*, 148173

Exploring the Catalytic Properties of Extra-Large Pores ZEO-1 Zeolite

Nourrdine CHAOUATI[1], Mohammad Fahda[1], Svetlana Mintova[1],
Ludovic Pinard* and Valentin Valtchev[1]*
[1]*Laboratoire de Catalyse et Spectrochimie, LCS, UMR 6506, ENSICaen, France*
* ludovic.pinard@ensicaen.fr, * valentin.valtchev@ensicaen.fr

Introduction

Zeolites are unique crystalline microporous materials used in different industrial applications, such as catalysis and adsorption-separation processes. Their microporous structure is the origin of their shape selectivity, but limits their application for bulkier molecules. Recently, a promising extra-large pore aluminosilicate zeolite, ZEO-1 (JZO), with relativel low Si/Al ratio (~15-20) and high hydrothermal stability, has been prepared.[1] ZEO-1 has a 3D framework with three types of supercages formed by interconnected 16x16, 16x12, and 16x12 member rings (MR) channels. As ZEO-1 is a relatively recent discovery, studies on its catalytic properties remain limited. Since the zeolite was recently discovered and its synthesis is difficult to reproduce, there are a few publications devoted to its catalytic properties.[1,2]

To shed light in ZEO-1's catalytic potential, we investigated its fundamental properties through model reactions: activity was assessed via n-hexane cracking at 540 °C, [2] selectivity through phenol alkylation with tert-butyl alcohol at 80 °C, [2] and stability via coking reactions with propene at 450 °C. Additionally, spent catalysts were analyzed using various methods to identify deactivation modes.

Materials and Method

The materials used in this study include ZEO-1 (16 MR: 10.62 × 9.41 ↔ 10.54 × 9.64; 12 MR: 7.24 × 6.60 ↔ 7.18 × 5.48) and commercial Beta (12 MR: 6.6 x 6.7 ↔ 5.6 x 5.6) and USY (12 MR: 7.4 x 7.4) zeolites, with their key properties detailed in Table 1. The catalytic tests for n-hexane cracking and propene transformation were conducted in a fixed-bed reactor at 540 °C and 450 °C, respectively, using a nitrogen-to-hydrocarbon molar ratio of 11. The alkylation reaction of phenol with tert-butyl alcohol was performed in the liquid phase using a batch reactor. For this reaction, 200 mg of zeolite catalyst was mixed with 565 mg of phenol and 445 mg of tert-butanol. The reactants were homogenized with 769 mg of nonane, and the reaction was carried out at 80 °C for 4 hours.

The spent catalysts obtained after various durations of propene conversion were analyzed to evaluate residual properties. N_2 physisorption was used to assess porosity, pyridine adsorption followed by FTIR determined acidity, and elemental analysis quantified coke content. The composition of the coke was further characterized by GC/MS after its separation from the zeolite framework.

Table 1. Main properties of studied materials.

Catalyst	ZEO-1	USY	Beta
Si/Al (mol/mol)	22.5	6	13.7
[PyH$^+$]* (µmol/g)	480	481	641
V_{micro} (cm^3/g)	0.31	0.27	0.22

*Pyridine adsorption-desorption at 150 °C monitored by FTIR.

Results and Discussion

The strength of Brønsted acid sites was evaluated using the rate of monomolecular cracking of n-hexane, normalized to the concentration of acid sites determined through pyridine adsorption (Figure 1a). The turnover frequency (TOF) results show that ZEO-1 displays slightly greater activity than USY zeolite but significantly lower activity than Beta zeolite. This indicates that ZEO-1 has acid sites with a strength comparable to those of USY.

Phenol alkylation with tert-butyl alcohol is a classic Friedel–Crafts reaction that produces ortho-butyl phenol (o-TBP), para-butyl phenol (p-TBP), and 2,4-di-tert-butyl phenol (2,4-DTBP). The pore size and the channel geometry influence the selectivity for these products.[2] ZEO-1, Beta, and USY achieved phenol conversion rates of 84%, 71%, and 90%, respectively.

USY showed minimal product selectivity, yielding similar proportions of o-TBP and 2,4-DTBP, with slightly less p-TBP. In contrast, Beta demonstrated a strong selectivity to p-TBP while producing negligible amounts of o-TBP and 2,4-DTBP. ZEO-1 exhibited a selectivity pattern similar to Beta, favoring p-TBP significantly over the other products (Figure 1b). Although ZEO-1 features a supercage structure with dimensions comparable to USY, its preference for p-TBP over 2,4-DTBP suggests that most active acid sites are located within its 12-MR channels. This conclusion aligns with DFT modeling, which highlights the stability of key tetrahedral sites within these channels. [2]

The stability of the catalysts was assessed by monitoring their activity decay during propene transformation (Figure 2c). After 60 minutes of reaction, ZEO-1 maintained a much higher proportion of its initial activity compared to Beta and USY, demonstrating its superior stability and resistance to coking. This improved stability is likely due to the limited number of acid sites within ZEO-1's 16-MR channels, which facilitates efficient molecular diffusion. Moreover, the coke molecules formed during propene conversion on ZEO-1 are primarily linear polyaromatics, such as alkyl-naphthalenes and anthracenes, whose sizes match well with its 12-MR channels. In contrast, Beta zeolite produces coke predominantly in the form of alkyl-pyrenes, which become trapped in the channel intersections, accelerating deactivation.[3]

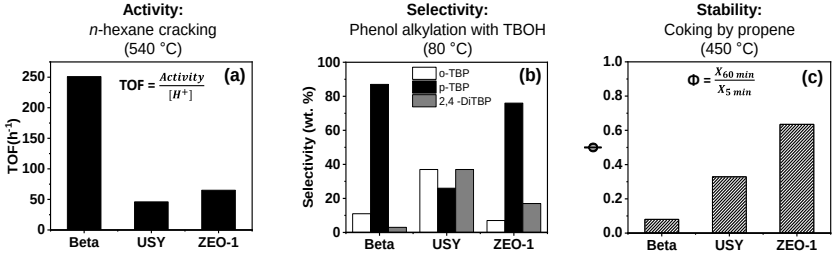

Figure 1. Catalytic activity (a), selectivity (b) and stability (c) of ZEO-1 in comparison with Beta and USY zeolites. Φ: deactivation function, TBOH: tert-butanol, TBP: terbutyl phenol.

Significance

The results of the catalytic tests indicate that ZEO-1 zeolite holds significant potential for acid catalysis applications in oil refining, petrochemistry, and sustainable chemistry. Its cracking performance is comparable to that of USY, while its shape selectivity appears to be governed by the 12-MR channels. Furthermore, the 16-MR channels contribute to its enhanced stability, making ZEO-1 a promising candidate for industrial processes that demand efficiency and durability, as well as for advancing greener and more sustainable chemical transformations.

References

1. Q-F. Lin, Z. R. Gao, C. Lin, S. Zhang, J. Chen, Z. Li, X. Liu, W. Fan, J. Li, X. Chen, M. A. Camblor, F-J. Chen, Science **2021**, 374, 1605–1608.
2. M. Fahda, J. Fayek, E. Dib, H. Cruchade, N. Pichot, N. Chaouati, L. Pinard, P. Petkov, G. N. Vayssilov, A. Mayoral, B. Witulski, L. Lakiss, and V. Valtchev, Chem. Mater. **2024**, 36, 5405−5421.
3. L. Pinard, S. Hamieh, C. Canaff, F. Ferreira Madeira, I. Batonneau-Gener, S. Maury, O. Delpoux, K. Ben Tayeb, Y. Pouilloux and H. Vezin, J Catal, **2013,** 299, 284–297.

Designing Pt/TiO_2 catalysts for efficient dehydrogenation of perhydrobenzyltoluene

Nataliia Marchenko[1], Mohamad Kharma, Franck Morfin, Laurent Piccolo,
Nuno Rocha Batalha, Valérie Meille*
IRCELYON, CNRS, UCBL, 69100 Villeurbanne, France
*valerie.meille@cnrs.fr

Introduction

In the context of the ongoing transition towards renewable energy, hydrogen is recognized as a promising vector for energy storage and transportation. While physical storage of hydrogen is widely used, Liquid Organic Hydrogen Carrier (LOHC) technology has emerged as another promising way to store and release hydrogen.[1] Among the various LOHC candidates, the perhydrobenzyltoluene (H12BT)-benzyltoluene (H0BT) couple (Figure 1a) attracted significant attention in recent years due to its optimal physical and ecotoxic properties as well as its competitive H_2 gravimetric storage density (6.2 wt%).[2] To release hydrogen from H12BT, Pt catalysts are currently employed both in industry and academia. Our study investigates the impact of the phase composition of TiO_2 support on structural and catalytic properties of Pt nanoparticles (NPs), aiming to achieve higher activity and selectivity than with a Pt/Al_2O_3 commercial reference.

Materials and Methods

TiO_2 supports were selected from commercial sources (P25 and P90 (anatase-rutile mixtures, Evonik), TiO_2-rutile (Merck), and G5 (anatase, Tronox)), some of which were subjected to heat treatment to change the ratio of polymorphs in the sample. TiO_2 supports are named A*x*, where *x* stands for the percentage of anatase phase in the titania. The 0.4 wt% Pt/γ-Al_2O_3 catalyst was provided by Heraeus. Pt/Ax catalysts were synthesized via incipient wetness impregnation using $Pt(NH_3)_4(NO_3)_2$ precursor with subsequent calcination and reduction treatments. The loading of Pt was 0.5 wt% unless otherwise stated.

Catalytic tests were performed in a glass semi-batch reactor (continuous removal of hydrogen) connected to a GC-TCD. The initial dihydrogen productivity (*P*) was calculated from the initial slope of the degree of dehydrogenation (DoD) of H12BT versus time (obtained by GC-FID analysis) and by GC-TCD measurements of the gas outlet.

Results and Discussion

The preparation of Pt/Ax catalysts resulted in the formation of Pt NPs of 1.0-1.6 nm in average size. When increasing the loading of Pt and/or changing the heat treatment, Pt NPs of 2.3 nm (Pt/A86R200, where R stands for the reduction temperature) and 2.7 nm (Pt2/A86R600, where 2 stands for the loading of Pt) were obtained. The performance of the catalysts depends on the nature of the support as well as on the size of the particles. Compared to Pt/Al_2O_3, Pt/Ax catalysts show higher productivity and DoD, except for Pt/A100. In particular, using Pt/A0, 47 % of DoD was achieved with an initial productivity of 2.2 g(H_2)/g(Pt)/min, while for Pt/Al_2O_3 the values of DoD and *P* are 35 % and 1.4 g(H_2)/g(Pt)/min. The product distribution (H6BT/H0BT) is similar for all the catalysts at the same conversion. As for the selectivity, Pt/TiO_2 leads to less methylfluorene (MF) side-product (Figure 1b); namely at a H0 yield of 11 % using Pt/Al_2O_3, the MF yield reaches 0.40 %, whereas with Pt/A0 only 0.09 % MF is formed. This result could be explained by the lower acidity of titania compared to alumina and the lower acidity of rutile compared to anatase.[3] Currently, FTIR measurements with a pyridine probe are being conducted to rationalize this behavior. In addition, the MF production rate is found to depend on the size of the Pt NPs. The MF yield is lower using Pt2/A86R600 (2.7 nm) than using Pt0.5/A86 (1.5 nm) at the same H0 yield (Figure 1c). Pt sites of low coordination (steps, corners) can strongly adsorb H0BT, which can be subsequently converted into MF.[4] CO-DRIFTS analysis is being performed for Pt/Ax samples to evaluate structural differences between Pt NPs. The recent results will be presented during the conference.

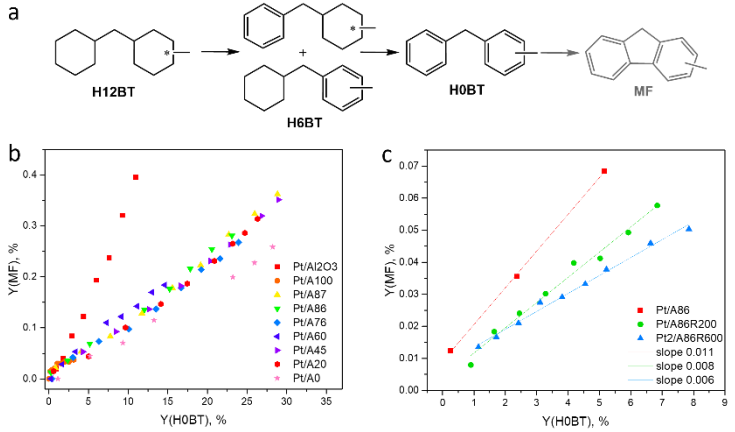

Figure 1. a) Scheme of H12BT dehydrogenation; b) Y(MF) vs Y(H0) for Pt/Ax and Pt/Al_2O_3 catalysts; c) Y(MF) vs Y(H0) for Pt/A86 (1.5 nm), Pt/A86R200 (2.3 nm), and Pt2/R600 (2.7 nm) catalysts. Reaction conditions: H12BT (20 g), catalyst (0.009 mol%), 260 °C, t = 4 h.

Significance

A series of Pt/TiO_2 catalysts was prepared and tested in H12BT dehydrogenation. Compared to Pt/Al_2O_3 reference, Pt/TiO_2 leads to less MF byproduct. Among the Pt/TiO_2 catalysts, the highest activity and H_2 selectivity were obtained with Pt/A0 (rutile), which may arise from the acidity of the support as well as from the structure of Pt NPs. A significant decrease in the amount of MF can potentially enhance the lifetime of both the catalyst and the LOHC.

References

1 F. D'Ambra and G. Gébel, *Sci. Technol. Energy Transit.*, **2023**, *78*, 32.
2 N. Brückner, K. Obesser, A. Bösmann, D. Teichmann, W. Arlt, J. Dungs and P. Wasserscheid, *ChemSusChem*, **2014**, 7, 229–235.
3 H. Li, M. Vrinat, G. Berhault, D. Li, H. Nie and P. Afanasiev, *Mater. Res. Bull.*, **2013**, *48*, 3374–3382.
4 F. Auer, A. Hupfer, A. Bösmann, N. Szesni and P. Wasserscheid, *Catal. Sci. Technol.*, **2020**, *10*, 6669–6678.

Investigations in the H_2-SCR pathways over a Pt/SiO_2-Al_2O_3 catalyst

Amira BEN ATTIA[1], Fabien CAN*[1], Xavier COURTOIS[1]*
[1] *IC2MP, Université de Poitiers-CNRS, 4 rue Michel Brunet TSA 51106 86073 Poitiers Cedex 9, France*
*fabien.can@univ-poitiers.fr ; xavier.courtois@univ-poitiers.fr

Introduction

H_2 internal combustion engine (H_2-ICE) could be a viable clean solution for heavy vehicles for decarbonizing the transport sector. However, a deNOx treatment could be necessary. One attractive approach is to implement a H_2-SCR after-treatment system. According to the literature, the H_2-SCR mechanism can be divided into two distinct routes, namely (i) the NO adsorption/dissociation based on a Langmuir-Hinshelwood mechanism and (ii) the oxidation–reduction pathways.[1] Regardless of the mechanism considered, a typical volcano shaped curve in NO_x conversion is obtained. This phenomenon is related to the competitive H_2 combustion reaction, which intensifies as the temperature rises, particularly above 150 °C on precious metals.

The oxidation–reduction mechanism the NO reduction process involves complex reactions between gaseous NO or weakly adsorbed oxidized species (NO^-, NO_2^-, NO_3^-) and adsorbed reduced N compounds (NH_x).[2] In this study, we investigate the reaction pathways of the H_2- SCR over a low loaded platinum-based catalyst, with a special focus on (i) the role of NH_3 as possible intermediate species and (ii) the origin undesired N_2O emission.

Materials and Methods

A 0.3%Pt/5%SiO_2-Al_2O_3 catalyst was prepared using a silica-alumina support provided by Sasol which was previously hydrotreated 4 h at 700°C (296 $m^2\ g^{-1}$). Platinum was added by wet impregnation from $Pt(NH_3)_2(NO_2)_2$ salt. After drying, the resulting powder was treated under N_2 at 700 °C, 4 h and finally hydrotreated at 600 °C, 4 h under synthetic air with 10 % H_2O (Pt dispersion of 35 %).

The catalytic behaviour of the sample (30 mg) was investigated under various reaction mixtures depicted in Table 1. The feed gas composition was monitored with a multigas infrared analyser (MKS 2030) for NO, NO_2, N_2O and NH_3. Additionally, a mass spectrometer (Pfeiffer Vacuum) was used to record the H_2 signal. The N_2 formation was calculated based on the assumption that only NO, NO_2, N_2O and NH_3 were formed as N-compounds.

Table 1. Reactional mixtures depending on the type of catalytic test (total flow: 150 mL min^{-1}).

Catalytic test	NO (ppm)	NH_3 (ppm)	H_2 (%)	O_2 (%)	N_2
H_2-SCR	400	-	1	2	balance
NO+H_2 reaction	400	-	1	-	balance
NH_3-SCR	400	400	-	2	balance
NH_3 oxidation	-	400	-	2	balance

Results and Discussion

As expected, the NO_x conversion under H_2-SCR conditions (Fig. 1A) showed a volcano-shaped curve. The conversion started below 50 °C, with N_2O as the main product. Interestingly, despite the high WHSV of 300 L h^{-1}/g_{cata} (30 mg catalyst for a total flow rate of 150 mL min^{-1}), some ammonia was detected starting from 70 °C, peaking near 100°C. At this temperature, full NO_x conversion was achieved and N_2 became the main reduction product. At higher temperatures, a secondary N_2O emission was observed. To explain these complex profiles, especially the role of NH_3 as potential intermediate and the origin(s) of the undesired N_2O emission, various reaction mixtures were used to study the NH_3 formation and its reactivity.

Removing oxygen (NO+H_2 reaction, Fig. 1B) showed no influence in the 50-100 °C temperature range, indicating that the actives sites were mainly covered by NO_x species, with N_2O as the main reduction product (accordingly, note that the H_2 conversion was shifted to lower temperatures when NO was removed from the reaction mixture, results not shown). The ammonia emission in Fig 1B started near 70 °C, which is consistent with the H_2-SCR conditions (Fig. 1A). In terms of ammonia reactivity, the NH_3-SCR (Fig. 1C) can occur from 70 °C, exhibiting significant activity from 100 °C. However, this reaction can only take place within the H_2-SCR process when both NH_3 and NO_x are simultaneously available, which occurs within a very narrow range (as shown in Fig 1A and confirmed varying the involved catalytic mass from 5 to 200 mg). Moreover, the distribution of N_2 and N_2O observed in NH_3-SCR (Fig. 1C) in the 100-350 °C temperature range differs significantly from that obtained in H_2-SCR (Fig. 1A). On the contrary, the second N_2O emission wave observed in H_2-SCR (Fig. 1A) closely correlated with the NH_3 oxidation by O_2, which led mainly to N_2 (Fig. 1D).

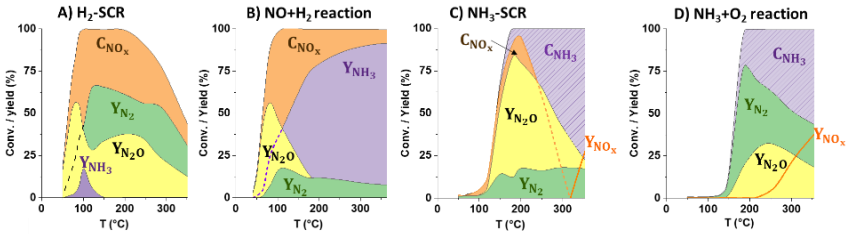

Figure 1. 0.3%Pt/5%SiO_2-Al_2O_3 catalytic behavior (C: conversion; Y: yield) depending on the reaction mixture reported in Table 1.

Significance

The pathways and mechanistic aspects of the H_2-SCR on platinum-based catalysts remain a topic of debate. In this study, we demonstrate that NO decomposition occurs mainly below 100 °C, leading principally to N_2O. The formation of NH_3 is observed starting at 70 °C and the NH_3-SCR reaction occurs only within the 70-120 °C temperature range, leading mainly to N_2O. Importantly, the H_2-SCR activity at T>120 °C is mainly driven by the NH_3 oxidation by O_2. To our knowledge, ammonia oxidation has not been considered yet as the main reaction in H_2-SCR.

References

1. Z. Liu, J. Li, S. Ihl Wooc, *Energy Environ. Sci.* **2012,** *5,* 8799-8814
2. J R. Burch, M. D. Coleman., *J. Catal.* **1999**, 188, 69-82

OC3: HDS, Biomass derivatives

Conversion of bio-derived levulinic acid, evaluation of conditions and catalyst performance

Chamorro S.[1*], Araque M.[1], Katryniok B.[1], Dominguez-Benetton X.[2], Martinez O.[2]
[1]*Univ. Lille, CNRS, Centrale Lille, Univ. Artois, UMR 8181-UCCS - Unité de Catalyse et de Chimie du Solide, 59000 Lille, France*
[2]*Separation and Conversion Technologies, VITO, 2400 Mol, Belgium*
**lchamorr@centralelille.fr*

Introduction

Due to the adoption of Europe's initial bioeconomy strategy in 2012 and the European Green Deal in 2020, industry is increasingly attracted to invest in areas that use renewable resources. It has been stated that the global chemical industry could reach revenues up to US$ 15 billion by the production of bio-based products.[1] Thus, sugars serve as a versatile starting point for a variety of important derived compounds in the chemical industry. Levulinic acid (LA), or 4-oxopentanoic acid, is a promising sugar-derived compound that can replace petroleum-based products. One of its most notable applications is in the synthesis of γ-valerolactone (GVL)**,** a compound used as a fuel additive, solvent, and intermediate in the production of polymers and fine chemicals. Frequently, the transformation of LA to GVL involves two-step process: hydrogenation and cyclization. In our study, we proposed the one-pot reaction without isolation of intermediates. The reaction was carried out at different reaction conditions of pressure and temperature using different loadings of mono- and bi-metallic Pt and Pd on TiO_2.

Materials and Methods

The following reagents and products were used as received from Sigma Aldrich: TiO_2 nanopowder, 21 nm primary particle size; PVP; PVA; $NaBH_4$ powder, ≥98.0%. As metal precursors: $Pt(NH_3)_4(NO_3)_2$ >50 Pt basis and $Pd(NO_3)_2 \cdot 2H_2O$ ~40% Pd basis.

The tested catalysts were synthetized by sol-immobilization technique, using PVA and PVP, since those biopolymers are good dispersing agents allowing to control the morphology and size of metal particles independently of the support.[2,3] Moreover, the catalysts were compared with catalysts prepared through conventional impregnation method using recovered metals derived from a gas-diffusion electrocrystallization process (GDEx).[4]

The reaction took place in liquid phase during 4 hours in a Screening Pressure Reactor (SPR) (Unchained Labs). The required amount of catalyst (10 mg) was introduced into a reactor and then an aqueous solution containing 10 wt.% LA was added. Previous to the catalytic run, a purge was performed with nitrogen, followed by pressurization with H_2, and heating up to the desired temperature (50, 100, 150, and 200°C). After the reaction, the aqueous phase product samples were analyzed by High-Pressure Liquid Chromatography (HPLC). HPLC analysis was performed using a Shimadzu HPLC system equipped with a UV-VIS Detector (Shimadzu SPD 10-AV) and Refractive Index Detector (Shimadzu RID-6A) using Aminex 87-H column from Bio-Rad, mobile phase 0.5mM H_2SO_4 in H_2O, flow 0.5 mL min^{-1}, 60°C. The catalysts were characterized by Transmission Electron Microscopy (TEM), Induced Coupled Plasma (ICP), X-Ray Diffraction (XRD) and Thermogravimetric Analysis (TGA).

Results and Discussion

The loadings (<3.0 wt.%) of the metals were consisted with those reported in previous studies.[5,6,7] The preliminary screenings revealed that the reference catalysts (prepared via sol-immobilization) generally exhibited superior activity in converting LA (Figure 1), whereby no clear trend could be observed for this series. On the other hand, for the catalysts based on the impregnation-sonication method using the metal precursors from the GDEx process, a steady increase in the performance was observed with increasing Pd/Pt ratio. Thereby, highest performance was observed for $PtPd_3/TiO_2$. In comparison, the monometallic Pt catalyst ($0.5Pt/TiO_2$) barely reached 50% conversion. For the catalyst based on the GDEx these results suggest that the deposition of bimetallic particles may significantly enhance catalytic performance. Furthermore, the use of recovered metal by GDEx to synthetize catalysts might be an overall energy-efficient and scalable method.

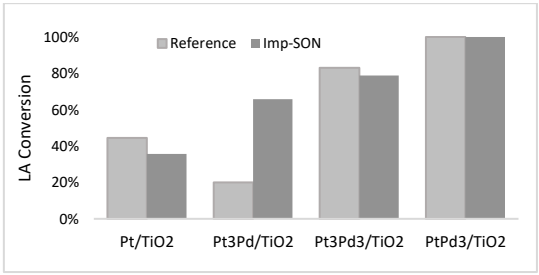

Figure 1. Comparison of the conversion between reference catalysts obtained by sol-immobilization method with PVP and the catalysts synthetized by impregnation-sonication (Imp-SON) using metals of GDEx process. Reaction conditions 200 °C, 30 bar H_2, 1ml of 10 wt.% LA in H_2O, 10 mg catalyst.

Significance

This research aligns with circular economy and green chemistry goals. The first by using recycling materials, which leads to reducing costs and dependence on environmentally impactful mining practices and the latter associated to the sustainable production of fuels and chemicals.

References

1. IEA Bioenergy Bio-based chemicals value added products from biorefineries. **2012**
2. Simakova, I.L., Demidova, Y.S., Gläsel, J., Murzina, E.V., Schubert, T., Prosvirin, I.P., Etzold, B.J.M., Murzin, D.Y. *CSTAGD* 6(24), 8490–8504, **2016**
3. Villa, A., Di Wang, Veith, G.M., Vindigni, F., Prati, L. *CSTAGD* 3(11), 3036, **2013**
4. Martinez-Mora, O., Pozo, G., et al. *RSSUAN*. 1, 454–458, **2023**
5. Filiz, B. C., Gnanakumar, E. S., Martínez-Arias, A., et al. *CALEER*. 147, 1744–1753, **2017**
6. Ruppert, A.M., Grams, J., Jedrzejczyk, et al. *CHEMIZ* 8(9), 1538–1547, **2015**
7. Sudhakar, M., Lakshmi Kantam, M., Swarna Jaya, V., Kishore, R., Ramanu-jachary, K.V., Venugopal, A. *CCAOAC* 50, 101–104, **2014**

This research is funded by the European Union under Grant Agreement No 101091715. Views and opinions expressed are however those of the author(s) only and do not necessarily reflect those of the European Health and Digital Executive Agency (HaDEA). Neither the European Union nor the granting authority can be held responsible for them.

Catalytic hydroconversion of enzymatic hydrolysis lignin into sustainable aviation fuels

Camille Pellegrin[1], Antoine Daudin[2], Nadège Charon[2], Christophe Geantet[1], Dorothée Laurenti[1]*

[1] *IRCELYON, University of Claude Bernard Lyon 1, 69626 Villeurbanne, France*

[2]*IFPEN, Rond-point de l'échangeur de Solaize, 69360 Solaize, France*

*dorothee.laurenti@ircelyon.univ-lyon1.fr

Introduction

Lignin is the world's largest source of renewable aromatics making it a promising candidate to produce aromatics and cycloalkanes within the range of jet fuels. While already co-produced in pulp industry, lignin will be soon available in greater quantities through emerging second-generation cellulosic bioethanol technology[1]. Nowadays, lignin is underutilized and is primarily recovered for its heating value. This thesis aims to improve the efficiency and sustainability of second-generation cellulosic bioethanol technology. The main challenge is therefore to depolymerize a technical lignin from enzymatic hydrolysis using bifunctional heterogeneous catalysts with variable metal sulfide/acid balance to monomers, and assess the effect of support's acidity. Those bifunctional catalysts can lead to C-O and C-C bonds cleavage of inter-linkage units[2,3], but also hydrogenation, hydrogenolysis, dehydration and also ring-opening reactions[4] in order to obtain SAF-compatible hydrocarbons i.e., aromatics, naphthenic and linear deoxygenated hydrocarbons.

Materials and Methods

The lignin from enzymatic hydrolysis of wheat straw is provided by IFPEN, as well as alumina-zeolite supports (shaped as extrudates). Lignin was characterized by elemental analysis (CHONS, XRF, ICP) along with thermogravimetric analysis (ATG). Major chemical functions were analyzed by ATR-IR, NMR analysis. Molar mass distribution is determined by Size Exclusion Chromatography (SEC-RID/DAD).

NiMoS catalyst supported on alumina-zeolite carriers were obtained by incipient wetness impregnation using $(NH_4)_6Mo_7O_{24}.4H_2O$ and $Ni(NO_3)_2.6H_2O$ as precursors, with a targeted loading of 10 wt% of Mo and 2.4 wt% of Ni. After maturation, the impregnated support is dried (120°C, 2h) and calcinated (450°C, 2h). Finally, sulfidation is performed at 400°C for 4 hours under a flow of H_2/ H_2S of 4 L/h (10%vol H_2S). A complete characterization of the supports and associated catalysts is conducted with various techniques (elemental analysis, textural properties, bronsted and lewis acidities, metals dispersion and phase crystallinity. The obtained catalysts are tested for lignin hydroconversion in a 300 mL stainless steel batch reactor, equipped with a magnetical stirring system and gas entrainment impeller. Typically, 3 g of lignin and 300 mg of catalyst are charged with 90 mL of solvent. The reaction is performed at 350°C under H_2 (50 bars). An appropriate product recovery protocol is applied to separate the liquid and solid fractions. Then, the liquid composition is given by GCxGC-FID/TOF-MS, molar mass distribution by SEC, and the elemental composition of the solid residue is determined by CHONS.

Results and Discussion

The first part of this study was devoted to lignin materials characterization. Beside usual alkylphenols structures commonly reported on lignin, our results revealed that lignin from enzymatic hydrolysis contains specifically a high ash content (7.6 wt%), including inorganic contaminants (Si, Ca) and also carbohydrate residues. NMR HSQC analysis confirmed the presence of Lignin-Carbohydrates Complexes (LCC), i.e, sugars bound to lignin. This composition results in low solubility of the crude lignin in THF solvent, however, washing the raw lignin with water increases THF solubility and remove some glucose monomers.

Regarding lignin hydroconversion, the main issue is the nature of the solvent; a hydrogen-donor solvent is preferred to optimize hydrogen diffusion in the liquid phase but often reacts during lignin depolymerization and hinders the analysis of the desired products. Solvent effect will therefore be discussed.

Table 1. Textural and acidic properties of supports

Samples	S_{BET} / $m^2.g^{-1}$	Av pore diam / nm	Total pore vol / $mL.g^{-1}$	Total acidity /$mmol.g^{-1}$
γ-Al_2O_3	212	12	0.64	0.375
γ-Al_2O_3-USY (Si/Al=40)	424	5.0	0.53	0.312
γ-Al_2O_3-USY (Si/Al=15)	448	4.7	0.53	0.407
γ-Al_2O_3-USY (Si/Al=2.6)	400	5.8	0.58	0.636
γ-Al_2O_3-HZSM5 (Si/Al=40)	287	7.8	0.56	0.334
γ-Al_2O_3-HZSM5 (Si/Al=25)	276	8.4	0.58	0.473
γ-Al_2O_3-HZSM5 (Si/Al=13)	278	8.3	0.58	0.582

Catalytic tests were carried out using NiMoS catalysts supported on Al_2O_3-HZSM5 and Al_2O_3-USY. The support acidity (Table 1) impacts the mass balance of the various fractions (liquid, THF-insolubles, THF-solubles, etc.) and the fractions composition. Additionally, for selected catalysts, we will present the influence of reaction time on the degree of raw lignin depolymerization assessed by SEC and NMR and the evolution of monomer products selectivity by using GCxGC characterization of the liquid phase. More precisely, the evolution of deoxygenated products of interest will be given according to the residence time.

Significance

This study offers a complete characterization of a real feedstock: a technical lignin from cellulosic ethanol biorefineries. It also investigates the reactivity of this increasingly available lignin by exploring the impact of textural and acidic properties of supports. This approach aims to produce a hydrocarbon mix, including aromatics and cycloalkanes, to address gaps in the composition of current certified SAFs.

Acknowledgment

The PEPR B-BEST is gratefully acknowledged for its financial support, through the project OPTISFUEL.

References

1. D.S. Bajwa et al., *Industrial Crops & Products* **2019,** 139, 111-526.
2. Z. Luo et al., *Nat. Chem. Eng.* **2024**, 1, 61-72.
3. *B. Joffres et al., Appl. Catal. B Environ., **2016,** 184, 153-162*
4. D. P. Gamliel et al., *Microporous Mesoporous Mater.* **2018**, 261, 18-28.

Development of non-noble metal catalysts for the dehydrogenation of formic acid

Sylvain Gigot[1,2], Émeline Charon[2], Mathieu Pinault[2], Caroline Genre[1], Thibault Cantat[1*]
[1]*Laboratoire de Chimie Moléculaire et Catalyse pour l'Énergie – NIMBE, CEA, CNRS, Université Paris-Saclay, Gif-sur-Yvette, France*
[2]*Laboratoire des Édifices Nanométriques - NIMBE, CEA, CNRS, Université Paris-Saclay, Gif-sur-Yvette, France*
* thibault.cantat@cea.fr

Introduction

Formic acid is among the most promising circular compounds for hydrogen storage. With 4.4 wt%H_2 content (53 g_{H2} L^{-1}), it is often considered as a Liquid Organic Hydrogen Carrier (LOHC)[1] and is part of the CO_2 economy.

Efficient homogeneous catalysts have been developed for formic acid dehydrogenation (FAD), with noble (Ru, Ir…) and non-noble metals (Fe, Mn…).[2] The main issue with those catalysts is their recovery. To tackle the issue, solid catalysts have been engineered, mainly with noble metals (Ru, Pd…). More recently, new non-noble metal materials have been explored with the development of single-atom catalysts, especially on carbon support. Cobalt single-atoms on N-doped carbon have demonstrated their efficiency for FAD.[3] As noble metal reserves decrease, finding efficient and cost-effective catalysts with non-noble metals is necessary. Here we describe the development, characterization and catalytic properties of highly-effective carbon supported single-atom manganese catalysts for the dehydrogenation of formic acid.

Materials and Methods

M-N-C catalysts are synthesized through a Zeolite Imidazole Framework (ZIF) decomposition method. A metallic precursor and zinc nitrate are dissolved in methanol. The solution is then mixed with an already prepared solution of 2-methylimidazole in methanol. Different metallic ratios between zinc and M (M = Mn, Co, or Fe) are considered, with Zn:M $\geq$ 1. After ageing, the ZIFs are pyrolyzed at temperatures comprised between 800 and 1000 °C under argon atmosphere.

The resulting materials are then analyzed by SEM, TEM, XPS, Raman spectroscopy and TGA among other techniques.

Reactivity tests are carried out at 100 °C in 50 mL batch reactors, with 30 mg of catalysts in 6 mL of propylene carbonate and 10 mmol of formic acid.

Results and Discussion

After the synthesis and tests of cobalt catalysts as benchmarks, manganese catalysts are currently synthesized and tested. The impact of key parameters, including the quantity of metal and nitrogen sites and the graphitization of the carbon support, on the catalytic performances will be presented.

Figure 1. SEM picture of Mn_1Zn_2-ZIF-950 °C (left) and Co_1Zn_2-ZIF-900 °C (right)

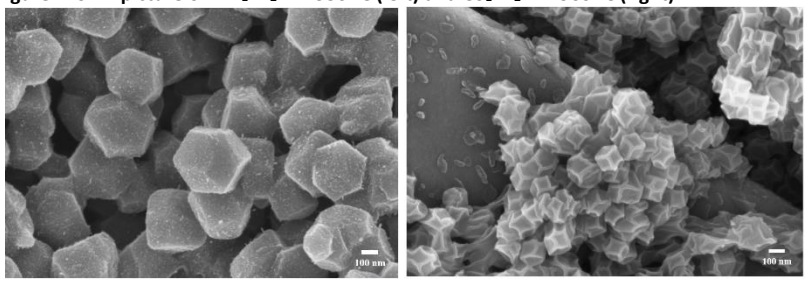

Figure 2. Comparison of the gaz pressure obtained with Zn_2Mn_1-ZIF-950 °C compared to Zn_2Co_1-ZIF-900 °C upon formic acid dehydrogenation at 100°C.

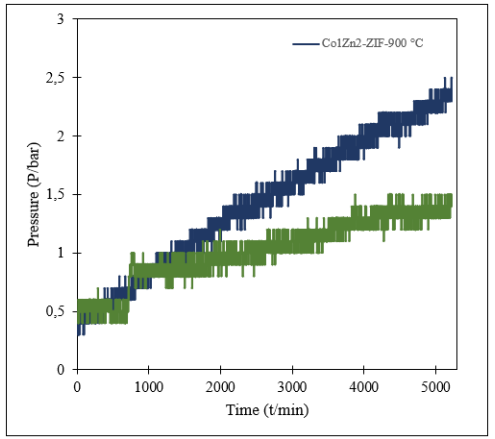

Significance

Manganese heterogeneous single-atom catalysts have not been described yet for formic acid dehydrogenation and are proposed as an alternative to ruthenium, palladium and cobalt catalysts.

References

1. J. Eppinger, K-W. Huang. *ACS Energy Lett.* **2017**, *2*, 1, 188–195
2. G. Laurenczy, M. Beller et al. *Chem. Rev.* **2018**, 118, 2, 372–433
3. M. Beller et al. *Angew. Chem. Int. Ed.* **2020**, *59* (37), 15849–15854.

Local and time-resolved characterization of a bimetallic Fe-Cu catalyst by environmental TEM and hyperspectral *in situ* Quick-XAS imaging

Aliou Sadia Traore[1], Ovidiu Ersen[1], Eric Marceau[2], Anthony Beauvois[3]* and Valérie Briois[3]
[1]*IPCMS - Institut de Physique et Chimie des Matériaux de Strasbourg, Strasbourg, France*
[2] *UCCS - Unité de Catalyse et Chimie du Solide, Lille, France*
[3] *Synchrotron SOLEIL, L'Orme des Merisiers, 91190 Saint Aubin, France*
**beauvois@synchrotron-soleil.fr*

Introduction

Bimetallic catalysts have been frequently used for the hydroconversion of platform molecules. In the case of nanoalloys, changes of their structural features usually allow one to trace the co-evolution of the two metals upon preparation and reaction. This is more difficult when the two metals do not form alloys, as is the case with Fe and Cu, but only coexist on the support. Synergetic phenomena explaining the characteristics of the catalyst (reducibility, higher selectivity in HDO products for Cu-Fe[1]) can be interpreted in terms of interfaces formed between the two metals but evidencing them is a challenging task. We show here that the latest methodological developments in imaging at different length scales have allowed us to understand the distribution and interplay of Fe and Cu during the reduction of a Fe-Cu/SiO_2 catalyst, at the nanoparticle scale, with environmental transmission electronic microscopy, and at the micrometer scale of the catalytic bed, with hyperspectral Quick-XAS imaging.

Materials and Methods

The Fe (10wt%)-Cu (10wt%)/SiO_2 catalyst was prepared by impregnation of Fe(III) and Cu(II) nitrates onto Sipernat-50 silica. After drying at 100°C (16h), calcination took place under a flow of synthetic air (100 mL min^{-1}) at 500°C during 5h (ramp rate 5 °C min^{-1}). Environmental transmission electronic microscopy analysis was carried out on a JEOL 2100F microscope by using a Protochips gas cell holder. Full Field (FF) Quick-EXAFS Hyperspectral Imaging, implemented at ROCK-SOLEIL,[2] was used to determine the evolution of the spatial distribution of Fe and Cu along the catalyst bed (length 2.3 mm, height 1.2 mm) during reduction under H_2 from 25 to 400°C (heating by gas blower), with a spatial resolution of 32.5 µm x 32.5 µm. 570 pixelated images at different energies of the XAS spectrum were recorded by the ORCA Flash 4.0 CMOS camera from 7070 to 9090 eV (one complete hyperspectral cube every 10.5 s). MCR-ALS[3] analysis was used for unraveling the Fe and Cu speciation at each pixel of the images.

Results and Discussion

On the calcined catalyst, Fe_2O_3 and CuO nanocrystalline phases (electron diffraction) coexist on the support as Janus nanoparticles presenting interfaces between the Fe and Cu oxidic domains identified as $CuFe_2O_4$ (STEM-EDX, elemental mapping at the Fe and Cu K lines and Fe and Cu K-edges EXAFS) (Fig. 1a). *In situ* EXAFS imaging shows that the reduction of Cu and Fe takes place through the succession of 3 Cu species ($CuO/CuFe_2O_4$, $CuO/CuFeO_2$ and Cu(0)) and 4 Fe species (a Fe(III) species encompassing the $Fe_2O_3/CuFe_2O_4$ and $Fe_2O_3/CuFeO_2$ compositions, a mixture of Fe_3O_4/FeO, and 2 Fe(0)-containing species). Between 121 and 133°C, reduction of Cu takes place at the interface by transforming $CuFe_2O_4$ to $CuFeO_2$, without affecting the formal trivalent oxidation state of Fe. Then the reduction of $CuO/CuFeO_2$ into Cu(0) will trigger the reduction of the iron(III) species into the Fe_3O_4/FeO second MCR-ALS isolated species, as evidenced by the co-localization of the phases in the catalytic bed (Fig. 1b; see the distribution of Fe_3O_4/FeO and Cu(0) at 144-148°C). H_2 activated by Cu(0) nanoparticles, fully formed at ≈200°C, then reduces Fe_3O_4/FeO to metallic Fe in the 200-300°C temperature range. EXAFS analysis for the third Fe(0) MCR-ALS species reveals a under-coordinated iron local order compared to the fourth one identified as Fe bcc. In conjunction with environmental microscopy, this finding has been interpreted by the formation of defective Fe nanoparticles resulting from the oxygen diffusion at the FeO_x/Fe/Cu interface and subsequent fragmentation of the Janus nanoparticles followed by Fe nanoparticles sintering at higher temperature.

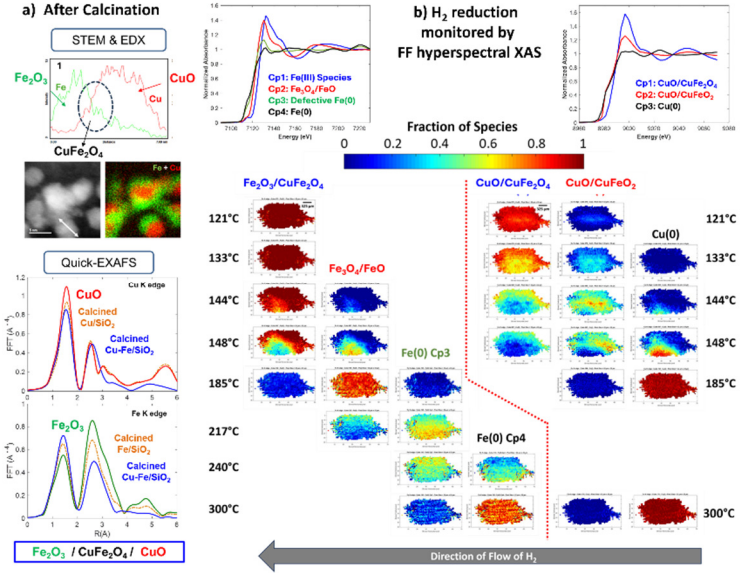

Figure 1. a) STEM-EDX and EXAFS results obtained after calcination. b) Speciation at the Fe and Cu K-edges measured during the monitoring of the reduction of the Fe-Cu catalyst under H_2. At the top, spectra of the successive Fe and Cu species extracted by MCR-ALS.

Significance

For the first time, the combination of local characterization and imaging at the micrometer scale in *in situ* conditions directly discloses synergetic phenomena taking place during the reduction of a Fe-Cu catalyst, and gives evidence for the formation of Fe/Cu interfaces that can explain the specific catalytic properties of this system with respect to a monometallic Cu catalyst.

References

1. For instance, H. Sheng and R. Lobo *ChemCatChem* **2016**, *8*, 3402.
2. V. Briois et al. *J Synchr. Rad.* **2024**, *31*, 1084.
3. A De Juan et al. *Analytical Methods* **2014**, *6*, 4964.

On the catalytic activity and structure of the CoReS phase in reactions involving hydrogen

Ryaboshapka Daria[1], Laurent Piccolo[1], Pascal Bargiela[1], Pavel Afanasiev[1*], Valerie Briois[2]
[1]*IRCELYON, Univ. Claude Bernard Lyon 1, 69626 Villeurbanne, France*
[2]*SOLEIL synchrotron, 91192 L'Orme des Merisiers , France*
*pavel.afanasiev@univ-lyon1.fr

Introduction

While MoS_2-based systems are widely studied in catalysis and electrocatalysis, ReS_2-based catalysts are often overlooked despite the better catalytic performance. Thus, in hydrodesulfurization (HDS) ReS_2 catalysts are several times more active than their Mo analogues.[1] They also demonstrate higher activity and better stability to the oxidizing atmosphere in electrochemical reactions.[2] For industrial applications MoS_2 catalysts are often promoted with Co which creates CoMoS sites and provides a considerable boost in activity. The structure of CoMoS phase while challenging to determine was proposed based on the X-ray absorption spectroscopy (XAS) and Density Functional Theory (DFT) calculations.[3,4] Modification with Co was also tried for ReS_2 catalysts and the increase of activity was achieved, but the existence of CoReS phase has never been demonstrated.[5] The goal of this work is to identify CoReS phase and to propose its structure on the basis of experimental and theoretical data.

Materials and Methods

The catalysts were synthesized via incipient wetness impregnation of mesoporous graphene (S_{BET} = 750 m^2/g) with NH_4ReO_4 and subsequent adsorption of $Co(acac)_2$, followed by sulfidation at 350 °C in two different atmospheres: H_2S/H_2 or H_2S/N_2. The initial samples are designated as 1Co10Re/G and 0.3Co0.6Re/G according to the metal loading; for sulfided samples H_2S/H_2 or H_2S/N_2 suffixes are added (1Co10Re/G H_2S/H_2). After sulfidation the catalysts were tested in HDS of thiophene (300-340 °C, 1 atm) and electrochemical hydrogen evolution reaction (HER) in acidic media. Sulfided samples were characterized by means of Raman, TEM/STEM-ADF (Scanning Transmission Electron Microscopy – Annular Dark-Field), XPS (X-ray Photoelectron Spectroscopy). *Operando* XAS at Co K edge and Re L edges was performed to estimate the state/local environment of metals. The evolution of the samples during sulfidation was studied by MCR-ALS (Multivariate Curve Resolution – Alternating Least Squares). The possible structures of CoReS phase were optimized using ORCA DFT software and then XANES (X-ray absorption Near Edge Spectra) spectra were simulated via FDMNES package. LCF (Linear Combination Fitting) for experimental XANES and EXAFS (Extended X-ray Absorption Fine Structure) spectra fitting were performed using ATHENA and VIPER software, respectively.

Results and Discussion

The synthesized CoReS catalysts demonstrated high activity in thiophene HDS: a promotion factor of 2 was achieved with respect to the non-promoted reference 10Re/G and 0.6Re/G catalysts containing ReS_2 (Fig. 1a). Similar results showing a significant improvement of activity due to addition of cobalt, were obtained for electrocatalytic HER. The references 1Co/G H_2S/H_2 and 1Co/G H_2S/N_2 demonstrated negligible activity in both reactions. By means of STEM-ADF microscopy we observed that the samples contained highly dispersed ReS_2 slabs and disordered ReS_x clusters. Though, neither electron microscopy, nor XPS or Raman study provided any information on the CoReS site. *Operando* XAS at Co K edge shows that though XANES of 1Co/G H_2S/H_2 and 1Co10Re/G H_2S/H_2 are expectedly similar, they demonstrate non-negligible differences at the pre-edge and above the edge. By means of DFT/FDMNES we constructed the possible structures of CoReS phase and simulated their XANES spectra (Fig. 1b). LCF fitting performed for 1Co10Re/G H_2S/H_2 suggests that Co species in this sample can be represented with 50% of 1Co/G H_2S/H_2, 20% of octahedral CoReS site and 30% of distorted tetrahedral CoReS site. As shows EXAFS fitting, the catalysts activated in different conditions (H_2S/H_2 vs H_2S/N_2) possess different proportions of octahedral and tetrahedral sites, with the predominance of tetrahedra for H_2S/H_2 and octahedra for H_2S/N_2. According to Re L edge *operando* spectroscopy, rhenium is invariably present as ReS_2 phase, which provides the edges for promoted CoReS sites.

In conclusion, for the first time we demonstrated the existence of highly active CoReS phase and proposed its structure based on the ensemble of computational and experimental characterizations. The real Co-Re-S/G catalyst contains 50 – 60% of sulfidic Co not involved in chemical interaction with Re and 40 – 50% of mixed CoReS sites with high activity.

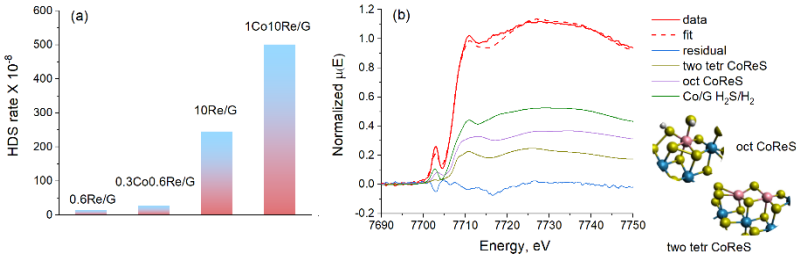

Figure 1. (a) Thiophene HDS rates for Re and CoRe catalysts sulfided in H_2S/H_2 at 320 °C, (b) LCF fitting for 1Co10Re/G H_2S/H_2.

Significance

This study shows for the first time formation of the promoted CoReS phase and might inspire further investigations on the structure of the CoReS species by means of other methods. By no means the application of such catalysts is limited by HDS or HER: their utilization can be extended to other reactions such as de-/hydrogenation, hydrodeoxygenation, photocatalytic HER etc.

References

1. T. A. Pecoraro et al, *J. Catal.* **1981**, *67*, 430
2. Y. Zhou et al, *ACS Nano.* **2018**, *12*, 4486
3. A. Rochet et al, *C. R. Chim.* **2016**, *19*, 1337
4. F. Caron et al, *J. Catal.* **2018**, *361*, 62
5. N. Escalona et al, *Appl. Catal.* **2005**, *287*, 47

OC4: H_2 activation, Hydrogenation of CO_2, propane

First observation of propylGa(III) active sites during non-oxidative propane dehydrogenation, by X-ray absorption spectroscopy

Jason A. Chalmers[1], Adam S. Hoffman[2], Fernando D. Vila[3], Simon R. Bare[2], and Susannah L. Scott[1,4]*

[1] *Department of Chemical Engineering, University of California, Santa Barbara, California 93106, United States.* [2] *Stanford Synchrotron Radiation Lightsource, SLAC National Accelerator Laboratory, Menlo Park, CA 94025, United States.* [3] *Department of Physics, University of Washington, Seattle, WA 98195, United States.* [4] *Department of Chemistry and Biochemistry, University of California, Santa Barbara, California 93106, United States.*

*sscott@ucsb.edu

Introduction

Non-oxidative propane dehydrogenation (PDH) is already used to produce >20 MMT propylene per year.[1] The annual demand for propylene is expected to increase from ca. 130 MMT today to 160 MMT by 2030, much of which will be supplied by PDH. Since the reaction is highly endothermic, it is important that propylene be made in the most efficient way possible. Ga has been investigated both as an active phase and a promoter in PDH catalysts.[2] Supported Ga catalysts can be highly selective (> 90 %) to propylene, although they are prone to deactivation. Despite many investigations, there is still much debate about the nature of the Ga active site(s), and how they evolve as the reaction proceeds. Like others before us, we interrogated their structures using *operando* X-Ray Absorption Spectroscopy (XAS). However, we started by establishing rigorous criteria for the use of XAS to determine the electronic structure and coordination of Ga.[3] Next, we applied these criteria to investigate Ga speciation in PDH conditions. Having clear and unambiguous signatures for the major Ga species makes it possible to detect and identify new Ga species generated under reaction conditions, and to correlate their abundance directly with the PDH rate.

Materials and Methods

Catalysts were synthesized by a pH-controlled impregnation method,[4] in which an aqueous solution of $Ga(NO_3)_3$ and citric acid were stirred with γ-Al_2O_3 at room temperature for 2 h. The pH of the slurry was initially adjusted to 10 with NH_4OH. The slurry was dried at 110 °C for 3 h, then calcined at 550 °C in O_2 (10 % in Ar) for 3 h.

Operando XAS measurements at the Ga K-edge were made in transmission mode at beamline 9-3 at the Stanford Synchrotron Radiation Lightsource. Catalysts were loaded into a specially-designed reactor[5] located between the first and second ionization chambers. The X-ray energy was calibrated by setting the maximum in the first derivative of the β-Ga_2O_3 spectrum to 10,375.1 eV. Each catalyst was heated to 600 °C in He, then the gas flow was switched to either H_2 or O_2 until the XANES was stable. The temperature was lowered to the reaction temperature (475 – 550 °C) and the feed was switched to propane (5 – 20 %, balanced in He, 30 mL/min, 1 atm). Hydrocarbon products were monitored with an online GC-FID (Agilent) and a Mass Spectrometer (Hiden).

Principal Component Analysis (PCA), Multivariate Curve Resolution with Alternative Least Squares (MCR-ALS), and Linear Combination Fitting (LCF) analysis were performed on the normalized Ga K-edge XANES spectra, over the range 10,340-10,420 eV.

Results and Discussion

Operando XAS data acquired during PDH for Ga/γ-Al_2O_3 pre-treated in H_2 show very large changes in Ga speciation during the first hour on-stream (Figure 1a). Analysis by MCR-ALS required three eigenspectra to describe the XANES. Chemical structures associated with these eigenspectra were identified by comparison to the XANES of known Ga materials (Figure 1b). Under PDH conditions, Ga(I) and $Ga(III)O_4$ co-exist as major species, with a minor fraction of propylGa(III) sites. The XANES of the minor sites closely resembles our previously-reported spectrum of $Ga(^iBu)_3$ grafted onto γ-Al_2O_3.[6] Linear combination fitting of the XANES as a function of time shows that the PDH rate is directly correlated with the fraction of these propylGa(III) sites (Figure 1c). This finding implicates propylGa(III) as a reactive intermediate in the catalytic cycle. Furthermore, the generation of propylGa(III) from Ga(I) indicates that oxidation of Ga(I) by propane may be an important step in catalyst activation. XANES recorded during PDH experiments at different temperatures, with and without co-fed H_2, and at different starting points of the Ga site distribution, allow us to optimize the fraction of these Ga sites and therefore the PDH activity.

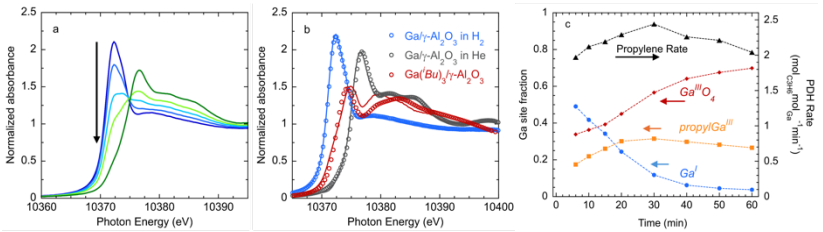

Figure 1. (a) Ga K-edge XANES for Ga/γ-Al_2O_3 recorded during the first hour of PDH in 20% propane at 475 °C, (b) comparison of eigenspectra (lines) and XANES reference spectra (points) used in the LCF, and (c) evolution of the PDH rate as a function of the fraction of each Ga species.

Significance

This study reports the first observation of a key alkylGa intermediate in the PDH catalytic cycle. It demonstrates the power of rigorous spectroscopic assignment and analysis, and provides a tool for studying mechanisms and adjusting the fraction of active sites.

References

1. Monai, M., Gambino, M., Wannakao, S., et al. *Chem. Soc. Rev.* **2021**, *50*, 11503.
2. Sattler, J.J.H.B., Ruiz-Martinez, J., Santillan-Jimenez, E., et al. *Chem. Rev*. **2014**, *114*, 10613.
3. Li, L., Chalmers J.A., Bare S.R., et al. *ACS Catal.* **2023**, *13*, 6549.
4. Getsoian, A., Das, U., Camacho-Bunquin, J., et al. *Catal. Sci. Technol.* **2016**, *6*, 6339.
5. Hoffman, A. S., Singh, J. A., Bent, S. F., et al. *J Synchrotron Rad*. **2018**, *25*, 1673.
6. Szeto, K. C., Jones, Z. R., Merle, N., et. al. *ACS Catal.* **2018**, *8*, 7566.

Tuning Ga-Sites and Acidity on Ga/Al_2O_3 Catalysts via H_2 Reduction or Co-Feeding: Insights into Propane Dehydrogenation Performance

Sebastian Amar-Gil[1], Catherine Especel[1], Francisco J. Passamonti[2], Viviana M. Benítez[2] and Florence Epron[1]*

[1]*CNRS, Université de Poitiers, Institut de Chimie des Milieux et Matériaux de Poitiers-IC2MP, Poitiers, France*

[2]*Instituto de Investigaciones en Catálisis y Petroquímica – INCAPE, Santa Fe, Argentina*

**florence.epron@univ-poitiers.fr*

Introduction

Propene, critical chemical for the production of various products, has growth its market demand in recent years. Propane dehydrogenation (PDH) offers an alternative method for the production of propene with economic benefits, but still faces challenges such as high costs, catalyst deactivation, and environmental concerns with Pt- and CrO_x-based catalysts.[1] Al_2O_3-supported Ga catalysts have shown promising selectivity, low toxicity, and cost. Tetracoordinated Ga3+ Lewis acid sites (LAS) have been proposed as active sites for PDH on Ga_2O_3-based catalysts,[2] where weak LAS drive propene formation, while Brønsted acid sites (BAS) favor by-product formation. Also, it has been demonstrated that Ga-hydrides are formed in the presence of the hydrogen produced during PDH, which may play a role on the reaction rate and the yield in propylene.[3]

For alumina-supported GaO_x catalysts, the hydride species and the state of Ga species after reduction have been thoroughly studied, but to our knowledge, acidity has only been studied before reduction, despite its importance on catalytic performance post-reduction. It would therefore seem that pre-treatment conditions, and the interactions between the support and the gallium, as well as test conditions have different impacts that need to be rationalized. In this work, the results obtained through a systematic study of the effects of H_2 co-feeding on Ga_2O_3/Al_2O_3 catalysts calcined or pre-reduced are presented.[4]

Materials and Methods

Ga_2O_3/Al_2O_3 catalysts, 5 wt.% Ga, were prepared via wet impregnation and calcination (Ga/Al), or calcination followed by reduction (Ga/Al_{red}). The materials were characterized in depth.[4] PDH reaction was carried out in a fixed-bed quartz reactor at atmospheric pressure at 575 °C for 4 h. The sample (100 mg) was pre-treated under N_2 (575 °C) or H_2 (650 °C, 1 h). The flow rate was kept constant at 100 mL min^{-1}, the concentration of C_3H_8 was fixed at 50 % balanced in N_2. H_2 co-feeding, 5 or 50%, was evaluated in the same conditions.

Results and Discussion

XRD and TEM analyses revealed that gallium species were well dispersed at the surface of the alumina support in all catalysts. Under the studied reaction conditions, i.e., high $C_3H_8/(N_2+H_2)$ ratio, adding 5% vol H_2 co-fed negatively impacted propane conversion and propylene in gas phase when the catalyst had not undergone reductive pretreatment before PDH. In contrast, reduction pretreatment before PDH reaction, performed in absence of H_2 co-feeding, reduced the activity (Figure 1 a, b). This decrease in activity was associated with a reduction in the amount of LAS, clearly observed by Pyridine-FTIR analysis, due to the decrease of GaO_x species at the surface of the catalysts. However, reduction pretreatment of the catalysts improved the propylene in gas phase, likely due to a reduction in the proportion of BAS (Figure 1 c), evaluated by an isomerization reaction test. TPR experiments revealed that reduction pretreatment performed at 650 °C could reduce a few Ga^{3+} species in Ga^{+}, approximately 3 %. In addition, the deactivation of the catalyst decreased as the amount of H_2 in the stream increased, linked to the constant recovery of active sites due to the removal of coke in the course of its formation, and the continuous formation of GaH_x sites on the surface of the catalyst as identified by FTIR analysis in the presence of hydrogen. Nevertheless, no direct relationship between the quantity of gallium hydrides species determined by FTIR on the catalysts and the catalytic performance in the propane dehydrogenation reaction was evidenced. The amounts of Lewis and Brønsted acid sites were demonstrated to be important parameter for good catalytic performance in terms of activity and production of propylene.

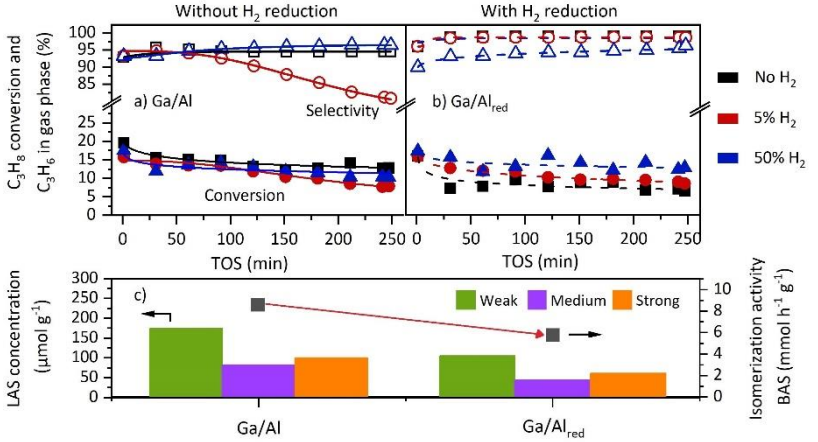

Figure 1. PDH at 575 °C under various H_2 co-feeding (5, 50 %) for a) Ga/Al and b) Ga/Al_{red}, c) Lewis acid sites (LAS) and Brønsted acid sites (BAS) evaluation for Ga/Al and Ga/Al_{red}.

Significance

Under harsh conditions (high propane flow rate), co-feeding H_2 enhances propane conversion and catalyst stability only if the Ga_2O_3/Al_2O_3 catalyst is reduced prior to the catalytic test. However, it does not have a beneficial effect on propylene formation.

References

1. A. Chernov, V. Sobolev, K. Koltunov. Catalysis Communications 170, 106495 (2022)
2. P. Castro-Fernández, D. Mance, C. Liu, et al. Journal of Catalysis 408, 155–164 (2022)
3. Y. Liu, G. Zhang, J. Wang, et al. Chinese Journal of Catalysis 42, 2225–2233 (2021)
4. S. Amar-Gil, C. Especel, F. Passamonti, et al. ChemCatChem Submitted, October 2024.

Pertinence of the assisted plasma catalysis for the valorization of CO_2 by hydrogenation

Nathan CORDIER[1*], Neha Choudhary[2], Patrick Da Costa2, Elodie Fourré[1] Catherine Batiot-Dupeyrat[1]

[1]*Institut de Chimie des Milieux et Matériaux de Poitiers (IC2MP), UMR-7285, Poitiers, France*

[2]*Sorbonne University, Institut Jean Le Rond D'Alembert (IJLRA), UMR 7190, St Cyr l'Ecole, France*

*nathan.cordier@univ-poitiers.fr

Introduction

Even though the current environmental politics are targeting the complete elimination of the CO_2 emissions from industrial and domestic origin, these goals won't be attained before the complete makeover of these sectors. During the transition period the CO_2 emissions could be limited by its utilization as a new carbon source, but due to its refractory characteristics the thermal catalysis isn't efficient enough to propose a cost-effective solution. The activation of small refractory molecules is exactly where the plasma activated catalysis shines, by both a low temperature activation and increased activity. But this activation ability is a double-edged blade, a lack of selectivity in plasma alone is often observed rendering the process unfitting for most applications. The widely adopted solution is the introduction of a catalyst inside the discharge, creating a plasma/catalyst synergy increasing both activity and selectivity [1]. This technology could be the key to CO_2 valorization, the objective pursued in this work is the formation of the C-C bond for the energy storage under the form of hydrocarbons. The main steps are the methanation reaction (1) followed by the methane coupling (2):

(1) $CO_2 + 4H_2 \rightarrow CH_4 + 2H_2O$

(2) $xCH_4 \rightarrow C_xH_y$

The current objective is the completion and control of the first reaction to perform the methane coupling in optimized condition as this last reaction is the most difficult to perform. The deep understanding of this reciprocal synergy between the catalyst and the discharge is essential to reach the optimized conditions both chemically and energetically. To achieve this objective the first step is the matching of performances with the best results from the literature. This is why the catalyst 15%wt. $Ni/Ce_{0.5}Zr_{0.5}O_2$ 4% Gd doped [2] was adopted as a benchmark for performances of the system. During testing, this catalyst displayed very good performances in the methanation reaction, reaching up to 85 % CO_2 conversion and near 100% selectivity matching the performances of the literature. Surprisingly, during the catalytic tests, traces of ethane were observed enabling us to make both a step in high performance methanation reaction and in the methane coupling. That why a deeper exploration and optimization of this catalyst was undertaken in sight of either designing a catalyst able to perform both reactions or a second independent catalyst optimized by the obtained knowledge.

Materials and Methods

A quartz DBD (Dielectric Barrier Discharge) type reactor was used with a discharge volume of 0.568 mm^3 and 22.3 mm in length. The discharge is modulated by a TTi TG1010A function generator coupled to a TREK model 30/20A amplificatory and the signals are recorded on a Wavesurfer 3054 z. The composition of the effluent is analyzed by a Scion He/H_2 Analyzer, PGA analyzer GC. The catalysts are completely synthesized in the laboratory, the supports are synthesized through the sol gel route and the metal are deposited via simple impregnation method. A flow of 50mL/min composed of a ratio 20:80 of CO_2:H_2 was used in all experiments and a power of 7.5 W at a frequency of 6.5 kHz was used for the catalytic tests.

Results and Discussion

High conversions of CO_2 along near 100% methane selectivity were obtained for the 3 temperatures studied as illustrated in the Fig. 1 along with the presence of ethane as a co-product. The comparison between the different nickel-based catalysts (Figure 1) is enabling us to determine that a real synergy is taking place. The pertinence of plasma assisted catalysis is highlighted when compared by conventional thermal catalytic. Furthermore, by comparing XRD and TPR analyses pre- and post-experiments, an effect of the plasma on the surface of catalyst can be observed, the comprehension of this modification could enable to tune the catalyst toward even more effective materials.

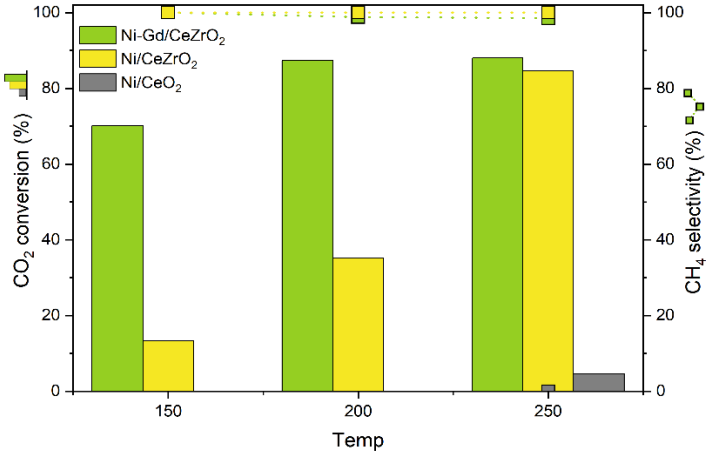

Figure 1. Conversion vs. temperature for Nickel based catalyst for different support and doping agents at 7.5 W under DBD.

Significance

The ability to form C-C bonds from CO_2 could shift its perception from waste to a valuable resource, enabling the establishment of a sustainable CO_2 utilization cycle.

References

[1] A. Bogaerts *et al.*, « The 2020 plasma catalysis roadmap », *J. Phys. Appl. Phys.*, vol. 53, n° 44, p. 443001, août 2020, doi: 10.1088/1361-6463/ab9048.

[2] M. Mikhail *et al.*, « Tailoring physicochemical and electrical properties of Ni/CeZrOx doped catalysts for high efficiency of plasma catalytic CO2 methanation », *Appl. Catal. B Environ.*, vol. 294, p. 120233, oct. 2021, doi: 10.1016/j.apcatb.2021.120233.

Insight into MoS_2 structure on the activity for CO_2 hydrogenation into syngas: A step towards H_2 economy

Oumayma Liaaychi[1,2]*, Amanda Sfeir[2], Pascal Blanchard[2], Christine Lancelot[2], Carole Lamonier[2], Said Laassiri[1], Jean-Philippe Dacquin[2], Sébastien Royer[2]

[1]*CBS-GPE, Mohammed VI Polytechnic University, 43150 Ben Guerir, Morocco;*

[2]*Unité de Catalyse et Chimie du Solide, UMR 8181, Université de Lille, CNRS, Centrale Lille, ENSCL, Université d'Artois, F-59000 Lille, France*

** E-mail: oumaima.liaaychi@um6p.ma*

Introduction

The hydrogenation of CO_2 using green hydrogen is a promising strategy for mitigating greenhouse gas emissions.[1] Various methods for converting CO_2 into valuable chemicals like methane, carbon monoxide, and methanol have been studied, with the reverse water-gas shift (RWGS) reaction being particularly important for producing CO, which serves as an intermediate for synthesizing chemicals and fuels. From a thermodynamic aspect, producing CO selectively remains highly challenging as the endothermic nature of RWGS reaction implies high operating temperatures (800°C) while at low temperature concurrent CO_2 methanation is favored (<500°C).[1] Transition metal dichalcogenides (TMDCs), such as MoS_2, have gained interest for their ability to activate CO_2 at temperatures below 200 °C.[2] Early in 1997, Osaki et al.[3] investigated the catalytic performance of metal disulfide catalysts for CO_2 hydrogenation. The MoS_2 catalyst exhibited high selectivity towards the reverse water-gas shift (RWGS) reaction, effectively converting CO_2 and H_2 into CO and H_2O.

In this study, we highlight the remarkable impact of dispersing the MoS_2 phase on SBA-15, significantly improving its reactivity for the hydrogenation of CO_2. The catalytic performance of MoS_2/SBA-15, with only 10% MoS_2 loading, was evaluated with respect to bulk MoS_2 over a temperature range of 200-800°C. The typically favourable formation of CH_4 at lower temperatures was entirely suppressed for both catalysts, leading to complete selectivity towards CO formation. Post-reaction characterization revealed that the MoS_2 phase underwent transformation to the Mo_2C phase under the reaction conditions (**fig.1**).

Figure.1. Dynamic transformation of MoS_2 catalysts to Mo_2C phase under RWGS reaction

Materials and Methods

MoS_2/SBA-15 was synthesized through gas-phase sulfidation of MoO_3/SBA-15 using 10% H_2S/H_2, while bulk MoS_2 was produced via a classical hydrothermal method involving $(NH_4)_6Mo_7O_{24}•4H_2O$ and thiourea. The mixed solution was heated at 200 °C for 24 hours in an autoclave. The catalysts were characterized using XRD, N_2-physisorption, SEM, HAADF-STEM, Raman spectroscopy, XPS, and H_2-TPR techniques.

Results and Discussion

XRD analysis confirmed the formation of MoS_2, with the absence of the (002) peak at 14.4° for MoS_2/SBA-15 suggesting the formation of few-layer or predominantly monolayer MoS_2 (**fig. 2a**). Raman spectroscopy showed characteristic peaks at 378 and 402 cm^{-1}, indicating the presence of Mo–S in-plane and out-of-plane phonon modes (**fig. 2b**). MoS_2/SBA-15 exhibited a higher specific surface area (522 m^2/g) compared to bulk MoS_2 (10.5m^2/g) (**fig. 2c**). Morphological analysis revealed flower-like structures for bulk MoS_2, whereas MoS_2/SBA-15 had finely dispersed, petal-like MoS_2 structures, providing better exposure of active sites (**fig. 3c**).

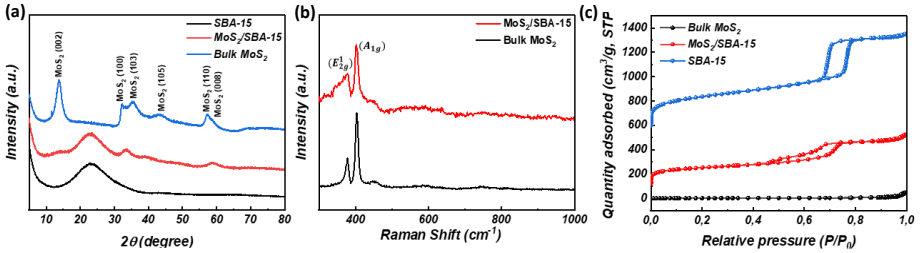

Figure.2. (a) XRD, **(b)** Raman, and **(c)** N2 physisorption isotherms for Supported and Bulk MoS_2

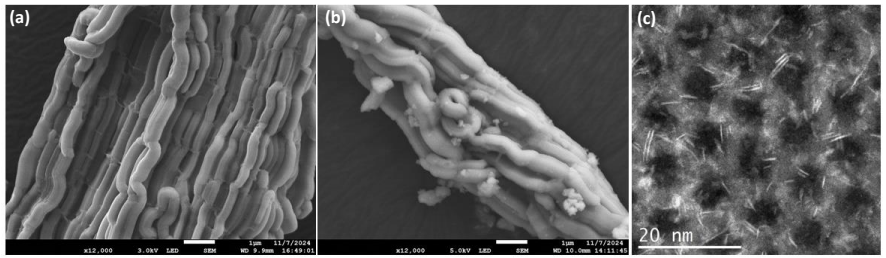

Figure.3. SEM images of (a) SBA-15, (b) and MoS2/SBA-15, (c) STEM-HAADF of MoS2/SBA-15

The MoS_2/SBA-15 catalyst demonstrated significantly enhanced catalytic activity, achieving a CO_2 conversion rate of 63% at 600 °C, compared to the bulk MoS_2 catalyst, which showed only 39% conversion under the same conditions. Furthermore, the 10%MoS_2/SBA-15 catalyst exhibited high stability, maintaining performance for over 100 hours at 800 °C.

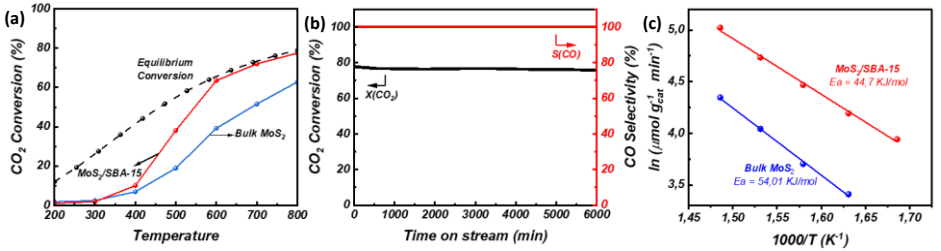

Figure.4. (a) CO_2 conversion, (b) stability test of the MoS_2/SBA-15, (c) Arrhenius plot for the RWGS reaction over MoS_2/SBA-15 and Bulk MoS_2.

Significance

The work presented in this study holds both industrial and fundamental significance of paramount importance related to (i) the effort for the development of novel approaches for greenhouse gas mitigation and (ii) providing useful insight into the correlation between physicochemical properties of the catalysts and their catalytic activity which is of high importance for the design of novel generation of catalysts for CO_2 Hydrogenation.

References

1. W. Jin Lee, C. Li, H. Prajitno, J. Yoo, J. Patel, Y. Yang and S. Lim, Catal Today, 2021, 368, 2–19.
2. J. Hu, L. Yu, J. Deng, Y. Wang, K. Cheng, C. Ma, Q. Zhang, W. Wen, S. Yu, Y. Pan, J. Yang, H. Ma, F. Qi, Y. Wang, Y. Zheng, M. Chen, R. Huang, S. Zhang, Z. Zhao, J. Mao, X. Meng, Q. Ji, G. Hou, X. Han, X. Bao, Y. Wang and D. Deng, Nat Catal, 2021, 4, 242–250.
3. T. Osaki, N. Narita, T. Horiuchi, T. Sugiyama, H. Masuda and K. Suzuki, J Mol Catal A Chem, 1997, 125, 63–71.

Batch heterogeneous catalytic selective hydrogenation of vegetable oils: regression of kinetic parameters from pseudo-first-order to detailed reaction mechanisms

Andrea Di Giuliano[1,2]*, Enza Pellegrino[1], Nicoletta Cancrini[1], Katia Gallucci[1]
[1]*Department of Industrial and Information Engineering and Economics, University of L'Aquila, 67100 L'Aquila, Italy*
[2] *Institut de chimie et procédés pour l'énergie, l'environnement et la santé, CNRS UMR 7515 - University of Strasbourg, 25 rue Becquerel, 67087 Strasbourg Cedex 2, France – (Invited researcher)*
*andrea.digiuliano@univaq.it

Introduction

Vegetable Oils (VO) contain mainly fatty acids with 18 carbon atoms and "i" unsaturations (C18:i in general, linolenic C18:3, linoleic C18:2, oleic C18:1, stearic C18:0). C18:i can become molecules of added-value for sustainable purposes, e.g., as building blocks for bio-plastics or bio-lubricant components[1]. Oleic acid (C18:1) is of industrial interest thanks to its higher chemical stability and lower solidification point in comparison to other fatty acids[1]. The Heterogeneous Catalytic Selective Hydrogenation (HCSH) of VO can maximize the fraction of C18:1 in a VO bulk [1].

Experimental data of HCSH of canola oil in batch reactor were taken from literature[2] and considered in this work. A modelling study was previously carried out by this research team[3] on those data[2], adopting reaction schemes based on pseudo-first-order kinetics for hydrogenation of double bonds: it turned out that experimental data could be properly regressed only by the hypothesis of two subsequent pseudo-first-order kinetic regimes, each one with its own kinetic constants; one was valid before maximization of C18:1, the other after this point[3]. This was associated with mechanistic details of different adsorption interactions between Lindlar catalyst and different C18:i [3,4]. In this work, a more in-depth analysis of reaction mechanisms is aimed, by overall-regression-approach of Bernas et al. [5].

Materials and Methods

Three tests from literature[2] were considered, all with: initial 200 mL of canola oil as the feedstock; 4 mg of commercial Lindlar catalyst (Sigma-Aldrich, 4-5% of metallic palladium on calcium carbonate, poisoned with PbO) per mL of canola oil; constant impeller rotation rate (650 rpm, the highest allowed in the reactor); different combinations of temperature (T) and H_2 pressure (p_{H2}) (Table 1); proper duration to observe the evolution of phenomena (t_{fin}, Table 1). Data were expressed as relative molar fractions of the four fatty acids C18:i (X_i), determined off-line by gas-chromatographic methods on sampled oil[2].

Table 1. Conditions of batch tests for heterogeneous catalytic selective hydrogenation

Test	T / °C	p_{H2} / MPa	t_{fin} / h
03	120 ± 5	0.8	6
04	180 ± 5	0.4	6
05	180 ± 5	1.2	5

The mass balances on the batch test system were formulated for the components C18:3, C18:2, C18:1, C18:0, imposing at each regression the expression of reaction rates resulting from the hypothesis of different reaction mechanisms (varying several features, e.g.: Hinshelwood-Langmuir or Eley-Riedal approaches; competition or not for active sites between H_2 and fatty acids; dissociative or molecular adsorption of H_2). Statistical indicators of the quality of regression were calculated and used to select the most plausible mechanism, such as determination coefficient R^2. All calculation were performed by MATLAB ®.

Preliminary Results and Discussion

As an example of mechanisms to be investigated, the one in Figure 1(a) involves elementary steps of non-competitive adsorption on sites Z for fatty acids and Z' for H_2, non-dissociative adsorption of H_2 on Z', direct Hinshelwood-Langmuir hydrogenation of unsaturated C18:i to C18:(i-1), adsorptions and desorptions in equilibrium.

The resulting regression functions (solid lines in Figure 1(b)) are compared to experimental data (points in Figure1(b)). The regression procedure of the kinetics parameters gave an overall R^2 of 0.99 on the data of the tests 03, 04, 05. The proposed mechanism is a good candidate to better interpret the selective hydrogenation of vegetable oil, in comparison with the approach of successions of different pseudo-first-order kinetic regimes during the same reactions, previously proposed by this research team[3] .

1) $Z' + H_2 \overset{K_1}{\leftrightarrow} Z'{-}H_2$
2) $Z + C18{:}3 \overset{K_2}{\leftrightarrow} Z - C18{:}3$
3) $Z + C18{:}2 \overset{K_3}{\leftrightarrow} Z - C18{:}2$
4) $Z - C18{:}3 + Z' - H_2 \overset{k_4}{\rightarrow} Z - C18{:}2 + Z'$
5) $Z - C18{:}2 + Z'{-}H_2 \overset{k_5}{\rightarrow} Z - C18{:}1 + Z'$
6) $Z - C18{:}1 + Z' - H_2 \overset{k_6}{\rightarrow} C18{:}0 + Z + Z'$
7) $Z - C18{:}1 \overset{K_7}{\leftrightarrow} Z + C18{:}1$

(a)

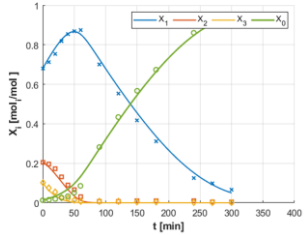

(b)

Figure 1. (a) Mechanism for the kinetic modelling of HCSH of VO; (b) Regression by batch reactor model with mechanism in (a), on experimental data from Test 05 (Table 1): solid lines are regressed functions (C18:3 yellow, C18:2 orange, C18:1 blue, C18:0 green); points are experimental data (C18:3 yellow ◊, C18:2 orange □, C18:1 blue x, C18:0 green ○).

Significance

The refinement of the kinetic modelling of the investigated reaction may help in simulative scale-up studies for industrial maximization of C18:1 production in different process configurations.

References

1. R. Uppar et al., *Environ. Dev. Sustain.* **2023**, *25*, 9011–9046
2. U.P. Laverdura et al., *ACS Omega* **2020**, *5*, 22901–22913
3. E. Pellegrino et al., Chem. Eng. J. **2024**, *488*, 150802
4. S. McArdle et al., *J Mol Catal A Chem*, **2021**, *351,* 179–187
5. A. Bernas et al., *Appl Catal A Gen,* **2009**, *353*, 166–180.

OC5: Structure, DFT, Simulation

Thermodynamic and kinetic origins of platinum single atoms supported on chlorinated γ–Al_2O_3: from calcined to reduced states

A. Hellier[1], A. T. F. Batista[1], C. Legens[1], A.-S. Gay[1], A. Aguilar Tapia[2], O. Proux[3], J.-L. Hazemann[4], Y. Joly[4], W. Baaziz[5], O. Ersen[5], C. Chizallet[1,*], P. Raybaud[1,6]

[1]*IFP Energies nouvelles, Rond-point de l'échangeur de Solaize, 69360 Solaize, France*
[2]*ICMG, UAR 2607 CNRS Université Grenoble Alpes, F-38048 Grenoble France*
[3] *OSUG, UAR 832 CNRS-Université Grenoble Alpes, F-38041 Grenoble, France*
[4]*Institut Néel, UPR 2940 CNRS Université Grenoble Alpes, F-38000 Grenoble, France*
[5]*IPCMS, CNRS-Université de Strasbourg, 67034 Strasbourg, France*
[6]*ENS Lyon, CNRS, Laboratoire de Chimie UMR 5182, 46 Allée d'Italie, 69364 Lyon, France*
*celine.chizallet@ifpen.fr

Introduction

Platinum (Pt) based catalysts supported on γ–alumina (γ–Al_2O_3) are used in a great variety of industrial chemical processes, including refining and biomass conversion. The activation steps (calcination and reduction) of these catalysts involve the transformation of oxidized mononuclear platinum precursors into a reduced active phase which may contain low nuclearity Pt clusters and Pt single atoms. However, deciphering the nature of these Pt SA species (oxidation state, type of ligands) and their transformation mechanisms during activation steps remain challenging, particularly in the presence of chlorine. By combining HR-electron microscopy, X-ray absorption spectroscopy (XAS) and density functional theory (DFT) calculations, we identify the thermodynamic and kinetic origins of oxidized[1] and reduced Pt SA formed during activation. We also reveal how chlorine enhances the stability of the Pt SA species, and how it impacts their structural and energetic features.

Materials and Methods

The catalysts samples (0.3 wt% Pt and 0.1 or 1.4 wt% Cl) were prepared[2] by diffusional impregnation of γ-Al_2O_3 extrudates (PuralSB3™) with a H_2PtCl_6 and HCl solution, followed by drying overnight and calcination at 520 °C for 2 h under dry air. These oxide catalysts were then reduced under H_2 flow at 500°C for 2h. High-resolution high-angle annular dark field in scanning transmission electron microscopy (HR-HAADF-STEM) imaging was carried out on a Cs-corrected JEOL JEM 2100F microscope, operated at 200kV, equipped with a JEOL HAADF detector. Pt L_3-edge XAS spectra, including both EXAFS and HERFD-XANES spectra, were acquired at the FAME-UHD beamline at ESRF. The thermodynamic stability and kinetic mechanisms were studied through a systematic determination of free energy profile by DFT calculations with VASP.[3] The catalysts were modelled by considering various $Pt(OH)_xCl_{4-x}(H_2O)_y$ anchored on the γ–Al_2O_3 (100) surface under various reaction conditions. The XANES simulation at Pt L_3-edge for the oxidized species obtained after calcination was undertaken with the FDMNES package.[4]

Results and Discussion

After calcination, EXAFS (including wavelet analysis) and HR-HAADF-STEM characterization revealed that oxidized Pt catalysts exhibit predominantly oxychlorinated Pt SA. In agreement with EXAFS, the thermodynamic DFT study of these Pt SA species shows that octahedral $Pt(OH)_xCl_{4-x}(H_2O)$ in interaction with the alumina surface are present. The first ligands' sphere of Pt depends on H_2O partial pressure and chlorine content, itself monitored by HCl pressure. Moreover, the simulated XANES spectra at the Pt L_3 edge for these complexes match well with the experimental HERFD-XANES. More quantitatively, they reveal that the bump feature observed between 11575 eV and 11585 eV (post-edge signal) is a tracer of the amount of Cl coordinated to Pt SA (Fig. 1 a). A quantitative comparison of the local structures of Pt SA obtained by EXAFS, XANES and DFT is finally provided.

After reduction, HR-HAADF-STEM highlights the presence of Pt nano-clusters and Pt SA (Fig. 1 c) whose respective proportion depends on the chlorine content. Starting from the most relevant oxychlorinated Pt SA models stabilized after calcination, we simulate by DFT their reduction mechanisms into Pt^0 SA (Fig 1 b). We find that chlorine enhances the thermodynamic stability of Pt^{II} SA intermediate, such as square planar $PtCl_2$ and HPtCl, anchored on γ–Al_2O_3 site by increasing the reduction temperature. Moreover, from a kinetic point of view, chlorine hardens Pt^{II} reduction into Pt^0 by increasing the activation barrier up to 174 kJ/mol for $PtCl_2 \rightarrow$ Pt and by involving a HPtCl intermediate strongly stabilized on the support. In addition, an easy diffusion of $PtCl_2$ onto an alumina surface site is computed, where $PtCl_2$ cannot be reduced. Conversely, for non-chlorinated oxidized Pt species, the activation barrier for reduction is lower and the one for diffusion to the SA stabilizing site is higher (Fig. 1.b)) which explains the higher proportion of Pt SA observed experimentally in the presence of chlorine.

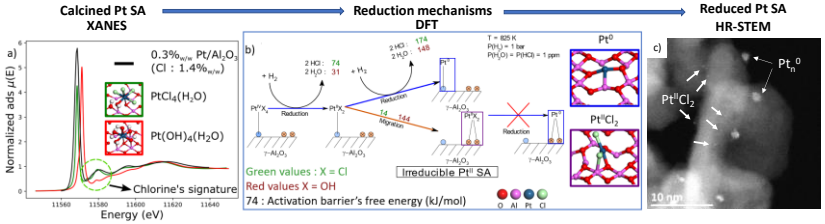

Figure 1. a) Comparison of experimental and computed XANES spectra of calcinated catalyst. Experimental spectrum is in black while simulated spectra are in green and red. b) DFT scheme of the chlorine impact on the kinetics of platinum reduction. Relevant molecular models of Pt SA on the (100) γ–Al_2O_3 surface are illustrated in insets. c) HR-HAADF-STEM picture of the reduced catalyst.

Significance

Our study provides experimental and theoretical insights into the origin of platinum single atoms present on the γ–alumina support and how it can be modulated by chlorine. It paves the way to better control of the properties of Pt/γ–Al_2O_3 catalysts by tuning activation conditions.

References

1. A. Hellier, et al. , *J. Catal*. **2024**, 429, 115212.
2. A.T.F. Batista, et al. *ACS Catal*. **2020**, 10, 4193; Nanoscale **2022**, 14, 8753.
3. G. Kresse, J. Hafner *Phys. Rev. B* **1994**, 49, 14251
4. O. Bunău, Y. Joly, *J. Phys.: Condens. Matter* **2009**, 21, 345501

Relationships between Structure, Stability and Size of Pd Nanoparticles Investigated by Ab Initio Models

Emmanuel IKWA[1,2]*,Mickael RIVALLAN[1],Thibaud NARDIN[1],Antoine HUGON[1],David LOFFREDA[2]
[1]*IFP Energies nouvelles, Rond-point de l'échangeur de Solaize, BP 3, 69360 Solaize, France*
[2]*CNRS, ENS de Lyon, UCB Lyon 1, LCH, UMR 5182, 69342, Lyon cedex 07, France*
*emmanuel.ikwa@ifpen.fr

Introduction

Metallic **n**ano**p**article**s** (**NPs**) play a crucial role in many heterogeneous catalytic processes.[1] Among them, Pt- and Pd-based NPs are widely used in the energy sector. At the level of chemical reactivity, the key role of the surface metallic coordination change has been suggested many times in the literature.[1] At an industrial scale, the reduction of required resources is a long-time quest, particularly the use of small NPs, which exhibit preponderant lowly-coordinated surface atoms. In this context, being able to establish the relationships between shape, stability and size of these NPs in operating conditions is a prerequisite for the design of cost-efficient catalytic processes.[2,3]

In theoretical literature, these relationships are usually studied by global optimization approaches and empirical interatomic potentials[4] for Pt and Pd NPs in vacuum. Studies with more accurate computational methods such as DFT are scarce, especially for NPs of several nanometers.[3] In the case of Pd, there is no study dealing with ab initio models of large NPs up to date. Therefore, in this work, we introduce DFT models of high-symmetry structures of **Pd NPs**, by examining relationships between crystallinity, size, shape and stability.

DFT Methods

Geometry optimizations were performed by using VASP[5] in accurate computational conditions (large 3D box and tight convergence criteria). The choice of the electronic exchange-correlation function was based on a careful comparative analysis of the predictions of standard GGA and van der Waals corrected functionals. Spin polarization was also considered. **Six different high-symmetry morphologies**[3] (Mackay-icosahedral, FCC cuboctahedral, FCC truncated octahedral (**TO**), decahedral, ino-decahedral, Marks-decahedral) were selected to model Pd NPs in the range 7–1415 atoms (0.5 nm – 3.9 nm). Mackay-icosahedral, decahedral, ino-decahedral and Marks-decahedral NPs are not crystalline, while FCC NPs are.

Results and Discussion

At the level of benchmarking functionals, standard GGA PBE and van der Waals PBE TS IHP functionals showed the best compromise in predicting structural, energetic, magnetic and compressibility properties of the Pd bulk. Concerning the different morphologies of NPs, we explored ordered structures in a quite exhaustive way, leading to sets containing from 6 to 11 NPs (see the corresponding calculated points in **Figure 1**). To investigate the stability order, the total cohesion energy (E_{coh}) of Pd NPs normalized to the total number of atoms **N** was systematically computed for the considered structures. By linearizing E_{coh} as a function of the different types of atoms present in the NPs, one can plot the stability against $N^{-1/3}$. Thanks to linear correlations, we can assess the relative stability of different set of morphologies.

Figure 1 shows the GGA PBE results without spin polarization. At this level of calculation, the **TO** morphology appears as the most stable one starting from 79 atoms. For smaller clusters there is a competition between non-crystalline Marks-decahedral clusters, presenting lateral concavities, and crystalline convex **TO** clusters. Cuboctahedral, icosahedral and decahedral clusters are never competitive in the explored range of sizes. Interestingly, these conclusions do not change when magnetism and dispersion (van der Waals interactions) are considered in the DFT models.

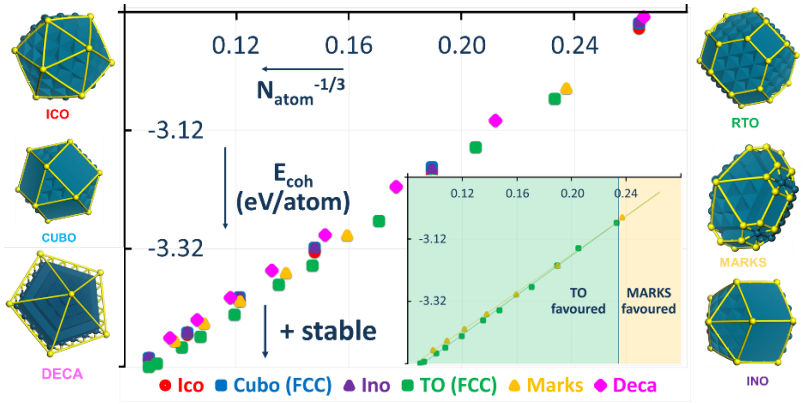

Figure 1. Pd NPs DFT models: evolution of the normalized E_{coh} against $N^{-1/3}$. Linear correlations for Marks and TO morphologies are reported as they are the most stable ones.

Significance

Among ordered structures, we suggest the **crystalline character** of Pd NPs larger than 79 atoms (ca. 1.20 nm) therefore concluding on an early transition between Marks-decahedra and TO clusters, in apparent contradiction with previous results based on global optimization methods and effective interatomic potentials (above 10^3 atoms).[4] Our conclusions agree with EXAFS analyses showing FCC core regions of Pd NPs bigger than 1.3 nm.[6] Additionally, the impact of magnetism and dispersion on Pd NPs seems to be minimal considering the relative stability, supporting the robustness of the study. An article will soon summarize these assessments,[7] and further work considering the catalytic properties of Pd NPs in the context of new energy carriers and sustainable developments are in progress.

References

1. J.K. Nørskov *et al.*, *Chem. Soc. Rev.*, **2008**, *37,* 2163-2171
2. N. Tarrat & D. Loffreda, *Environ. Sci. Nano*, **2023**, *10, 7,* 1754-1767
3. J.E.M. Cardona *et al.*, *J. Phys. Chem. C.*, **2023**, *127, 36,* 18043-18057
4. F. Balleto *et at.*, *J. Chem. Phys.*, **2002**, *116, 9,* 1856-2863
5. G. Kresse & J. Furthmüller, *Phys. Rev. B*, **1996**, *54, 16,* 11169-11186
6. V.V. Srabionyan *et al.*, *J. Phys. Chem. Solids*, **2014**, *75, 4,* 470-476
7. E. Ikwa *et al.*, *J. Phys. Chem. Lett.*, **2024**, *in preparation*

Periodate activation by zero valent iron particles embedded into nitrogen rich biochar for bisphenol A degradation: efficiency and mechanism

Jin Kang[1,2]*, Jean-Philippe Dacquin[2], Sébastien Royer[3], Hui Zhang[1]

[1] *Environmental Catalysis Laboratory, Wuhan University, 430000 Wuhan, China*

[2] *Unité de Catalyse et Chimie du Solide, UMR 8181, Université de Lille, CNRS, Centrale Lille, ENSCL, Université d'Artois, F-59000 Lille, France*

[3] *Université Littoral Côte d'Opale, UR 4492, UCEIV, Unité de Chimie Environnementale et Interactions sur le Vivant, Dunkerque, F-59140 France*

*jin.kang@univ-lille.fr

Introduction

Endocrine Disrupting Chemicals (EDCs) have aroused significant concerns due to their adverse effects on aquatic ecosystems and human health.[1] Periodate-based advanced oxidation processes (PI-AOPs) are an effective method for producing reactive species to degrade EDCs[2] Many researchers reported that PI can be converted to iodate (IO3−) through an oxygen-atom transfer process without forming toxic byproducts.[3] Fe-based transition metal activators are commonly used in PI-AOPs because their low cost and excellent activation efficiency. However, Fe leaching from these catalysts causes secondary pollution, highlighting the need for alternatives. In this study, Fe particles embedded in nitrogen-rich biochar (NBC) were synthesized via a simple pyrolysis method using corn straw and metal–organic frameworks as precursors. This work not only provides an efficient PI-AOPs system for wastewater decontamination, but also offers significant insights into the oxidation mechanism of PI-AOPs.

Materials and Methods

FeC@NBC were prepared by a one-step facile pyrolysis method using corn straw as precursor of NBC and MOF-Fe as iron source. BPA was analyzed by a high-performance liquid chromatography (HPLC, Shimadzu LC-20A, Japan) with a C-18 column. The optimization of the calculation model was used the DMol3 package of Material Studio software.

Results and Discussion

The surface morphology and structure of FeC@NBC were analyzed using SEM and TEM images (Fig. 1). TEM-EDS mapping confirmed the presence of Fe, C, N, and O in FeN@BC (Fig. 1c). XRD analysis (Fig. 2a) indicated that Fe species were mainly in the Zero Valent Iron state. N_2 adsorption-desorption isotherms (Fig. 2b) showed that all catalysts had a mesoporous structure. Raman spectra (Fig. 2c) revealed that FeC@NBC had a higher ID/IG ratio than Fe@NBC, indicating more defects in its carbon structure, which is linked to its more uniform loading on biochar surfaces.

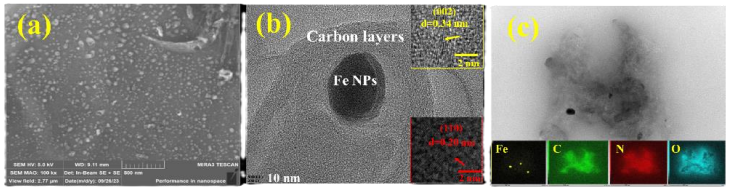

Fig. 1 (a) SEM image, (b) TEM images, (c) EDS mapping of the FeC@NBC

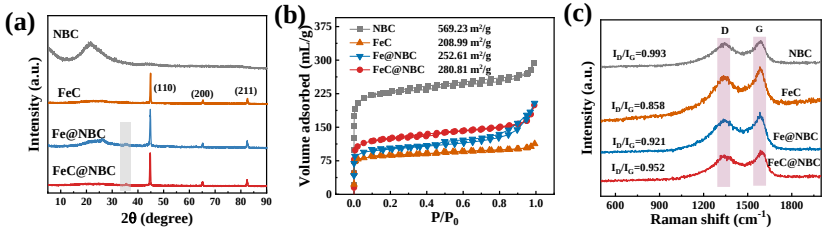

Fig. 2 (a) XRD, (b) BET and (c) Raman of catalysts

The degradation experiments indicating that PI could not degrade BPA. When FeC@NBC and PI coexist, 98.7% of BPA was degraded after 30 min reaction (Fig. 3a). The quenching experiments and EPR confirmed that BPA was oxidized via electron-transfer process and IO3• (Fig. 3b, c). Due to the formation of metal embedded in the biochar structure, the metal leaching concentration in the system is below 0.1 mg/L even after five cycles of testing. Last, Theoretical calculations (Fig. 4) revealed that PI adsorption on FeC@NBC had a higher charge density than on NBC, suggesting enhanced electron transfer, which facilitated the oxidation of PI at electron-deficient sites.

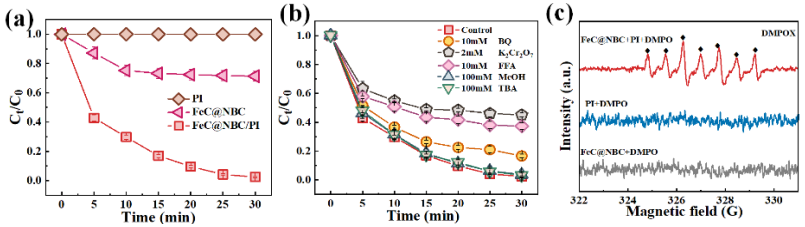

Fig. 3 (a) BPA degradation, (b) quenching experiments (c) EPR. Conditions: [catalysts]=0.1 g/L, (d) metal leaching experiment, [PI] = 1 mM, BPA=0.02mM, pH=7

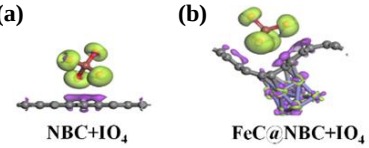

Fig. 4 Theoretical calculations simulate the adsorption of PI molecules over the NBC (a) and FeC@NBC (b)

Significance

This work opens up a new perspective for cost-effective biochar waste recycle and broadens out the avenue for PI-based AOPs in the treatment of refractory organic micropollutants.

References

1. B. Petrie, R. Barden, B. Kasprzyk-Hordern, *Water Res*, 72 (2015) 3-27.
2. E.T. Yun, H.Y. Yoo, W. Kim, H.E. Kim, G. Kang, H. Lee, S. Lee, T. Park, C. Lee, J.H. Kim, J. Lee, *Appl Catal B-environ*, 203 (2017) 475-484.
3. Y. Yao, H. Chen, J. Qin, G. Wu, C. Lian, J. Zhang, S. Wang, *Water Res*. 101 (2016) 281–291.

Influence of nanocrystals morphology in the stabilization of oxidized Pt single atoms on γ-Al_2O_3

M. Cotoni[1]*, F. Moreau[1], L. Lemaitre[1], M. De Mello Timm[1], V. Rouchon[1], D. Gioffrè[2], A. Cabiac[1], C. Bouchy[1], C. Copéret[2], C. Chizallet[1]

[1]*IFP Energies nouvelles, Rond-point de l'échangeur de Solaize, 69360, Solaize, France*

[2]*Department of Chemistry and Applied Biosciences, ETH Zürich, CH-8093 Zürich, Switzerland*

**martin.cotoni@ifpen.fr*

Introduction

Platinum catalysts supported on γ-Al_2O_3 are key players in a variety of industrial applications. Interaction of platinum atoms with the γ-Al_2O_3 surface sites is expected to impact the platinum dispersion, which in turn affects the catalytic properties. Notably, despite decades of research, the presence of Pt single atoms (Pt_1) has only been recently identified[1] and the location of their anchoring sites for these platinum single atoms remains an open question. The combination of experiments and DFT calculations has revealed that some properties of the support play a crucial role in stabilizing Pt_1. For instance, the presence of unsaturated penta-coordinated Al^{3+} ions[1] on specific crystallographic facets[2] of the support have been proposed as a key factor for stabilization of platinum. However, surface hydroxyls at the edge of faces may also play a major role in stabilizing single atoms. Here, we investigate key factors that favor the formation of single atoms prepared using surface organometallic chemistry, with the combination of ^{1}H MAS-NMR and high-resolution microscopy as characterization methods.

Materials and Methods

We selected two aluminas samples: 1) a commercial boehmite (Dequagel/F-Dequachim), presenting ill-defined nanocrystals (denoted D), and 2) a recently reported one[3], presenting well-defined needle-shape nanocrystals (denoted N). The two γ-Al_2O_3 were first prepared by calcination of boehmite samples at 600 °C (6h - 1°C/min ramp), followed by a dehydration under high vacuum at 500 °C (8h - 5 °C/min ramp). The density of surface hydroxyl groups of each support was then measured by titration with a Grignard reagent $MgBn_2$[4]. Next, the platinum catalysts, were prepared, under inert atmosphere, by deposition of a pentane solution of $MeCpPtMe_3$ on the dehydrated alumina in suspension in pentane, to reach a density of 0.03 Pt/nm^2, corresponding to a loading of 0.1 wt% Pt and 0.27 wt% Pt for N and D supports, respectively. The materials were then calcined under a dry air flow at 450 °C (2h - 2°C/min ramp). In addition, the alumina supports were also subjected to the same activation procedure without introduction of Pt. The samples were denoted calcined Pt/N and Pt/D or Calcined N and D. The samples were also characterized by ^{1}H MAS solid-state NMR (Bruker Avance, 400 MHz, 9.4T, 14 kHz, the proton spectra were externally referenced to the proton peak of adamantane to 1.87 ppm) and by high resolution HAADF-STEM (HR-HAADF-STEM, JEOL JEM-NeoRAM).

Results and Discussion

The ^{1}H NMR spectra strongly depend on the nature of the support and the presence of Pt, in particular regarding the signal below 0 ppm, assigned to μ_1-OH species at the edge of alumina platelets[5]. Deconvolution of the NMR spectra and normalization to the total OH surface concentration determined by Grignard titration (3.2 and 2.3 OH.nm^{-2} respectively for dehydrated N and dehydrated D) enable to evaluate the amount of these OH groups. Note that sample D exhibits lower concentration of edge μ_1-OH compared to N one, and that, the presence of platinum induces a disappearance of these μ_1-OH species, partially for calcined Pt/N and almost completely for calcined Pt/D (Figure 1).

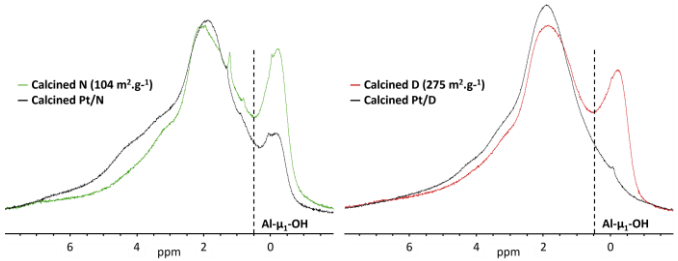

Figure 1. ^{1}H MAS-NMR spectra of calcined alumina and calcined Pt/alumina

Characterization with HR-HAADF-STEM shows a sintering of platinum on calcined Pt/D, whereas calcined Pt/N presents mostly platinum single atoms (Figure 2).

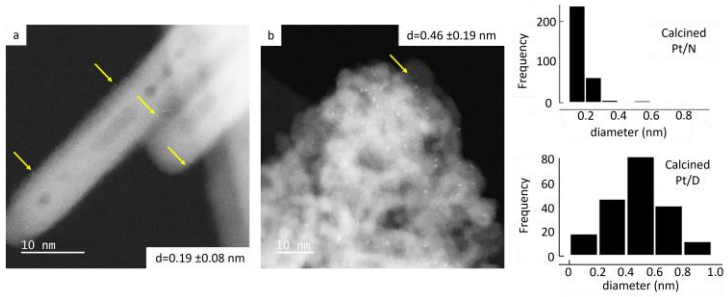

Figure 2. HR HAADF-STEM of: (a) Calcined Pt/N and (b) Calcined Pt/D with their respctive histograms in size of particles (yellow arrows point toward single atoms)

Comparison of the two materials highlights the influence of the support morphology on the stabilization of platinum single atoms: N with well-defined nanocrystals shapes display large fractions of single atoms on its well-defined edges, with a dispersion of 61.2 % in single atom. We propose that this is due to the presence of a higher concentration of edge μ1-OH in N compared to D. Understanding this trend is currently being pursued by exploring alternative alumina nanocrystals shapes and computational modelling.

Significance

Thanks to ^{1}H MAS NMR and HR-HAADF-STEM, we show that Pt_1 single atoms are stabilized on specific edges of alumina nanocrystals, possibly because of the presence of μ_1-OH species. This study opens a first step towards understanding of the influence of the support morphology in promoting single atoms. This could have a significant implication on the performances of the catalysts.

References

1. J.H. Kwak et al., *Science*, **2009**, *325*, 1670
2. A. Hellier et al., *J. Catal.,* **2024**, *429*, *115212*
3. L. A. Völker et al., *J. Phys. Chem. C*, **2022**, *126*, 6351
4. D. Gioffrè et al*, Helv. Chim. Acta*, **2022**, *105, e202200073*
5. A. T. F. Batista et al., *ACS Catal.* **2023**, *13*, 6536

Microkinetic study of acid gas valorization on Na faujasite

Marco Fabbiani[1], Syeda Rabia Batool[1], Ludovic Pinard[1], Raman Ghassemi[2], Soroush Zare Ghorbaei[2], Jeroen Lauwaert[2], Joris Thybaut[2], Valentin Valtchev[1]*
[1]*Laboratory of Catalysis and Spectrochemistry (LCS), CNRS-ENSICaen-UniCaen, Caen, France*
[2]*Laboratory for Chemical Technology (LCT), Ghent university, Ghent, Belgium*
*valentin.valtchev@ensicaen.fr

Introduction

In 2022, the production of electricity and heat remained the largest contributor to global CO_2 emissions, accounting for approximately 38% of the total, with emissions reaching a record high of 14.9 Giga tons (Gt)[1]. In industrial applications, fossil fuel combustion is a primary method for generating the heat required for chemical reactions, with about half of the chemical industry's CO_2 emissions attributed to fuel combustion for heat supply. Refineries and petrochemical industries alone are responsible for approximately 1.24 Gt of CO_2 emissions annually[2]. Additionally, this sector manages over 3.6 million tons (Mt) of hydrogen sulfide (H_2S) each year, often mixed with CO_2 as acid gas, which is encountered in refining, in exploration and production (as components of natural gas reservoirs), and in biogas treatment (as natural components of the gas mixture from a digester), etc. Current acid gas treatment predominantly relies on the Claus process to recover sulfur from H_2S-rich gas streams, a method that requires supplemental fuel for lean H_2S sources (less than 55%). However, existing technologies do not enable the simultaneous reduction of CO_2 and H_2S. As the chemical industry transitions toward a low-carbon economy, there is a pressing need to reduce fossil fuel dependence by decarbonizing processes, particularly through electrification. The project eCODUCT [3] introduces an innovative two-step technology for acid gas valorization:

i) conversion of CO_2 and H_2S into carbonyl sulfide (COS) in a fixed-bed reactor, via the reaction:

$$H_2S(g) + CO_2(g) \rightleftharpoons COS(g) + H_2O$$

ii) COS conversion into carbon monoxide (CO) and elementar sulfur (S_x) using an electrothermal fluidized bed (ETFB) reactor.

In this work, we address the first step (i) by studying the role of FAU-type basic zeolites on the competitive desorption and reaction of CO2 and H2S supported by the development of a microkinetic model.

Materials and Methods

Adsorption and reaction of CO_2 and H_2S were performed at atmospheric pressure in a fixed-bed quartz reactor (9 mm diameter) at variable temperatures from 45 to 120°C. The reactor was fed with a mixture of H2S (Linde, purity: 95%v in N_2) and CO_2 at different dilutions (3-12%v) using a constant flow of 4.8 L/h (STP). Before testing, catalyst (commercial 13X zeolite) was compacted under 5 tons, crushed, and sieved to obtain homogenous particles (0.2-0.5 mm), then loaded in the reactor. All samples were pre-treated at 350°C under nitrogen flow 1.8 L/H (STP) for 8-10 h before being fed with the acid gas mixture with different flow sequences.

Results and Discussion

At low temperatures, both physisorption and chemisorption must be taken into account. These contributions are experimentally distinguished by saturating the zeolite with a single component followed by a thermal desorption process. For both H_2S and CO_2 adsorbed individually on 13X zeolite, the amount is less than 10%, corresponding to a very low ratio relative to the sodium cation (0.6 mol/g for 13X). The overall interaction strength of H_2S with the adsorption site is greater than CO_2, likely due to a dissociative adsorption mechanism on the sodium cation [4,5]. A series of experiments was conducted on 13X zeolite samples (Table 1) pre-saturated with H_2S to investigate the kinetics of COS formation (Figure 1).

Table 1. Textural properties of microporous material 13X.

Sample	S_{BET} / $m^2.g^{-1}$	Pore size / Å	Si/Al
13X	800	7.3	1.2

Chemisorbed H2S is completely converted upon reaction with CO_2. COS production profile passes through a maximum and then decreases with the reaction time evidencing the progressive deactivation of the catalyst. Temperature significantly influenced the reaction, with conversion rates increasing from 5% at 45°C to 12% at 120°C. The highest COS yield was observed at 100°C. The experimental data were used to develop a microkinetic model based on the Langmuir-Hinshelwood-Hougen-Watson (LHHW) kinetic. This model incorporates the role of sodium cations within the faujasite supercages as active adsorption and reaction sites and considers water, a reaction co-product, as the primary factor driving catalyst deactivation over time.

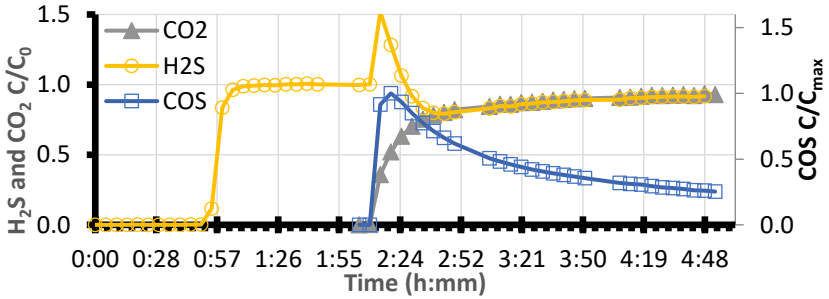

Figure 1. Relative concentrations vs. time of H_2S, CO_2 and COS over 13X zeolite.

Significance

This work provides a comprehensive understanding of the conversion of CO_2 and H_2S into the intermediate molecule COS, supported by a detailed microkinetic model. This approach not only sheds light on the reaction mechanisms and the role of active sites but also has significant implications for greenhouse gas mitigation and the reduction of industrial waste impacts.

References

1. The Paris Agreement UNFCCC, May **2023**.
2. https://www.iea.org/data-and-statistics/data-tools/greenhouse-gas-emissions-from-energy-data-explorer
3. https://e-coduct.eu, Horizon Europe Grant Agreement n. 101058100.
4. Yum et al., Separations **2022**, 9, 229.
5. Khabazipour et al., Ind. Eng. Chem. Res. **2019**, 58, 22133−22164,

News from CeO_2 catalysts : an unreported cerium oxyhydroxide phase and *operando* monitoring of H_2 activation as surface hydrides

Rémi F. André[1*], G. Rousse,[2] J.-J. Gallet,[3] F. Bournel,[3] Sophie Carenco[1*]
[1]*Laboratoire de Chimie de la Matière Condensée de Paris (LCMCP), Sorbonne Université*
[2]*Chimie du Solide-Energie, UMR 8260, Collège de France & Sorbonne Université*
[3]*Laboratoire de Chimie Physique Matière et Rayonnement (LCPMR), Sorbonne Université*
*remi.andre@enscm.fr

Introduction

Cerium oxide is a pivotal compound in catalysis, both as a support and as an active phase, in particular for vehicle three-way exhaust clean-up. However, its fine features, such as the Ce(III) to Ce(IV) ratio, strongly depend on the protocol used to prepare it. While the literature contains tens of protocols to prepare cerium oxide nanoparticles from Ce(III) precursors, there is still an open question regarding the time at which the cerium oxidation occurs and the role of hydroxide phases in this process. Besides, cerium oxides recently appeared as possible substitutes to precious metals for hydrogenation reactions, in particular for olefins and carbonyls.[1,2] The nature of the active sites and the feature of the material to optimize, such as the exposed facet or the density of oxygen vacancies, are however still debated in literature, as well as the conditions ruling the H_2 activation between the heterolytic (H^+ and H^-) and the homolytic (2 H·) pathways, both possible on several metal oxides.[3]

Materials and Methods

Cerium hydroxides/oxides were obtained *via* hydrothermal pathway starting from $Ce(NO_3)_3.6H_2O$ and KOH. Characterization of the nanomaterials includes PXRD, TEM, neutron diffraction (ANSTO), XAS (LUCIA, SOLEIL synchrotron) and FTIR. NAP-XPS experiments were conducted on CeO_2 nanoparticles deposited on a gold-coated silicon wafer at the TEMPO B beamline of SOLEIL synchrotron. XPS data were treated with CasaXPS software.

Results and Discussion

While reproducing literature results claiming efficient hydrogenation catalysts as CeO_{2-x},[4] we evidenced an unreported phase upon air oxidation of small $Ce(OH)_3$ nanoparticles (Figure 1).[5] A structure with a pseudo 6-fold symmetry, identified as an oxyhydroxide, was proposed based on a Rietveld refinement of PXRD data, comforted by the analysis of the degree of oxidation of cerium by XAS, among other techniques. Besides, a thermodiffraction experiment clearly evidenced $CeO(OH)_2$ as an intermediate between $Ce(OH)_3$ and CeO_2 upon air calcination in the 50-75 °C range, thus separating the oxidation and dehydration steps.

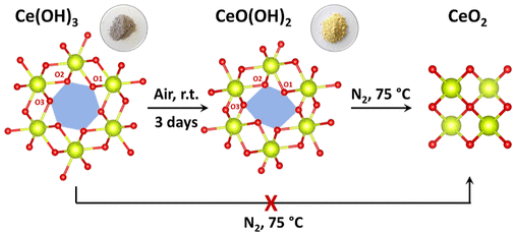

Figure 1. Evolution of the crystal structure of the Ce–O skeleton of cerium trihydroxide $Ce(OH)_3$ exposed to air and/or thermal treatment.

The so-formed defective CeO_2 nanoparticles from $CeO(OH)_2$ calcination were compared with classical hydrothermal, and thermally reduced, CeO_2 NPs for the activation of H_2 *via* Near-Ambient Pressure XPS (NAP-XPS), prelude of an activity in hydrogenation reactions (Figure 2).[6] The concentration of Ce(IV) dropped in both cases to *ca.* 43 %, and re-increased progressively to 57 % upon exposure to 0.14 and 0.5 mbar of H_2. Similar works on CeO_2 surfaces concluded on the activation of H_2 as two surface hydrides H^-, leading to an oxidation of two Ce(III) sites related to an oxygen vacancy.[7] The extent of the phenomenon was more reduced in their case with a Ce(III) fraction evolving from 6 % to 9.2 %, underlining the importance of defective surfaces in our case.

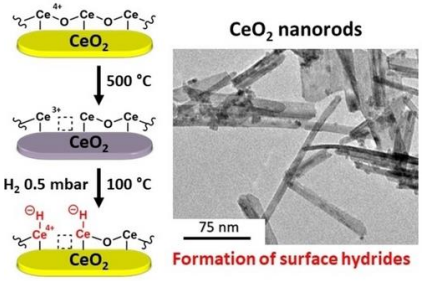

Figure 2. NAP-XPS experiments evidence the reduction of surface cerium atoms of CeO_2 upon thermal treatment (in vacuum), followed by an oxidation upon addition of H_2, attributed to the formation of surface hydrides.

Significance

As to the $CeO(OH)_2$ phase, the description of this phase will allow a better understanding of the mechanism of formation of CeO_2, critical considering the versatile Ce(III)/Ce(IV) switch. Note that the authors found on several occurrences a misattribution of the PXRD pattern as the phase was not reported. As to the surface hydride formation, the results unambiguously extend known results on clean CeO_2 surfaces to more relevant objects for effective catalysts (*i.e.* defective nanoparticles), on the hot topic of hydrogenation by non-platinoid compounds.

References

1. G. Vilé, …, J. Pérez-Ramirez, *Angew. Chem. Int. Ed.* **2012**, *51*, 8620
2. Z. Zhang, …, J.-Q. Lu, *ACS Cat.*, **2020**, *10*, 14560
3. M. Garcia-Melchor, N. Lopez, *J. Phys. Chem. C*, **2014**, *20, 10921*
4. S. Zhang, …, Y. Qu, *Nat. Commun.* **2017**, *8*, 1
5. R. F. André, …, S. Carenco, *Chem. Mater.* **2023**, *35*, 5040
6. R. F. André, …, S. Carenco, *ChemCatChem* **2024**, *16*, e202400163
7. Z. Li, …, H. Freund, *Angew. Chem. Int. Ed.,* **2019**, *58*, 14686

OC6: Biomass

Carbon supported metal oxides nanoparticles and their applications in biomass valorization

Ali Djellali*, Juliette Blanchard
Laboratoire de Réactivité de Surface, Sorbonne Université, 75005 Paris, France
*ali.djellali@sorbonne-universite.fr

Introduction

Activated carbon made from olive waste is an eco-friendly material derived from agricultural by-products, offering high surface area and porosity ideal for catalytic applications. When modified with metal oxide nanoparticles (NPs) like zirconium dioxide (ZrO_2) and titanium dioxide (TiO_2), its catalytic properties are enhanced, enabling effective biomass conversion processes.

In this context, the modified activated carbon serves as a catalyst for converting glucose and fructose into 5-hydroxymethylfurfural (HMF), a valuable platform chemical for biofuel and bioplastic production. ZrO_2 and TiO_2 deposition improves the carbon's acidity and stability, facilitating selective dehydration to HMF. This approach not only utilizes renewable feedstocks but also addresses waste management issues, promoting sustainable chemical production.

Materials and Methods

Two activated carbons were synthesized from olive waste through chemical activation using $ZnCl_2$ and H_3PO_4 (AC-Zn and AC-P) followed by calcination [01]. Metal oxide nanoparticles (NPs, ca. 5 nm) were subsequently deposited onto the activated carbons, and the resulting samples were thoroughly characterized. Nitrogen adsorption was employed to assess changes in specific surface area, while X-ray diffraction (XRD) was used to confirm the incorporation of NPs, and TGA for evaluation of metal oxide loading. The nanocomposites were then tested as catalysts for the conversion of fructose and glucose into 5-hydroxymethylfurfural (HMF) in a water/organic solvent-based reaction system. High-performance liquid chromatography (HPLC equipped with RI and UV detectors) was utilized to quantify the reaction products, providing insight into the catalytic performance of the materials.

Results and Discussion

N_2-adsorption analysis of the AC confirms their high surface area (1400-1600 m2.g-1) and reveals that AC-P contains a significant fraction of mesopores. For composites samples, increasing nanoparticle loadings decreased the textural properties of both nanocomposites, beyond what was expected from the nanoparticle weight fraction, suggesting metal oxide NPs occupy AC pores. XRD patterns revealed TiO_2 and ZrO_2 diffraction peaks (respectively anatase and cubic zirconia), in samples with higher loadings (above 10 wt%), while their absence in other samples may be due to low concentrations, small crystallite size, or incomplete crystallization.

The AC/NPs catalysts were evaluated for the conversion of fructose into 5-hydroxymethylfurfural (HMF) using three different solvent mixtures: NaCl-saturated H_2O/THF, H_2O/DMSO, and H_2O/MIBK. Experimental conditions (amount of catalyst, temperature, duration) were optimized for each solvent using a design of experiments approach [02]. Notably, the HMF yield was highly dependent on the choice of solvent, following the trend DMSO > THF > MIBK.

Adding the metal oxide NPs increased the yield of HMF for the two AC and in all solvent mixtures. However, in DMSO AC-ZrO_2 outperforms AC-TiO_2, reaching an HMF yield of about 90% for a ZrO_2 loading of 10wt%. ZrO_2 and supported ZrO_2 NPs have seldom been used as catalyst for this reaction and this exceptional performance highlights the potential of AC-P-ZrO_2 as an efficient catalyst for HMF production, offering a promising pathway for sustainable biomass conversion [03]. Further characterization of the fresh and spent catalysts, focusing on their acid-base properties (NH_3- and CO_2-TPD) is underway to better understand the origin of this high selectivity of ZrO_2 NPs for this reaction. HMF yield of mechanical mixture of commercial ZrO_2 or TiO_2 samples with our AC are currently being performed to better understand the complex interplay between these two materials. The results we obtained will be analyzed and discussed with regards to existing literature and acid-base balance.

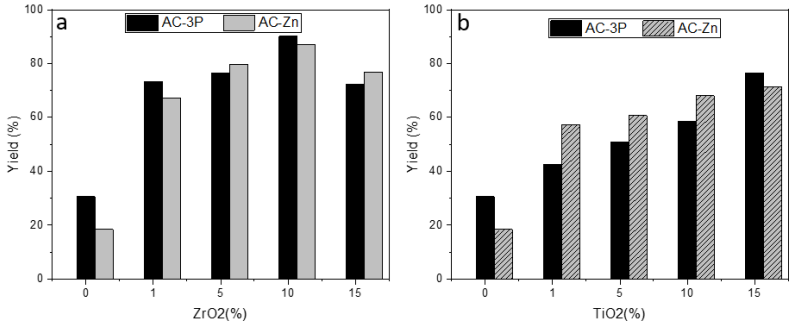

Figure 1. a) HMF yield vs the amount of ZrO_2 in the samples (AC-P and AC-Zn) after 5 h of heating under stirring at 160°C in water/DMSO mixture. b) HMF yield vs the amount of TiO_2 in the samples (AC-P and AC-Zn) after 5 h of heating under stirring at 160°C in water/DMSO mixture.

Significance

This work presents a sustainable method for producing HMF, a key biofuel precursor, by converting fructose using activated carbon from olive waste. This approach valorizes agricultural by-products, reduces fossil dependence, and achieves high yields with eco-friendly catalysts, highlighting its potential for industrial biorefineries and green chemistry applications.

References

1. H Boustila, S Tazibet. *Chem. Eng. Technol.* **2022**, *45*(2), 258-265.
2. S. Karoui, A. Amrane. *J. Hazard. Mater.* **2020**, *387*, 121675.
3. A. Veluturla, S., Saranya. *J. Chem. Techol. Biotechnol*, **2024**, *99*(7), 1477-1492.
4. Q. Kong, Y. Fu. (2020). *Fuel Process. Technol*. **2020**, *209*, 106528.

Functionalization of lignocellulosic biomass for the production of bio-binders

Nolwenn Daridon[1], Christophe Geantet[1], Dorothée Laurenti[1]*
[1]*IRCELYON, CNRS-Univ Lyon 1, UMR5256,*
2 avenue A. Einstein 69100 Villeurbanne, France
*dorothee.laurenti@ircelyon.univ-lyon1.fr

Introduction

Pavement of the roads uses a huge quantity of bitumen coming from petroleum derivatives. In order to limit the use of fossil resources, new bio-binder formulations are highly expected. The aim of the Post-Oil Pavement project is to develop a bio-binder formulation made with maleinized used edible oils (UEO) mixed to lignocellulosic materials. Currently, bio-based substitutes can be used to partially replace bitumen[1,2]. For example 10 to 20 % of lignin can be introduced into a binder without altering its rheological properties but if the percentage of lignin is increased, undesirable effects appear[3,4]. It can affect the fatigue performance, decrease the self-healing ability of the bitumen or the diffusion coefficient[3] and even crystallized particles could be observe[4].

In this work, our target is to modify lignin and/or cellulose by esterification or etherification of the hydroxyl functions using catalytic methods to increase their lipophilicity. Functionalization of these biomasses, when mixed with UEO, would enable to obtain materials with rheological properties close to those of the bitumen used in industry.

Materials and Methods

The starting materials for the reactions are commercial microcrystalline cellulose and Kraft lignin containing around 18,5 and 6,50 mmol/g of OH groups respectively. O-Alkylation of lignin was realized with different trialkyl(R3)phosphate with R=ethyl, butyl, or 2-ethylhexyl. The O-alkylated lignins were obtained by reacting with the trialkyl phosphate (10 eq.) for 3h at 140°C. Different kind of catalysts were tried: K_2CO_3, DIPA, DBU, H_3PO_4 and amino functionalized silica gel. Esterification of cellulose with UEO was performed by solubilizing the cellulose (5 wt%) in a switchable solvent[5]: DMSO/DBU/CO_2, where CO_2 is added (10 bars), for 3 min at room temperature. The solution of solubilized cellulose is then added to 3 eq. of UEO per OH, for 24h at 115°C**.** All the starting materials and solids obtained were analyzed by ^{1}H, ^{13}C, ^{31}P NMR, SEC, TGA, ATR-IR and CHONS. Unreacted free OH groups on lignin were quantified by ^{31}P NMR after phosphitylation to determine the degree of substitution and discriminate aliphatic, aromatic and carboxylic positions.

The functionalized biomass samples were mixed in UEO using a heating protocol going from 100°C to 230°C. The change in rheological properties is observed even during the heating and then at room temperature.

Results and Discussion

The O-ethylated lignins obtained thanks to triethylphosphate and using K_2CO_3 as the catalyst, have a degree of substitution (DS) between 21 % and 82 % depending on the time and reaction temperature. The highest DS was obtained at 3h and 140°C. With other trialkyl phosphate having longer carbon chains like tributyl phosphate and tris(2-ethylhexyl) phosphate, under the same operating conditions, total DS of 44% and 18% have been obtained respectively. Unsurprisingly, the DS are lower due to steric hindrance with no selectivity to specific hydroxyls type.

The impact of the nature of the catalyst has been studied. Different homogeneous and heterogeneous catalysts were chosen with various acid or basic properties. We observed varying reactivity of the OH groups depending on the acidity/basicity properties. With a basic catalyst, the O-ethylation tends to happen on the aromatic hydroxyls while with an acidic catalyst, the aliphatic hydroxyls are mainly O-ethylated. With amino catalyst, the catalysts deactivated in the presence of the trialkylphosphates[6] and therefore the catalytic activity decrease after longer residence time. We attempted to use heterogeneous catalysis (silica-supported amines) where some results have been achieved without any leaching however activity is lower than with homogenous catalysts. It's a first step towards the heterogenization of the O-alkylation of lignin.

Concerning the cellulosic material, after the transesterification by the UEO, we obtained a solid that is soluble in DMSO, which indicates clearly that the esterification reaction of OH groups happened. The substitution degree was calculated by ^{1}H NMR by comparing the integration of the vinyl proton with the proton on the C1 of the anhydroglucose unit. A DS of 0,5/3 was reached. We used glyceryl trioleate as a model molecule for UEO to understand better the mechanism behind the reaction. The impact of the carbon chain length of triglycerides and presence of fatty acids on the DS was studied.

By mixing transesterified cellulose or ethylated lignin with the UEO maleinized or not, we observed an increase in the viscosity of the mixtures at room temperature with variation depending of the starting LC material and type of functionalization.

To conclude, the lignin and cellulose were successfully functionalized and when added to UEO, a change in rheological properties of the mixture was observed and suggest that we can get a bio-binder by this way.

Significance

Due to the high amount of bitumen needed (11,3 million tons each year in the EU), it is necessary to develop sustainable solutions for petroleum bitumen by identifying new resources allowing the development of an alternative binder while maintaining the performance and usage properties offered by reference solutions.

Act of acknowledgment: The French National Research Agency is thanked for its funding.

References

1. E. Gaudenzi, *Construction and Building Materials,* **2023**, *362*, 129773
2. H. Soenen, *Rheol Acta.,.* **2015**, *53*, 741-754
3. S. Ren, *Construction and Building Materials*, **2021**, *287*, 123058
4. I.P. Pérez, *Journal of Cleaner Production*, **2019**, 220, 87-982
5. KN. Onwukamike**,** ACS Sustainable Chem Eng., **2018, *6*,** 8826-8835
6. A. Banerjee, *Synthesis,* **2023**, *55*, 315-332

A bottom-up approach to design new catalytic systems for the mild oxidation of furan derivatives

Lénaïck Hervé[1†], Franck Rataboul[1], Catherine Pinel[1], Amandine Cabiac[2], Maria Fernandez Espada Pastor[2], Laurent Djakovitch[1*]

[1]*IRCELYON, CNRS, 69626 Villeurbanne, France*

[2]*IFP Energies nouvelles, 69320 Solaize, France*

* laurent.djakovitch@ircelyon.univ-lyon1.fr

† lenaick.herve@ircelyon.univ-lyon1.fr

Introduction

To reduce our dependence on fossil resources and promote sustainability, biomass is a key carbon source. Carbohydrate-rich biomass yields a variety of valuable molecules, including 2,5-furandicarboxylic acid (FDCA) and 2,5-diformylfuran (DFF), which can be produced through the catalytic oxidation of 5-hydroxymethylfurfural (5-HMF) for applications as monomers or pharmaceuticals.

Since 2010, many studies have investigated the selective oxidation of 5-HMF, primarily using noble metal-supported catalysts (Au, Pd, Pt, Ru) and several equivalents of soluble base.[1] However, the high cost of these metals, combined with wastewater treatment issues, highlight the need for new approaches. In this context, a bottom-up strategy appears promising. “Quasi-homogeneous” catalysis through metallic colloids stable in solutions may provide an effective way to identify the most suitable metal(s) for the catalytic system. This method has been relatively underexplored for 5-HMF oxidation. Some systems, such as core-shell Pt-Fe_3O_4 nanoparticles, have been applied to FDCA formation[2], while $NH_4.V_3O_8$-Fe_3O_4 nanoparticles have been used for DFF.[3]

In the context of a project funded by PEPR BBEST-FURFUN (2023-2026) focused on bio-sourced furan valorization, we will present in this communication our strategy for developing an “ideal” catalytic system through a bottom-up approach: this is the creation of a "quasi-homogeneous" colloidal phase and then the progression to stable and efficient heterogeneous catalysts (Figure 1). We will detail here our developments for the synthesis of stable palladium colloids in aqueous media for the selective oxidation of HMF to either DFF or FDCA under mild conditions.

Materials & Methods

We prepared PVP-stabilized palladium colloids (Pd NPs) through a reliable method.[4] Na_2PdCl_4 and PVP (10 eq.) were separately dissolved in water, combined, and stirred vigorously for 0.5 hours. Pd NPs were then formed by reduction with $NaBH_4$ (2.5 eq.) at room temperature and stirring for 1 day. The Pd NPs were characterized by ICP and TEM, and the colloidal solution has shown to be stable over weeks.

For catalytic experiments, 40 mL of a 0.5 wt% HMF solution in water, Na_2CO_3 (≤1.2 eq./HMF) and palladium colloidal solution (0.55 mol.%), were placed in a three-neck flask, exposed to a flow of wet air, and stirred at 1000 rpm at 25 or 80°C for 48 hours. Reaction mixtures were analyzed via HPLC.

Results & Discussion

Palladium is renowned for the catalytic oxidation of carbonyl compounds, and we present initial results on “quasi-homogeneous” catalysis using palladium colloids, that will serve as a baseline for comparison with non-critical metals (e.g., Cu, Ag, Au). First analysis focused on particle size and stability of Pd NP solutions in aqueous media, as well as the effect of palladium colloids on the activity and selectivity for 5-HMF oxidation. Various catalytic tests examined parameters like base concentration, temperature, and air/O_2 flow rate to clarify their roles in the reaction pathway, with the support of existing literature.

TEM analysis revealed uniform particles of around 3.5 nm with a narrow size distribution and stable, as colloidal solution for at least one month. As an example of catalytic conditions variations, temperature effect showed that at 25°C, HMF conversion reached 70% with 80% selectivity into HMFCA, while at 80°C, HMF was fully converted with 100% selectivity into FDCA.

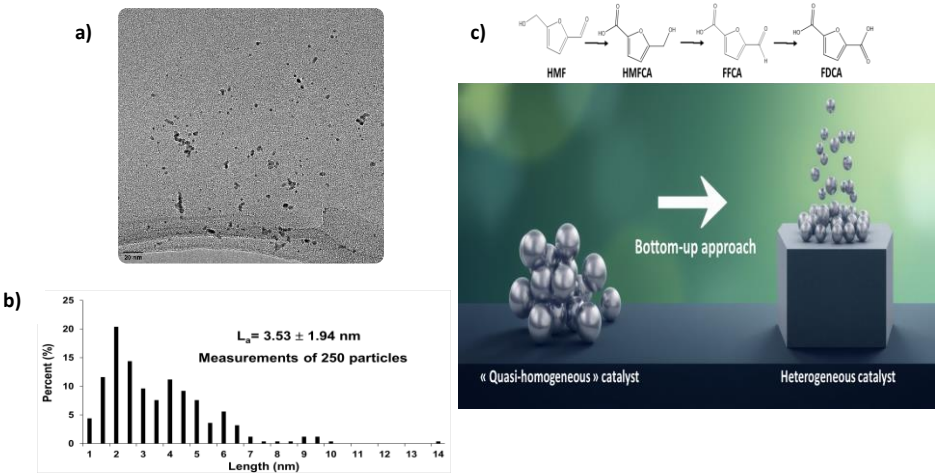

Figure 1. TEM analysis (a) and distribution of the particles size (b) of the Pd colloid; (c) sketch of the reaction mechanism and the bottom-up strategy.

Significance

This study participates to the advances towards the implementation of robust routes for the very important reaction of oxidation of 5-HMF into DFF or FDCA, particularly by using more eco-friendly procedures limiting the use of oxygen pressure, as well as expensive reagents and solvents.

References

1. Z. Zhang, K. Deng, ACS Catal., **2015**, *5*, 11.
2. Y. Zhang, Z. Xue, J. Wang, X. Zhao, Y. Deng, W. Zhao, T. Mu, RSC Adv., **2016**, *6*, 56.
3. J. Lai, S. Zhou, F. Cheng, D. Guo, X. Liu, Q. Xu, D. Yin, Catal. Lett., **2020**, *150*, 1301.
4. D. Bourbiaux, S. Mangematin, L. Djakovitch, F. Rataboul, Catal. Lett., **2021**, *151*, 3239

Unlocking the Potential of Au-Pt Core-Shell Catalysts: A Microemulsion Approach for Enhanced Glucose Oxidation to Glucuronic Acid in base free media

ELHALLAL Maher[1]*, ORDOMSKI V. Vitaly[1], CAPRON Mickael[1]
[1]*UCCS-UMR CNRS 818, université de Lille, 59655 Villeneuve d'Ascq cedex, France*
*maherhallal@univ-lille.fr

Introduction

The selective oxidation of glucose to high-value chemicals is a crucial process in the valorization of biomass-derived feedstocks. Glucuronic acid, a key intermediate in pharmaceutical and food industries, can be obtained through glucose oxidation. However, achieving high selectivity and yield remains challenging. This study presents a novel Au-Pt/TiO_2 catalyst with a unique core-shell nanostructure for the efficient oxidation of glucose to glucuronic acid.

Materials and Methods

The catalysts used in the experiments was prepared using a microemulsion method[1]. This method involved reducing by hydrazine hydrate solution, an aqueous phase containing metallic precursors ($HAuCl_4$ and/or $H_2PtCl_6{\cdot}6H_2O$) with an oil phase (cyclohexane) and an amphiphilic surfactant (AOT), along with the addition of TiO_2. The catalysts, denoted as $Au_xPt_{(100-x)}/TiO_2$ (x = 0, 25, 50, 75, 100), were prepared with a total metal loading of 2.5 wt%. Catalyst characterization was performed using TEM, EDX, TITAN, BET, BJH, XRD, ICP-AES, and XPS.
Catalytic reactions were conducted in a 300 mL stainless steel reactor with 200 mL glucose solution (0.5M). Reaction parameters including catalyst mass (0-0.4 g), time (5-9 h), temperature (100-140 °C), and O_2 pressure (10-30 bar) were optimized. Products were analyzed by HPLC with RI and UV detectors.

Results and Discussion

Optimization studies revealed optimal reaction conditions of 5 h, 120 °C, 15 bar O_2, and 0.3 g of catalyst.
Under optimized conditions, Au-based catalysts exhibited superior catalytic activity (71% conversion) while Pt-based catalysts showed the highest product selectivity (66% glucuronic acid selectivity). Notably, the $Au_{50}Pt_{50}/TiO_2$ catalyst demonstrated a synergistic effect, achieving both high conversion (68%) and selectivity (58%), outperforming monometallic counterparts **(figure 2).** Remarkably, TEM and EDX analyses unveiled a unique Au Core-Pt shell nanostructure in the bimetallic catalysts **(figure 1).** This core-shell structure is believed to be responsible for the enhanced catalytic performance observed. XPS results corroborated the formation of bimetallic nanoparticles, while BET and BJH analyses showed good surface areas and well-defined mesoporous structures. ICP-AES confirmed the intended metal loadings and ratios.

The enhanced performance of the bimetallic catalyst is attributed to the unique core-shell structure, where the Au core facilitates rapid electron transfer[2], while the Pt shell provides optimal active sites for selective oxidation[3]. This synergistic effect results in improved catalytic efficiency and selectivity towards glucuronic acid.

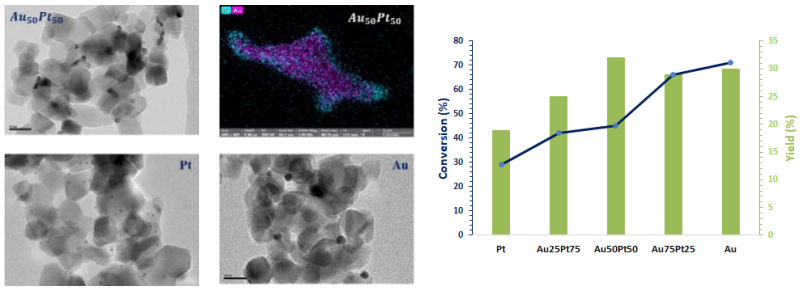

a b

Figure 1. a) TEM Images and EDX analysis of Au,Pt and $Au_{50}Pt_{50}$. b) glucose conversion and glucuronic acid yield for *$Au_xPt_{(100-x)}/TiO_2$ (x = 0, 25, 50, 75, 100). 0.5M glucose, 200mL solution, 5 h, 120 °C, 15 bar O_2, and 0.3 g catalyst.*

Kinetic studies showed $Au_{50}Pt_{50}/TiO_2$ had the highest rate constant for glucose conversion compared to Au/TiO_2 and Pt/TiO_2. Gluconic acid formed rapidly, then converted to glucuronic acid. Glucuronic acid selectivity peaked at 5 hours. Optimizing reaction time and oxygen pressure as well as reaction temperature maximized glucuronic acid yield while minimizing by-products and humins formation. The bimetallic catalyst showed improved resistance to deactivation likely due to its unique core-shell structure.

Significance

This study presents a novel Au-Pt core-shell nanostructure supported on TiO_2 for efficient glucose oxidation. The synergistic effect observed in the bimetallic catalyst offers a promising approach for the selective production of glucuronic acid. These findings contribute to the development of more efficient and sustainable processes for biomass valorization, with potential applications in pharmaceutical and food industries.

References

1. R. Wojcieszak et al, "Selective oxidation of glucose to glucuronic acid by cesium-promoted gold nanoparticle catalyst"
2. Changhui Tan et al, "A self-supporting bimetallic Au@Pt core-shell nanoparticle electrocatalyst for the synergistic enhancement of methanol oxidation"
3. América Higareda et al, "Synthesis of Au@Pt Core—Shell Nanoparticles as Efficient Electrocatalyst for Methanol Electro-Oxidation"

Effect of the replacement of Mg^{2+} by Zn^{2+} in metallic silicates on acid-base properties and on their activity in γ-valerolactone ring opening reaction

Albert Issa[1,2], Thomas Onfroy[1], Guillaume Laugel[1], Jean-François Hochepied[2], Hélène Lauron-Pernot[1]*

[1]*Laboratoire de Réactivité de Surface, Sorbonne Université, 75005 Paris, France*

[2]*ENSTA UCP, IP Paris, 91120 Palaiseau, France*

*helene.pernot@sorbonne-universite.fr

Introduction

Transesterification reactions play a pivotal role in a wide array of applications within the field of bio-sourced molecules valorization, for instance, transforming γ-valerolactone (GVL) through a ring-opening reaction with methanol. This reaction results in the production of methyl-pentenoates, which are used as intermediates in the synthesis of Nylon (Figure 1(a)). Previous studies have evidenced the potential of magnesium silicates (MS), as catalysts for transesterification reaction of GVL[1]. The preparation of Magnesium Silicate Hydrate (MSH) phase by co-precipitation (via 2 distinct process: micromixer or doublejet) allow to get solid with wide range of Mg/Si ratio that affect their acid-base properties. More interesting, selectivity of the products of the GVL ring-opening reaction is controlled by the acid-base properties. Unfortunately, a loss in the carbon balance has been evidenced for all samples during catalytic test that is associated to strongly adsorbed carboxylates.

In this contribution, we will evidence the impact of changing the cation from Mg^{2+} to Zn^{2+} on the acid-base properties of the materials, which will be characterized using the 2-methyl-but-3-yn-2-ol (MBOH) decomposition test[2] (Figure 1(b)) and pyridine adsorption followed by FTIR, and their impact on the activity and selectivity of the materials in the GVL ring-opening reaction and notably on the loss in the carbon balance.

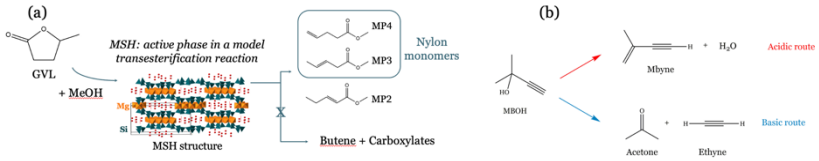

Figure 1. (a) the GVL ring-opening reaction, (b) the MBOH decomposition reaction.

Materials and Methods

The co-precipitation of zinc silicate (ZS) has been performed using the protocol described by Payan et al.[2] for the synthesis of MS using a micromixer. The MBOH test is processed in the gas phase using N_2 as a carrier gas and a reaction temperature of 130 and 170°C. The pyridine desorption at various temperature from 150 to 300 °C was followed by FTIR spectroscopy. The GVL ring-opening reaction is performed in gas phase. Methanol and GVL in N_2 (MeOH/GVL molar ratio = 30) is introduced into a reactor between 270 and 330°C. Reactants and products were then analyzed by GC.

Results and Discussion

A set of zinc silicates (ZS) solids prepared by co-precipitation using micromixer was obtained with wide range of Zn/Si ratio (from 1.08 to 0.44).

The study of acid-base properties, using the model reaction of MBOH conversion, has shown that all ZS catalysts are significantly more active than magnesium silicates (MS) ones. However, ZS present narrower acid-base properties compare to MS one but for both families sample presenting the highest K/Si (K originating from silicate precursor) show the lowest acid selectivity. According to pyridine adsorption results, only Lewis acid sites are detected at the surface of ZS. Furthermore, samples with the highest K/Si ratio exhibits a low amount of acid sites. As in the case of MS samples, this finding was attributed to the blocking of acid sites by K^+ ions.

Zinc samples showed a tendency toward higher K/Si ratios, in comparison to the MS ones, with two samples displaying slightly higher acid selectivities due to their lower K/Si ratios. These two samples, in particular, stood out for their significantly higher GVL conversion rates (about 20%) compared to the others ZS and a low carbon balance loss (about 3%). So, mainly 17% of the converted GVL is transformed into products, with MP4 selectivities approaching 70%, which is a strong performance. Indeed, MS counterpart present a lowest GVL conversion (about 15%), a highest carbon balance loss (about 7%) and a lower selectivity in MP4 (about 60%).

Furthermore, attempts to enhance the activity of these two zinc samples by increasing the reaction temperature from 270 to 330°C). This increase in temperature resulted in higher product conversion (from 17 to 37%) with a stable loss in carbon balance (from 3 to 5% whatever the temperature). However, a slight reduction in MP4 selectivity to around 60% is observed, which still represents a favorable outcome Figure 2.

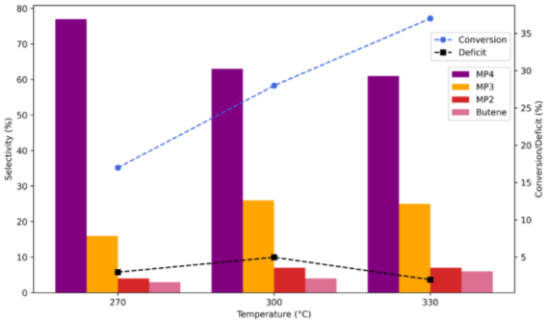

Figure 2. Products conversion, carbon balance deficit and selectivities for a ZS at different temperatures

Significance

This study evidence how the replacement of Mg^{2+} by Zn^{2+} in metallic silicate is able to modify the acidic and basic properties of these catalysts. This replacement allow to strongly improve catalytic performances in the GVL ring-opening reaction in terms of conversion, carbon balance and selectivity into the most suitable products (those serving as bio-sourced Nylon precursors).

References

1. A. Issa et al., ICC 2024, Lyon ; A. Issa et al. Article in preparation
2. Lauron-Pernot et al., Catal. Rev., **2006**, 48, 315-361
3. F. Payan et al., Catalysts, **2023**, 13, 1393

Investigation of Liquid Organic Hydrogen Carriers (LOHC) Issued from Biomass Resources

Issam Nciri, Christophe Coutanceau, Karine De Oliveira Vigier*
IC2MP, UMR 7285, CNRS - Université de Poitiers, Poitiers, France ;
**karine.vigier@univ-poitiers.fr*

Introduction

The use of Liquid Organic Hydrogen Carrier (LOHC) is a promising way of simplification of hydrogen storage and transport. The handling of a liquid instead of hydrogen gas presents a similar level of complexity to that of hydrocarbons already in use worldwide, with the advantage of hydrogen as sustainable energy vector. Hydrogen storage and transport using LOHCs are based on two-step cycles, such as (i) loading/storage of hydrogen by catalytic hydrogenation of H_2-lean compounds and (ii) unloading/releasing hydrogen by dehydrogenating the resulting H_2-rich liquids.

Most of LOHCs considered have hydrogen capacities around 6 wt% if the hydrogenation – dehydrogenation reaction is complete. However, the liquids usually considered such as toluene, ethylcarbazole, phenylcarbazole, 2-(N-methylbenzylpyridine) or dibenzyltoluene are produced from fossil sources and present a toxicity which can make their transport and long-term storage hazardous. Also, the renewal of LOHC partly lost in the hydrogenation/dehydrogenation process decreases the sustainability of the process.

To improve the safety and sustainability of LOHC, it is proposed to use compounds which can be biosourced and present a low toxicity, such as ethylene glycol (EG), from syngas produced by biomass pyrolysis or catalytic transformation of cellulosic material, and glycerol (GLY) produced by alcoholic fermentation of sugars or as a sacrificial compound from the synthesis of biodiesels by the transesterification of fatty acids in oilseed plants, animal fats or used vegetable oils. The selective oxidation of one or two terminal alcoholic functions leads respectively to two or four H_2 molecules for EG (M = 62 g) and GLY (M = 92 g):

$$R\text{-}CH_2OH + H_2O \rightarrow R\text{-}COOH + 2\,H_2$$

$$CH_2OH\text{-}R'\text{-}CH_2OH + H_2O \rightarrow COOH\text{-}R'\text{-}COOH + 4\,H_2$$

which would correspond to a weight storage from 6.4 % to 12.8 % for EG and from 4.3 to 8.7 % for glycerol. Here in we have studied the use of ethylene glycol as a LOHC.

Materials and Methods

All the chemicals were purchased from sigma Aldrich. For the dehydrogenation of ethylene glycol, the protocol used is as follows. A catalytic ink is prepared by mixing in MilliQ water the electrocatalyst and a suspension of Nafion® 5 wt% in aliphatic alcohols and deposited on a 0.3 mm diameter glassy carbon working electrode. The counter electrode is a glassy carbon plate of 2 cm². The reference electrode is a reversible hydrogen electrode (RHE). The electrolyte composed of alkaline or acidic media containing ethylene glycol with different concentrations is purged with inert gas prior to the linear sweep voltammetry between 0.05 and 1 V vs RHE at 5 mV s^{-1} and 25 °C. For the hydrogenation of the corresponding acid (oxalic acid), a batch reactor of 75 mL was used. The reaction was carried out in the presence of a Ru-Based catalyst. The products obtained were analysed by high performance liquid chromatography using a refractometer index detector.

Results and Discussion

The selective electrocatalytic oxidation, without breaking of the C-C bonds, of some of these compounds will be investigated. With convenient electrocatalysts the oxidation reaction at the anode of an electrolysis cell starts at around 0.3 V vs. RHE (instead of 1.23 V under standard conditions for water electrolysis), with production of hydrogen at the cathode, the total cell voltage being below 1.0 V. The electrical energy used for producing H_2 is then very low, making the process viable [1-3].

On the other hand, the reaction products (particularly carboxylic acids without breaking the C-C bonds) were hydrogenated. The results demonstrated that after the optimization of the reaction conditions a selectivity to ethylene glycol of around 70% can be obtained in the case of the hydrogenation of oxalic acid in the presence of a Ru-based catalyst (Figure 1). All these results as well as the reaction pathway will be discussed.

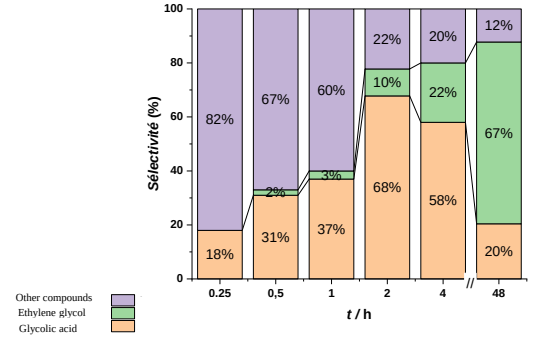

Figure 1. Hydrogenation of oxalic acid in the presence of a Ru-based catalyst. Evolution of the selectivity to different products.

Significance

In this work, we have shown that bio-sourced polyols are good candidates as LOHCs and that bimetallic electrocatalysis can be used for the dehydrogenation of ethylene glycol to oxalic acid and that this acid can be hydrogenated to ethylene glycol as a main product.

Acknowledgements.

This work was performed in the framework of the BHyoLOHC project funded by the "France 2030" government investment plan managed by the French Research Agency, under the reference "ANR-22-PEHY-0016". The authors also acknowledge financial support from the European Union (ERDF) and Région Nouvelle Aquitaine. This work pertains to the French government program "Investissements d'Avenir" (EUR INTREE, reference ANR-18-EURE-0010).

References

1. L. Demarconnay, S. Brimaud, C. Coutanceau, *J. Electroanal. Chem* **2007**, 601, 169-180.
2. C. Coutanceau, S. Baranton, R.S.Bitty Kouamé, *Front. Chem.* **2019**, 7, article 100.
3. C. Lamy, C. Coutanceau, S. Baranton, in "*Hydrogen and Fuel Cells Primers", B. G. Pollet (Editor), Elsevier, Academic Press*, **2020,** pp. 1-122.

OC7: Hydrogenation, NH_3

Heterogeneous noble-metal-free catalysts for the semi-hydrogenation of alkynols under mild conditions

Ajay Tomer[1]*, Laurent Djakovitch[1], Noémie Perret[1]

[1][1]*Institut de Recherches sur la Catalyse et L'environnement de Lyon (IRCELYON) UMR 5256 - CNRS / Université Lyon 1, 69626 Villeurbanne Cedex, France*

*ajay.tomer@ircelyon.univ-lyon1.fr

Introduction

The semi-hydrogenation of alkynols to corresponding enols is a crucial process in the industrial production of pharmaceuticals, agrochemicals, fragrances, and flavors.[1] For example, enols such as 2-Methyl-3-buten-2-ol (MBE) are important intermediates in the synthesis of vitamin E. A plethora of active mono- and bi-metallic (Pd-, Pt-based) catalysts have been reported in the literature; however, the reports on Ni-based catalysts are limited as they often result in over-hydrogenated products.[2] Selective hydrogenation of alkynols is typically carried out in hydrothermal environment and thus demands highly water-resistant catalysts. In addition, catalysts should be able to suppress the hydrogenolysis or hydrodeoxygenation side reactions. Therefore, a rational design of an efficient and environmentally friendly heterogeneous catalyst is needed to address the limitations of current catalytic systems.

In this work, we report a series of titania-supported nickel catalysts synthesized by wet impregnation method varying the calcination temperature, metal loading, and titania phase compositions. The catalytic performances of Ni/TiO_2 catalysts were evaluated for the first time in the aqueous phase hydrogenation of 2-Methyl-3-butyn-2-ol (MBY) under mild conditions. The influence of particle size distribution, surface nickel species, surface acidity, and metal-support interaction on both activity and product distribution was investigated

Materials and Methods

5 & 10 wt.% Ni catalysts were prepared on different titania supports (P25, UV100, and HPX400) by wet impregnation followed by calcination (300-500 °C) and reduction under H_2 at 500 °C. The catalysts were characterized by XRD, UV-Vis, H_2-TPR, NH_3/MBY-TPD, TEM, and XPS to assess their physicochemical properties. The semi-hydrogenation reactions were carried out in a 300 mL Parr reactor with 1g of MBY and 0.1 g of reduced catalyst in 40 mL H_2O at 30-50 °C and 10 bar H_2 for 2-6 h. The products were analyzed by gas chromatography.

Results and Discussion

The hydrogenation of MBY on Ni/TiO_2 resulted in the formation of the targeted semi-hydrogenated MBE along with the fully hydrogenated MBA (2-methyl-3-butanol) as main by-product. The conversion and yield were dependent on the support and calcination temperature as shown in Figure 1. The pure anatase 10Ni/UV100 catalyst exhibited the highest conversion and MBE yield (~80%) while the pure rutile-based catalyst (10Ni/HPX400) favored mostly MBA. Some of the main properties of the catalysts are included in Table 1. The crystallite size of Ni was lower (D_{Ni} = 11.5 nm) in UV100 and HPX400 catalysts than with P25 (24.7 nm), and the size increased with the calcination temperature. Reducibility results demonstrated that mixed and rutile-phased titania interacted with Ni nanoparticles more strongly than anatase phase, as evidenced by their higher reduction activation energies (Red. E_a, Table 1). UV-vis analysis showed greater O2*p* → Ni*d* charge transfer in UV100 than P25. MBY-TPD results revealed stronger adsorption of reactant MBY on anatase titania catalyst compared to other titania (Table 1). Better adsorption of MBY facilitates MBE formation. Results clearly illustrate the effect of crystal phases of titania and metal-support interaction on both conversion and product distribution. The higher conversion and the improved MBE yield for 10Ni/UV100 catalyst is attributed to smaller Ni nanoparticles, greater charge transfer, weak to moderate metal-support interaction, and higher MBY adsorption strength.

Table 1. Physicochemical properties of titania-supported Ni catalysts

Samples	S_{BET} ($m^2.g^{-1}$)	% Anatase/Rutile	D_{Ni} (nm)	Red. E_a ($kJ.mol^{-1}$)	MBY Des. ($\mu mol.g^{-1}$)
10Ni/P25_500	40	83/17	24.7	68.2	61.5
10Ni/UV100_300	186	100/0	10.8	17.5	158.0
10Ni/UV100_400	172	100/0	11.2	20.7	133.2
10Ni/UV100_500	78	100/0	11.5	24.1	90.2
10Ni/HPX400_500	51	0/100	11.8	86.5	55.8

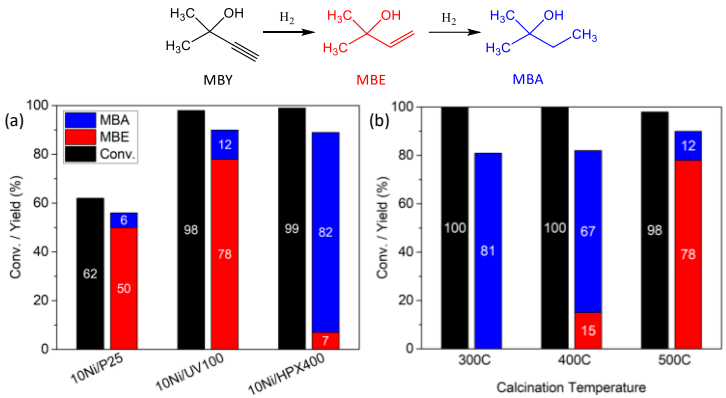

Figure 1. a) Catalytic activities of different Ni/TiO_2 catalysts, b) Effect of calcination temperature in 10Ni/UV100 catalyst. Reaction conditions: MBY- 1g, H_2O- 40g, Catalyst- 0.1g, Time- 6h, Temp.- 30 °C, H_2- 10bar, RPM- 900.

Significance

Our results showed promising performances of Ni/TiO_2 catalysts in MBY semi-hydrogenation under mild conditions (30 °C, 10 bar) without using any additives or promoters. Findings of this work can pave the path for selective chemical transformations with the potential to supersede the current industrial route (Lindlar catalyst) to alkenol production.

References

1. Á. Molnár, A. Sárkány, M. Varga, *J. Mol. Catal. A*, **2001**, 173, 185–221.
2. X. Chen, C. Shi, C. Liang, *Chinese J. Catal.*, **2021**, 42, 2105-2121.

Tuning the hydrogenation selectivity by playing with the carbide speciation in Mo-W mixed carbides

P. Azimov[1*], C. Guibert, C. Sayag, X. Carrier
[1] *Sorbonne Université, CNRS, Laboratoire de Réactivité de Surface, LRS, F-75005 Paris, France*
**parviz.azimov@sorbonne-universite.fr*

Introduction

Transition **m**etal **c**arbides (**TMC**s), particularly those of molybdenum (Mo) and tungsten (W), are recognized as promising alternatives to noble metal catalysts due to their similar electronic structures, resilience to poisoning agents, and economic advantages. Additionally, their catalytic properties can be finely tuned, further enhancing their performance.[2] For example, in Mo-W bimetallic carbides, the combination of the metallic functionality of Mo carbides with the oxophilic properties of W carbides can lead to the formation of a bifunctional catalysts with optimized and more versatile catalytic properties.[3] This approach provides a unique opportunity for specific reactions that demand both high activity and selectivity. In this study, we report on the structure-activity relationship of carbon-supported Mo-W mixed carbides synthesized via **t**emperature-**p**rogrammed **c**arburization (**TPC**) for the selective hydrogenation of acetylene.

Materials and Methods

Carbon-supported mono- and bimetallic Mo/W carbides were synthesized via TPC in a U-shaped quartz reactor under 20 vol% CH_4/H_2 atmosphere for 2 h at 873 K, then passivated in 1 vol% O_2/He for 2h. Bimetallic Mo-W samples with a Mo:W ratio of 3:1 (7.5 wt% Mo and 4.8 wt% W, noted Mo_3W_1-C) were prepared using two approaches: co-impregnation-carburization or sequential impregnation-carburization of Mo and W precursors. The influence of the preparation method on the catalysts was investigated by X-ray diffraction (XRD), transmission electron microscopy (TEM) and energy dispersive X-ray analysis (EDX).

Catalytic performances of the materials were assessed with the selective hydrogenation of acetylene at 623 K. In a typical experiment, the passivated catalyst was reduced in H_2 at 723 K for 2 hours before introducing the reactant stream containing 20 vol% H_2 and 1 vol% C_2H_2 balanced with He. The effluent gas was analyzed online using a micro gas chromatograph.

Results and Discussion

XRD of the mono-metal samples (not shown) reveal that the W sample exhibits reflections at 2θ = 40°, 58°, 73°, and 86°, corresponding to the cubic W-metal phase only. In contrast, the Mo sample shows only reflections of the cubic carbide phase (α-MoC_{1-x}), with no metallic phase detected. Further, XRD analysis was performed on Mo_3W_1-C samples in order to gain insight into the evolution of crystallographic phases in the bimetallic samples prepared either by co-impregnation-carburization or sequential impregnation-carburization (Figure 1a). As can be seen from the diffractograms, no significant differences are observed between the sample prepared by co-impregnation (Co-impr.) and sequential impregnation-carburization starting with W (W-first). In both samples, peak reflections at 2θ = 36°, 42° and 62° attributed to a cubic carbide phase can be distinguished. Analysis of single particles by EDX revealed simultaneous presence of Mo and W showing that TPC of the co-impregnated samples or sequential impregnation starting with W (W-first) leads to the formation of mixed bi-carbides particles and not to a mixture of two mono-metal carbides. Remarkably, when the sequential impregnation-carburization starts with Mo (Mo-first), XRD pattern of the product contains a mixture of peaks belonging to the cubic carbide phase (α-MoC_{1-x} , 2θ = 36°, 42° and 62°) and to the cubic metal W phase (2θ = 40°, 58°, 73° and 86°). These results are further confirmed by TEM analysis, which reveals two types of particles, with interplanar distances corresponding to the carbide phase (d_{111} = 0.24 nm) and to the W metal (d_{110} = 0.22 nm).

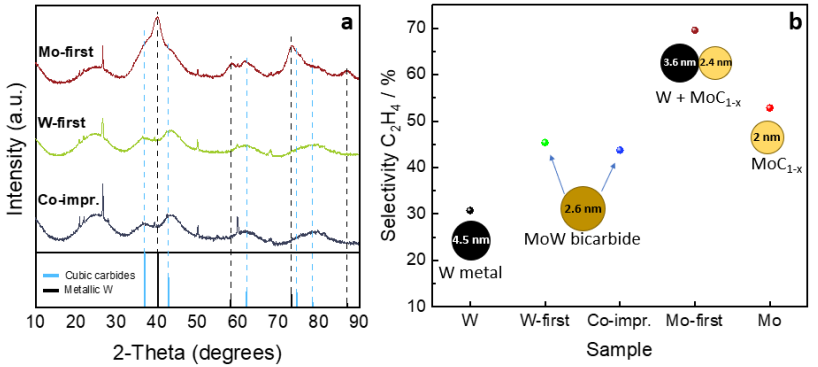

Figure 1. (a) X-ray diffraction (XRD) patterns of catalysts prepared via different methods. (b) Selectivity to ethylene during acetylene hydrogenation at 623 K as a function of catalyst composition and preparation method.

The results of acetylene hydrogenation are shown in Figure 1b for monometallic and bimetallic samples (Mo_3W_1-C). The structure-activity relationship between the bimetallic and monometallic samples reveals that the highest selectivity towards ethylene in acetylene hydrogenation is achieved with the Mo-first Mo_3W_1-C sample, which contains both α-MoC_{1-x} carbide and metallic W phases. Pure W metal, pure Mo carbide as well as a homogeneous MoW bimetallic carbide give lower selectivity. This suggests a synergistic effect in the Mo-first Mo_3W_1 sample between Mo carbide nanoparticles and metallic W that enhance the adsorption and further hydrogenation of acetylene, resulting in improved ethylene selectivity. The carburization sequence plays a critical role, as starting with Mo leads to a material with higher catalytic performance compared to co-impregnated or W-first methods, where mixed carbides without metallic W were formed.

Significance

The findings contribute to a deeper understanding of how a bimetallic synergy within TMCs can be optimized to design efficient and cost-effective catalysts for selective hydrogenation processes. Extension to other catalytic processes is underway.

References

1. M. Führer et al., Catal. Sci. Technol., **2020**, *10*, 6089
2. J. Zhu et al., Catal. Sci. Technol., **2020**, *10*, 3635.
3. Ch-C. Tran, Catal. Sci. Technol., **2019**, *9*, 1387

Selective C–O hydrogenolysis of erythritol over monometallic rhenium catalysts in aqueous phase

Theresa AL BAYEH[1], Catherine PINEL[1], Franck RATABOUL[1], Noémie PERRET [1]*
[1]*Ircelyon, CNRS, Université Lyon 1, 69266 Villeurbanne, France*

* noemie.perret@ircelyon.univ-lyon1.fr

Introduction

In the field of biomass valorization, polyols are of great interest due to their potential to form valuable chemicals through catalytic hydrogenolysis/deoxygenation and dehydration reactions under hydrogen leading to (partly)deoxygenated long chain products. These transformations involve competing C—O (desired) and C—C (undesired) bond cleavage pathways, with supported metal catalysts.[1] Literature indicates that monometallic catalysts based on noble metal (Ir, Rh, Pt) do not show a strong preference for C—O hydrogenolysis. In contrast, bimetallic catalysts, combining such a noble metal for hydrogen activation with an oxophilic promoter (Re, Mo) for polyol adsorption, have proven highly effective for C—O cleavage over C—C.[2] Polyol's sorbitol (C6) and glycerol (C3) have mainly been investigated. Besides, erythritol, a C4 polyol has rarely been studied despite its interest in giving C4 molecules, particularly butanediols that can be used as building blocks for polymer syntheses.

We aim to explore alternative solutions to reduce reliance on costly noble metals or bimetallic systems. Rhenium is a promising non-noble metal for hydrogenation reactions but has been investigated in very few biomass conversion reactions,[3] and there is no report on erythritol hydrogenolysis. We will present here our promising results obtained on monometallic rhenium supported on TiO_2 catalysts in erythritol hydrogenolysis, focusing on their activity and selectivity toward the C_4 linear deoxygenated product.

Materials and Methods

The monometallic catalyst, $4_{wt}\%ReO_x/TiO_2$, was synthesized through classical wet impregnation with NH_4ReO_4 and TiO_2 P25, followed by calcination (500 °C), reduction (450 °C), and passivation (25 °C). The catalysts were thoroughly characterized, including XRD, ICP, TGA, TPR/TPD, XPS, and STEM. Catalytic reactions were performed in continuous and batch reactors at 240°C using a 0.4 mol/L erythritol solution in water. In the continuous reactor, 1.26 g of catalyst was mixed with silicon carbide and tested under 85 bar H_2 pressure, while in the 300 mL batch reactor, 1.4 g of catalyst was used at 120 bar. Quantitative analysis was performed using HPLC (RID detector, Coregel 107H column).

Results and Discussion

The characterization revealed the presence of well-dispersed particles of rhenium (< 2 nm) on TiO_2. The characterization by XPS indicates a partial reduction of rhenium oxides after reduction at 450 °C and exposure to air with no metallic rhenium. This is not surprising since monometallic rhenium is known for its oxophilic properties. However, after in situ reduction under the same conditions as the catalytic test (240 °C), the amount of metallic rhenium increases to 32% as shown in Figure 1.

In a batch reactor, we studied different titanium dioxide supports, varying the anatase-to-rutile ratios, along with different calcination and reduction temperatures and various Re loadings. Here, we present the best results obtained so far. The reaction reached full conversion after 6 hours, achieving a high selectivity of 70% toward linear deoxygenated products, primarily 1,2-butanediol, demonstrating a strong preference for C—O hydrogenolysis at the C_3 and C_4 positions. Interestingly, the catalyst showed excellent conversion stability and high selectivity after 35 hours of continuous reaction in a packed-bed reactor with no detectable rhenium leaching (ICP analysis) in the aqueous phase.

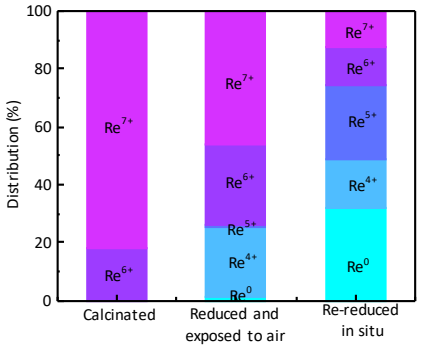

Figure 1. Distribution of rhenium oxide species in $ReOx/TiO_2$ after calcination at 500°C, reduction at 450°C and exposure to air, and in situ reduction at reaction temperature (240°C).
Obtained by XPS analyses.

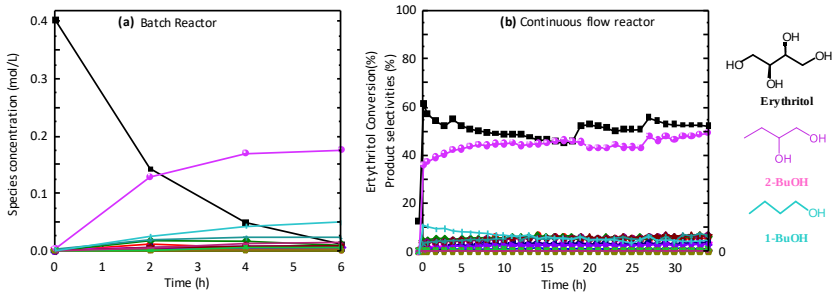

Figure 2. (a) Evolution of the concentration vs. time of reactant and products in a batch reactor, (b) Evolution of the conversion and selectivity vs. time in a continuous flow reactor.

Significance

We will present a detailed study on using supported monometallic rhenium as a non-noble metal catalyst for the catalytic hydrogenation of erythritol in the aqueous phase. This low-cost catalyst can be used under continuous flow conditions and shows very promising conversion and selectivity, as well as good stability over time.

References

1. Y. Amada, K. Tomishige, ChemSusChem, 2012, 00, 1.
2. A. said, ChemCatChem, 2017, 9, 2768.
3. J. Luo, ACS Catal., 2024, 14, 7032.

Promoting Ru Electron Density by basic Hydroxyapatite Supports for H_2 Storage as NH_3 under mild conditions

Sabrina Akrour[1], Alexandre Vimont[2], Sandra Casale[1], Guylène Costentin[1] and Cyril Thomas[1]*
[1]*Sorbonne Université, CNRS, Laboratoire Réactivité de Surface, LRS, Paris, 75005, France*
[2]*Normandie Université, Laboratoire Catalyse et Spectrochimie, 14000 Caen, France*
*cyril.thomas@sorbonne-universite.fr

Introduction

Ammonia (NH_3) plays a dual role as a key fertilizer in global agriculture and as a promising hydrogen (H_2) carrier for renewable energy storage[1]. Traditionally, NH_3 synthesis via the Haber-Bosch process requires severe conditions, high temperatures (400-600 °C) and pressures exceeding 200 bar, accounting for nearly 2% of global energy consumption and producing substantial greenhouse gas emissions[2]. Improving this process to achieve efficient NH_3 production under milder conditions remains a significant challenge. Ru catalysts have been reported to be more active than conventional iron (Fe) and nickel (Ni) catalysts[3] and Ru/MgO has been considered as a benchmark catalyst for NH_3 synthesis[4]. It has been suggested that the basic nature of the support enhances the electron density of Ru, which facilitates the dissociation of the nitrogen triple bond N≡N that is claimed to be the rate-limiting step in NH_3 synthesis.

The present study investigates original hydroxyapatite-supported Ru catalysts for NH_3 synthesis. Hydroxyapatite (HAp) is an environmentally friendly calcium phosphate known both for its high ability for metal dispersion[5] and for its basic properties that can be tuned by modifying its composition (Ca/P ratio) by adjusting the pH of the precipitation medium[6]. The influence of the synthesis conditions on the basic properties of the HAp supports, on the dispersion and electronic density of the Ru nanoparticles (NPs) are studied and discussed in line with the evolution of the turnover frequency (TOF) for NH_3 synthesis.

Materials and Methods

HAp supports were synthesized by adding a phosphorus precursor solution ($NH_4H_2PO_4$) to a $Ca(NO_3)_2$ solution at 80 °C, at stationary pH ranging from 6.5 to 9.0 by controlled addition of NH_4OH and by using an Optimax 1001 workstation (Mettler Toledo). Subsequently, Ru (1-5 wt%) was deposited by wet impregnation of $Ru(NO)(NO_3)_3$ and the metallic nanoparticles were obtained by reduction under H_2 at 450 °C for 2 h. ICP-OES chemical analysis, N_2 sorption, XRD, SEM, TEM and N_2-FTIR were used to characterize Ru/HAps and the catalytic conversion of 2-methylbut-3-yn-2-ol was used as a model reaction to investigate the acid-base properties of HAps. Ammonia synthesis was performed in a fixed-bed flow reactor (FR-100, Micromeritics) with a 50 mL/min H_2:N_2 (3:1) flow at 1 bar using 100 mg of catalyst diluted with 4.8 g of SiC. The NH_3 concentration at the reactor outlet was recorded every 5 seconds using an on-line MKS 2030 infrared analyzer.

Results and Discussion

Properties of the Ru/HAp catalysts: Crystalline (XRD) rod-like (SEM) HAps with a global increase in Ca/P ratio with increasing precipitation pH were successfully prepared. All of them show very similar specific surface areas of about 35 m^2/g. For all of the HAp_pH supports, well-dispersed Ru NPs of 2.1 ± 0.2 nm (TEM) were obtained after reduction. This particle size was maintained with increasing Ru loading.

Catalytic performance: Ru/HAp catalysts were found to be active and stable with time on stream (at least 3 days) for NH_3 synthesis. The catalytic measurements showed that varying the Ru content on HAp had a limited effect on the TOF values for NH_3 production. In contrast, the Ca/P ratio of the HAp support, modulated by the precipitation pH, significantly affected the TOF, reaching an optimum of 0.41 min^{-1} at 400 °C for Ru (2 wt%)/HAp_7.6. This TOF was found to be about 60 % higher than that of a Ru/MgO benchmark catalyst (**Figure 1a**). This finding is consistent with the higher basicity of the corresponding support as measured by the 2-methylbut-3-yn-2-ol model conversion reaction. In addition, N_2 adsorption on Ru^0 NPs at 100 K followed by FTIR showed the most pronounced shift of the maximum of the N_2 absorption band toward lower wavenumbers (2191 cm^{-1}) for Ru (2 wt%)/HAp_7.6 (**Figure 1b**), which is consistent with an increased electron density of the Ru^0 NPs for such a sample.

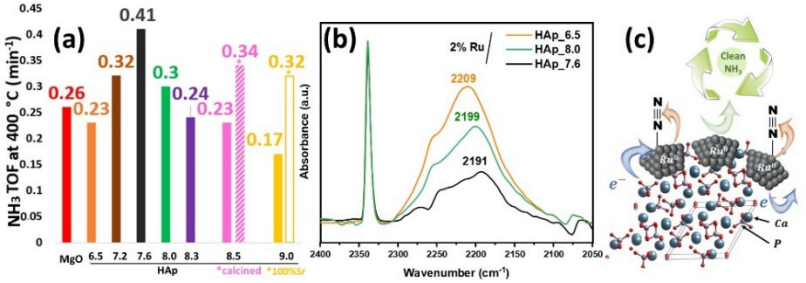

Figure 1. (a) NH_3 TOF at 400 °C and 1 bar over Ru/MgO and Ru/HAp_pH catalysts, (b) N_2-FTIR spectra at 100 K. (c) Schematic representation of the influence of HAp basicity on NH_3 synthesis.

Optimization paths: Better dispersion of the Ru NPs was achieved by performing a calcination step at 600 °C of the HAp support prior to Ru deposition. This reduced the size of the Ru NPs to 1.7 nm and resulted in an increase in TOF of about 50% for the calcined HAp_8.5 support compared to uncalcined HAp_8.5 (**Figure 1a, purple bars**).
Sr bulk-substituted HAp (Sr-HAp) was also prepared by coprecipitation, and the Sr-HAp support was found to be more basic than its Ca counterpart. This resulted in an increase in NH_3 TOF of about 90% for Ru/Sr-HAp_9.0 compared to Ru/HAp_9.0 (**Figure 1a, yellow bars**).

Significance:

These results not only highlight the potential of HAps and modified HAps as supports for Ru in NH_3 synthesis, but also provide a clear proof of concept of the critical role of the basic properties of the support on the electronic density of the Ru particles, and in turn on the activation of N_2 (**Figure 1c**).

References

(1) A. Afif et al., *Renew. Sustain. Energy Rev.* **2016**, *60*, 822.
(2) Q.Wang et al., *J. Energy Chem.* **2019**, *36*, 25.
(3) H. Fang et al., *ACS Catal.* **2022**, *12*, 3938.
(4) X. Ju et al., *ChemCatChem.* **2019**, *11*, 4161.
(5) M. Akri et al., *Nat. Commun.* **2019**, *10*, 1.
(6) T. Tsuchida et al., *J. Jpn. Petrol. Inst.* **2009**, *52*, 51.

Straightforward synthesis of highly active inorganic electride composites for green ammonia synthesis

Aissam ADDOU[1,2*], Amanda sfeir[2], Jean-Philippe Dacquin[2], Sébastien Royer[2,3], Said Laassiri[1]

[1]*Chemical & Biochemical Sciences, Green process Engineering (CBS), Mohammed VI polytechnic university, UM6P, 43150, Benguerir, Morocco.*

[2]*Université de Lille, CNRS, ENSCL, Centrale Lille, Univ. Artois, UMR 8181-UCCS-Unité de Catalyse et de Chimie du Solide, F-59000 Lille, France.*

[3]*Université Littoral Côte d'Opale, UR 4492, UCEIV, Unité de Chimie Environnementale et Interactions sur le Vivant, Dunkerque, F-59140 France.*

*aissam.addou@univ-lille.fr

Introduction

To consider ammonia as an energy carrier, it is essential to develop efficient catalysts for ammonia synthesis under milder conditions (e.g; 400°C - 50 bars). Recently, electride-based materials attracted significant attention as highly active and stable catalysts for ammonia synthesis[1]. In electrides, electrons function as anions (nucleus-free) within the lattice structure, facilitating nitrogen bond cleavage by enhancing electron donation to the active phase. This electron donation reduces the energy barrier for nitrogen bond dissociation and shifts the rate-determining step of the reaction from bond cleavage to the formation of reaction intermediates. This property leads to improved catalytic performance while inhibiting hydrogen poisoning on Ru metal surface, making electrides serious candidates for producing green ammonia under intermittent conditions at low T(°C) and low P(MPa). Among electride-type catalysts, notable examples include C12A7: e^-, Ca_2N, $BaO_xN_ye^-_z$, Ba_2N, and LaRuSi (an intermetallic Ru-based electride). These materials have demonstrated the ability to promote ammonia synthesis over Ru at low temperatures, with a low apparent activation energy (49-67 kJ/mol), which is clearly lower than that of conventional Ru catalysts (120 kJ/mol). Recently, $BaAl_2O_{4-x}H_y$ has been introduced as a 3D lattice structure oxyhydride electride, showcasing impressive catalytic performance for ammonia synthesis when promoted both with noble (665 mmol g_{Ru}^{-1} h^{-1} at 340°C and 0.90 MPa) and with non-noble metals (500 mmol g_{Co}^{-1} h^{-1} at 340°C and 0.90 MPa)[2]. However, the synthesis of electrides is often complex, requiring high-temperature of reduction and metal reducing agents such as Al, Ca, and metal hydrides like BaH_2. The objective of this study is to develop a simplified approach for the preparation and activation of electrides, characterized by surface area retained and elevated electron density.

Materials and Methods

$BaAl_2O_{4-y}e^-_y$/C was synthesized using a sol-gel method coupled with carbothermal reduction process under nitrogen at 1400°C for 4 hours. First, the xerogel was prepared using nitrate precursors in distilled water, with the addition of citric acid and ethylene glycol in a molar ratio of n_{CA}/n_{EG} = 4. The xerogel was then transformed into an oxy-electride composite support at high temperature under nitrogen gas flow. The resulting powder was impregnated with $Ru_3(CO)_{12}$ in tetrahydrofuran and treated in N_2 at 250°C for 2 hours, producing 0.6 wt% and 1.1 wt% Ru/$BaAl_2O_{4-y}e^-_y$/C catalysts. All catalysts were then tested without any further pretreatment under the following conditions: N_2/H_2 = 1:3, 60 ml/min, 250-400°C, 0.1 MPa. The catalysts were characterized using XRD, Raman, HAADF-STEM, TGA, EPR, H_2-TPR, iodometry, and N_2 adsorption-desorption techniques.

Results and Discussion

Characterization results revealed that $BaAl_2O_{4-y}e^-_y$/C exhibits key features of electride-based materials, including a high electron density (5.72 × 10^{21} cm^{-3}, quantified via iodometry). XRD confirmed that $BaAl_2O_4$ is the main phase. The surface area of the prepared support measured to be 41 m^2/g, which is higher compared to conventional methods for preparing inorganic electrides (1–2 m^2/g). These properties are attributed to the presence of 20 wt.% residual graphitized carbon in the material, confirmed by Raman spectroscopy, which identified the G and D bands. STEM analysis revealed that the carbon in the material forms a fibrillar-like structure surrounding the particles. The Ru particle sizes averaged 1.7 nm for 0.6 wt% Ru/$BaAl_2O_{4-y}e^-_y$/C and 2.0 nm for 1.1 wt% Ru/$BaAl_2O_{4-y}e^-_y$/C.

The 0.6 wt% Ru/$BaAl_2O_{4-y}e^-_y$/C oxy-electride composite demonstrated an ammonia synthesis rate of 3090 µmol $g^{-1}_{Catalyst}$ h^{-1} at 400°C and 0.1 MPa, with an activation energy (Ea) of 60 kJ/mol. For comparison, 2.5 wt% Ru/$BaAl_2O_{4-y}e^-_y$/C showed a rate of 1377 µmol $g^{-1}_{Catalyst}$ h^{-1} and an Ea of 74 kJ/mol (Figure 1-a, b, and c). These catalysts outperformed conventional Ru-based catalysts (e.g., Ba-Ru/AC, Ru/MgO) and other electride-based Ru catalysts (e.g., BaOxNye-z, C12A7: e^-)[3]. Furthermore, the catalysts maintained good stability for over 9 days under synthesis conditions, with no observed loss of activity. The composite carbon-electride support induce strong promotional effects on the Ru. It reduces the energy barrier for synthesis, which could be associated to a strong interaction between the support and the Ru. This interaction, coupled with the stabilization of small Ru particles enhancing the density of active B5 sites, facilitates nitrogen bond cleavage under mild conditions.

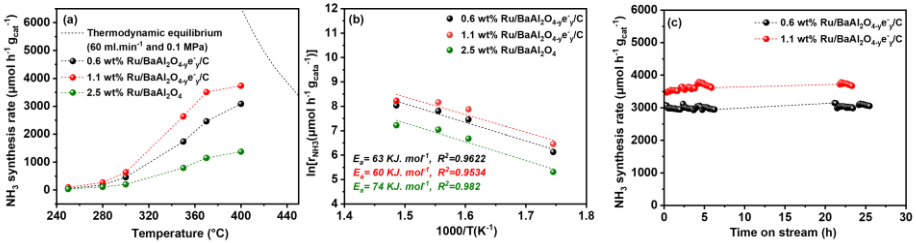

Figure 1. (a) Temperature dependence of the NH_3 synthesis rates over 0.6 wt% Ru/$BaAl_2O_{4-y}e^-y$/C and 1.1 wt% Ru/$BaAl_2O_{4-y}e^-y$/C. (b) Arrhenius plots in the temperature ranges of 573-673K. (c) Reaction time profile for ammonia synthesis over 0.1g of catalyst at 400°C and 0.1 MPa under 60 ml/min of 75%H_2/N_2 gas flow.

Significance

The present work demonstrates a straightforward approach to synthesizing oxy-electride composites via a carbothermal reduction process. $BaAl_2O_{4-y}e^-_y$/C promotes ammonia synthesis on Ru at low temperatures and exhibits high structural and catalytic stability, maintaining good catalytic performance for green ammonia synthesis.

References

1. Kitano M, et al. *Nat Chem*. **2012,** 4, 934.
2. Jiang Y, et al. *J Am Chem Soc*. **2023**, 145, 10669.
3. Li J, et al. *Adv Energy Mater*. **2023**, 13, 2302424.

H_2-Assisted Synthesis of $Ni_2P/Ni_{12}P_5$ Nanocatalysts for Low Temperature Phenylacetylene Hydrogenation

Bakkouche K.[1], Carenco S.[1]*

[1] *Laboratoire de Chimie de la Matière Condensée de Paris, CNRS, Sorbonne Université, 4 place Jussieu, 75005 Paris, France*

*sophie.carenco@sorbonne-universite.fr

Introduction

Given the wide range of unique magnetic, redox, and catalytic properties of transition metal phosphides, developing nanoscale synthesis methods with precise control of the size, shape, and composition presents a considerable challenge.[1–3] Among the strategies, colloidal synthesis routes lead to readily dispersed metal phosphide nanoparticles directly suitable for use in catalytic reactions. In the literature, there are many reports that describe the synthesis of metal phosphide nanoparticles and particularly nickel phosphide using oleylamine as both the solvent and the reducing agent.[4] . In contrast, we propose a novel method for the synthesis of well-crystallized monodisperse nickel phosphide (mixture of Ni_2P and $Ni_{12}P_5$) nanoparticles under hydrogen, using mesitylene as a non-coordinating solvent. Although nickel nanoparticles have been synthetized under hydrogen using different nickel precursors, this approach marks the first instance of nickel phosphide being produced in such conditions.

Nickel phosphide nanocatalysts were then evaluated in the phenylacetylene hydrogenation as a colloidal nanocatalyst in the presence of an additional Lewis base (tri-n-butylphosphine). We proved that the catalytic activity of the mixture Ni_2P and $Ni_{12}P_5$ nanoparticles could be boosted by the presence of P^nBu_3. This enhancement of the catalytic activity could concern either the substrate conversion or a product selectivity. At high temperature (80 °C and 100 °C), the phosphine allowed an enhancement for styrene selectivity, while at low temperature (60 °C, 40 °C, 30 °C and 0 °C), the addition of P^nBu_3 is required for the reaction to occur.

Materials and Methods

Nickel phosphide nanocatalysts were synthesized in an autoclave under 3 bar of hydrogen using $Ni(acac)_2$ and tri-n-octylphosphine (TOP) as nickel and phosphorus precursors. The crystalline phase of nanoparticles was then characterized X-Ray Diffraction and high resolution TEM. The size of NPs was determined by TEM and the surface state was studied by XPS. These nanocatalysts were then used in phenylacetylene hydrogenation in the presence of tri-n-butylphosphine $(P^nBu)_3$. The catalytic reaction was monitored by liquid ^1H NMR and ^{31}P NMR.

Results and Discussion

Briefly, we developed a new robust synthesis method of nickel phosphide (Ni_2P and $Ni_{12}P_5$) nanoparticles with a narrow size distribution and tunable crystallographic phase achieved by decomposition of $Ni(acac)_2$ in the presence of TOP as the ligand and the phosphorus precursor, under a reducing atmosphere (H_2). The control of the crystallographic phase was possible by adjusting TOP concentration and the reaction temperature. Moreover, the synthesis provided NPs with a high chemical yield, allowing their use in catalysis.

Then, we demonstrated the phosphine effect on the catalytic hydrogenation of phenylacetylene at different temperatures from 0 °C to 100 °C as shown in figure 1. At high temperature (80 °C and 100 °C), the addition of the phosphine has no effect on the conversion, a significant enhancement of selectivity for the styrene was obtained from 0 % to 40 % at 100 °C and from 0 % to 68 % at 80 °C. in contrast, at lower temperature (30 °C, 40 °C and 60 °C), the presence of phosphine is necessary for the reaction to occur since there was no conversion observed without adding P^nBu_3.

Remarkably, in the presence of both nickel phosphide nanoparticles and P^nBu_3, 22% of conversion was obtained when the reaction temperature is lowered to 0°C. In other words, the combined action of both NPs and the phosphine allows the phenylacetylene hydrogenation reaction to occur at significantly milder conditions where usually Pt and Pd catalysts are required.

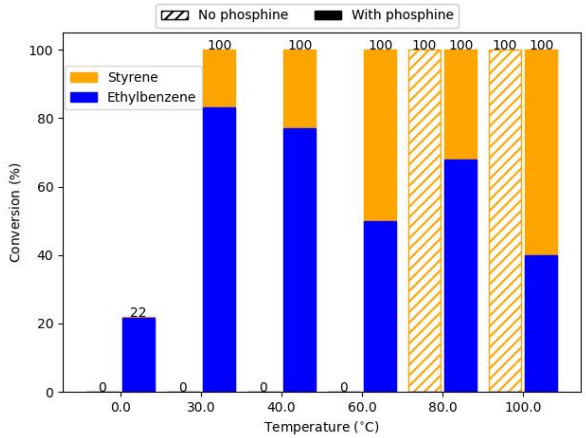

Figure 1. Influence of the temperature on the catalytic activity of the mixture Ni_2P and $Ni_{12}P_5$ NPs with and without phosphine $(P^nBu)_3$. Reaction conditions : phenylacetylene (1 mmol), NPs (0.1 mmol), P^nBu_3 (0.2 mmol), anisole (0.33 mmol), toluene (2 mL), 16 h, H_2 (7 bar).

Significance

This work focuses of the development of new, cost-effective synthesis methods of highly efficient catalysts for low-temperature hydrogenation reactions, in the presence of Lewis bases, such as phosphines.

References

1. S. Brock, et al, *J. Solid State Chem.* **2008**, *181* (7), 1552–1559
2. E. Popczun, *Angew. Chem. Int. Ed.* **2014**, *53* (21), 5427–5430.
3. S. Carenco, *Chem. Rev.* **2013**, *113* (10), 7981–8065.
4. E. Muthuswamy, *ACS Nano* **2011**, *5* (3), 2402–2411.

OC8: Adv. characterization, Kinetics, Sorption

Probing surface reaction dynamics using calorimetry vs gas chromatography: The case of isopropanol dehydration

T. Cabanis[1]*, A. Auroux[1], J.-L. Dubois[2], N. Sbirrazzuoli[3], G. Postole[1]
[1]*Universite Claude Bernard Lyon 1, CNRS, IRCELYON, UMR 5256, Villeurbanne, F-69100.*
[2]*Trinseo Netherlands B.V., Innovatieweg 14, 4542 NH Hoek, The Netherlands*
[3]*Institut de Chimie de Nice (ICN) – UMR CNRS 7272, Université Côte d'Azur (UCA), 28 avenue Valrose, 06108 Nice Cedex 2, France*
*tristan.cabanis@ircelyon.univ-lyon1.fr

Introduction

The study of chemistry at the catalyst surface is the key for understanding the fundamental mechanism in heterogenous catalysis taking a vital role in numerous industrial processes.[1] Thermal analysis and calorimetry are one of the powerful tools for catalyst characterization. For example, the quantification of active site strengths through interactions with probe molecules allows direct correlation between site strength and number to catalytic efficiency of a material.[2] Moreover, thermal analysis signals shape is correlated to the kinetics of the thermal effect being observed. Computations on these signals have already allowed for the determination of kinetic parameters and models of several solid-state reactions.[3] Knowing how kinetics is important in catalysis research, applying these methods to a catalytic thermal event would provide interesting information to the field.

This work introduces a novel operando system allowing the measurement of the heat flow signal involved during a heterogeneous catalytic reaction. A pulse catalytic test is set inside a Calvet-type calorimeter and directly linked to a gas chromatograph. Catalytic dehydration of isopropanol to propylene is used as a standard reaction.

Materials and Methods

Pulse experiments were carried out in a quartz microreactor placed in a Setaram Calvet differential scanning calorimeter (DSC) connected to a gas chromatograph (GC). The reaction cells are 1/4' in diameter quartz tubes fitting perfectly into the DSC. Typically, 15 mg of the catalyst with controlled particle size of 300 µm to 425 µm is loaded. The catalyst is constantly flushed with a 30 mL.min^{-1} helium flow. A 6-port valve set inside the GC and equipped with a calibrated sample loop is used to admit a fixed amount of reagent into the carrier gas flow. The outlet of the microreactor is directly connected to a Porapak Q column and to thermal conductivity (TCD) and flame ionization detectors (FID) placed in series.

Results and Discussion

Figure 1.a displays the typical heat flow signal obtained after injection of 1.15 µmol of isopropanol on a commercial alumina catalyst supplied by Grace Davison, at 250 °C. The first exothermic peak refers to the adsorption of isopropanol, while the subsequent endothermic peak is attributed to both the reaction and the product desorption. The thermogram was therefore deconvoluted in exothermic and endothermic peaks as shown in Figure 1.b.

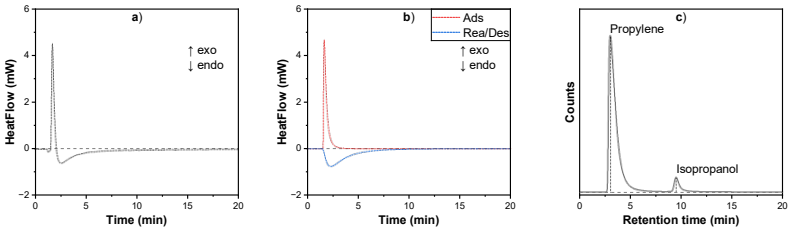

Figure 1. Typical measured (a), deconvoluted (b) heat flow and FID (c) signals as a function of time when reaction occurs at 250 °C, at steady state.

The conversion rate and the enthalpy of each exothermic/endothermic effect were therefore calculated using the opposite integrated values from thermograms and the amounts of adsorbed/reacted isopropanol from GC results (Figure 1.c). At 250 °C, 1.09 µmol of isopropanol, representing a conversion rate of 94.7%, was adsorbed (exothermic peak) and converted (endothermic peak) to propylene with complete selectivity. The enthalpy of adsorption was calculated to be −98 kJ.mol^{-1}, and the enthalpy of reaction/desorption to be +114 kJ.mol^{-1}. Based on the literature values of water and propylene desorption heats, the standard enthalpy of the reaction has been evaluated.

Obtained values of adsorption and desorption/reaction enthalpies are in good agreement with the values obtained by density function theory (DFT) from the literature. Indeed, Larmier et al.[4] calculated the adsorption enthalpy of isopropanol on γ-alumina to be −89 kJ.mol^{-1} and a reaction enthalpy of +125 kJ.mol^{-1} in the case of a E2-type mechanism. The differences can be explained through different statements used in DFT.

Significance

This novel system of a pulse catalytic test set inside a DSC is trusted to be an interesting tool for energetic and mechanistic studies through experimental data. Moreover, further analysis of the endothermic and exothermic contributions as a function of time and temperature can be used to determine the kinetic parameters and lead to an accurate description of each step of the catalytic process.

References v

1. G. A. Somorjai, Y. Li in Introduction to Surface Chemistry and Catalysis, John Wiley & Sons, **2010**.
2. A. Auroux in Calorimetry and Thermal Methods in Catalysis, Springer Berlin, Heidelberg, **2013**.
3. S. Vyazovkin, A. K. Burnham, J. M. Criado, L. A. Pérez-Maqueda, C. Popescu, N. Sbirrazzuoli, Thermochimica Acta, **2011**, 520 (1–2), 1–19.
4. K. Larmier, C. Chizallet, N. Cadran, S. Maury, J. Abboud, A; F. Lamic-Humblot, E. Marceau, E, H. Lauron-Pernot, ACS Catal. **2015**, 5 (7), 4423–4437.

This work is part of PYROCO2 project that has received funding from the European Union's Horizon 2020 research and innovation programme under grant agreement No. 101037009.

Isobutanol dehydration catalyzed by HFER: mechanism insights from FT-IR and kinetic modelling

Eleonora Vottero[1]*, Reda Aboulayt[1], Alexandre Vimont[1], Philippe Bazin[1], Karine Thomas[1], Sylvie Maury[2], Céline Chizallet[2] and Arnaud Travert[1]
[1]*Univ Caen Normandie, ENSICAEN, UNICAEN, CNRS, LCS, 14000 Caen, France*
[2]*IFP Energies Nouvelles, 69360 Solaize, France*
*eleonora.vottero@unicaen.fr

Introduction

The dehydration of alcohols derived from biomass provides an interesting alternative to oil refinement for the production of alkenes, which constitute a fundamental building block in the petrochemical industry. In the frame of the MAMABIO project (B-BEST PEPR, contract ANR-22-PEBB-0009), our current work focuses on the investigation of the reaction mechanism and kinetics of the isobutanol dehydration reaction catalyzed by HFER. This process is of particular interest as HFER exhibited a remarkable selectivity for the direct conversion of isobutanol to linear butenes,[1-2] as opposed to most other solid acid catalysts which lead to the formation of the direct dehydration product (isobutene) instead.[3-4] The exact reaction pathway and the nature of the catalytic sites, however, remains elusive.

Materials and Methods

Isobutanol dehydration is being investigated on an HFER catalyst with Si/Al ratio = 12.5 and exhibiting a large external surface area (47 m^2/g) provided by the IFPEN laboratories. Their reactivity in the presence of isobutanol along a temperature ramp lasting 2 h and ranging from 40 to 264°C has been investigated by *in situ* FT-IR spectroscopy by employing the custom "Jumpipe" setup, which allows for the alternate measurement of the gas present in the cell and of the pelletized zeolite. The concentration profiles of the reactant, intermediates and products were obtained by analyzing the IR spectra dataset with nnls (non-negative least squares) and multivariate curve resolution with alternating least squares (MCR-ALS). Finally, the concentration profiles were used to fit a kinetic model and calculate the corresponding kinetic parameters. All the chemometric analysis was performed with Spectrochempy.[5]

Results and Discussion

The isobutanol dehydration reaction intermediates and products on the investigated HFER catalyst were identified and quantified by nnls fit analysis (for the species in the gas phase) and MCR-ALS (for the species adsorbed on the catalyst during the reaction). The resulting experimental concentration profiles are shown in Figure 1 (continuous lines).
The first gas phase products (Figure 1A) are H_2O and 2-butene, then the concentration of the latter decreases in favor of the formation of isobutene and (at last) 1-butene. Isobutanol does not access the internal porosity of the catalyst: the first intermediate observed after adsorption on the external surface is 2-butanol (Figure 1B), which then dehydrates to 2-butene. This observation strongly suggests that the reaction started on the external surface with the alcohol isomerization to the linear isomer, then followed by dehydration to linear 2-butene, as supported by DFT studies.[6] The Brønsted acid sites (BAS) inside of the pores are the last ones to be affected, following the adsorption of H_2O and butenes. The latter interacted with the BAS to form oligomers and at last coke which, in turn, are likely to be involved in secondary reactions contributing to the isomerization of 2-butene to isobutene and 1-butene.
These considerations permitted to elaborate a preliminary reaction mechanism, which was then included in the kinetic model used to fit the experimental concentration profiles (dashed lines, Figure 1). The kinetic parameters calculated by the fit will be later compared with those calculated by DFT simulations to finalize the rationalization of the reaction mechanism.

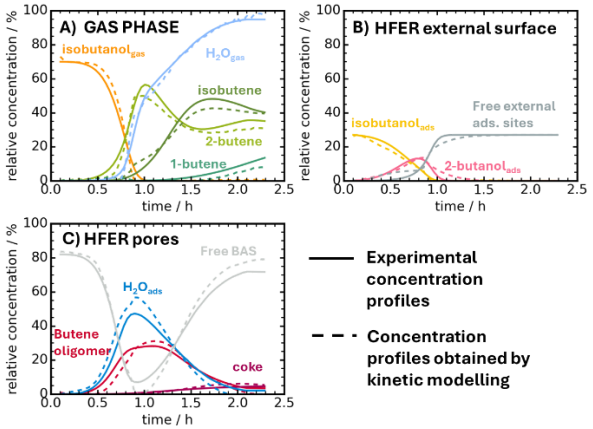

Figure 1. Experimental profiles for the reactant, the reaction intermediates and products (continuous lines) compared with the corresponding profiles calculated by kinetic modelling fit (dashed line). For readability, the species observed in the gas phase are reported in panel A, those at the external surface of the HFER crystals in panel B, and those formed within the zeolite pores in panel C.

Significance

Isobutanol dehydration on HFER is a promising alternative for the direct production of linear butenes.[1-2] Our study strengthens previous hypotheses about the reaction mechanism, in particular confirming that the reaction starts with the isomerization of isobutanol into 2-butanol at the external surface of the HFER crystals, followed by dehydration to 2-butene (as proposed by computational studies[6]). A better understanding of such an unusual reaction mechanism is not only of theoretical interest, but it is also fundamental to rationally optimize the catalyst to the target application.

References

1. Z. Buniazet *et al, Applied Catalysis B: Environmental*, **2019** 243 594-603
2. S. Van Daele *et al*, *Applied Catalysis B: Environmental*, **2021** 284 119699
3. H. Knözinger *et al, Journal of Catalysis*, **1972** 24 57-68
4. J.D. Taylor *et al*, *Topics in Catalysis*, **2010** 53 1224-1230
5. A. Travert, C. Fernandez, *Zenodo* **2024** DOI: 10.5281/zenodo.3823841
6. M. Gešvandtnerová *et al*, *Journal of Catalysis* 413 **2022** 786–802

Highlighting the Positive Impact of Zeolite on Platinum-Catalyzed Hydrogenation through a High-Throughput Infrared Study

Maya El Zayed[1], Philippe Bazin[1] and Ludovic Pinard[1]*

[1]*Laboratoire Catalyse et Spectrochimie (LCS), Université de Caen, CNRS, F-14000, Caen, France*
*ludovic.pinard@ensicaen.fr

Introduction

The hydrogenation of unsaturated molecules is a crucial industrial reaction, essential for the production of numerous petrochemicals. While catalyst performance is primarily associated with the nature of metallic sites, the support material plays a pivotal role in influencing hydrogenation activity[1,2]. Using high-throughput infrared spectroscopy, this work provides a large library of kinetic data, highlighting the synergistic interplay between zeolite and platinum during pyridine hydrogenation.

Materials and Methods

Experiments were carried out using the innovative "Caroucell" infrared cell[3], enabling real-time monitoring of pyridine hydrogenation across 10 samples at 110°C under varying hydrogen pressures. Pt/SiO_2 acted as the metallic component, promoting hydrogen dissociation, while the ZSM-5(11) zeolite content was varied to evaluate its influence on catalytic performance. The mixtures tested included 25%, 50%, and 75% zeolite proportions.

Results and Discussion

The hydrogenation of pyridine was strongly influenced by the hydrogen pressure within the system. On 0.6 wt% Pt/SiO_2 mixture with ZSM-5(11) in a 1:1 mass ratio, the formation of piperidine (band at 1473 cm^{-1}) occurred slowly at 15 Torr (figure 1a). However, increasing the hydrogen pressure within the infrared cell significantly boosted pyridine conversion. This demonstrates that higher hydrogen pressures enhance hydrogenation efficiency by promoting the diffusion of activated hydrogen species (H_{SP})[1]. The presence of zeolite in the catalyst further enhanced hydrogen adsorption via hydrogen spillover, a key mechanism for transferring activated hydrogen to the reaction sites[2,3].

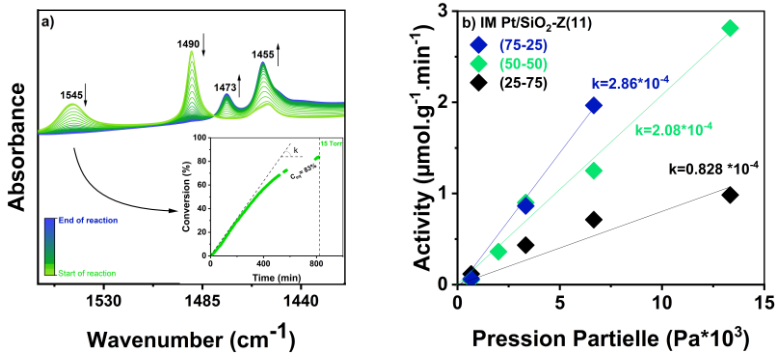

Figure 1. a) Tracking Reaction Dynamics: Analysis of 1000 Infrared Spectra Over 15 Hours at 15 Torr and Conversion vs. time b) Catalyst Activity vs. Hydrogen Pressure

Additionally, surface diffusion played a crucial role in the effective conversion of adsorbed pyridine, with its contribution increasing as the applied pressure in the IR cell was elevated. To gain deeper insights into the role of zeolite on surface diffusion and diffusion time, the reaction rate constant (k) was calculated for mixtures containing 25%, 50%, and 75% zeolite, respectively.

As depicted in (figure 1b), the first-order reaction kinetics reveal that the optimal reaction rate constant was achieved with the 25% zeolite mixture, outperforming those with 50% and 75% zeolite. This finding indicates that the reaction rate constant (k) is directly influenced by the diffusion time of hydrogen species traveling from the Pt/SiO_2 to the zeolite. Therefore pyridine, plays a dual role in this system—not only as a reactant but also as an active participant driving the spillover process. Acting as a "pumping machine," pyridine facilitates the transfer of hydrogen species across the catalyst, ensuring effective interaction with Brønsted acid sites within the zeolite[4].

Notably, a minimum diffusion distance is required for the pumping effect of pyridine to operate effectively, with the optimal arrangement observed at a 3:1 ratio of $Pt-SiO_2$ to protonated zeolite, regardless of the zeolite's acidity emphasizing the significance of spatial arrangement within the catalyst. These findings are consistent with previous hydrogen chemisorption analyses investigating the spillover mechanism, which revealed that the degree of hydrogen spillover is highly sensitive to catalyst composition. The most efficient performance was achieved with a 75% Pt/SiO_2 and 25% zeolite mixture (table 1). This specific composition strikes an optimal balance between hydrogen adsorption and spillover activity while ensuring the necessary number of acidic sites for effective catalytic operation[2]. The enhanced performance of this mixture underscores the importance of precisely tailoring catalyst proportions to achieve maximum bifunctional synergy.

These findings illustrate the interplay between catalyst design, hydrogen spillover dynamics, and reaction kinetics, highlighting how the structural and compositional optimization of catalysts can profoundly influence their performance.

Table 1. Acidity and spillover hydrogen amount measurements for mixtures

Pt/SiO_2 wt.%	ZSM-5(11) wt.%	n_{H2} (µmol.g^{-1})[a] 40°C	110°C	[PyH^+] [b] µmol.g^{-1}
75	25	22	20.4	128
50	50	13.9	13.6	251
25	75	6.2	6.5	378

[a] H_2 Chemisorption; [b] number of protonic sites able to retain pyridine at 150°C (µmol.$g_{catalyst}^{-1}$)

Significance

This work provides a deeper understanding of the bifunctional mechanisms driving hydrogenation processes. The findings demonstrate how zeolite-metal interactions, facilitated by hydrogen spillover and driven by pyridine dynamics, can be harnessed to design more efficient catalysts.

References

1. N. Batalha, J. D. Comparot, A. Le Valant, L. Pinard., *Catal. Sc. Tech*. **2022**, *12*, 1117-1129
2. J. Chupin, N.S. Gnep, S. Lacombe, M. Guisnet, *Appl. Catal.* **2001**, *206*, 43-56
3. V. Zholobenko, P. Bazin et al., *J. Catal.* **2020**, *385*, 52-60
4. H. Shin, M. Choi and H. Kim, J. Phys. *Chem. C.* **2016**, *18*, 7035–7041

ME-PSD IR Spectroscopy to study CO oxidation reaction under Pt/Al_2O_3 catalyst

Nassar N., Djaafri A., Richard M., Dujardin C., Tougerti A., Cristol S.*
University of Lille, CNRS, Centrale Lille, ENSCL, University of Artois, UMR 8181-UCCS- Unité de Catalyse et Chimie du Solide, F-59000 Lille, France
*Sylvain.cristol@univ-lille.fr

Introduction

Dynamic behavior investigation of actives species involved in catalytic reaction is still highly challenging since a catalytic pathway is a combination of rapid adsorption and desorption of reactants/intermediates/products on ill-defined active surface sites.[1] Furthermore, the spectroscopic signal arising from non-active sites (spectators) is frequently stronger than that of actives sites, overwhelming key information on catalysis. One way to mitigate this problem is to apply Modulation Excitation Spectroscopy (MES)[2] which consists in a periodic perturbation of the state of the system by the variation of external parameter such as temperature, pressure, concentration... This rapid periodic perturbation of the system state will influence only the concentration profile of the active species which will oscillate at the frequency of the periodic excitation but with a phase delay. The concentration profile of species not responding to the periodic excitation (*i.e.* spectator species) will remain constant making possible their removal from the global signal by a post data acquisition mathematical treatment known as PSD (Phase Sensitive Detection). In this study we aim to monitor the dynamic behavior of actives species formed on the Pt/Al_2O_3 catalyst's surface during CO oxidation reaction by applying ME-PSD infrared (IR) spectroscopy (rapid looping from ^{12}CO to ^{13}CO while simultaneously recording time-resolved IR spectra). Indeed, although the Alumina-supported Pt catalyst (commonly used for CO and unburned hydrocarbon oxidation) has been extensively studied, the reaction mechanism of CO oxidation remains unclear and is still widely debated. Over 20 different steps have been proposed in the literature to explain this mechanism.[3]

Materials and Methods

Catalyst Synthesis. Pt/Al_2O_3 catalyst is prepared by incipient wetness impregnation of ɣ-Al_2O_3 support (specific surface area of 225 m^2g^{-1} and a pore volume of 0.76 cm^3g^{-1}) with platinum (II) acetylacetonate (Fluka) precursor salt to obtain 1 wt% metal loading. The sample was dried overnight at 85 °C, calcined 2 h under air flow at 500 °C (ramp 10 °C/min) and reduced with dihydrogen 2.5 h at 400 °C (ramp 5 °C/min).

ME-experiments. The catalyst is introduced in a home-made transmission IR reactor composed of 6 inlet and outlet channels (diameter 200 µm), in form of a square pellet (~10 mg and 1.21 cm^2) to perform *operando* experiments. The low dead volume of the reactor used here inferior to 0.5 cm^3, a required condition to obtain more relevant kinetic data for ME application. Spectra are obtained by using a ThermoScientific Nicolet 6700 FTIR spectrometer equipped with a MCT detector enable millisecond order spectra acquisition in rapid-scan mode. The cell is connected on one side to an automatic gas distribution system (Beckhoff®) composed of 4-way pneumatic valve upstream of the transmission IR reactor in order to switch the gas phase composition in isobaric and isotherm conditions. The ME PSD IR experiments are started once the system reach its steady state, only then the switching of the reactant from ^{12}CO to its labelled counterpart ^{13}CO is performed (sending 2000 ppm of $^{12}CO + O_2$ for 15s on the catalyst surface, then we switch to 2000 ppm of $^{12}CO + O_2$ also for 15s, the gas flow rate was 12ml/min), under a constant temperature of 119°C. This $^{12}CO \rightarrow {}^{13}CO$ gas switch step was repeated 100 times.

Results and Discussion

"Figure 1 (top) shows IR spectra recorded during the ME-IR experiment (time domain), along with demodulated spectra obtained after PSD signal processing (Figure 1, bottom). In the 'CO adsorbed on Pt' region, the isotope peak exchange is visible in the time domain. However, in the 'carbonate and CO adsorbed on 2 Pt' regions, the isotope peaks become distinctly evident following PSD signal processing.

Similar peaks between 1400 and 1900 cm^{-1} are observed for both fundamental and harmonic frequencies. However, in the CO adsorbed on Pt region, two additional peaks appear at 2043 and 2093 cm^{-1} in the harmonic frequency. This is clear evidence of the presence of two distinct kinetic processes. Indeed, since k3 reflects the behavior of species reacting at a higher frequency than the system's fundamental perturbation, we can conclude that carbonate species and CO bridging on two Pt atoms exhibit a slower exchange rate than CO adsorbed on a single Pt atom. Note also that the exchange between ^{12}CO and ^{13}CO is a simpler reaction when adsorbed in a bridging position between two platinum atoms, whereas it is much more complex when adsorbed on a single platinum atom (additional peaks at 2043 and 2093 cm^{-1} for harmonic frequency).

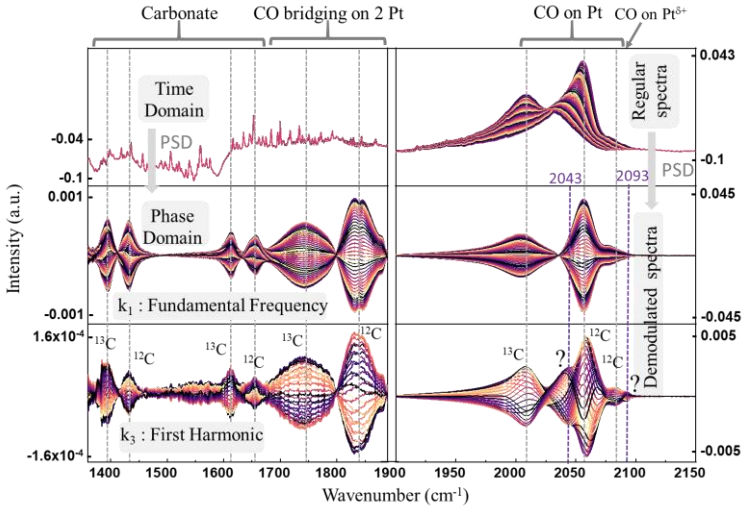

Figure 1. Upper. IR spectra recorded during $^{12}CO/^{13}CO$ looping experiment (time domain). Bottom. ME-IR spectra after PSD processing (demodulated spectra at k_1 and k_3)

Significance

Applying ME-PSD IR spectroscopy shine new insights of CO oxidation reaction mechanism occurring Pt/Al_2O_3 catalyst. Based on these experiments, a new decomposition of the IR spectra of adsorbed CO is proposed.

References

1. D. S. Santilli and B. C. Gates, *Hydrocarbon Reaction Mechanisms*, Weinheim, Wiley-VCH., **2008**.
2. Müller P, Hermans I. *Applications of modulation excitation spectroscopy in heterogeneous catalysis*. Industrial & Engineering Chemistry Research, **2017**, 56(5): 1123
3. S. Salomons, R. E. Hayes, M. Votsmeier, A. Drochner, H. Vogel, S. Malmberg and J. Gieshoff, Appl. *Catal. B Environ*., **2007**, 70, 305–313

Cu_2O Nanocatalysts: Morphology-Dependent Reactivity and Operando Insights from NAP-XPS

M. De Rocco[1]*, A. Capitaine[2], A. Dabbous[2], B. Sciacca[2], J.-J. Gallet[3,4], F. Bournel[3,4], D. Pierucci[5,6], S. Cristol[1], P. Simon[1], H. Tissot[1]

[1]*Université de Lille, CNRS, UCCS, UMR 8181, 59655, Villeneuve d'Ascq, France*

[2]*Aix-Marseille Université, CNRS, CINaM, Marseille, France*

[3]*Sorbonne Université, LCPMR, F-75005, Paris, France*

[4]*Synchrotron SOLEIL, L'Orme des Merisiers, Saint-Aubin, BP 48, F-91192 Gif-sur-Yvette, France*

[5]*Sorbonne Université, UPMC Univ. Paris 06, UMR 7588, INSP, F-75005, Paris, France*

[6]*CNRS, UMR 7588, Institut de NanoSciences de Paris, F-75005, Paris, France*

*michele.de-rocco@univ-lille.fr

Introduction

Cu_2O-based catalysts show great potential as alternatives to noble metal-based catalysts in several key reactions, including the water-gas shift reaction, CO hydrogenation or oxidation, and propylene oxidation.[1] However, their practical application is limited by deactivation caused by oxidation to CuO or reduction to Cu.

The catalytic activity of Cu_2O is highly dependent on its morphology, particularly on the specific crystallographic surfaces exposed, as demonstrated in studies on single-crystal surfaces. For this reason, model systems such as nanoparticles with high uniformity in shape and size allow to separate contributions and observe behaviours of the specific type of surface as well as to investigate the role of particle size in the mechanism.[2] In this context, Cu_2O nanoparticles with well-defined cubic morphology (nanocubes) and tuneable sizes ranging from 10 to 300 nm were synthesized. Surface modifications under various gas atmospheres and CO oxidation reactions were monitored in operando using Near-Ambient Pressure X-Ray Photoelectron Spectroscopy (NAP-XPS).

Materials and Methods

Cu2O nanocubes were synthesized following Ke et al.[3] method, using $CuSO_4$ as precursor in aqueous solution with NaOH and ascorbic acid (AA, used as a reducing agent).

Shape, size and surface composition for as-prepared nanocubes (12, 40, 120, and 290 nm) were analysed by UV-Visible, SEM and XPS in UHV after deposition on a gold-coated silicon wafer. NAP-XPS experiments were performed on the Surface Analysis platform NAP-XPS of Institut Chevreul and at the TEMPO beamline of Soleil synchrotron. Samples were exposed to single gas and gas mixture atmosphere up to 2 mbar (O2, H2, CO, CO:O2) The sample was heated under these atmospheres from room temperature to 400 K.

Results and Discussion

The synthesized Cu_2O nanocubes were initially characterized using UV-Vis spectroscopy, SEM, and XPS under UHV conditions to optimize synthesis parameters for achieving the best size distribution and shape uniformity. Additionally, the surface composition, particularly, CuO presence on the surface, hydroxyl group density and carbon contamination, were analysed as a function of synthesis parameters and nanoparticle size to ensure a thorough understanding of the interface prior to gas exposure.

The nanocubes were then exposed to O_2 to study surface oxidation and the removal of carbon contamination. These results were compared with previous studies by Wang et al. on (100) and (111) single crystal surfaces.[1] Under 1 mbar of O_2, the nanocubes developed a thin CuO layer. At 400 K, this CuO layer proved to be unstable, consistent with earlier findings on CuO thin films.[4]

The size of the nanocubes significantly influenced their behavior: larger nanocubes (e.g., 290 nm) demonstrated surface reactivity comparable to single crystals, while smaller nanocubes exhibited distinct surface compositions during reactions and reduced at different temperatures. The study was further extended to CO adsorption and CO oxidation reactions. SEM imaging conducted after the experiments confirmed that the nanocubes retained their shape throughout the process.

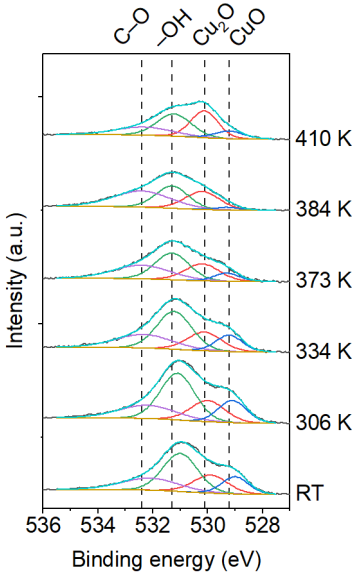

Figure 1. Variation of the O 1s spectrum of the 290 nm cubes during the temperature ramp.

Significance

The fundamental significance of this work lies in advancing our understanding of catalytic mechanisms at interfaces. This research specifically focuses on Cu_2O nanoparticles, investigating how their shape and size influence their properties in gas-phase environments and during catalytic reactions. By studying these nanoscale systems, we aim to uncover the relationships between morphology, surface reactivity, and catalytic behaviour. The findings will provide valuable insights into the principles governing catalytic processes and contribute to the development of efficient, morphology-tailored catalysts.

References

1. C. Wang, H. Tissot, C. Escudero, V. Perez-Dieste, D. J. Stacchiola, J. Weissenrieder, *J. Phys. Chem. C* **2018**, *122* (50), 28684-28691
2. Q. Hua, T. Cao, H. Bao, Z. Jiang, W. Huang, *Chem. Sus. Chem.* **2013**, *6*, 1966-1972
3. W.-H. Ke, C.-F. Hsia, Y.-J. Chen, M. H. Huang, *Small* **2016**, *12* (26), 3530-3534
4. A. B. Gurevich, B. E. Bent, A. V. Teplyakov, J. G. Chen, *Surf. Sci.* **1999**, *442* (1), L971-L976

Sorption-Enhancement Reaction Process (SERP) with in-situ water removal for an Intensified Methanol Production from CO_2: from experiment to modelling

Enrico Antonuccio, David Edouard, Guillaume Aubert, Laurent Vanoye, Pascal Fongarland*
[1]*CP2M, University of Lyon1-CPE- 69100 Villeurbanne, France*
*pascal.fongarland@univ-lyon1.fr

Introduction

The necessity to find an alternative route from fossil carbon for the synthesis of valuable fuels imposes the use of CO_2-rich syngas. Methanol is identified since several years as an good candidate with advantages: liquid at room temperature, high energy, and valuable building block for chemicals. However, the main drawbacks are related to the thermodynamical limitations and the presence of a side reaction, the reverse water gas-shift (rWGS).[1]

$$CO_2 + 3H_2 \underset{-Q}{\Leftrightarrow} CH_4O + H_2O$$

$$CO_2 + H_2 \underset{+Q}{\Leftrightarrow} CO + H_2O$$

To improve the yield of methanol, one strategy lies in the use of a sorbent (zeolites or MOF) that could adsorb water and/or methanol in situ and shift the equilibrium limitation. It is possible then to develop a cycling process with one step for reaction/adsorption and a second for regeneration/desorption called 'SERP' (Sorption Enhanced Reaction Process) technology.[2] The aim of our project is to better understand of the interaction between the various contributions (mass and heat transfer, catalytic reaction and sorption) using an experimental and modeling/simulation approaches; to optimize the process via relevant operating parameters like duration and nature of cycles, integration of operations, scale-up issues …. Despite some simulation works already published, a very few of experimental wors have been achieved up to now about SERP process.

Materials and Methods

For experimental part, a lab-scale fixed-bed reactor was filled with a commercial catalyst ($Cu/ZnO/Al_2O_3$) and different adsorbents (3A, 4A, 5A, 13X zeolites (molecular sieves)). To continuously analyze the downstream products (CO, CO_2, H_2, CH_3OH, H_2O) the exiting gas was sampled and sent to a GC and 2 TCD while inlet gas was supplied via mass flow controllers. Temperature and pressure are kept constant inside the insulated oven that hosts the reactor via a backpressure regulator and an electrical resistance.

For the modeling part, a dynamic, heterogeneous, non-ideal plug flow reactor model has been designed.[3] Mass and energy balance equations was numerically integrated using Matlab software for time integration considering linear driving force model for the sorption step on the sorbent. Intrinsic kinetic model was taken from the well-known literature related to Methanol synthesis as well as isotherm adsorption for water and methanol on zeolite-type sorbent.

Results and Discussion

In a first time, residence time distribution (RTD) was determined in the experimental set-up to establish the hydrodynamic pattern of the set-up. Breakthrough curves of water, MeOH and CO_2 have been obtained for the different sorbents for a range of temperature from 200 and 300 °C (15 bar) to evaluate the maximum sorption capacity in reaction conditions. Steady-state catalytic activity was also measured without sorbent to set the kinetic model parameters. It was then possible to confirm the catalyst stability for several days. SERP experiments was then performed by studying the effect of different operating parameters such as the nature of cycles (pressure and/or temperature swings, time of cycling), reaction step temperature, total pressure, contact time and the nature of the sorbent. Figure 1 presents experimental SERP at 235 °C and 15 bar, under stoichiometric conditions using the commercial catalyst adsorbent 4A with a 1:3 mass ratio. The effects of the intensifications are appreciable in the overshoot in CO concentration, that flattens at the equilibrium only when the breakthrough of water and methanol occurs, indicating that the adsorbent is saturated and can no longer boosts the equilibrium. Two cycles are presented in the figure, each spaced out by a temperature and purge swing under nitrogen (at 250°C). Co-adsorption role of water and methanol was investigated as well as the impact of SERP on sorbent and catalyst integrity due to the cycles. All experiments were fully modelled in dynamic to better understand the interaction between all coupled phenomena.

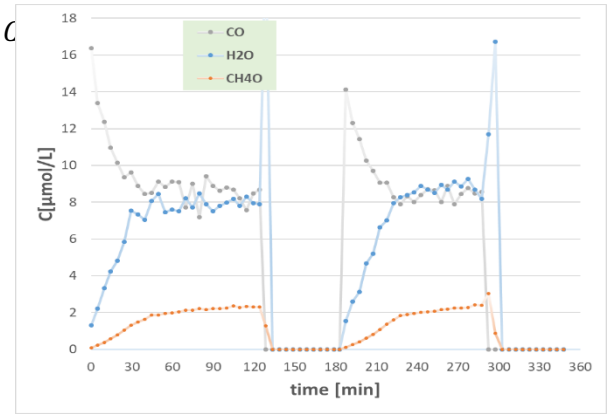

Figure 1. Concentration vs. time at the reactor outlet for the products: water (blue), CO (gray), methanol (orange). Feed flowrate = 60 NmL/min, 1g of $Cu/ZnO/Al_2O_3$ catalyst., 235 °C, 15 bar.

Significance

This work is between a fundamental and applied study where the main objective is to better understand the impact of cycles on methanol synthesis during SERP and gives data to obtain a model able to scale the SERP approach at a larger scale.

References

[1] Terreni, J.; Trottmann, M.; Franken, T.; Heel, A.; Borgschulte, Energy Technology **2019**, 7 (4).
[2] Dobladez, J. A. D.; Maté, V. I. Á.; Torrellas, S. Á.; Larriba, M.; Pascual Muñoz, G.; Alberola Sánchez, R. Sep. Purif. Technol. **2021**, 262.
[3] Guffanti, S.; Visconti, C. G.; Groppi, G., Ind. Eng. Chem. Res. **2021**, 60 (18), 6767–6783.

OC9: Photo, electro

Molecular Understanding of Heterogeneous Organometallic Photocatalysts

R. Jabbour,[1] Q. Perrinet,[2] T. Robinson,[1] A. Ranscht,[3] A. Solé-Daura,[4] A. Ghosh,[3] J. Canivet,[3] V. de Waele,[2] C. Mellot-Draznieks,[4] A. Lesage,[1] F. M. Wisser[3,5]*

[1]*Centre de RMN à Très Hauts Champs, Université de Lyon, 69100 Villeurbanne, France*

[2]*LASIRE, Université de Lille, 59000 Lille, France*

[3]*IRCELYON, Université de Lyon, 69626 Villeurbanne Cedex, France*

[4]*Collège de France, 75231 Paris Cedex 05, France*

[5]*Erlangen Center for Interface Research and Catalysis (ECRC), Friedrich-Alexander-Universität Erlangen-Nürnberg, 91058 Erlangen, Germany*

*florian.wisser@fau.de

Introduction

Photocatalytic CO_2 reduction reactions have gained enormous interest as they offer sustainable routes to provide renewable fuels and small building blocks for chemicals. However, efficient, selective and long-term active photosystems and well-understood molecular structures of the active sites are still scarce. To fully explore the potential of photochemical CO_2 valorization, understanding of the reaction mechanism and of the roles of the different molecules involved are of utmost importance.[1,2] This concerns in particular the role of amines, which are often supposed to be only a sacrificial electron donor.

Materials and Methods

Porous organic polymer (POP) based photocatalysts were prepared by palladium mediated cross coupling reaction in organic solvents, rhodium^{III} pentamethylcyclopentadienyl (RhCp*) active sites were infiltrated post-synthetically. Photochemical CO_2 reduction was performed in acetonitrile/triethanolamine (TEOA) mixtures. Solid-state Magic Angle Spinning (MAS) Dynamic Nuclear Polarization (DNP) NMR characterizations were performed on 400 or 800 MHz Bruker spectrometer. Prior to DNP measurements, the samples were impregnated with a 16 mM solution of TEKPOL in tetrachloroethane. Time-resolved spectroscopic techniques were performed in nitrile/TEOA mixtures, similar to photocatalysis. Radical trapping and characterization were performed using a X-band EPR spectrometer.

Results and Discussion

Here we will present a set of completely heterogeneous photocatalysts. In these systems, both the photosensitizer and the catalyst are integrated into the same framework. Different organic photosensitizers will be evaluated in terms of their light absorption properties as well as in terms of their catalytic activities. The presented fully heterogeneous photosystems allow for a constant and efficient transformation of CO_2 into formic acid, without any deactivation for at least four days. The reasons for their superior performance, caused by an ultrafast visible photo-induced electron transfer, will be explained based on time-resolved spectroscopy and density function theory (DFT) calculations.[3]

We will also present a rational approach for the design of heterogenized catalysts, to control in a predictable way the catalytic activity of the active site.[4] Combining advanced solid-state characterization techniques and computational methods provide a clear picture of the confined RhCp* catalyst within amorphous POPs (Figure 1a). Importantly, the confinement does not affect the molecular structure of the active RhCp* moiety.[5]

Finally, we will shed light on the role of triethanolamine in heterogeneous photocatalysis using a combination of EPR, solid-state NMR and time-resolved spectroscopy together with molecular dynamic (MD) simulations. Our results suggest that in case of fully heterogeneous photosystems, TEOA modulates charge transfer from the photosensitizer to the catalytically active site, while in case of heterogeneous catalysts and homogeneous $Ru(bpy)_3$-based photosensitizers it acts as (i) a proton source close to the catalytic Rh center (Figure 1b) and (ii) as an efficient electron relay between photosensitizer and catalyst.

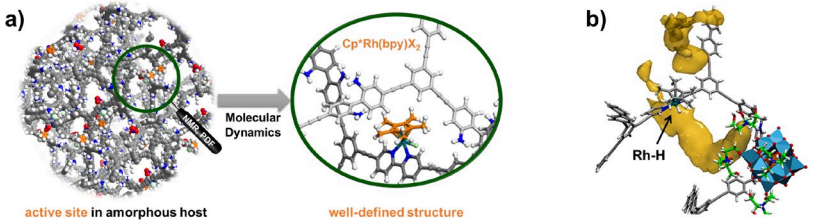

Figure 1. a) Molecular structure of the catalytic RhCp* moiety confined in an amorphous POP, b) Time averaged TEOA distribution (yellow cloud) around the catalytically active site in a POP based heterogeneous catalyst obtained by MD simulations and based on the structural model shown in (a). Solvent molecules are omitted for clarity.

Significance

The analytical power of the proposed methodologies is highlighted by (i) revealing precise knowledge of the molecular structure of organometallic complex heterogenized within a porous support and of its interactions with the surrounding pore, (ii) disclosing the role of TEOA in the rection and (iii) establishing the Hammett parameter as a descriptor of the catalytic activity of heterogenized organometallic catalysts. This work demonstrates rational design rules for the synthesis of highly active and completely heterogenized photocatalysts.

References

1. Renato N. Sampaio, D. C. Grills, D. E. Polyansky, D. J. Szalda, E. Fujita, *J. Am. Chem. Soc.* **2020**, *142*, 2413
2. J. Canivet, F. M. Wisser, *ACS Appl. Energy Mater.* **2023**, *6*, 9027
3. F. M. Wisser, M. Duguet, Q. Perrinet, A. C. Ghosh, M. Alves-Favaro, Y. Mohr, C. Lorentz, E. A. Quadrelli, R. Palkovits, D. Farrusseng, C. Mellot-Draznieks, V. de, Waele, J. Canivet, *Angew. Chem. Int. Ed.* **2020**, *59*, 5116
4. F. M. Wisser, P. Berruyer, L. Cardenas, Y. Mohr, E. A. Quadrelli, A. Lesage, D. Farrusseng, J. Canivet, *ACS Catal.* **2018**, *8*, 1653
5. R. Jabbour, C. W. Ashling, T. C. Robinson, A. H. Khan, D. Wisser, P. Berruyer, A. C. Ghosh, A. Ranscht, D. A. Keen, E. Brunner, J. Canivet, T. D. Bennett, C. Mellot-Draznieks, A. Lesage, F. M. Wisser, *Angew. Chem. Int. Ed.* **2023**, 62, e202310878.

Exploring $BaTiO_3$-Derived Materials for Advancing SOFC Electrode Performance

Valerie Theuns[1]*, Donovan Ledru[2], Marie-Hélène Chambrier[2], Aurélie Rolle[1], Anne-Sophie Mamede[1], Héloïse Tissot[1], Elise Berrier[1]

[1] Univ. Lille/ [2]Univ. Artois, CNRS, Centrale Lille, Univ., UMR 8181 - UCCS – Unité de Catalyse et Chimie du Solide, [1]F-59000 Lille/ [2]F-62300 Lens, France

* valerie.theuns@univ-lille.fr

Introduction

One of the current challenges in solid oxide fuel cell (SOFC) development is the removal or reduction of critical raw materials (CRMs), like Co, La and Sr[1], in electrode materials while maintaining adequate electrochemical activity and ionic conduction. On the other hand, non-critical alternatives such as barium titanate $BaTiO_3$ (BTO) show significantly lower activity. The objective of the present work is to take advantage of the capability of ABO_3 perovskite oxides to accommodate various cation substitutions at A- and/or B-site to embed the needed functions. In practice, we target the design of BTO-derived perovskites with increased redox activity and improved ionic conductivity, which is a promising starting point for low-CRM materials.

For example, substituting Ti^{4+} by Fe^{3+} at B-site of $BaTiO_3$ is expected to bring additional redox functions, while modifying the total cationic charge leads to structural rearrangements to maintain neutrality. In general, varying the ionic radii, the formal charge of the cations or the A/B ratio is expected to cause structural disorders which can sustain ionic conductivity or favor the ex-solvation of an additional crystal phase.[2] Moreover, A-site deficient perovskite materials have demonstrated improved redox activity over the stoichiometric counterparts.[3]

In this work, we target the selection of BTO-based oxides modified by the substitution of A-site cations (Ba^{2+}) and/or B-site cations (Ti^{4+}). To this end, the following dopants were chosen to substitute the A- and B-sites of BTO, to form a series of BTO-derived samples: Ca^{2+} and La^{3+} ions for the A-site, and Pr^{3+}, Ni^{2+}, Fe^{3+} and Cu^{2+} ions for the B-site.

Our research focuses on a comprehensive investigation of BTO-derived perovskites, examining their structure, including minority phases, redox properties, surface composition and ionic conductivity.

Materials and Methods

The $BaTiO_3$-derived samples were prepared using the citrate complexation method, accompanied by some samples synthesized with the conventional ceramic (solid-state) method and samples made with an autocombustion synthesis.

Several characterization techniques (SSA, TGA-DSC, TPR-TPO, XRD, and XPS) were used. Moreover, operando Raman spectroscopy was run by means of a dedicated environmental cell (Harrick Scientific) and a HR800 Horiba spectrometer equipped with several lasers allowing excitation wavelengths of 633, 532 or 457nm. XPS has been performed by means of a Kratos Analytical Axis UltraDLD spectrometer. Quasi *in-situ* measurements were made using the catalytic cell, where the samples were thermally pretreated under gaseous reactant flow at atmospheric pressure and transferred to the analysis chamber under UHV.

Results and Discussion

XRD, Raman, and XPS analyses revealed ex-solved crystalline phases in some of the samples. Preliminary results of a $Ba_{0.85}Ca_{0.15}Ti_{0.80}Fe_{0.20}O_3$ sample show some reducibility by TPR, making it suitable for H_2 reduction. Fig. 1 shows *in-situ* Raman spectra collected during H_2/O_2 cycling. H_2-TPR induced clear spectral modifications beyond thermal effects, notably a shift to lower frequencies, decreased intensity at 505 cm^{-1}, and increased intensity at 730 cm^{-1}. O_2-TPO restored the initial Raman spectrum, indicating sample regeneration upon redox cycling.

The sample's reducibility correlates with its iron content, as evidenced by the quasi *in-situ* XPS spectra in Fig. 1. Metallic iron is formed after reduction at 800°C and disappears upon reoxidation, suggesting that the observed reduction is linked to Fe cations. Further analysis using complementary techniques will provide a detailed discussion of this phenomenon

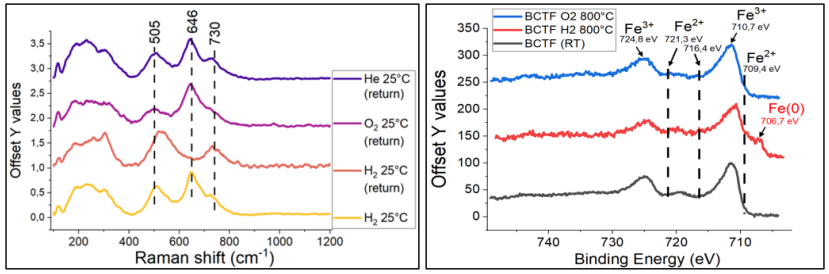

Figure 1. Left: evolution of the Raman spectra at λ = 633 nm of $Ba_{0.85}Ca_{0.15}Ti_{0.80}Fe_{0.20}O_3$ during in-situ measurements. Right: quasi in-situ XPS spectra of $Ba_{0.85}Ca_{0.15}Ti_{0.80}Fe_{0.20}O_3$ showing the Fe 2p orbitals after H_2 reduction at 800°C and O_2 oxidation at 800°C.

In conclusion, combining in-situ Raman experiments, XPS measurements, and the other characterization techniques, it becomes possible to estimate the performance of a possible SOFC electrode material. Additionally, the activity of the perovskite materials is influenced by their synthesis method.

Significance

The present work has significance in contributing to the discovery of new air-electrode materials with lowered Co and La content, while simultaneously developing a methodology of characterization for future novel materials.

References

1. European Commission, (…), Veeh, C., Publications Office of the European Union, 2023
2. Zakeri, F., (…), Khataee, A., Al-Ce co-doped BaTiO3 nanofibers as a high-performance bifunctional electrochemical supercapacitor and water-splitting electrocatalyst. *Scientific Reports*, 2024, 14(1), 9833.
3. Sun, Y., (…), Luo, J., A-site deficient perovskite: the parent for in situ exsolution of highly active, regenerable nano-particles as SOFC anodes, *Journal of Materials Chemistry A*, 2015, 3(20), 11048-11056.

Catalytic electroreduction of CO_2 to methanol on cobalt phthalocyanines: effect of macrocycle functionalization

Tabaries C.[1*], Capitolis J. [1], Prévot M.[1], Piccolo L.[1], Khodadadi A. [2], Zanotti G. [2], Flammini R. [2], Contini G. [2]

[1] *IRCELYON, CNRS & Université Claude Bernard Lyon 1, Villeurbanne, France*

[2] *Istituto di Struttura della Materia, CNR, Roma, Italy*

*camille.tabaries@ircelyon.univ-lyon1.fr

Introduction

2023 marks a new record for fossil CO_2 emissions worldwide: 37.5 billion tons of carbon, an increase of 1.1% compared to 2022.[1] Progressing in the development of technologies such as electrochemical CO_2 reduction (CO2RR) for valorizing CO_2 into high added value chemicals becomes a necessity.[2] Converting CO_2 to methanol ($CO_2 + 6H^+ + 6e^- \rightarrow CH_3OH + H_2O$) is particularly interesting, as methanol is a pivotal chemical compound for the chemical industry, which also presents a high energy storage capacity.[3] One specific advantage of methanol compared to other CO_2 reduction products (CO, CH_4, C_2H_4) is that it is liquid under ambient conditions, which facilitates its transport and storage. However, producing methanol by CO2RR remains a challenge, as very few efficient electrocatalysts have been reported for this process, compared to other CO_2 reduction routes.[4] Still, recent studies have shown increasing methanol productivity with cobalt phtalocyanines (CoPc) dispersed on carbon nanotubes, leading to faradaic efficiencies towards methanol in the 10-30% range at – 1 V vs. the reversible hydrogen electrode (RHE).[5-6] While these results are indeed promising, the reported overpotentials remain high and little has been investigated regarding the influence of the chemistry of the macroligand on the electrocatalytic performances. Here we propose to address these shortcomings by functionalizing the reference CoPc with four electron-donating n-butoxy groups.

Materials and Methods

The electrocatalysts were homemade CoPc and $(nBuO)_4$CoPc (Figure 1a) supported on carbon nanotubes (CNTs). Both derivatives were synthesized in a single step via the cobalt(II)-templated tetramerization of phthalonitrile or 4-butoxyphthalonitrile, using a low-environmental-impact glycerol/anisole solvent mixture in the presence of the organic base 1,8-diazabicyclo[5.4.0]undec-7-ene (DBU), achieving moderate-to-good yields. 90 mg of the CNTs were dispersed in 90 mL of 0.05 mg/ml CoPc in DMF solution. The mixture was sonicated for 30 min and stirred for 48 h, then centrifugated, and washed with DMF and ethanol before drying. A catalyst ink was prepared by dispersing 10 mg of electrocatalyst in 2 ml ethanol with 10 µl of 5 wt% Nafion solution. The ink was sonicated for 30 min and 16 µL of it was deposited on a glassy carbon electrode of 12 mm in diameter (mass loading 0.8 µg). Electrochemical measurements were performed inside a H-cell equipped with a 3-electrode setup (counter electrode: Pt wire, reference electrode: Ag/AgCl/3M KCl). The electrolyte was 0.5M $KHCO_3$. The cathode and anode compartments were separated by an Aquivion membrane. CO_2 was continuously bubbled into the electrolyte during electrolysis at a flow rate of 50 mL/min. The gas products were analyzed using on-line gas chromatography. The liquid products were quantified after testing using 1H NMR in D_2O with an internal standard.

Results and Discussion

The CO2RR performance comparison of unsubstituted and n-BuO substituted CoPc is shown in Figure 1b. Functionalization of the macroligand leads to a reduction in overpotential: the highest methanol yield is obtained at – 1.2 V vs RHE for CoPc, while it is shifted to – 1 V vs. RHE for $(nBuO)_4$CoPc. Moreover, by carefully controlling the loading of $(nBuO)_4$CoPc on CNTs, the methanol faradaic efficiency increased from 10% to over 15% in our most efficient system, while no such improvement could be achieved on unsubstituted CoPc. We attribute this increase to the possibility of loading a higher amount of $(nBuO)_4$CoPc without molecular stacking at the surface of the CNTs compared to CoPc, which is enabled by the steric hinderance brought by the alkyl chains.

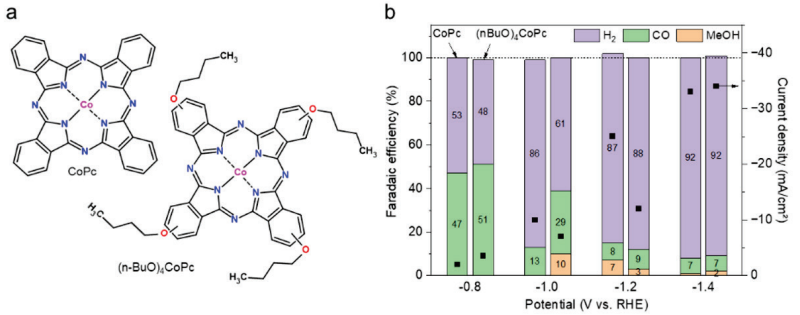

Figure 1. a) CoPc molecular catalysts. b) Comparison of the electrocatalytic performances of CoPc/CNT and $(nBuO)_4$CoPc/CNT.

Significance

This work demonstrates a promising molecular engineering strategy to significantly boost CO2RR performance for methanol production. It paves the way for a new generation of efficient molecular electroacatalysts capable of increasingly higher selectivity and activity for this challenging reaction.

The ERANET-ACT3 NEXTCCUS project funding is greatly acknowledged.

References

1. P. Friedlingstein *et al.*, *Earth System Sci. Data* 15, 5301, 2023
2. R.I. Masel *et al.*, *Nat. Nanotechnol.* 16, 118, 2021
3. Y.R. Wang, *Angew. Chem. Int. Ed.* 61, e202212162, 2022
4. A. Bagger *et al.*, *ChemPhysChem* 18, 3266, 2017
5. Y.S. Wu *et al.*, *Nature* 575, 639, 2019
6. E. Boutin *et al.*, *Angew. Chem. Int. Ed.* 58, 16172, 2019

Photoelectrocatalytic valorization of glycerol with zinc oxide photoanode

Yacine Djerroud[1], Jie Yu[1], Frederic Dappozze[1],
Chantal Guillard[1], Philippe Vernoux[1], Jesús González-Cobos[1,*]
[1]*Université Claude Bernard Lyon 1, CNRS, IRCELYON, UMR 5256, Villeurbanne, 69100, France*
*jesus.gonzalez-cobos@ircelyon.univ-lyon1.fr

Introduction

Global population growth, which has doubled since 1960 and is projected to reach 9 billion by 2050 [1], is significantly increasing energy demand. Renewable resources, such as biomass and biodiesel, have become essential last years to reduce the dependence on fossil fuels. However, biodiesel production generates crude glycerol as by-product, which account for 10% of synthesized biodiesel, amounting to over 2.2 million tonnes annually [2]. Glycerol wastes contain several contaminants (salts, free fatty acids, methanol) and their treatment by incineration leads to environmental concerns due to the emission of CO_2.

The selective oxidation of glycerol into value-added products, such as glyceraldehyde (GAD) and dihydroxyacetone (DHA), is attracting increasing interest for its economic and ecological benefits. These products are key precursors in the cosmetics, polymer, and emulsifier industries [3]. Conventional processes, such as combustion and pyrolysis, are energy-intensive and emit CO_2, prompting the exploration of alternative approaches like photoelectrochemical (PEC) processes.

PEC systems using semiconductor-based catalysts (e.g., TiO_2, WO_3) for glycerol oxidation while generating hydrogen have shown great promise [3]. In our group, we have recently developed the first PEM photoelectrocatalytic reactor for the glycerol valorization using WO_3 photoanode showing a synergetic effect between photo-catalysis and electrocatalysis.[4]

Herein we propose for the first time ZnO as a promising photoanode material for the selective glycerol valorization. Different parameters (temperature, applied potential, charge separation) have been optimized to maximize the production of GAD and DHA on the anode and H_2 on the cathode.. Besides, the PEC reaction mechanism has been discussed based on a systematic study of the PEM photoelectrolyser performance under different thermo- (TC), photo- (PC), electro- (EC), and photoelectrochemical (PEC) conditions.

Materials and Methods

Photoanode preparation:

The photoanode consisted of ZnO supported on a carbon cloth support, which was prepared by spray deposition of an ink containing commercial ZnO catalyst, isopropanol as solvent, and Nafion as ionomer. The ZnO:Nafion ratio was 1:1, and the final catalyst charge on the electrode was 3.5 mg/cm².

Membrane-electrode assembly and PEM cell setup:

The membrane-electrode assembly (MEA) was composed of the ZnO/carbon cloth photoanode, PFSA Aquivion as a proton exchange membrane, and a commercial a Pt- (20% wt)/C cathode supported on carbon cloth. The PEM cell reactor was modified to host a quartz window on the anode side to allow light irradiation on the photoanode. The setup featured temperature control, a potentiostat for electrochemical monitoring, and a peristaltic pump for water and an aqueous glycerol solution circulation on the cathodic and anodic sides, respectively.

Product analysis :

A comprehensive system enabled efficient analysis of all glycerol oxidation products. A mass spectrometer was integrated to on-line detect all the gases: H_2 at the cathode and CO_2, CO, and (eventually) O_2 at the anode. The anodic liquid products were sampled and analyzed by HPLC and the eventual H_2O_2 generation was determined by UV-vis spectroscopy.

Results and Discussion

The photoelectrocatalytic oxidation of glycerol using ZnO photocatalyst was analyzed under different operation conditions. For example, Fig. 1 shows the time variation of the concentration of the two main oxidation products, GAD and DHA at 60ºC, with UV light irradiation (PC), with an applied voltage of 1.2 V (EC) and with both (PEC).

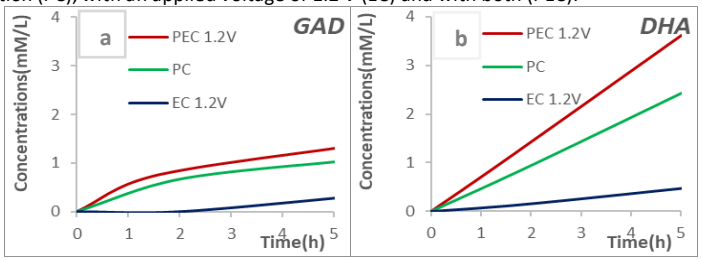

Figure 1. Time evolution of a) GAD and b) DHA concentration in the anodic solution at 60ºC comparing 3 processes: PEC (1.2 V, UV light), PC (only UV light) and EC (only 1.2 V).

PEC conditions showed to be optimum to maximize the production of both value-added products, GAD and DHA. Besides, the increase in the temperature and in the applied voltage under PEC conditions significantly enhanced the yields in terms of GAD and DHA on the anode as well as the obtained current and H2 generation on the cathode, while EC operation led to overoxidation to CO_2. The key role of the H2O2 generation by the photocatalytic activity of ZnO and of the synergy between EC and PC has been investigated and the obtained results open new perspectives for the development of ZnO-based photoanode materials for the selective glycerol valorization and H2 co-generation.

The authors thank CNRS and Agence Nationale de la Recherche (ANR) for the financial support for this work.

Significance

This study combines photo- and electrocatalysis in a flow-PEM cell to selectively oxidize glycerol and co-generate H_2, showing promising proprieties of ZnO as photoanode in this field.

References

1. Miguel-Angel Perea-Moreno, et al. Biomass as renewable energy: Worldwide research trends,2019.
2. Narasimharao Kondamudi, et al. Simultaneous production of glyceric acid and hydrogen from the photooxidation of crude glycerol using TiSi2,2012, 126:180–185
3. Zhenao Gu,et al. Interface-modulated nanojunction and microfluidic platform for photo-electrocatalytic chemicals upgrading,2021, 282:119541
4. Jie Yu, et al. First PEM photoelectrolyser for the simultaneous selective glycerol valorization into value-added chemicals and hydrogen generation,2023, 327:122465

OC10: CO_2 Methanation, Dehydrogenation

Powdery metal nanoparticle-based catalysts prepared by spark ablation for CO_2 methanation

P. Hongmanorom[1], D.P. Debecker[1]*
[1]*Institute of Condensed Matter and Nanoscience, UCLouvain, Louvain-La-Neuve, Belgium*
*damien.debecker@uclouvain.be

Introduction

Wet chemical methods are the most common processes implemented for both lab- and industrial-scale production of metal nanoparticles and supported metal nanoparticles. These processes usually generate large amounts of liquid waste, making use of solvents, ligands, surfactants, counter ions, etc. Also, they mostly rely on multi-step energy-intensive procedures, such as aging, drying, calcination, and reduction.[1] Spark ablation is a compelling alternative to traditional wet chemical methods, primed to reduced environmental impact (i.e., no use of solvents, precursors, salts, ligands, or high-temperature treatments). It was developed to generate nanoparticles, using electrical discharges between two electrodes of a target material in inert gas flow. This physical process yields primary metal particles in the 1-10 nm size range. The well-controlled deposition of generated metal nanoparticles onto flat surfaces has been well documented.[2, 3] Yet, for heterogeneous catalysis, powdery materials are needed. We propose for the first time to modify a spark nanoparticle generator to allow a direct deposition onto pulverulent materials.[4] The concept relies on the aerosolization of a powder, which is gas-transported and injected in the path of metal nanoparticle formation. Herein, TiO_2 powder is used as the catalyst support, while Ni electrodes are used to generate Ni nanoparticles as the active phase, forming the Ni/TiO_2 catalyst for CO_2 methanation.

Materials and Methods

In Figure 1 (Left), TiO_2 P25 (Degussa) powder was aerosolized from a mechanically vibrating reservoir by a 4-jet vortex fed with N_2 (99.9%; 3 L/min). The aerosolized powder was transported through a venturi for de-agglomeration before injection into the spark generator. Sparks generated between the Ni electrodes (99.99%; 3mm diameter) with a gap voltage of 1.3 kV and a charging current of 10.4 mA produced Ni clusters, which were carried by N_2 (99.9%; 3 L/min) to form Ni nanoparticles deposited onto TiO_2 particles. The resulting Ni/TiO_2 catalyst was collected on filter paper. The catalyst (200 mg) was reduced at 500°C for 2 h under a flow of 20 mL/min (50% H_2/50% He) prior to the reaction testing in the 200-400°C range with a gas mixture of 20 mL/min (10% CO_2 and 40% H_2 diluted in He). Catalyst characterization was performed using N_2 physisorption, H_2-TPR, XRD, ICP-AES, and HR-TEM.

Results and Discussion

The pristine TiO_2 support and the as-prepared Ni/TiO_2 catalyst exhibit a H3-type hysteresis loop, resulting from the interparticle voids in the loose aggregates of non-porous TiO_2 particles. After Ni loading (2.3 wt% determined by ICP-AES) and CO_2 methanation reaction, the TiO_2 diffraction peaks are unchanged in intensity, positions and width, which suggests that TiO_2 crystallites are unaffected by the catalyst preparation and reaction conditions. Additionally, the main diffraction peaks of Ni ($2\theta = 44.6°$) or NiO ($2\theta = 43.1°$) crystalline phases are not detectable in the XRD pattern of the as-prepared Ni/TiO_2 catalyst, excluding the presence of Ni/NiO crystallites larger than 5 nm. TEM images further confirm this observation, showing many small Ni nanoparticles (<5 nm) well-dispersed on TiO_2. HRTEM images also reveal the lattice fringes with inter-planar distances of 2.0-2.1 Å and 2.35-2.45 Å, corresponding to the (111) crystal plane of cubic Ni and NiO, respectively. It should be noted that the homogeneity of the deposit is still not optimal, as some "floating" Ni/NiO nanoparticles can also be observed, not being in contact with TiO_2 support. Despite no interaction with TiO_2 support, these nanoparticles are very small (<5 nm). Although the Ni loading, Ni particle size and metal-support interaction have not been fully optimized, the Ni/TiO_2 catalyst achieves satisfactory CO_2 conversion of 53% and CH_4 selectivity of 76% at 400°C, as shown in Figure 1 (Right). After the reaction, HRTEM images show that small Ni nanoparticles (a few nanometer), well-dispersed on TiO_2 support, remain stabilized after reductive pretreatment and subsequent reaction. Nevertheless, few large particles (50-80 nm) can also be found, likely stemming from the sintering of "floating" Ni nanoparticles without interaction with TiO_2. The presence of few large Ni nanoparticles is consistent with the small and relatively narrow XRD peak at 44.6° of the spent Ni/TiO_2 catalyst. The homogeneity of deposition could be further improved by improving the design of the mixing zone and better controlling the powder aerosolization. Additionally, the scope could be expanded to other metals (e.g., Ru, Rh, Pd, Co, and Fe), which have been reported as active and selective metal catalysts for CO_2 methanation.

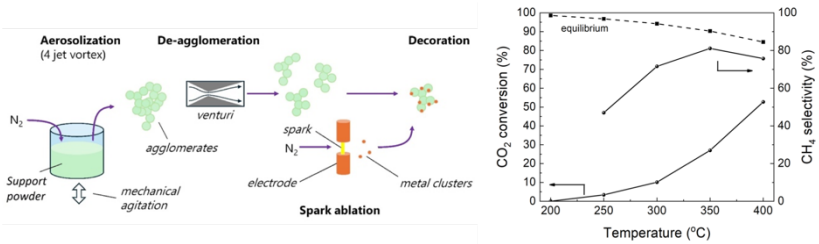

Figure 1. (Left) Schematic view on the set-up used to prepare powdery Ni/TiO_2 catalyst. (Right) CO_2 conversion and CH_4 selectivity of Ni/TiO_2 catalyst as a function of temperature.

Significance

We report the first synthesis of the powdery heterogeneous catalyst using spark ablation technology. The resulting Ni/TiO_2 catalyst is readily active in the hydrogenation of CO_2 to CH_4. This disclosed method opens new avenues for heterogeneous catalyst preparation.

References

1. N.D. Jaji, H.L. Lee, M.H. Hussin, H.M. Akil, M.R. Zakaria, M.B.H. Othman, *Nanotechnol Rev.* **2020**, *9*, 1456.
2. T.V. Pfeiffer, J. Feng, A. Schmidt-Ott, *Adv. Powder Technol.* **2014**, *25*, 56.
3. S. Drdova, M. Gao, O. Sambalova, R. Pauer, Z. Zhou, S. Dimitriadou, A. Schmidt-Ott, J. Wang, *Environ. Sci.: Nano.* **2024**, *11*, 1023.
4. D.P. Debecker, P. Hongmanorom, T.V. Pfeiffer, B. Zijlstra, Y. Zhao, S. Casale, C. Sassoye, *Chem. Commun.* **2024**, *60*, 11076.

Silica-supported DFM catalysts for CO_2 methanation: Comparative study with Al_2O_3-based catalysts

Lidia Castoldi[1]*, Giuseppe Nava[1], Sergio Molina-Ramírez[2], Cinzia Cristiani[2], Barbara Di Credico[3], Elisabetta Finocchio[4], Luca Lietti[1], Roberto Scotti[3]

[1]*Dipartimento di Energia (Laboratory of Catalysis and Catalytic Processes), Politecnico di Milano, Milano, Italy.*

[2]*Dipartimento di Chimica, Materiali e Ingegneria Chimica Giulio Natta, Politecnico di Milano, Milano, Italy.*

[3]*Dipartimento di Scienza dei Materiali, Università Milano-Bicocca, Milano, Italy.*

[4]*Dipartimento di Ingegneria Civile, Chimica e Ambientale, Università di Genova, Genova, Italy.*

**lidia.castoldi@polimi.it*

Introduction

The growing concern about global warming and climate change has driven many countries to act and generate new policies for environmental protection. Although decarbonization technologies and strategies show rapid and steady development, they are still incipient and require high investments. CO_2 Capture and Storage and Utilization (CCSU) catalytic strategies have emerged to prevent the CO_2 release and reduce its atmospheric concentration. In this context, dual-function materials (DFM) are potentially proposed for cyclic CO_2 capture and methanation technology, acting both as solid adsorbents for capturing CO_2 and as catalysts for fuel (i.e. methane) production upon H_2 exposure[1]. In literature, successful DFMs consist of redox metals supported mostly over alumina and doped with alkaline or alkaline-earth oxides[2]. However, the growing interest in the use of more economical materials within the idea of circular economy has positioned silica as a possible effective alternative as catalytic support for DFMs due to its interesting morphological, physical, and chemical properties. Moreover, the recovered silica from industrial waste could be employed and reused as support.

This work aims to compare the catalytic performance of DFMs supported on silica (both commercial and waste) with DFMs supported on alumina in the catalytic CO_2 methanation reaction.

Materials and Methods

Silica-supported catalysts were prepared by sequential impregnation, incorporating Ru (0.5% wt), and different Alkaline(-earth) oxides such as Ba and K (16% wt)[2]. These catalysts, together with the binary formulations (Me/SiO_2) and the support (commercial and waste silica) were characterized by N_2 physisorption, XRD, SEM-EDX, CO_2 TPD, H_2-TPR, among others. Microreactor experiments were carried out in a quartz tubular reactor with a total flow of 100 ml/min. The gases leaving the reactor were analyzed through a mass spectrometer, an FT-IR spectrometer, and a micro gas chromatograph. CO_2 capture/reduction cycles were performed at constant temperature in the range 250-400°C. Every cycle is composed of an adsorption phase (1% CO_2/He) and a reduction phase (4% H_2/He), separated by an inert purge. Advanced spectroscopy characterization methodology was carried out to investigate acidity and basicity and surface OH groups distribution. CO_2 adsorption / desorption was also investigated using in situ FT-IR techniques.

Results and Discussion

The catalytic performance data for CO_2 reduction with H_2 are presented in Table 1 for the commercial support. CO_2 conversion achieved by Ru-Ba catalysts appears to be independent of the support material (Al_2O_3 or SiO_2). However, Ru-Ba/SiO_2 shows a higher methane selectivity compared to Ru-Ba/Al_2O_3 with the same composition at lower temperature range, achieving comparable values beyond 400°C. The CO_2 storage capacity of Ru-Ba/SiO_2 was approximately 230 $\mu mol/g_{cat}$ (43% lower than that of the Al_2O_3-supported catalyst), producing 63 $\mu mol/g_{cat}$ of CH_4 in the subsequent reduction with H_2. This observation implies that not regenerable carbonate species may remain on the surface after the reduction step which does not participate in the methanation reaction.

Table 1 - TPR experiment results: temperature ramp (from RT to 500°C @10°C/min) in CO_2 (1% v/v) + H_2 (4% v/v) He-balanced

Temperature (ºC)	Ru/SiO_2		Ru-Ba/SiO_2		Ru-Ba/Al_2O_3	
	$X_{CO_2}(\%)$	$S_{CH_4}(\%)$	$X_{CO_2}(\%)$	$S_{CH_4}(\%)$	$X_{CO_2}(\%)$	$S_{CH_4}(\%)$
300	20.0	95.1	11.7	86.1	4.4	41.1
400	29.5	58.2	33.1	39.2	32.0	16.1
500	52.8	20.3	53.6	12.9	53.2	6.8

Experiments conducted with FTIR analysis of the species arising from CO_2 adsorption revealed the formation of a complex population of carbonate-type species, also depending on the support material employed. Both samples exhibited an initial population of bulky carbonates related to the presence of Ba (1400–1500 cm^{-1} region) stable up to 500°C. Adsorbed surface and carbonates (likely bidentate species) are detected on both samples, remaining stable following degassing. Hydrogen carbonate species observed in the Al_2O_3-supported catalyst (1227 cm^{-1}) are likely due to the interaction of CO_2 with the support itself, while the same species could be formed over the silica-supported catalysts following the interaction of CO_2 with the basic oxide phase. However, in the Ru-Ba/Al_2O_3 sample, signals around 1560 and 1355 cm^{-1}, linked to the presence of bidentate carbonates on the Ba phase, shifted in the silica-supported material, indicating a different nature of these species, which remained present only in Ru-Ba/Al_2O_3 after degassing.

Significance

This study highlights silica as a sustainable alternative support for dual-function materials (DFMs) in CO_2 capture and conversion functionalized with Ru and Alkali(-earth). The utilization of Ru-Ba/SiO_2 improved methane selectivity and generated more labile carbonate species than alumina-supported materials. Silica's use, particularly when sourced from industrial waste, aligns with circular economy principles reducing environmental impact.

References

1. M. Duyar, M. Treviño, R. Farrauto, *Applied Catalysis B,* **2015**, *168-169*, 370
2. A. Porta, R. Matarrese, C. Visconti, L. Lietti, *Energy&Fuels,* **2023**, *37*, 7280

The promoter effect of MgO on the performance of Ni(acac)$_2$-grafted hydroxyapatite in the Sabatier reaction

Nassima Berroug, Miguel A. Gutiérrez-Ortiz, Juan R. González-Velasco, Zouhair Boukha*
Chemical Technologies for Environmental Sustainability Group, Department of Chemical Engineering, Faculty of Science and Technology, University of the Basque Country UPV/EHU, P.O. Box 644, E-48080, Bilbao, Spain
*zouhair.boukha@ehu.eus

Introduction

The strategies based on the use of green hydrogen (GH2) are expected to lead the energy transition towards achieving climate neutrality in compliance of the ambitious European Green Deal targets consisting of (i) energy transition plan by 2030 and (ii) a fully decarbonized European energy system by 2050. Therefore, finding solutions for GH2 storage and transport has become essential to widespread its effective application. In this sense, the use of renewable hydrogen to convert CO_2 into synthetic natural gas (SNG) is one of the most attractive strategies, meant for taking advantage of the available NG facilities [1,2]. The current research, dealing with the CO_2 methanation reaction, is mainly focused on the design of catalyst formulations to improve the performance of the active metals like Ni or Ru. Since the activation of CO_2 mainly occurs on the basic sites, surface modification of the used support through incorporation of basic materials appears to be of crucial importance for a high catalytic performance. Therefore, a wide series of basic oxides have been investigated as chemical promoters, e.g. CaO, MgO, K_2CO3, Na_2CO_3, CeO_2 and La_2O_3 [1,2]. The present contribution deals with the study on the promotional effect of Mg addition on the performance of Ni supported on hydroxyapatite (HAP) catalysts. The improved catalytic properties of the Mg promoted samples were linked to the occurrence of suitable surface chemistry and the dispersion of the Ni active phase.

Materials and Methods

Ni/Mg(x)/HAP catalysts were prepared through a modification of the HAP support with Mg and, subsequently, Ni(acac)$_2$ complex was grafted in a toluene solution. First, Mg-doped HAP samples were prepared by impregnation, by using solutions with different amounts of $Mg(NO_3)_2.6H_2O$ salt. The resulting samples, Mg(x)/HAP, were dried at 120 °C for 12 h, and then calcined at 500 °C for 4 h. Thereafter, the Ni/Mg(x)/HAP catalysts were synthesized by grafting method to obtain a Ni content close to 4 wt.%. The Ni(acac)$_2$ precursor was dissolved at 60 °C in toluene. Then, the solution temperature was adjusted to 30 °C, followed by addition of Mg-modified HAP support (6 g) under vigorous stirring. After 3 h stirring, the resulting suspension was filtered, washed with pure toluene and then dried at 80 °C for 12 h. Finally, the samples were calcined at 500 °C for 4 h. The prepared catalysts were characterized by using several techniques, including XRF, DRS, TGA, WDXRF, FTIR, BET, XRD, CO_2-TPD, H_2-TPR and TEM.

The CO_2 methanation catalytic tests were performed in a tubular reactor (ID = 9 mm) working at atmospheric pressure. The pre-treatment of the catalysts (500 mg, 160-250 µm) consisted of their reduction at 500 °C under a 20% H_2/N_2 for 1 h. The reaction mixture was composed of 16% CO_2, 64% H_2 and 20% N_2, with a total flow of 250 cm^3 min^{-1}, corresponding to a WHSV of 30,000 cm^3 g^{-1} h^{-1}. The analysis system consisted of a gas chromatograph (Agilent 490 Micro GC) equipped with a TCD detector.

Results and Discussion

Table 1 lists the actual promoter loadings, textural and catalytic properties of the grafted catalysts promoted with Mg. It can be observed that the progressive addition of Mg induces a smooth decrease in the specific surface area (from 51 to 45 m^2 g^{-1}).

Table 1. Textural properties and chemical analysis for the grafted Ni-Mg(x)-HAP catalysts.

Sample	Mg, wt.%	S_{BET}, m^2 g^{-1}	d_p, nm	V_p, cm^3 g^{-1}
HAP	0	51	27.6	0.39
Ni-Mg(1)-HAP	0.7	49	27.2	0.33
Ni-Mg(2)-HAP	1.6	47	27.1	0.34
Ni-Mg(3)-HAP	2.4	46	28.5	0.33
Ni-Mg(4)-HAP	3.2	45	26.7	0.32

Fig. 1a shows the light-off curves for the activated Ni-Mg(x)-HAP samples in the CO_2 methanation. The activity seems to depend on the Mg content and follows this general trend: Ni-Mg(2)-HAP > Ni-Mg(4)-HAP > Ni-Mg(1)-HAP > Ni-Mg(3)-HAP. Interestingly, the samples reach their maximum conversion at relatively low temperatures (425 °C). Moreover, according to Fig. 1b, upon increasing the reduction temperature (500-750 °C), the activity of the optimized sample systematically improves, suggesting an increase in the number of active sites composed of Ni metallic phase. Work is in progress to shed light on the parameters influencing the activity of this novel series of active materials.

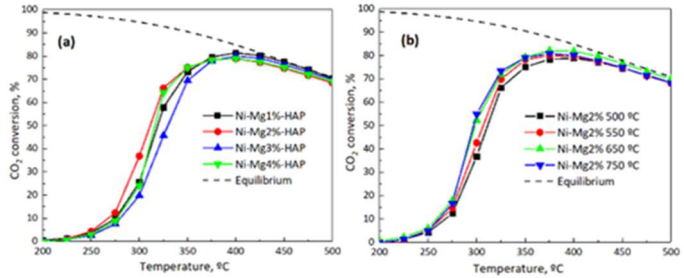

Figure 1. Catalytic activity in the Sabatier reaction of (a) Ni-Mg(x)-HAP catalysts and (b) Ni-Mg(2)-HAP reduced at different temperatures (WHSV = 30,000 cm^3 g^{-1} h^{-1}).

Significance

Here, we report the activity of a novel series of active Ni/Mg/HAP catalysts in the Sabatier reaction. It should be outlined that the observed performance outperforms that observed over a number of reference basic materials, reported in the literature.

References

1. Z. Boukha, A. Bermejo-López, U. De-La-Torre, J. R. González-Velasco, Appl. Catal. B-Environ. 338 (2023) 122989.
2. Z. Boukha, A. Bermejo-López, B. Pereda-Ayo, J. A. González-Marcos, J. R. González-Velasco, Appl. Catal. B-Environ. 314 (2022) 121500.

CO_2 methanation catalysts derived from Ni-alkaline earth metal carbonates

Sharad Gupta[1*], Sebastien Royer[1], Edmond Abi-Aad[1], and Christophe Poupin[1]
[1]*Université du Littoral Côte d'Opale, Unité de Chimie Environnementale et Interactions sur le Vivant (UCEIV), UR4492, 145, Avenue Maurice Schumann, Dunkerque 59140, France*
*sharad.gupta@univ-littoral.fr

Introduction

The continuous increase in the world energy demand has increased greenhouse gases mainly CO_2 into the atmosphere. There is a pressing demand across the globe to develop materials and processes to reduce the harmful emission.[1] CO_2 methanation using a catalyst obtained from earth-abundant materials offers a promising option to economically reduce anthropogenic CO_2. Alkaline earth metal carbonates are interesting and relevant candidates with respect to CO_2 methanation as it is available in large quantities in the form of low-cost natural mineral resourses.[2] In this work, we have explored the use of supported Ni catalysts derived from alkaline earth metal carbonate. We obtained the catalysts from the thermal decomposition of respective carbonate precursors under H_2 stream and studied its catalytic activity and stability in CO_2 methanation reaction

Materials and Methods

$NiMgCaCO_3$ with different Ni:Mg:Ca ratios (NMC) were synthesized via a simple co-precipitation method using Na_2CO_3 as the carbonating agent. Under H_2 reduction condition, $NiCaMgCO_3$ decomposed to $Ni/Ca(OH)_2$-CaO/MgO and formed an active catalyst for CO_2 methanation. Under reaction condition hydroxide/oxide phase adsorbs CO_2 and formed a carbonate phase, which cyclically converted into oxide with the release of CH_4 in the presence of H_2 and metallic Ni.

Results and Discussion

Screening of catalysts revealed that the active Ni catalyst originating from the decomposition of $MgCaCO_3$ exhibited good activity for CO_2 methanation. At 340 °C, NMC-154 showed 84% CO_2 conversion and 99.7% CH_4 selectivity. The developed catalytic system operated efficiently over 100 h on a stream without catalyst deactivation. Detailed structural characterization of these catalysts showed the phase-dependent generation of active species. From XRD and BET analysis it is revealed that, an increasing concentration of Mg in carbonates improves the textural properties and dispersion of Ni nanoparticles. The local reducing environment generated by the formation of CH_4 from the decomposition of alkaline metal carbonates maintains the reducibility of the catalyst. However, more detailed characterization studies must understand the structure-activity correlation of catalysts.

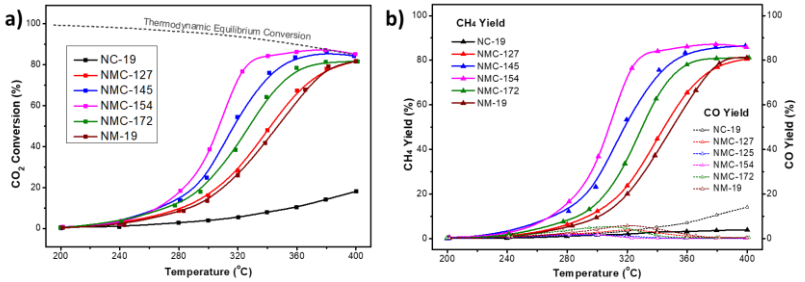

Figure 1. a) Catalytic CO_2 conversion, b) CH_4 and CO yield with respect to reaction temperature.

Significance

The methanation reaction is an interesting reaction from an industrial point of view. Indeed, it could allow the storage of hydrogen, limit CO_2 emissions and produce methane for injection into existing networks. The kinetic limitation of CO_2 methanation reaction requires the use of a catalyst. The aim of this study is therefore to find an efficient catalyst that is also stable over time with the possibility of large-scale synthesis in order to facilitate industrial use.

References

1. Wang, W.; Wang, S.; Ma, X.; Gong, J. *Chem. Soc. Rev*. **2011,** 40, 3703-3727.
2. Lux, S.; Baldauf-Sommerbauer, G.; Siebenhofer, M. ChemSusChem 2018, 11, 3357-3375.

Rhenium-based materials for integrated carbon capture and utilization

S. Scognamiglio[1,2,3], F. Morfin[1], R. Checa[1], J. Ivañez[1], G. Landi[2], L. Piccolo[1]*
[1] *Institut de recherches sur la catalyse et l'environnement de Lyon (IRCELYON), CNRS & Université Lyon 1, Villeurbanne, France*
[2] *Institute of Science and Technology for Sustainable Energy and Mobility – CNR, Naples, Italy*
[3] *Dipartimento di Scienza Applicata e Tecnologia (DISAT), Politecnico di Torino, Italy.*
*laurent.piccolo@ircelyon.univ-lyon1.fr

Introduction

An analysis of the International Energy Agency in 2023 reported that in this year the total energy-related CO_2 emissions increased by 1.1%, but clean energy usage is leading to a slowdown in the growth of emissions, in particular due to the global capacity additions of wind and solar sources [1]. By converting captured CO_2 into useful products, carbon capture and utilization (CCU) may further contribute to environmental sustainability and generate economic value, transforming a wasted product into a resource [2, 3].

This work investigates the performance of rhenium-based dual-function materials (DFMs) for the integrated CCU (ICCU) to methane [4], and compares them with nickel counterparts. Conventional CO_2 methanation was used as a reference test to evaluate the impact of dilution with an adsorbent material and its relationship with ICCU performance.

Materials and Methods

Ammonium perrhenate and nickel nitrate were used as metal precursors. Commercial γ-alumina was used as catalyst support. The catalysts were prepared by wet impregnation, drying then calcination in air, and reduction in H_2 flow. To obtain DFMs, the catalysts were diluted in a commercial layered double hydroxide (LDH) synthetic hydrotalcite, which acts as a CO_2 sorbent.

The materials were characterized using elemental analysis (ICP-OES), scanning transmission electron microscopy (STEM), and temperature-programmed techniques. The methanation and ICCU tests were performed in a plug flow fixed bed reactor at atmospheric pressure coupled with a gas analyzer. The samples were pretreated *in situ* under H_2 flow at 400 °C. For CO_2 hydrogenation, the feed comprised CO_2 (10%) and H_2 (40%) in N_2. ICCU cycles at 300 °C included CO_2 adsorption (7.5% CO_2/N_2, 4 min) and hydrogenation (10% H_2/N_2, 4 min) steps separated by N_2 purges. Fifty cycles were performed to assess the DFM stability.

Results and Discussion

Table 1 reports the main characteristics of the four samples. STEM shows that the metal is in the form of small clusters on alumina. The CO_2 hydrogenation results reveal that the undiluted catalysts exhibit not only higher activity but also higher methane selectivity (Fig. 1a), whereas under repetitive CO_2 adsorption-hydrogenation cycles (ICCU tests), the LDH-diluted samples outperform the catalysts, demonstrating enhanced stability and methane productivity (Fig. 1b), with full selectivity to methane. Temperature-programmed CO_2 desorption or hydrogenation experiments allow correlating these performances to CO_2 adsorption capacity and desorption temperature. Moreover, although Re/Al_2O_3 is much less efficient than Ni/Al_2O_3 for conventional CO_2 methanation, the Re DFM appears twice more active on a molar metal basis than the Ni DFM in ICCU.

Table 1. Sample characteristics

Sample	Dilution factor	Label	wt% metal
Re/Al_2O_3	0	RAL_0	5.2
Re/Al_2O_3 + LDH	4	RAL_4	
Ni/Al_2O_3	0	NAL_0	2.2
Ni/Al_2O_3 + LDH	4	NAL_4	

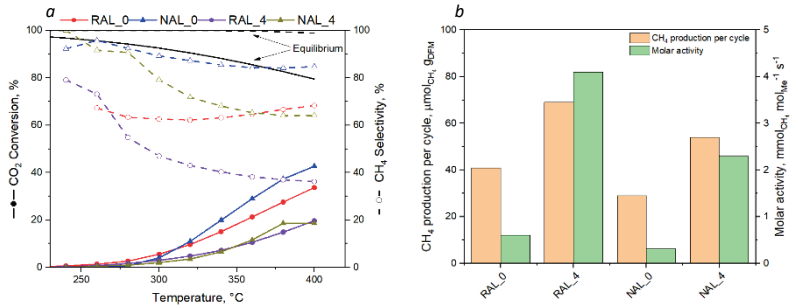

Figure 1. Performance comparison of materials a) in CO_2 hydrogenation to methane (the only other carbon product is CO), and b) in ICCU cycling at 300 °C (100% CH_4 selectivity).

Significance

These findings suggest that rhenium-based dual-function materials are a valuable choice for cyclic CO_2 capture and conversion.

The ANR-DuCaCO2 project funding is greatly acknowledged.

References

1. CO_2 Emissions in 2023 – Analysis. IEA 2024. https://www.iea.org/reports/co2-emissions-in-2023 (accessed November 5, 2024).
2. T. A. Atsbha, T. Yoon, P. Seongho, C.J. Lee, *Journal of CO_2 Utilization* 44, 101413 (2021).
3. F. Marocco Stuardi, F. MacPherson, J. Leclaire, *Current Opinion in Green and Sustainable Chemistry* 16, 71 (2019).
4. J. Chen, Y. Xu, P. Liao, H. Wang, H. Zhou, *Carbon Capture Science & Technology* 4, 100052 (2022).

Posters

CO_2 Purification of Industrial Flue Gas: Effect of Physico-Chemical Properties obtained by different Preparation Methods on CoCuAl oxide for the Selective Catalytic Reduction Process

Abou Rahhal A.[1], Genty E.[1], Cousin R.[1], Ponchel A.[2], Noel S.[2], Poupin C.[1], Siffert S.[1]*
[1]*Univ. Littoral Côte d'Opale, UR 4492, UCEIV, Unité de Chimie Environnementale et Interactions sur le Vivant, F-59140, Dunkerque, France*
[2]*Univ. Artois, CNRS, Centrale Lille, Univ. Lille, UMR 8181, Unité de Catalyse et de Chimie du Solide (UCCS), rue Jean Souvraz, SP 18, 62300 Lens, France*
*stephane.siffert@univ-littoral.fr

Introduction

In recent decades, environmental and human health have become a critical concern due to various atmospheric pollutants mainly greenhouse gases such as CO_2. Therefore, it is essential to minimize the amount of CO_2 released to the atmosphere by carbon capture facilities for either its utilization or storage[1]. Industrial flue gas is composed of various gases, primarily CO_2, combined with other pollutants mainly NO and CO that are harmful to environment and human, as well as oxygen and water vapor[2]. Consequently, and prior to CO_2 valorization, CO_2 purification is a crucial step to remove both NO and CO using selective catalytic reduction (SCR) process based on the following reaction: $NO + CO \rightarrow CO_2 + ½ N_2$. Indeed, recent work[4] has shown that copper and cobalt based transition metal oxides derived from layered double hydroxides (LDH) are promising catalysts for CO_2 purification. Layered double hydroxide material provides suitable route to prepare mixed oxide catalysts with good dispersion and high thermal stability. Various strategies are implemented to promote the activity and selectivity of these catalysts. The primary approach is based on the influence of the LDH precursor synthesis method (microwave or hydrothermal assistance) to obtain better crystallinity and enhanced active site dispersion[5]. In addition, the use of cyclodextrins is known to be an effective approach in the preparation of heterogeneous catalysts[6] and is a promising modification to enhance the selective catalytic reduction of industrial flue gas. Anionic β-cyclodextrin can intercalate in LDH structures promoting enhanced reducibility and dispersion of active species[7]. Therefore, the aim is to study the effect of various layered double hydroxide modified methods on the physico-chemical properties of CoCuAl mixed oxide catalysts for the selective catalytic reduction of industrial flue gas.

Materials and Methods

The cobalt-copper based catalysts (CoCuAl) were prepared following different co-precipitation routes. LDH were synthesized by precipitating respective amounts of metal nitrates over either sodium carbonate (classical way) or carboxymethyl-β-cyclodextrin solution maintaining a constant pH using sodium hydroxide followed by maturation step under different conditions: room temperature (classical way), hydrothermal treatment or microwave assistance. The solution was then filtered, washed and dried to obtain CoCuAl LDH samples.

The samples were characterized by various techniques including X-ray diffraction (XRD), thermogravimetric analysis (TGA), Fourier-transform infrared spectroscopy (FTIR), Temperature Programmed Reduction (H_2-TPR), and Raman spectroscopy. Catalytic tests for thermally treated samples were conducted in a continuous-flow reactor under simulated flue gas conditions (20.5% CO_2, 8.8% O_2, 8.2% H_2O, with 1300 ppm of CO and 500 ppm of NO) at temperatures ranging from 100 to 400 °C.

Results and Discussion

In comparison of classical LDH preparation route, microwave irradiations for few minutes tends to promote higher surface area catalysts with smaller particle size distribution, which will enhance the catalytic performance within SCR process. Hydrothermal treatment also enhances the textural properties with higher specific surface areas, higher amount and easier reducibility of active species. Both techniques promote better crystallinity and therefore an efficient and selective catalyst for CO_2 purification. The intercalation of cyclodextrins within the LDH structure promotes different physico-chemical properties and modified mesoporosity after calcination defined by several characterization techniques such as XRD, FTIR, TGA, and Raman. Therefore, the presentation will figure out the influence/evolution of various physicochemical properties obtained by modified LDH preparations in relationship with the catalytic activity.

Significance

This work presents insights into various LDH preparation methods that improve the physio-chemical properties of CoCuAl catalysts and therefore enhances CO_2 purification efficiency in industrial setting, hence technologies for clean energy and providing a scalable pathway for mitigating NO_x and CO emissions in captured CO_2 streams.

Acknowledgments

The authors would like to thank the PIA Dunkerque l'Energie Créative and Université du Littoral Côte d'Opale as well as MatHyBioCat project and CPER BiHautsEcodeFrance for their financial support to this research work.

References

1. Ma J, Li L, Wang H, et al. *Engineering*. 2022, 14, 33–43.
2. Larki I, Zahedi A, et al. *Sci. Total Environ.* 2023, 903, 166108.
3. Liu S, Gao J, et al. *J. Chem. Eng*. 2024, 486, 150285.
4. Akil, J., Siffert, S., Cousin, R., Poupin, C. *Appl. Catal. A*: *General*, 2023, 653, 119066.
5. Abou Serhal, C., Mallard I., Poupin C, Labaki M, Siffert S, Cousin R. *EurJIC*. 2019, 26.
6. L. Bai, F. Wyrwalski, J., E. Monflier, A. Ponchel et al., *J. Catal.* 2016, 341, 191–204.
7. Demeester, A., Douma, F., Cousin, R., Noël, S. et al Int. J. Mol. Sci., 2024, 25(12), 6390.

Catalytic Oxidative desulfurization of Marine fuel oil: investigating catalyst deactivation

Joy Alakari[1*], Teddy Roy[1], Line Poinel[1], Christine Lancelot[2], Pascal Blanchard[2], Carole Lamonier[2]
[1]*SEGULA Technologies, 44550 Montoir De Bretagne, France*
[2]*Univ. Lille, CNRS, Centrale Lille, ENSCL, Univ. Artois, UMR 8181 – UCCS – Unité de Catalyse et Chimie du Solide, 59000 Lille, France*
*joy.alakari@segula.fr

Introduction

Maritime transport contributes to 3% of global greenhouse gas emissions, with a 10% rise recorded between 2012 and 2018[1]. To prevent further increases in emissions, the International Maritime Organization (IMO) has tightened sulfur limits in marine fuels under MARPOL Annex VI, reducing sulfur content to 0.1% in Sulfur Emissions Control Areas (SECAs) and 0.5% elsewhere. Hydrodesulfurization (HDS) is commonly used but is costly due to high temperature, pressure, and hydrogen requirements. Moreover, its effectiveness is limited, in heavy fuel oil, due to the presence of refractory sulfur compounds.

Catalytic oxidative desulfurization (ODS) can offer a cost-effective alternative[2], transforming sulfur compounds into sulfones for further removal. It operates under mild conditions (low temperatures <100°C and atmospheric pressure). While most ODS studies focus on model compounds or light cuts, its application to marine fuel oil in batch reactors or continuous flow processes is rarely studied[3]. Furthermore, catalyst deactivation during ODS of heavy feed remains largely unexplored, underscoring the need for our research to understand the underlying phenomena to develop robust catalysts for this process.

Materials and Methods

A 20% MoO_3/Al_2O_3 catalyst was prepared using the incipient wetness impregnation method with ammonium heptamolybdate, followed by maturation, drying, and calcination.

ODS tests were conducted on RMG380 marine fuel oil (1.3 wt.% S), diluted with dodecane (x5) and centrifuged (20 min at 8000 rpm), referred to as RMG380-DC. The deactivation phenomena of the catalysts were first studied using a batch process. A 100 mL glass reactor was used, where 30 g of the prepared RMG380-DC and 600 mg of catalyst were heated to 80°C under reflux, with H_2O_2 added, and the catalyst was recovered by filtration. To further investigate catalyst deactivation, the process was transitioned to a continuous flow setup. The fuel was fed into a fixed-bed reactor alongside H_2O_2 at a flow rate of 0.88 mL/min, maintaining an oxidant-to-sulfur ratio of 10. The stream passed through a catalytic bed heated to 80°C. Another continuous test was conducted using a model feed (DBT in dodecane) with sulfur content matching that of the diluted fuel (0.26 wt.% S) to identify the deactivation phenomena observed with the real feed and evaluate the influence of its complex composition on the system.

Catalyst performance was evaluated by monitoring dibenzothiophene (DBT) conversion using GC-SCD. Deactivation causes were studied by analyzing the catalyst after the batch-test and after drying, and the catalyst after the continuous-test and after washing with toluene for its recovery from the fixed-bed reactor. Both catalysts were characterized by XRF and CHNS to assess changes in composition.

Results and Discussion

The four successive batch tests with RMG380-DC revealed progressive catalyst deactivation, as shown in Figure 1 (Left). Possible causes were investigated: active phase leaching and sulfone adsorption, which are major deactivation factors with model molecules[4], as well as the effects of water (byproduct) and heavy hydrocarbon (HC) deposition, which are less commonly addressed in the literature. XRF analysis evidences the absence of active phase leaching (Table 1). Around 2% of sulfur retention after four runs indicates that in a batch process, sulfone adsorption is negligeable (0.83 wt.% sulfur by CHNS). However, the high H/C ratio of 1.5 suggests adsorption of HC on the catalyst surface which may contribute to the deactivation.

Table 1. CHNS analysis and XRF analysis on used 20%MoO_3/Al_2O_3 in batch and continuous process

	CHNS analysis				XRF analysis	
	C (%)	H (%)	N (%)	S (%)	Al_2O_3 (%)	MoO_3 (%)
20Mo/Al – Batch (4 runs)	17.51	2.16	0.09	0.83	ND	18.6
20Mo/Al – Continuous	4.70	1.60	0.02	0.20	80.1	18.8

Using a fixed bed reactor, a continuous activity loss is also observed (Figure 1, right). The absence of leaching is evidenced, and CHNS analysis also shows negligible sulfur content, suggesting that sulfones are either not adsorbed or removed during washing (Table 1). To evaluate the role of water, a test with the model fuel was performed. It shows a nearly cyclical behavior, with strong deactivation attributed to sulfone adsorption due to reduced solubility in model feeds, followed by an increase in activity, probably due to progressive sulfone release in the charge during the flow process. The full recovery of DBT conversion after 300 min indicates that the presence of water did not negatively affect the catalyst surface.

This investigation helps to identify the potential causes leading to the deactivation phenomena observed in both batch and continuous processes in the ODS of marine fuel. Leaching, sulfone adsorption, and the effect of water have been excluded as significant factors in both processes. Therefore, the primary hypothesis remains the precipitation/adsorption of hydrocarbons. Further work will focus on exploring this hypothesis and developing strategies to mitigate this phenomenon.

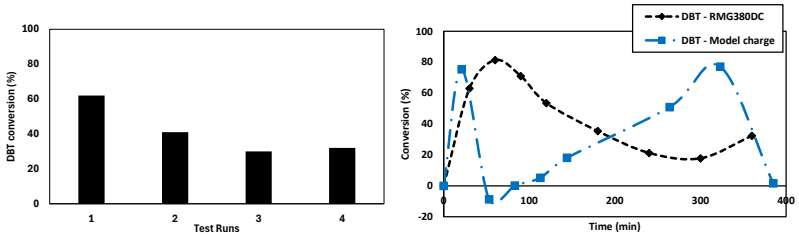

Figure 1. 20%MoO_3/Al_2O_3 ODS activity on DBT conversion in a batch reactor (Left) and in a fixed bed reactor (Right) for RMG380_DC (black) and in model charge (blue) (Ox/S=10, 80°C)

Significance

Identification of deactivation phenomena helps to design an efficient and robust ODS catalyst.

References

1. International maritime organization. Fourth IMO GHG Study 2020: Full report and annexes.
2. Prerana, S.; Vijayalakshmi, G.; Verraboina, S. An overview of conventional and alternative technologies for the production of ultra-low-sulfur fuels. Reviews from chemical engineering 2018, 35, 669-705.
3. Houda, S.; Lancelot, C.; Blanchard, P.; Poinel, L.; Lamonier, C. Ultrasound Assisted Oxidative Desulfurization of Marine Fuels on MoO_3/Al_2O_3 Catalyst. Catal. Today 2021, 377, 221–228.
4. Estephane, G.; Lancelot, C.; Blanchard, P.; Dufaud, V. ; Chambrey, S. W-SBA based materials as efficient catalysts for the ODS of model and real feeds. Applied Catalysis A: General 2019, 571, 42-50.

Influence of Water Vapor Treatment for NH_3-TPD on Zeolites

Dr. Bilal Amoury[1], Dr. Jürgen Adolphs[2] *, Dr. Serkan Gökpinar[2], Dr. Yuko Konishi[3]
[1]*Microtrac Formulaction, 3 Paule Raymondis Street, 31200 Toulouse, France*
[2]*Microtrac Retsch GmbH, Retsch-Allee 1-5, 42781 Haan, Germany*
[3]*Microtrac BEL Corp., Tokyo, Japan*
*j.adolphs@microtrac.com

Introduction

Temperature programmed desorption of ammonia (NH_3-TPD) is commonly used to evaluate the acidity (acid amount, acid strength) of solid acid catalysts such as zeolites. In many cases, there are two peaks, *l*-peak (low temperature) and *h*-peak (high temperature) in the TPD spectrum.

Materials and Methods

The *l*-peak is derived from ammonia molecules which are adsorbed by hydrogen bonding on NH_4^+ cation on acid sites and is not considered to indicate the acidity. However, in the case of zeolites with weak acidity, such as Y-type zeolites, the *l*-peak and *h*-peak overlap, making it difficult to evaluate acidity. NH_3 TPD measurement with steam treatment is considered being effective to eliminate the *l*-peaks. In this contribution the procedure, and precautions are described. Ammonia as probe molecule is adsorbed onto the zeolite sample until it reaches equilibrium. Then the temperature of the sample is continuously increased, causing an enrichment with the desorbed molecules in the inert carrier gas (Helium). The standard TCD (Thermal Conductivity Detector) measures the total adsorbed amount and not the specific desorbed constituents. However, since zeolite adsorbs water in its pores, it is necessary to use a detector that can detect water and ammonia separately when measuring TPD. Also, since water vapor is introduced at high temperature, this method is not applicable to samples whose properties are changed by water vapor. Therefore, a quadrupole mass spectrometer is used to detect the desorbing ammonia at mass number 16. Mass number 17 was not used because the peak at 17 can be affected by the desorbed water.

NH_3-TPD measurements were performed under the following conditions:

Measuring equipment	: BELCAT II + BELMASS
Sample	: MFI, 50 mg
Temperature ramp rate and target temperature	: 10°C/min, 610°C
Adsorption gas	: NH_3/He 5%

According to Igi et al., in their experiments the steam treatment was performed by repeating the evacuation of the sample cell with following steam introduction. Differently, the catalyst analyzer BELCAT II is a dynamic flow type equipment operating permanent at atmospheric pressure. Fully saturated water vapor is generated by an advanced bubbling method with inert gas at room temperature under atmospheric pressure.[1]

Results and Discussion

The experimental results show that steam treatment eliminates the *l*-peak and leaves the *h*-peak shape almost unchanged, indicating that steam treatment in NH_3-TPD measurement is very effective for eliminating the *l*-peak and examining the *h*-peak in detail. To perform NH3-TPD measurement with BELCAT II, the vapor option and a quadrupole mass spectrometer BELMASS is necessary.

References

1. Igi, H.; Katada, N.; Niwa, N. *Proc. 12th Intl. Zeol. Conf.*, **1999**, 2643.

Valorization of Greenhouse and Acid Gas by Low-Silica Zeolite Catalyst

Syeda Rabia B.[1], Marco F.[1], Ludovic P.[1]*, Alexey N.[2], Helene R.[2], Valentin V.[1]*
[1]*LCS, CNRS-ENSICaen-UniCaen, 14000 Caen, France.* [2]*Saint Gobain Research Provence and NORPRO, Cavaillon, France.*
*ludovic.pinard@ensicaen.fr; *valentin.valtchev@ensicaen.fr

Introduction

One persistent challenge in recent times is the indiscriminate emission of greenhouse gases such as CO_2 into the atmosphere, leading to global warming and environmental degradation. The lack of mature technologies for CO_2 conversion into value-added compounds is the major obstacle to the circular economy and Net Zero target. Refineries and petrochemical industries emit 1.24 Pty of CO_2 and at the same time process large quantities of hydrogen sulfide (H_2S). The admixture of later with CO_2 is called "acid gas".[1] Current acid gas treatment methods, like the Claus process, have limitations and require additional fuel, whereas CO_2 reduction techniques need high-purity CO_2, necessitating effective separation from acid gas. Hence, no existing technologies allow simultaneous CO_2 and H_2S reduction.[2] A new technology aims to electrify a simultaneous chemical conversion of acid gas components into platform molecule carbonyl sulfide COS, followed by the conversion of COS into CO and marketable Sulphur[3]. As COS serves as a building block for this technology, its formation in continuous mode from CO_2 and H_2S is the first and most important stage of this process as follows:

$$H_2S(g) + CO_2(g) \rightleftharpoons COS(g) + H_2O(l) \qquad (i)$$

The conversion of H_2S without catalyst is very low (0.5%), whereas it is reported to be over 70 % in the presence of a zeolite.[4] Zeolites catalyze the COS formation via dissociative adsorption, where the SH- group of H_2S orientates to weakly coordinated cations while the proton interacts with lattice oxygen. This leads to high H_2S reactivity to catalyze COS formation.[3] The benchmark material reported for this very reaction is zeolite NaX[4], however, the literature lacks devoted efforts on the optimization of this reaction. In this work, we explore different zeolites for acid gas conversion, aiming to develop a superior performance catalyst that enables high yields of COS per pass and low energy demand for regeneration.

Materials and Methods

Saint Gobain and UOP provided zeolite samples. The potassium exchanged 13X sample is denoted as 13X-K. The sieved zeolite catalysts (Table 1, particle size 0.2-0.5 mm) were loaded in a fixed-bed quartz reactor (9 mm diameter), and the reactor was fed with a mixture of H_2S (Linde, purity: 95%v in N_2) and CO_2 at different dilutions (3-12%v) using a constant flow of 1.8 L/h (STP). The conditions used for adsorption and reaction of CO_2 and H_2S are WHSV= 0.0247h^{-1}, P=1.1 bar, T=45-350°C. Catalysts in two different states were employed for the reaction (i) fully dry (pre-treated at 100-350°C under nitrogen flow 1.8 L/h (STP) for 6 h) and (ii) water-saturated catalysts.

Results and Discussion

The catalytic conversion at 100°C is minimum on zeolite Y amongst all dry zeolites (Figure 1).

Even though 13X has the same framework as that of zeolite Y, it has very high catalytic conversion followed by slower catalyst deactivation. Zeolite 4A outperforms all the catalysts, giving the maximum COS yield during the first hour of the reaction (Figure 1). After that, the reaction in 4A proceeds by a deactivation profile faster than that of 13X and 13X-K. The catalytic performance of 13X-K is intermediate between 13X and 4A, giving a COS formation peak like zeolite 4A followed by a slower deactivation profile like 13X.

Table 1. Properties of zeolite catalysts employed in this work.

Material	Si/Al ratio	S_{BET}(m^2/g)	Density (g/ml)	Hydration (%)
13X	1.2	900	0.65	24
4A	0.97	400	0.4	20.6
Y	2.5	700	-	23.8
13X-K	1.2	900	0.65	21.5

A series of catalytic tests at 45-350°C temperature range are carried out to gain further insights on the reaction profile of these zeolites as a function of temperature. As water is one of the reaction products, deactivation of zeolite occurs due to poisoning of the active sites by water.[5] This was confirmed by the negligible acid gas conversion on water-saturated zeolites. Therefore, we employ different conditions of pretreatment and the systematic comparison with the results of thermal gravimetric analysis (TGA) that enables an understanding of the hydration level of different zeolites and its role in the formation of COS.

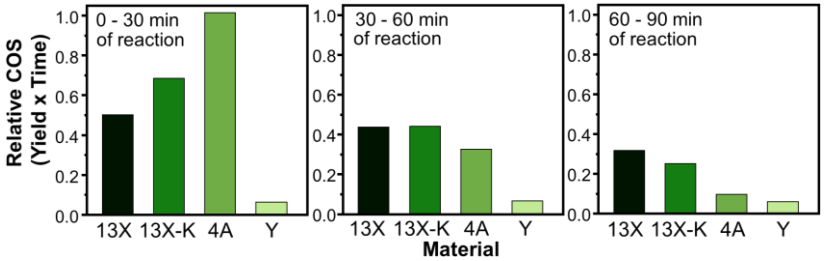

Figure 1. Relative COS formed at 100°C over dry zeolites at different times on stream (TOS).

Significance

This research work will contribute significantly to integrating COS production in a continuous process by maximizing the COS yield per pass with still reasonable times on stream (TOS). This will also aid in circularity in the processes of acid gas mixture and industry stream conversion.

References

1. The Paris Agreement UNFCCC, (May 2023), unfccc.int/process-and-meetings/the-paris-agreement
2. T. Yu, Z. Che, Z. Liu, J. Xu, and Y. Wang. Separations. ***2022*** 9(9), 229.
3. https://e-coduct.eu/
4. P. Fellmuth, W. Lutz, and M. Bülow. Zeolites. ***1987***, 7(4), 367-371.
5. S. Pfeifer, C. Pase, … D. Bathen. Microporous and Mesoporous Materials. ***2024***, 113408.

Versatile Macroligand Strategy for the Heterogenized Ni-Catalyzed Direct C-H Arylation of Benzothiophenes

Jerome Canivet,* Emilien Chaigne--Tarlotin, Elsje Alessandra Quadrelli
IRCELYON, Univ. Lyon 1, CNRS UMR 5256, Villeurbanne, France
*jerome.canivet@ircelyon.univ-lyon1.fr

Introduction

The use of earth-abundant metals for the direct C-H activation through a heterogeneous protocol would allow reaching appealing sustainability for the synthesis and derivatization of fine chemicals since this approach would enable at the same time (i) the use of accessible resources, (ii) a beneficial atom- and step-economy of non-activated substrates, and (iii) the ability to reuse the catalyst and to easily separate it from products. To change the paradigm of molecular catalytic processes for fine chemical synthesis, we introduced recently the concept of solid porous macroligand for heterogenized molecular catalysis. Having molecularly-defined active sites, porous macroligands have been found to drive the activity and the selectivity of heterogenized catalytic processes on a similar way as molecular ligands but with the advantage of the structuration in a three-dimensional framework and the confinement within a porous nanospace. Here we show the heterogenization of an earth-abundant molecular nickel complex within the structure of a bipyridine- and N-heterocyclic carbene-based porous organic polymers (POP) used as a porous macroligand. The molecularly-defined Ni-based heterogeneous catalyst allows the efficient and fully C2-selective arylation of benzothiophenes, thiophenes and selenophene, maintaining the intrinsic activity of molecular Ni-sites with advantageous stabilization and recycling ability.

Materials and Methods

Typical catalysis experiments are ran on 0.25 mmol of heteroaryl substrate using 1 mol% Ni catalyst (ca. 13 mg solid). The flask was sealed with a silicon septum and transferred out of the glove box. The reaction was stirred and heated to 120°C. After 16 h, the reaction mixture was quenched with 2 mL of dry methanol. The catalyst was separated by centrifugation and washed twice with dry methanol to be reused.

Results and Discussion

First, A nickel-based catalytic system for the regiospecific C2–H arylation of benzothiophene has been established. $NiCl_2$(bpy) is used as a catalyst in combination with LiHMDS.[1] The catalytic system is applicable to a variety of functionalized benzothiophenes, as well as other heteroarenes including thiophene, benzodithiophene, benzofuran and selenophene in combination with iodo aryl electrophiles. The role of LiHMDS as a uniquely potent base and a postulated mechanism have been unravelled. Then, bipyridine units covalently incorporated into the backbone of a porous organic polymer, named BpyMP-1, were used as a porous macroligand for the heterogenization of a molecular nickel catalyst. A controlled nickel loading within the porous macroligand is achieved and the nickel coordination to the bpy sites is assessed at the molecular level using IR and solid-state NMR spectroscopy.[2] The heterogenized Ni-bpy catalyst **Ni@BpyMP-1** was successfully applied to the direct and fully selective C2 arylation of benzothiophenes, thiophene and selenophene, as well as for the arylation of free NH-indole (Figure 1). Recyclability of the catalyst was achieved by employing hydride activators such as $NaBH_4$ to reach a cumulative turnover number of more than 300 after seven cycles of catalysis, which corresponds to a total productivity of 12 grams of 2-phenylbenzothiophene, chosen as model target biaryl, per gram of catalyst. More recently, a novel porous organic polymer platform with imidazolium functionalities (IM-POP) has been synthesized through radical polymerization.[3] N-heterocyclic carbene (NHC) has been subsequently generated from imidazolium moiety via base treatment and followed by the coordination of nickel salt giving access to single-site Ni-NHC catalyst inside the polymeric network. The nature and coordination of the Ni sites have been assessed by various spectroscopic techniques. The **$NiCl_2$@NHC-POP** was found to heterogeneously catalyze the direct selective C2-H arylation of (benzo)thiophenes using various aryl electrophiles with turnover number up to 75, reaching cumulative TON of ca. 400 after recycling for six consecutive runs (Figure 1). Both Bpy and NHC systems were postulated to proceed through similar pathways with the deprotonation of the benzothiophene to form the corresponding lithiated species as primary step, followed by transmetallation with (aryl)Ni species in a Ni(I)/Ni(III) redox catalytic cycle.

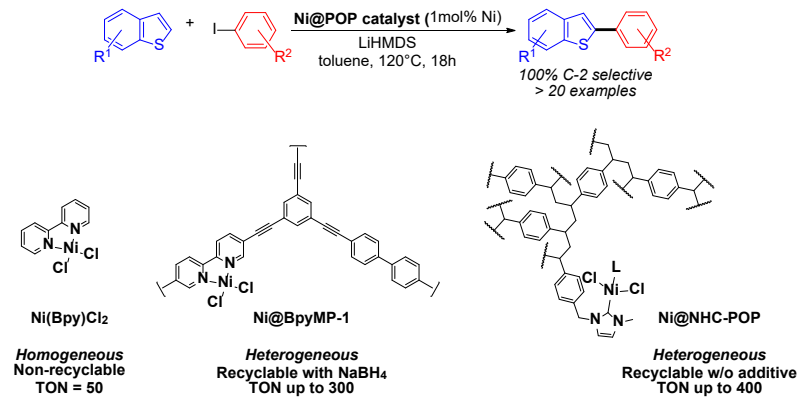

Figure 1. Comparison of molecular Ni-catalysts for the direct and fully selective C2-phenylation of benzothiophene.

Significance

Considering their robustness and their potential processability, the porous organic polymers used as macroligands for molecular catalysts further pave the way to molecularly defined and robust heterogeneous systems for a more sustainable synthesis of fine chemicals.

References

1. Mohr *et al.*, *Green Chem.* **2020**, *22*, 3155
2. Mohr *et al.*, *ACS Catal.* **2021**, *11*, 3507
3. Samanta *et al.*, *Catal. Sci. Technol.* **2023**, *13*, 5825

Porous Organic Polymers for Heterogeneous CO_2-to-HCO_2H Photoreduction

Emilien CHAIGNE--TARLOTIN*, Jérôme CANIVET, Elsje Alessandra QUADRELLI
Université Claude Bernard Lyon 1, CNRS, IRCELYON - UMR 5256, 2 Avenue Albert Einstein, 69626 Villeurbanne Cedex, France
**emilien.chaigne@ircelyon.univ-lyon1.fr*

Introduction

The promise of photocatalytic CO2 reduction reactions to offer sustainable routes for producing renewable fuels and necessary chemical building blocks has garnered a lot of interest. However, there is still a lack of effective, long-lasting, and selective photocatalysts as well as a thorough knowledge of the molecular makeup of active sites. Immobilizing isolated active sites within a supportive framework is a potential strategy in the creation of molecularly specified heterogeneous catalysts.

A significant challenge still exists in integrating catalytically active centers into a solid support while preserving performance on par with homogeneous counterparts. We have recently put up the idea of solid porous macroligands for heterogenized molecular catalysis in an effort to revolutionize the field of molecular catalytic processes for precise chemical synthesis and the manufacture of green fuel.[1] Similar to molecular ligands, these porous macroligands with molecularly-defined active sites have shown promise in boosting the activity and selectivity of heterogenized catalytic processes. They also enjoy the advantages of a three-dimensional structure and confinement in a porous nanospace.[2]

Results and discussion

When compared to homogeneous catalysis, heterogeneous catalysis offers a number of benefits, including simple product separation from the catalyst and recyclability. Solids that function as macroligands for site-isolated molecular complexes can be used to heterogenize molecular catalysts. For the CO2 to formic acid photoreduction, we have previously shown that fully heterogeneous systems based on the porous organic polymer macroligand POP exhibited exceptional productivity and stability over time (Figure 1).

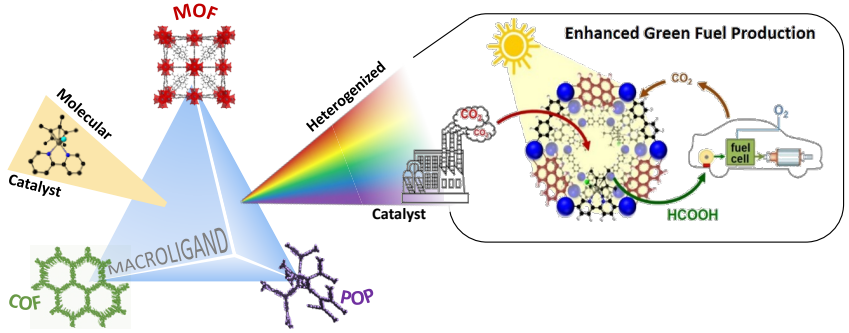

Figure 1: Porous hybrid solids as macroligands for photocatalytic CO2 conversion

We switched from the previously reported palladium catalyzed macroligand synthesis to radical polymerization with the aim to increase the sustainability of the photocatalysts synthesis. This novel synthetic approach, which would begin with vinylated monomers, would give the POP macroligand new optical and electrical characteristics as well as flexibility. The objective would be to construct whole heterogeneous systems with PS and coordination sites serving as catalyst macroligands, based on the same composition as the prior POP synthesis. The Rh catalyst heterogenized in N-POP material and utilized with an external photosensitizer completed preliminary testing. In this work, the photophysical and photocatalytic properties of a porous organic polymer structure are preserved through the successful integration of an organic photosensitizer. With organic dyes and a molecular Rh catalyst acting as single sites in a non-conjugated porous matrix, this invention seeks to develop all-in-one heterogeneous photocatalysts. The POP effectively facilitates light harvesting and electron-hole creation since it is built around perylene or polythiophene units. The coordination of organometallic active sites as isolated single-site molecular catalysts for CO2 reduction is made possible by the presence of bipyridine co-monomers, resulting in the production of formic acid as the only carbon-based product.

Acknowledgements

This work has benefited from French State aid managed by the Agence Nationale de la Recherche under France 2030 plan, bearing the reference code ANR-22-PESP-0010: Projet ciblé "POWERCO2" within the PEPR project SPLEEN

References

1. Wisser et al., *ChemCatchem* **2020**, *12*, 1270-1275.
2. Rajapaksha et al., *Chem. Soc. Rev.*, **2023**, *52*, 8059-8076.
3. Fávaro et al., *ChemCatChem* **2023**, *15*, e202300197.
4. Wisser et al., *Angew. Chem. Int. Ed.* **2020**, *59*, 5116–5122.
5. Newar et al., *Adv. Energy sustainabilit Res.*, **2024**, 5, 2300209.

An Old Yet Indispensable Method: *n*-Hexane Cracking for Composite Zeolite Characterization

Ruizhe Zhang[1,2], Nourrdine Chaouati[2], Bo Wang[1], Jiani Xu[1,3], Honghai Liu[4], Hongjuan Zhao[4], Jiujiang Wang[4], Shuta Xu[3], Francesco Dalena[2], Zhengxing Qin[1], Xionghou Gao[4], Svetlana Mintova[1,2*], Ludovic Pinard[2*]

*ludovic.pinard@ensicaen.fr and svetalana.mintova@ensicaen.fr

[1]China University of Petroleum (East China), Qingdao, China; [2]LCS, UMR 6506, ENSICAEN, France; [3]Institute of Chemical Physics, Chinese Academy of Sciences, Dalian, Liaoning; [4]PetroChina Company Limited, Beijing, P. R. China; [e]ICPEES, UMR 7515,

Introduction

Zeolitic materials are extensively utilized in catalytic and separation-adsorption processes due to their high activity and exceptional selectivity. However, their application is restricted by narrow porosity, which limits their efficiency in the transformation and separation of bulkier molecules. To address this limitation, composite zeolites with hierarchical porosity have been developed. These hybrid materials combine the intrinsic properties of two distinct structures and benefit from enhanced diffusion capabilities provided by hierarchization, making them more versatile catalysts suitable for a broader range of applications. Characterization of such complex materials using conventional physicochemical techniques poses challenges, as these methods often fail to directly assess the reactivity of acid sites and, consequently, their catalytic properties. This gap can be bridged by employing model reactions.

One of the most commonly used catalytic tests is n-hexane cracking, a reaction initially introduced by the Mobil company in the 1960s and still widely applied under the term "α-test." [1] This reaction proceeds via either monomolecular or bimolecular cracking mechanisms. The rate of monomolecular cracking is particularly sensitive to the strength of Brønsted acid sites (BAS).[2] The strength of these sites is closely linked to their local environment, which includes the zeolite's structural and compositional framework, the precise location of acid sites within the framework, and the presence of extra-framework species.[3] Consequently, this catalytic test serves as a powerful tool to probe the acidic properties of composite zeolites. It provides valuable insights into the reactivity of these hybrid materials and reveals potential synergistic, additive, or intimacy effects within the hierarchical structures.

Materials and Methods

The physicochemical properties of the materials were determined as follows: the Si/Al ratio was measured using X-ray fluorescence (XRF), the concentrations of Brønsted and Lewis acid sites (BAS and LAS) were quantified through pyridine adsorption-desorption at 150 °C, assisted by infrared spectroscopy (IRTF), and the morphology was examined using transmission electron microscopy (TEM). The transformation of n-hexane was conducted in a four-parallel fixed-bed reactor system. To ensure an accurate estimation of the reaction rate, the experiment was performed at four different contact times by varying the amounts of the same catalyst. The catalyst, with a particle size of 0.2–0.4 mm, was pre-treated at 540 °C under a nitrogen flow for 12 hours. A diluted n-hexane/nitrogen mixture was then injected into the reactors at 540 °C, maintaining a molar ratio of 11.

Results and discussion

The catalytic activities of two series of catalysts USY, with a Si/Al ratio ranging from 2.5 to 40, and HZSM-5, with a Si/Al ratio from 9 to 75, are compared to those of USY/ZSM-5 mixtures (containing 41 % USY and 59 % of ZSM-5) and a composite with a USY/ZSM-5 ratio. The composite consists of hierarchical zeolite Y (41 wt. %) and nano-sized ZSM-5 (59 wt%), produced through partial interzeolite conversion from USY. The key characteristics of this material are presented in Table 1.

The activity is directly proportional to the number of BAS non-exalted by aluminum extraframework (Figure 1A). Accordingly, the turnover frequencies (TOF) of these sites are determined from the slopes of the linear plots of cracking activity versus the concentration of acid sites, measured by pyridine probing at 150 °C. The USY/ZSM-5 composite exhibits the same TOF as the series of mechanical mixtures with similar proportions but different concentrations of BAS (Figure 1A). Therefore, the activity of the composite materials corresponds to an algebraic sum of the activities of pure zeolite Y and ZSM-5. This indicates that the composite retains the distinct acidic properties of its individual components.

Table 1. Main properties of studied catalysts.

Sample	USY/ZSM-5 (wt. %)	Si/Al (mol/mol)	[PyH$^+$] (µmol/g)	[PyL] (µmol/g)
USY/ZSM-5 Composite	41/59	20	148	104

The paraffins-to-olefins ratio (P/O), calculated from initial reaction rates, is influenced by the zeolite framework but decreases notably with increasing BAS concentrations (Figure 1B) as a result of enhanced secondary cracking. At comparable BAS concentrations, the composite exhibits a significantly lower P/O ratio compared to the mechanical mixture, pure ZSM-5, or pure USY. This difference is likely due to the close interaction between the crystallites of the two zeolitic phases. The texture and intimate contact between these phases (as shown in the TEM image, Figure 1A) influence the balance between primary and secondary cracking, likely by improving the accessibility of acid sites.

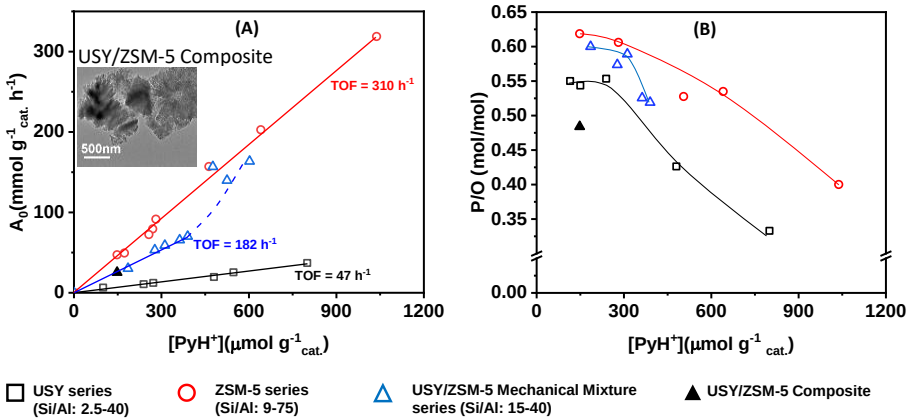

Figure 1. Variation of initial activity (A) and paraffins to olefins ration (B) as function of concentration of BAS probed by pyridine at 150 °C. A_0: initial activity of n-hexane cracking, P/O initial paraffins to olefins ratio.

Significance

The n-hexane cracking reaction (α-test) is demonstrated to be and remain a highly effective characterization tool for probing the catalytic properties of porous materials. Initial activity measurements reveal that the USY/ZSM-5 composite exhibits the intrinsic acidic characteristics of both USY and ZSM-5. Moreover, the interaction and proximity between the crystallites of the two structures significantly influence the material's selectivity. Consequently, this hybrid material displays promising catalytic properties, making it suitable for applications in the petroleum industry, fine chemical production, and the conversion of renewable resources.

References

1. J. A. Lercher, A. Jentys and A. Brait, in Mol. Sieves Vol. 6, Berlin, Heidelberg: Springer Berlin Heidelberg, 2008, pp. 153–212.
2. S.M. Babitz, B.A. Williams, J.T. Miller, R.Q. Snurr, W.O. Haag, H.H Kung, Applied Catalysis A: General, **1999**, 179, 71-86.
3. M. Guisnet, L. Pinard, Catalysis Reviews, **2018,** 60, 337-436.

A variety of environments of Lewis acid sites and hydroxyl groups of USY zeolites deciphered by DFT and high-resolution ^{1}H Solid-State NMR

T. Jarrin[1], Z. Wang[2], T. de Bruin[3], G. Pirngruber[1], M. Rivallan[1], A. Lesage[2], C. Chizallet[1,*]
[1]*IFP Energies nouvelles, Rond-point de l'échangeur de Solaize, 69360 Solaize, France*
[2] *Centre de RMN à Très Hauts Champs, Université de Lyon, 69100 Villeurbanne, France*
[3]*IFP Energies nouvelles, 1 et 4 Avenue de Bois Préau, 92852, Rueil-Malmaison, France*
*celine.chizallet@ifpen.fr

Introduction

Faujasite zeolite is widely employed for its catalytic properties, in the form of Ultra-Stable Y (USY), obtained after steaming and/or acid leaching. Bulk bridging Si-(OH)-Al sites are the main origin of the Brønsted acidity of zeolites. However, many reactions also take place at the surface of the material and of its mesopores. This study aims at unraveling the nature of USY bulk and surface acid sites. Using density functional theory (DFT), we propose some models for bulk defects and for external surface sites of the crystallites, investigate their dehydration properties, study their Brønsted and Lewis acidity via the adsorption of pyridine,[1] and compute dealumination barriers from bulk and external surface sites.[2] Experimentally, we investigate four faujasite zeolites at different stages of the dealumination process. By implementing NMR at high field and very fast MAS, we obtain high resolution ^{1}H NMR spectra interpreted with two-dimensional ^{1}H multiple-quantum correlations (two-, three and four-quanta), ^{1}H{^{27}Al} dipolar-based heteronuclear multiple quantum correlation experiments, and DFT calculations of chemical shifts based on the defect and surface models developed.

Materials and Methods

Periodic DFT calculations were performed with the VASP code (PBE+D2). Bulk cells at Si/Al = 47 and 3 were built, making use of the Loewenstein and Dempsey rules. External surface models were built by cleaving the crystal structure in the (111) orientation, experimentally known to be the most relevant. Dealumination barriers were computed thanks to the Nudged-Elastic Band method refined by a quasi-Newton optimization of the transition states. The GIPAW approach was used to compute chemical shifts. Four commercially available Y zeolites (from Zeolyst) were investigated: CBV300 ($Na(NH_4)Y$), CBV500 (obtained from CBV300 by steaming and full NH_4^+ exchange), CBV600 (steaming of CBV500) and CBV712 (acid-leached to remove Extra-Framework Aluminum - EFAL). The samples were dehydrated at 450°C under vacuum. ^{1}H single-resonance experiments were performed at 18.8 T on a Bruker NEO narrow-bore spectrometer equipped with a 1.3 mm ^{1}H/^{13}C/^{15}N triple-resonance probe capable of spinning up to 65 kHz for MAS. The ^{1}H-^{27}Al double-resonance experiments were carried out at 13.5 T on a Bruker NEO wide-bore spectrometer with a 1.3 mm ^{1}H/X double-resonance probe capable of spinning up to 65 kHz for MAS.

Results and Discussion

Several terminations of the (111) faujasite external surface exhibit similar stabilities according to DFT calculations. There, Al-H_2O groups are found to be more stable than classical bridging groups. Upon heating, dehydration of the Al-H_2O groups leads to Al_{III} and Al_{IV} species depending on the local environment in the vicinity of the Al-H_2O sites. Calculated temperatures of water desorption from those sites are highly dependent on the ability of the network to rearrange into an Al_{IV} species, and to the Si/Al ratio. The simulation of the adsorption of pyridine shows that these environments generate Brønsted acid sites of various strengths, and strong Lewis acid sites, even in the absence of extra-framework species. Defects and external surface sites affect the barrier of the initiation of dealumination, a variety of subtle local effects entering into play, such as the proximity with surface silanols. Al–O bond breaking is made easier from a kinetic perspective on some sites of the external surface. By NMR, experimentally, an extensive array of surface species, totaling 15 peaks, could be resolved and monitored in the course of dealumination (Fig. 1B). These resonances were assigned, some unambiguously, by combining the NMR information with DFT calculations of ^{1}H chemical shifts. Dense clusters of more than four Si-(OH)-Al were highlighted in sodalite cages. Similarly, a set of six Si-OH resonances were resolved and assigned to either isolated or clustered silanols, whether in proximity to Al atoms or not. The presence of $Al(OH)_{0/1/2}(H_2O)_{2/1/1}$ species is shown. Isolated Al-OH in multinuclear EFAL species or in amorphous silica-alumina domains are also identified. In contrast, the presence of alumina-like domains is excluded as free μ_1-Al-OH groups are not observed. The evolution of the hydroxyl groups was tracked during the dealumination process through quantitative analysis of the NMR spectra.

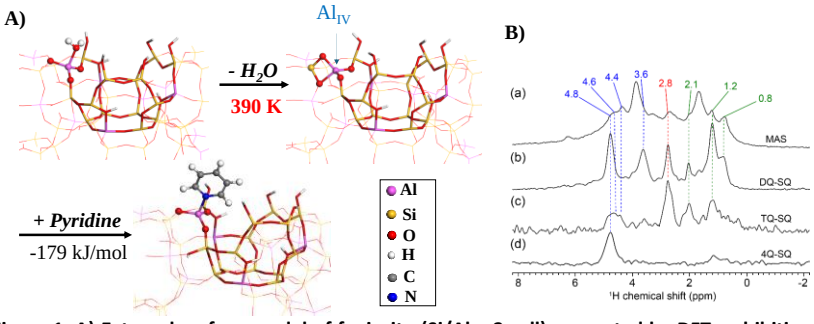

Figure 1. A) External surface model of faujasite (Si/Al = 3 cell) computed by DFT, exhibiting one Al-(H_2O) group, that dehydrates for T>390K and reveals a strong Lewis acid site probed by pyridine. B) ^{1}H MAS spectra (a) and the SQ-dimension projections extracted from the 2D ^{1}H DQ-SQ (b), TQ-SQ (c) and 4Q-SQ (d) correlation spectra of a USY sample obtained by steaming and acid leaching.

Significance

An unequalled level of details is thus reached in the description of the surface groups in presence after the various treatments. The presence of hydroxyl groups influences the Brønsted acidity of the samples, while Lewis acidity is shown to be due not only to EFALs but also to external surface sites. This opens the way to the rational control of the reactivity depending on pre-treatment conditions.

References

1. T. Jarrin, T. de Bruin, C. Chizallet, *ChemCatChem.* **2023**, *15*, e202201302
2. T. Jarrin, T. de Bruin, C. Chizallet, *ACS Catal.* **2024**, *14*, 1639

Impact of Limonene on the Products of Catalytic Pyrolysis of Polyethylene

Souha Denguezli[1*]; Sophie Duquesne[2]; Anthony Dufour[3]; Jean-François Lamonier[1]
[1]*Univ. Lille, CNRS, Centrale Lille, Univ. Artois, UMR 8181, Unité de Catalyse et Chimie du Solide (UCCS), Lille, 59000 (France)*
[2]*Univ. Lille, CNRS, Centrale Lille, INRAE, UMR 8207, Unité Matériaux et Transformations (UMET), Lille, 59000 (France)*
[3]*Univ. Lorraine, CNRS, UMR 7274, Laboratoire Réactions et Génie des Procédés (LRGP), Nancy, 54000 (France)*
**souha.denguezli@univ-lille.fr*

Introduction

This thesis project explores the catalytic pyrolysis of low-density polyethylene (LDPE) contaminated with limonene, used as a model contaminant. The choice of limonene is justified by an extensive literature review highlighting its presence in orange juice and its high affinity for LDPE, as demonstrated by several researchers[1],[2]. The study examines the effect of this pollutant on the thermal and catalytic degradation of LDPE, as well as the impact of the ZSM-5 zeolite on the degradation of LDPE. ZSM-5, recognized as the most widely used catalyst for the catalytic pyrolysis of LDPE, is investigated for its efficiency in enhancing the conversion of LDPE into valuable hydrocarbons.

Materials and methods

Low-density polyethylene (LDPE, DOW 310E) and d-limonene (Alfa Aesar) were used to study the sorption of limonene by LDPE. For each experiment, 3 g of LDPE pellets were divided into three aluminum supports (1 g per support) and placed in an airtight desiccator containing 12 mL of limonene in a beaker. The setup was incubated in an oven at 40°C. Sorption was monitored by weighing the LDPE after 12 days to determine the amount of absorbed limonene.The pyrolysis was performed in a stainless steel tubular reactor at 450°C, with a nitrogen flow rate of 200 mL/min. The chemical transformations of pure and absorbed limonene were analyzed by FTIR. The yields of the three fractions (gas, liquid, and solid) obtained during pyrolysis were calculated using the equations described below, and the liquid fractions were characterized by GC-MS.

Table1 : Equations Used for Yield Calculations

Yields without pollutants	Yields with pollutants
$Wax + Oil(wt\%) = \frac{Mass\ wax + oil}{Mass\ de\ LDPE} \times 100$	$\frac{m\ wax + oil}{m\ LDPE + m\ pollutant} \times 100$
$Coke\ (wt\%) = \frac{Mass\ coke}{Mass\ de\ LDPE} \times 100$	$\frac{m\ coke}{m\ LDPE + m\ pollutant} \times 100$
$Gas(wt\%) = 100 - Wax + Oil(wt\%) + Coke\ (wt\%)$	$Gas(wt\%) = 100 - Wax + Oil(wt\%) + Coke\ (wt\%)$

Results and Discussions

The results of limonene sorption by LDPE showed that, at 40°C, between 150 and 160 mg/g of LDPE were absorbed over 12 days. The experiment, repeated twice, yielded consistent results, demonstrating good reproducibility. The thermal and catalytic pyrolysis of LDPE contaminated with limonene at 450°C was conducted, with each experiment repeated three times for consistency, the thermal pyrolysis showed a decrease in the liquid phase yield (33%) and an increase in the gaseous phase (63%) compared to pure LDPE. During catalytic pyrolysis, a reduction in both the liquid and solid phases was observed, in favor of the gaseous phase. The thermal pyrolysis of LDPE predominantly produces alkanes (55%) and alkenes (35%), while the addition of limonene promotes the formation of cyclic structures. In catalytic pyrolysis with ZSM-5, the LDPE primarily generates BTEX, while limonene alone predominantly forms cycloalkenes (57%). When combining LDPE, limonene, and ZSM-5, the product distribution

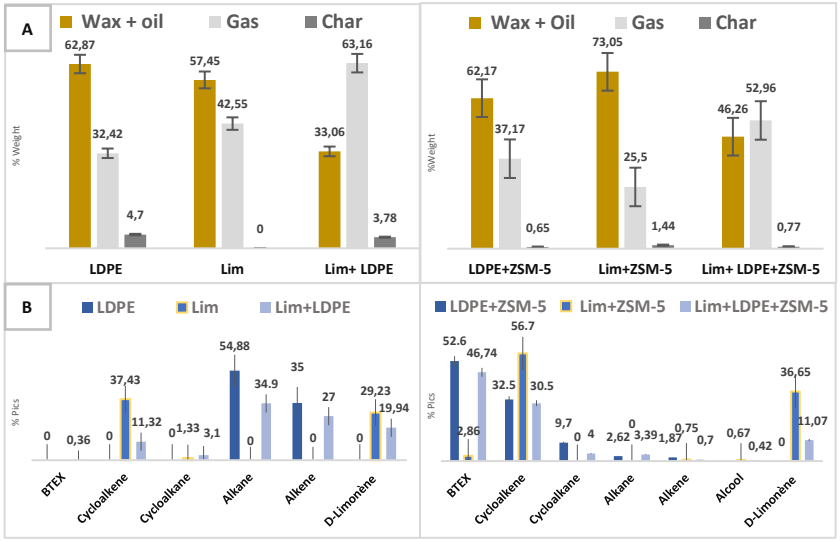

Figure 1: (A) Yields of the different phases from the thermal and catalytic pyrolysis of LDPE, Limonene, and LDPE+Limonene at 450°C respectively ;(B) Composition of the liquid fraction after the thermal and catalytic pyrolysis of LDPE; Limonene; LDPE+Limonene respectively

shows an increase in cycloalkenes (30.5%) and a slight reduction in BTEX (47%), indicating the influence of limonene on catalytic mechanisms.

Significance

The investigation of interactions between limonene and LDPE demonstrated significant sorption of limonene by LDPE. Additionally, the study examined the catalytic influence and the effect of limonene on the distribution of gaseous, solid, and liquid fractions during pyrolysis.

References

[1].R. W. G. Van Willige, « Effects of flavour absorption on foods and their packaging materials », 2002. doi: 10.18174/121284.
[2].R. W. G. van Willige , « Influence of food matrix on absorption of flavour compounds by linear low-density polyethylene: proteins and carbohydrates »,doi:10.1002/1097-0010(20000915)80:12<1779::AID-JSFA726>3.0.CO;2-F.

Porosity control of hierarchical zeolites provides effective catalyst for continuous-flow methyl oleate skeletal isomerization

Jonathan F. Sierra-Cantor[1], Olinda Gimello[1], Anne Aubert-Pouëssel[1], Carlos-Alberto Guerrero Fajardo[2], Francesco Di Renzo*[,1], Corine Gérardin[1], Nathalie Tanchoux[1]
[1] *ICGM, Université de Montpellier-CNRS-ENSCM, Montpellier, France,*
[2] *Departamento de Quimica, Universidad Nacional de Colombia, Bogotá, Colombia.*
*francesco.di-renzo@umontpellier.fr)

Introduction

Biodiesel worldwide production is still rising and will do so for many years, as the delays of electrification of the fuel production for heavy-duty transport justify an intermediate introduction of bio-based renewables. Shift to continuous-flow processes and improvement of the properties of enoic esters from vegetable or recycled oils require new custom-tailored heterogeneous catalysts. The recrystallization of zeolites in cetyltrimethylammonium (CTA) solution is an accepted method to open a hierarchical micro-mesoporous network and improve the accessibility of the active sites.[1] Micro-mesoporous hierarchical zeolites can provide significant improvements in selectivity and stability of the methyl oleate isomerization in flow reactors, overcoming previously observed site passivation.[2]

Materials and Methods

Parent ferrierite (FER-PAR) and dealuminated faujasite (Y30-PAR) were proton exchanged, recrystallized in cetyltrimethylammonium (CTA) solution, and calcined at 550°C, obtaining recrystallized FER-REC and Y30-REC catalysts. Textural data and composition of the catalysts are reported in Tab. 1. Methyl oleate isomerization was carried out in batch autoclaves (solventless, 285°C, 6 h) or in continuous flow reactor (285°C, 20 bar, N_2 flow, WHSV 3.5 h^{-1}).

Results and Discussion

The CTA recrystallization treatment has been applied to two kinds of zeolites with different microporosity - 10-member ring (10MR) medium size-micropore ferrierite and 12MR large-micropore high-silica faujasite - producing different structural mesoporosity in the two kinds of zeolites, with formation of MCM-41-like wormlike mesopores in faujasite and opening of a constrained negative-crystal mesoporosity in ferrierite (see Fig. 1A).[3]

Table 1. Composition and textural properties of materials

Catalyst	Si/Al	Micropore volume	Mesopore volume	Surface area ($m^2\ g^{-1}$)	
		$cm^3\ g^{-1}$	$cm^3\ g^{-1}$	BET	αS
a) Y30-PAR	30.2	0.253	0.181	716	110
b) Y30-REC	24.4	0.111	0.488	837	583
c) FER-PAR	9.7	0.145	0.054	394	15
d) FER-REC	6.6	0.107	0.252	427	159

Results of methyl oleate skeletal isomerization at 285 °C on faujasite and ferrierite catalysts are reported in Fig. 1B and 1C, respectively. In batch experiments (color bars in the figures), the yield on the parent zeolites was 27% on Y30-PAR and 55 % on FER-PAR. CTA recrystallization induces a limited yield improvement of 2% for Y30-REC and 4 % for FER-REC. In the case of the flow reactor experiments (lines with dots in Fig.1B and 1C), the yield of branched products on the parent zeolites is always lower than in the batch experiments and rapidly decreases with time-on-flow, until 4 % on Y30-PAR and 8 % on FER-REC after 7 h. When the recrystallized catalysts are used, for Y30-REC, no stability improvement are observed, with only a small increase of yield. In the case of FER-REC, the yield of branched monoenoic methyl esters rapidly rises to 53% and remains stable around this value for 8 h time-on-flow, at 98 % oleate conversion, a value similar to the results of batch tests, suggesting that the condensate in the constrained porosity of FER-REC exert a washing effect on the poisoning deposits on the Brønsted acid sites, similarly to the effect of the pressurized liquid phase in the batch reactors.

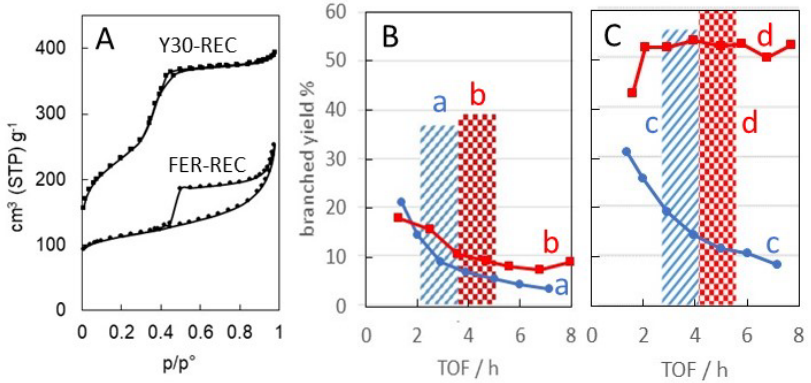

Figure 1. N2 sorption isotherms for recrystallized samples (A) and yield of branched isomers on faujasite (B) and ferrierite (C) catalysts (bars are batch results, lines and dots are flow reactor results vs. time-on-flow) Y30-PAR (a), Y30-REC (b), FER-PAR (c) and FER-REC (d).

Significance

A correct choice of both micropore and mesopore architecture of hierarchical zeolites allows to overcome the stability limitations of heterogeneous catalysts for the fatty ester skeletal isomerization in flow reactors.[2]

References

1. R. Chal, C. Gérardin, M. Bulut, S. Van Donk, *ChemCatChem*, **2011**, *3*, 67-81.
2. J. F. Sierra-Cantor, O. Gimello, C.-A. Guerrero-Fajardo, F. Di Renzo, H. Petitjean, M. Rivière, C. Gérardin, N. Tanchoux, *Appl. Catal. B: Environ*. **2024**, *344*, 123602.
3. X. Cheng, T. Cacciaguerra, D. Minoux, J.-P. Dath, F. Fajula, C. Gérardin, *Micropor. Mesopor. Mat*. **2018**, *260*, 132-145.

Novel time-resolved IR/isotopic exchange methodology for the mechanistic investigation of CO_2 hydrogenation to methanol

Amira Djaafri[1], Mélissandre Richard[1*], Christophe Dujardin[1], Isabelle De Waele[2]

[1] *Univ. Lille, CNRS, Centrale Lille, Univ. Artois, UMR 8181 – UCCS – Unité de Catalyse et Chimie du Solide, F-59000 Lille, France.*

[2] *Univ. Lille, CNRS, UMR 8516, LASIRE, Laboratoire de Spectroscopie pour les interactions, la Réactivité et l'Environnement, F59 000, Lille, France*

* melissandre.richard@centralelille.fr

Introduction

Studying reaction mechanisms in heterogeneous catalysis under real conditions and on short timescales is a major challenge.[1,2] In this contribution we present a novel approach combining time-resolved *operando* infrared spectroscopy (TR-IR) and steady-state isotopic transient exchange (SSITE). This method enables the investigation of reaction steps on timescales ranging from milliseconds to nanoseconds offering new insights into molecular processes occurring at the active site.

The feasibility of the TR-IR/SSITE coupling was initially demonstrated by studying the CO oxidation reaction on Pt/Al_2O_3, where the very first moments of isotopic exchange of carbonyl species were observed. Our aim is now to apply our methodology to further investigate the hydrogenation of CO_2 to methanol over Cu-ZrO_2 catalyst, focusing on the dynamics of Cu-bound formates and their role in the catalytic process. Indeed, recently Meunier *et al.* suggested that Cu formates are key intermediates in this reaction as their decomposition rates align with methanol formation.[3]

Materials and Methods

The TR-IR/SSITE tests were carried out on CO_2 hydrogenation reaction on a 6%$_{wt}$ Cu/ZrO_2 catalyst at 220 °C and 3 bar using alternately the following gas feed (12 mL min^{-1}): 20% **$^{12}CO_2$**/60% H_2/He or 20% **$^{13}CO_2$**/60% H_2/He-Kr. Long-period were first conducted switching the isotopic reactant every 5 min, followed by faster switch period up to 0.5 seconds.

The catalyst pellet (1.21 cm^2, ~12.8 mg) was loaded in the homemade IR cell with an internal dead volume inferior to 0.5 cm^3 and equipped with KBr windows. The cell was connected upstream to an automatic regulator for gas supply and control of the switching valves. Prior the reaction, the catalytic material was pre-treated at 350 °C during 1 h under 80% H_2/He. The evolution of adsorbed species at the catalytic surface was monitored using either Thermo Scientific Nicolet 6700 or Bruker Vertex 70V FTIR spectrometers equipped with an MCT detectors, respectively. IR spectra were collected in rapid-scan mode with a spectral resolution of 2 or 8 cm^{-1}.

Results and Discussion

The difference IR spectra between $^{12}CO_2$ and $^{13}CO_2$ feeds during both long (5 min) and fast (0.5 s) switching periods are presented in **Figure 1**. The spectra reveal key bands characteristic of formate species adsorbed on the catalyst surface. Specifically, the bands at 1570, 1385, and 1369 cm^{-1}, observed during the long-period switch, have been attributed to bidentate formates adsorbed on ZrO_2 support. A red shift of this bands upon $^{13}CO_2$ exchange is observed, giving rise to bands at 1526 and around 1330 cm^{-1} corresponding to the ^{13}C-labelled bidentate formate.

In addition, difference spectra obtained at the very start (< 0.5 s) of the isotopic exchange reveal new bands at 1690, 1630, and 1341 cm^{-1}. These have been assigned to monodentate formate species adsorbed on copper, suggesting a faster exchange kinetics compared to the formates adsorbed on ZrO_2. The appearance of these bands highlights the dynamic nature of surface interactions during the reaction. As the switching period decreases, the isotopic exchange allows us to selectively observe only the species that exchange rapidly on the catalyst surface. This provides valuable insights into the dynamics of reactive intermediates and their role in the reaction mechanism.

Further, additional bands were observed during the short-period switch, pointing to the presence of other adsorbed species or intermediates. These features require further investigation to elucidate their exact nature and contribution to the catalytic process.

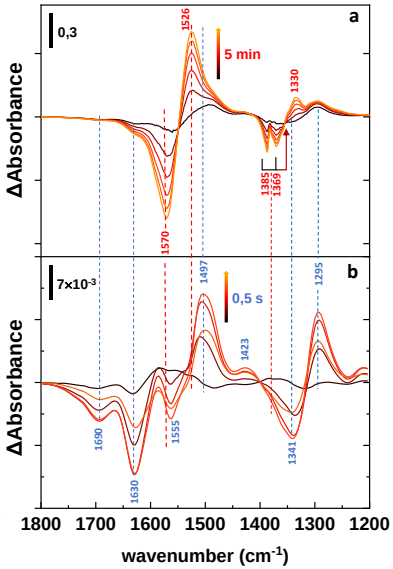

Figure 1. Difference between $^{13}CO_2$ and $^{12}CO_2$ IR spectra on Cu-ZrO_2 in the formates range at 220 °C and 3 bar; (a) 5 min long-period switch, (b) 0.5 s fast-period switch

Significance

The TR-IR/SSITE approach offers significant potential for exploring new details of the dynamics of heterogeneous catalytic reactions and examining reaction steps at the molecular level under realistic steady-state conditions on a short timescale.

References

1. Kalz, K. F. *et al.*, *ChemCatChem,* **2017***, 9*, 17–29.
2. Bañares, M. A. & Daturi, M., *Catalysis Today,* **2023***, 423*, 114255.
3. Meunier, F. C., Dansette, I., Paredes-Nunez, A. & Schuurman, Y., *Angewandte Chemie International Edition*, **2023**, *62*, e202303939

Financial - This study was financially supported by the French *Agence Nationale de la Recherche (ANR)* – project ANR-21-CE29-0030-01. The authors want to thank also Centrale Lille Institute, the Ministère de l'Enseignement Supérieur et de la Recherche (CPER IRENE and CPER ECRIN) and the European Fund for Regional Economic Development for their support.

Polyolefins recycling: Mechanism of the polyolefin bifunctional hydrocracking from a polymer approach.

*J. Florez[1], S. Maury[1], R. Martinez-Franco[1], J. Fernandes[1], V. Monteil[2]
[1]*IFP Energies Nouvelles, 69360 Solaize, France*
[2]*Catalysis, Polymerization, Processes and Materials laboratory CP2M, 69616 Villeurbanne, France*
*julia.florez-ablan.@ifpen.fr

Introduction

Bifunctional hydrocracking of alkanes is a well-established process in the refining industry, with extensive literature available on the topic. However, its application to polyolefin recycling is relatively new, necessitating a deeper understanding of the reaction dynamics, selectivity, and mechanisms. Currently, most publications focus on optimizing fuel cuts yields by studying the influence of the catalyst features, such as the solid acid type and metal component.[1,2] Although the catalyst approach is important, a polymer-based approach should not be disregarded. The structure and properties of the polyolefin have a real and significative impact on the reaction mechanism and its main products. Some authors have proposed different hydrocracking mechanisms for Polypropylene and Polyethylene, nevertheless, most studies overlook the feedstocks structural differences which can lead to inaccurate statements. Here, three types of polyolefins were evaluated: Polypropylene (PP), High Density Polyethylene (HDPE) and Low-Density Polyethylene (LDPE). For a better understanding of the mechanism, the hydrocracking reaction was evaluated at several processing conditions. For the preliminary trials, the polyolefins grades were chosen to match and compare the results with current literature.

Materials and Methods

A commercial USY zeolite (Si/Al=17) from Zeolyst was impregnated with an aqueous solution of H_2PtCl_6 to obtain a Pt content of 0,5wt%. The solid was then dried at 110°C and calcinated at 450°C for 3h. For a better handling the catalyst was milled and sieved into particles of 200-500µm. The platinum reduction took place in a hydrogen flux of 2l/h/g at 150°C for 30min and 2h at 400°C.

The hydrocracking reactions were carried out in a High-throughput system of four batch reactors using 12g of polyolefin and 1,2g of catalyst. The polyolefins grades were acquired from Sigma Aldrich. The liquid and solid yields were estimated by gravimetric analysis. The reaction gaseous products were quantified by a flowmeter Rytter and analysed by online Gas Chromatography GC-FID. The liquid yields composition was determined with an off-line GC-FID employing a quantification method. The partially cracked polyolefin was extracted and separated from the used catalyst by a "Soxtherm" system with Xylene for 3h at 250°C. Ethanol was added to the xylene solution that was then vacuum filtrated to recover the precipitated polyolefin. The recovered catalyst and polyolefin were then dried at 90°C for 2h. The polyolefin molar mass was characterized by size exclusion chromatography (SEC), infrared analysis (IR), parallel plates rheometer and differential scanning calorimetry (DSC). The catalysts were characterized by IR and thermogravimetric analysis (TGA).

Results and Discussion

As shown in Figure 1 the behaviour of the tested PP, HDPE and LDPE considerably differ. By compiling the characterization results of the gas and liquid and solid, reaction mechanisms are proposed separately for each polyolefin type.

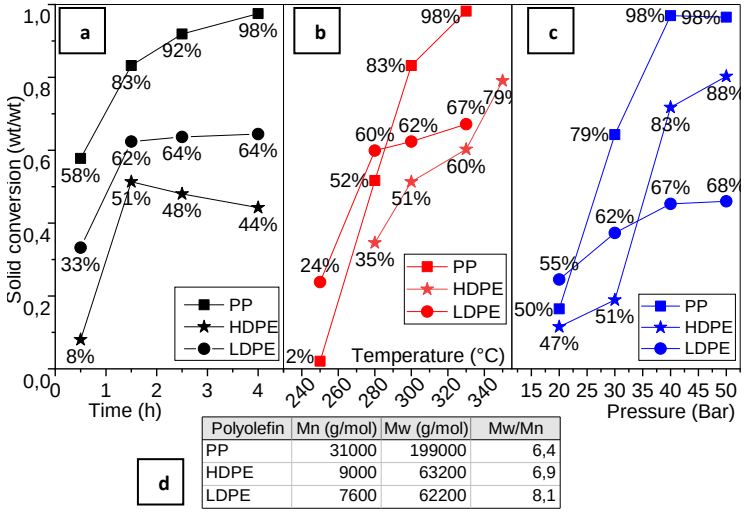

Polyolefin	Mn (g/mol)	Mw (g/mol)	Mw/Mn
PP	31000	199000	6,4
HDPE	9000	63200	6,9
LDPE	7600	62200	8,1

Figure 1. Solid conversion of PP, HDPE and LDPE in function of (a) Time at 30bar H_2 300°C, (b) Temperature for 1,5h at 30bar H_2 and (c) Pressure at 300°C for 1,5h and (d) SEC results of the virgin polyolefins.

Nevertheless, the number average molar mass (M_n) and the dispersity of the molar mass distribution ($Đ$) of the tested polyolefin grades is not the same, making comparisons between them even more challenging. Current literature does not adequately address the impact of initial M_n and $Đ$, so any inference about the reaction mechanisms, based on a comparison of the different polyolefins that overlooks molar mass could be misleading. To bring more clarity to this topic, HDPE samples with similar $Đ$ but varying M_n will be synthesized and tested. This study will reveal the impact of initial chain size on the reaction's activity and selectivity, as well as on the initial viscosity of the polymer in hydrocracking conditions.

Significance

The study proposes a new approach to the evaluation of the reaction mechanisms and intends to explore in more detail the influence of the feedstock characteristics on the selectivity and reactivity of the reaction.

References

1. Kots P.A., Vance B.C., Vlachos D.G. Reaction Chemistry & Engineering, 2021, 7, 1, 41-54.
2. Dong Z., Chen W., Xu K., Liu Y., Wu J., Zhang F. ACS Catalysis, 2022, 12, 24.

Influence of preparation method of CuAl mixed oxide issued from LDH catalytic total oxidation of model fumes issued from biomass combustion

Eric Genty*, Pierre Edouard Danjou, Christophe Poupin, Stéphane Siffert, Renaud Cousin

Université du Littoral Côte d'Opale, Unité de Chimie environnementale et Interactions sur le Vivant (UCEIV), 145 avenue Maurice Schumann, 59140 Dunkerque, France.

eric.genty@univ-littoral.fr

Introduction

Emission of volatile organic compounds (VOCs) into the environment is now strictly regulated due to harmful to public health and atmospheric environment. Moreover, in many industrial applications and for the fumes issued from biomass combustion, emissions often contain CO. Catalytic total oxidation of CO into CO_2 is considered to be a good route for the reduction of CO toxic effects from motor engines and industrial processes exhausts. Among many technologies available for VOCs control, the catalytic oxidation of these pollutants to carbon dioxide and water has been recognized as one of the most promising technologies [1, 2]. In the aim to obtain a reaction economically competitive, it is necessary to explore higher active catalysts performing at low temperatures.

Transition metal oxides, especially cobalt, copper and manganese oxides, offer a low-cost alternative to metal noble based catalysts which are presently the most active catalysts in the complete oxidation of VOCs at low temperatures. An interesting way to obtain mixed oxides catalysts is through the use of layered double hydroxides (LDH) as precursors. Indeed, after calcination treatment mixed oxides are formed and possess unique properties like a high surface area, good thermal stability, good mixed oxides homogeneity and basic properties. The partial or the total substitution of Mg^{2+} and Al^{3+} is possible by divalent cation or trivalent cation in the LDH structure [3, 4]. For synthetized the LDH compounds, the coprecipitation is the method widely applied. Recently, microwaves (MW) radiation heating [5, 6] and ultrasound (US) [7] have been applied to the synthesis of hydrotalcite with different chemical compositions as an alternative to the conventional hydrothermal treatments. In fact, there are several advantages such as shorter treatment times to achieve enhanced crystallinity degrees, higher specific surface areas, and increase the metallic dispersion. In the present study, Cu- Al LDH as precursors are characterized and investigated for total oxidation of CO and Toluene mixture.

Materials and Methods

LDH precursors Cu_6Al_2 were prepared by three methods: conventional synthesis (CT), microwaves treatment (MW) and ultrasound treatment (US). An aqueous solution containing appropriate amounts of copper and aluminum nitrates was added, whilst stirring, dropwise into one containing Na_2CO_3 and NaOH. For CT synthesis compounds, the temperature and the pH were maintained respectively at 60 °C and 9.5. The solution was dried at 60 °C during 18 h. For the second solids (MW), the gel obtained was aged on a monomode reactor Synthewave Prolabo 402 (300 W) equipped with infrared pyrometer control and stirring mechanically, at 60°C for 1 h. For the third material (US), the gel obtained was aged on ultrasound irradiation Branson sonifier 450 (20 kHz). This procedure was carried out at atmospheric pressure and at 80°C. The three precipitates were filtered, washed to eliminate the alkali metals and the nitrate ions until the pH 7, and a dried at 60°C for 48 h. The calcination treatment was performed under air (4L h^{-1}; 2°C.min^{-1}; 4 hours at 500°C). The materials are characterized by XRD, XPS, N_2 sorption, H_2-TPR.

The toluene and CO mixture oxidation reactions were conducted at atmospheric pressure in a micro reactor containing 100 mg of catalyst. Catalytic tests were made using a gas mixture containing of 1000 ppm C_7H_8 and/or 1000ppm CO and 20% O_2 in He. The feed gases were analyzed by an Agilent 490 Micro gas chromatography and ADEV 4400 IR CO- CO_2 analyzer

Results and Discussion

A beneficial effect of a MW and US method was observed on the preparation of mixed oxides. The characterization of these solids revealed several textural and physicochemical differences (specific surface areas, crystallites size, reducibility, …). The use of MW or US synthesis procedure was induced a variation of Cu/Al atomic ratio on the surface and O_{ads}/O_{bulk} observed by XPS analysis. Catalytic performances for toluene oxidation in presence or absence of CO according the T_{50} values (temperature corresponding to 50% of toluene conversion) show an increase of activity for the solid prepared by US and MWs (Figure1 a). Relations between physicochemical properties and catalytic activity have been established (Figure1b), indicating a Mars Van Krevelen mechanism for toluene total oxidation in presence of CO in the reactional mixture.

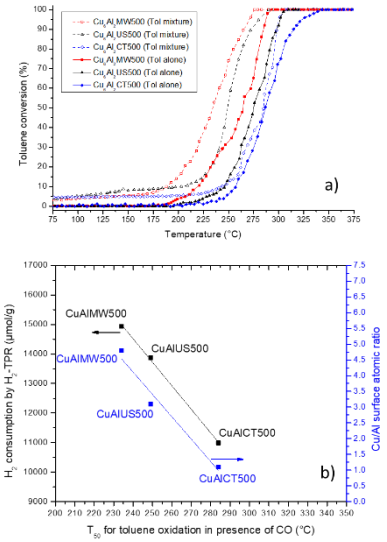

Figure 1 a) Conversion vs. temperature of toluene in presence or absence of CO
b) relation between physicochemical characteristics and T_{50}

Significance

This work proves that it is possible to produce highly efficient catalysts issued from LDH precursors with low synthesis duration. Catalytic performance challenges the expensive noble metal-based systems for this this type of application. Moreover, the complexification of reaction mixture enhances the total oxidation of toluene indicating potential applications of this type of materials for the depollution of fumes issued from biomass combustion.

References

1. T. Barakat, J.C. Rooke, E. Genty, R. Cousin, S. Siffert, B.-L. Su, **2013,** *Energy Environ. Sci.* 6 371.
2. C. Gennequin, M. Lamallem, R. Cousin, S. Siffert, F. Aïssi, A. Aboukaïs, **2007**, *Catal Today* 122
3. E. Genty, R. Cousin, S. Capelle, C. Gennequin, S. Siffert, **2012** , *Eur. J. Inorg. Chem*. 2802.
4. F. Kovanda, T. Rojka, J. Dobešová, V. Machovič, P. Bezdička, L. Obalová, K. Jirátová, T. Grygar, **2006** *J. Solid State Chem* 179 812.
5. M. Climent, A. Corma, S. Iborra, K. Epping, A. Velty, **2004** *J Catal* 225 316.
6. P. Benito, F.M. Labajos, V. Rives, **2009** *Pure Appl. Chem* 81 1459.
7. O.R. Neto, N.F.P. Ribeiro, C.A.C. Perez, M. Schmal, M.M.V.M. Souza, 2010, *Appl. Clay Sci.* 48 542.

Electrochemistry Unlocks New Possibilities in Difluoromethylation of Alkenes

Hyunwoo Kim[1]*

[1]*Department of Chemistry, Pohang University of Science and Technology, 37673 Pohang, South Korea*

*khw7373@postech.ac.kr

Introduction

The difluoromethyl group (CF_2H) serves as an essential bioisostere in drug discovery campaigns according to Lipinski's Rule of 5 due to its advantageous combination of lipophilicity and hydrogen bonding ability, thereby improving the ADME properties. However, despite the high prevalence and importance of vicinal hydrogen bond donors in pharmaceutical agents, a general synthetic method for doubly difluoromethylated compounds in the vicinal position is absent. Here we describe a copper-electrocatalyzed strategy that enables the vicinal bis(difluoromethylation) of alkenes. By leveraging electrochemistry to oxidize $Zn(CF_2H)_2(DMPU)_2$–a conventionally utilized anionic transmetalating source–we paved a way to utilize it as a CF_2H radical source to deliver the CF_2H group in the terminal position of alkenes. Mechanistic studies revealed that the interception of the resultant secondary radical by a copper catalyst and followed reductive elimination is facilitated by invoking Cu(III) intermediate, enabling the second installation of CF_2H group in the internal position. The utility of this electrocatalytic 1,2-bis(difluoromethylation) strategy has been highlighted through the late-stage bioisosteric replacement of pharmaceutical agents such as Sotalol and Dipivefrine.

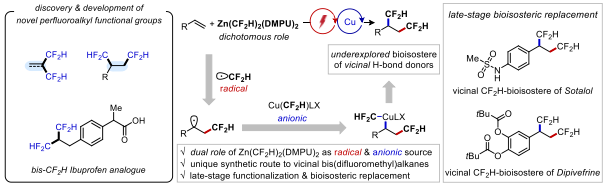

Figure 1. Electrocatalytic Bis(difluoromethylation).

Materials and Methods

An oven-dried, 10 mL two-neck glass tube was equipped with a magnetic stir bar, a rubber septum, a threaded Teflon cap fitted with electrical feed-throughs, a carbon felt anode (1.0 *0.5 cm^2) (connected to the electrical feedthrough via a 9 cm in length, 2 mm in diameter graphite rod), and a platinum plate cathode (1 x 0.5 x 0.02 cm^3). In a nitrogen-filled glove-box, $Cu(OTf)_2$ (0.02 mmol, 10 mol%) and L_1 (0.02 mmol, 10 mol%) were added, followed by the sequential addition via syringe of degassed DMSO (4.0 mL) and 2 (185.7 mg, 0.44 mmol, 2.2 equiv). After stirring 5 -10 minutes of the reaction vessel, $LiClO_4$ (85.1 mg, 0.8 mmol) and alkene substrate (0.2 mmol, 1.0 equiv) was added. The cell was sealed and removed from the glove-box. Then, a nitrogen-filled balloon was adapted through the septum to sustain a nitrogen atmosphere. Electrolysis was initiated at a constant current of 2.0 mA at r.t. for 12 h. The mixture was then diluted with DCM (30 mL) and then washed with water, brine, dried over anhydrous $MgSO_4$, and concentrated under reduced pressure. The residue was subjected to flash column chromatography on silica gel (eluted with hexanes/ethyl acetate) to yield the desired product.

Results and Discussion

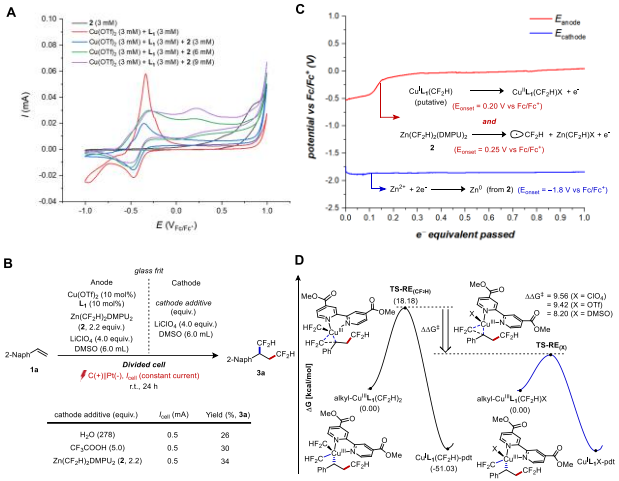

Figure 2. A. CV of reaction components. An increase in current at the second irreversible oxidation at 0.20 V vs Fc/Fc^+ upon the addition of more 2 suggest the formation of putative Cu(II)–CF_2H complex via transmetalation. B. Divided cell experiments. C. The voltaic profile of each electrode. It is conceivable for multiple oxidation events to occur simultaneously, involving the conversion of 2 to CF_2H radical (E_{onset} = 0.25 V vs Fc/Fc^+) and the putative L_1–Cu(I) –CF_2H complex to its Cu(II) analogue (E_{onset} = 0.20 V vs Fc/Fc^+). D. Computed relative free energies of reductive elimination step for different Cu(III) intermediates. Energy values are given in kcal·mol^{-1}. All data were computed at SMD (DMSO)-B3lyp-d3/SDD+6-311++G//B3lyp-d3/Lanl2dz+6-31G** level of theory (ΔG in kcal/mol). The reductive elimination from [alkyl–$Cu^{III}L_1(CF_2H)X$] proceeded with significantly lower activation energy compared to that from [alkyl–$Cu^{III}L_1(CF_2H)_2$] [$\Delta\Delta G^{\ddagger}$ {$TS\text{-}RE_{(CF2H)}$ and $TS\text{-}RE_{(X)}$} = 9.56, 9.42 and 8.20 kcal·mol^{-1} for X = ClO_4, OTf and DMSO respectively].**

Significance

We anticipate that this mechanistically distinct synthetic pro-tocol will widen the accessibility to a diverse array of vicinal bis(difluoromethylated) chemical entities, thereby facilitating the potential expansion of drug candidate libraries.

References

1. S. Kim, H. Kim, *J. Am. Chem. Soc.* **2024**, *146,* 22498–22508.
2. S. Kim, K. H. Hwang, H. K. Park, J. Kwak, H. Lee, H. Kim, *Commun. Chem.* **2022**, *5*, 96.
3. J. B. I. Sap, C. F. Meyer, N. J. W. Straathof, N. Iwumene, C. W. Am Ende, A. A. Trabanco, V. Gouverneur, *Chem. Soc. Rev.* **2021**, *50*, 8214-8247.

Catalytic activity of $MoO_x@SiO_2$ yolk-shell structures in propane dehydrogenation and subsequent propylene metathesis

Anna Rokicińska[1], Mariya Myradova[2], Mateusz Mandrela[1], Dominika Waśniowska[1], Marek Dębosz[1], Piotr Michorczyk[2], Piotr Kuśtrowski[1]*
[1]*Faculty of Chemistry, Jagiellonian University, Gronostajowa 2, 30-387 Krakow, Poland*
[2]*Department of Organic Chemistry and Technology, Cracow University of Technology, Warszawska 24, 31-155 Krakow, Poland*
*piotr.kustrowski@uj.edu.pl

Introduction

Olefin metathesis, a reaction involving the cleavage and reassembly of C=C double bonds, plays an essential role in the chemical industry. Particularly when combined with preliminary dehydrogenation of alkanes, this reaction provides an effective way to creating targeted, valuable unsaturated hydrocarbons from readily available raw materials. Typically, the industrial metathesis process is carried out in the presence of a WO_x/SiO_2 catalyst at relatively high temperatures (~350–450 °C). On the other hand, MoO_x-based materials, active at moderate temperatures (25–200 °C), are considered as promising alternatives to the commercial system.[1,2] In the presented work, core-shell structures, built from MoO_x nanoparticles deposited inside or onto $@SiO_2$ mesoporous shells, were synthesized. The introduction of active phase particles into the core-shell structure allows to improve their dispersion as well as to protect against aggregation while maintaining the structural integrity of the composite material.

Materials and Methods

Spherical polystyrene (PS) particles with uniform diameters in the range of 160–200 nm were coated with a SiO_2 precursor layer using a modified Stöber strategy. The formed silica support was subsequently modified with MoO_x (1-20 wt.% of Mo) using two various approaches. In the first one (path A) the active phase precursor was introduced into the $PS@SiO_2$ composite using wet impregnation and equilibrium-controlled adsorption followed by calcination at an oxidizing atmosphere. Alternatively, the same techniques were used for the modification of the calcined $@SiO_2$ support previously released from the polymer core (path B). The obtained MoO_x-containing yolk-shell materials were characterized in terms of morphology (SEM-EDS, STEM), chemical composition (XRF), structure (XRD), textural parameters (N_2 adsorption), surface composition (XPS), reducibility (H_2-TPR), as well as tested as catalysts in the propane dehydrogenation coupled with subsequent metathesis of formed propylene.

Results and Discussion

The synthesized spherical $PS@SiO_2$ particles exhibited a smooth surface and a high degree of monodispersity, retaining its morphological features even after removal of the polymer scaffold. Additionally, appropriate coating conditions and an addition of surfactant during deposition led to the generation of mesoporosity in the silica shell. The specific surface area of the unmodified SiO_2 material achieved 660 m^2/g after the elimination of the PS core. Such a high surface area and expanded mesoporosity opened up the possibility of generating various forms of the MoO_x active phase. The systems with MoO_x nanoparticles enclosed within the structure of the SiO_2 shell and deposited on its external surface were produced. On the other hand, the materials characterized by the intended yolk-shell structure with MoO_x nanoparticles introduced into the interior of $@SiO_2$ were also created. The expected amounts of MoO_x phase incorporated into the structure of spherical $@SiO_2$ supports were confirmed. The catalysts synthesized via path A exhibited lower crystallinity of the active phase and a higher specific surface area compared to those of path B. Example STEM images of the produced materials are shown in Figure 1.

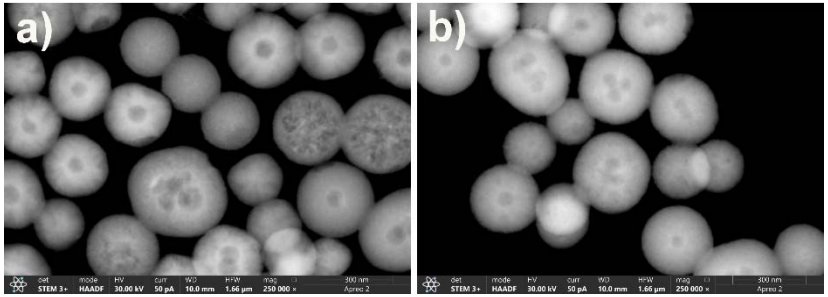

Figure 1. STEM images of (a) $@SiO_2$_A_Mo10 and (b) $@SiO_2$_B_Mo10 catalysts.

It was observed that the reaction rate increased with raising Mo content. For both series, the best catalytic performance was achieved over the samples containing 10 wt.% of Mo. Slight decreases in the conversion of propane (in the dehydrogenation step) and propylene (in the metathesis step) were found for the samples with the higher MoO_x loading. Generally, the materials prepared through path A exhibited higher catalytic activity in the dehydrogenation of propane, whereas the catalysts synthesized via path B demonstrated superior propylene conversions and greater stability over time during the metathesis step when compared to those synthesized via path A. The explanation of these effects related to the distribution of MoO_x particles on the surface of SiO_2 was discussed.

Significance

The work shows the possibility of very effective integration of the propane dehydrogenation with metathesis of its main product carried out in the presence of $MoO_x@SiO_2$ catalysts with a yolk-shell structure, which opens the prospect of using such a technology on an industrial scale.

Acknowledgment

We thank the National Science Centre of Poland for financial support in the implementation of research (grant no. 2022/45/B/ST8/01798).

References

1. M. Myradova, A. Węgrzynowicz, A. Węgrzyniak, M. Gierada, P. Jodłowski, J. Łojewska, J. Handzlik, P. Michorczyk, *Catal. Sci. Technol.* **2022**, *12,* 2134-2145
2. P. Michorczyk, A. Węgrzyniak, A. Węgrzynowicz, J. Handzlik, *ACS Catal.* **2019**, *9*, 11461–11467

Methane Pyrolysis into Hydrogen and Carbon material: A comparative study between Microwave vs. Conventional heating methods

Valentin L'hospital[1,*], Leandro Goulart de Araujo[1], Emmanuel Landrivon[1], Ariel Mello[2], Marilena Radoiu[2], Yves Schuurman[1], Nolven Guilhaume[1], David Farrusseng[1]

[1] *IRCELYON, CNRS-Université de Lyon, 69626 Villeurbanne, France*
[2] *Microwave Technologies Consulting, 69100 Villeurbanne, France*
*valentin.lhospital@ircelyon.univ-lyon1.fr

Introduction

Methane pyrolysis is emerging as a promising method for producing hydrogen while generating valuable solid carbon, offering a CO_2-free alternative to traditional steam methane reforming. This process involves the thermal cracking of CH_4 into H_2 and solid carbon, which could be valorized in different applications. Whereas thermal cracking (without a catalyst) requires temperatures exceeding 1200°C, catalytic processes allow to reduce the process temperatures down to 600-800°C, particularly on metal-based catalysts such as Ni or Fe[1].

However, rapid catalyst deactivation and heat transport limitations strongly penalize the efficiency and economics of catalytic pyrolysis. Whereas mechanism may differ, deactivation by coking occurs on all type of metal-based catalysts. Also, CH_4 pyrolysis is a highly endothermic reaction. As a consequence, reaction rates are usually controlled by heat transfer and very high CH_4 conversion levels are hardly achieved.

This work deals with the design and study of CH_4 and biogas pyrolysis in a fluidized-bed reactor using an iron-based catalyst heated by microwave (MW).[2,3] The combination of bed fluidization and direct catalyst heating by MW irradiation allows reaching full CH_4 conversion at high temperatures. Surprisingly, we can observe a significant apparent activation process on time on stream (TOS) in opposite to usual catalytic deactivation process.

Materials and Methods

The fluidized catalytic bed consists of a quartz tube filled with specific iron-carbon composite catalyst powder of 100-150 µm diameter. The MW heating device consists of a 1.3 kW solid state generator operating at 915 MHz (Leanfa, Italy) and a standard WR975 waveguide and monomode cavity (Muegge, Germany). The reaction temperature is controlled by a pyrometer while an IR camera monitors both the fluidization and the temperature of the different zones of the reactor.

Results and Discussion

The IR camera clearly shows that the fluidization enables the establishment of a homogenous temperature throughout the catalyst bed heated by MW. We carried out a comparative study using the same reactor size and catalyst amount, by varying the temperature from 750 up to 950°C and then down to 750°C, but one heated by a conventional electrical furnace and the other by MW. In the two reactions, CH_4 conversions increase with the temperature and follow similar trends (*Fig 1.*). For MW heating, the CH_4 conversion reaches thermodynamic equilibrium at 950°C. CH_4 is converted to pure H_2 and solid carbon without traces of C2 and C3 fractions. The produced carbon is deposited on the surface of the fluidized iron grain. Characterization of the carbon shell by XRD and Raman indicates a graphitic-type structure with a surface area of 10 $m^2 g^{-1}$. The carbon production rate is 4.6 g h^{-1}. Consequently, the bed volume builds up with time of stream (TOS).

For the two heating methods, we can observe that methane conversion increases with TOS over the 30 min of stabilized temperature. However, after 4 hours on TOS, CH_4 conversion has more than doubled, for example at 750°C (MW), 20% against 47%. We can attribute this apparent-activated process to the continuous increase of the bed volume and thus to the residence time, assuming that the deposited carbon plays the role of catalyst. Indeed, the residence time increases from about 2 sec to 6 sec. A power law kinetic model using the order of 0.6 estimated by Cherbański et al.[4] supports our hypothesis of catalyst built-up.

The apparent superior catalytic performances of MW heating and scalability issues of MW reactor heating will be discussed.

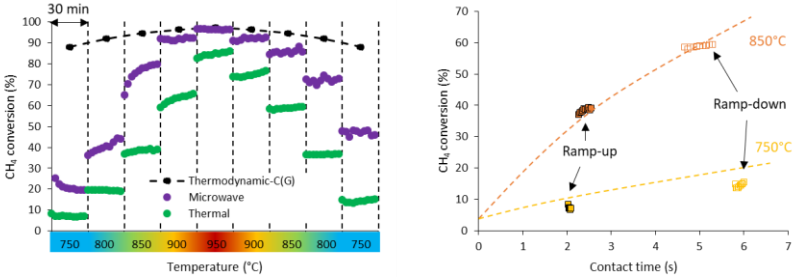

Figure 1 : CH_4 conversion (%) from 750 to 950°C (30 min for each temperature) by conventional and microwave heating (Left), impact of the contact time on methane conversion during CH_4 pyrolysis at 750 and 850°C.

Significance

Catalytic methane pyrolysis in a fluidized bed can achieve very high methane conversion (>90%) into hydrogen and solid carbon. Higher activity has been demonstrated in a MW-heated reactor. Equally important, the output stream is a mixture of H_2 and CO in a ratio of 2:1, an ideal ratio for Fisher-Tropsch synthesis if biogas (CH_4:CO_2 2:1) are used. This work opens up the prospect of converting biogas into liquid hydrocarbons in two catalytic steps without any gas separation

References

1. J. Prabowo *et al. Carbon,* **2024,** *216*, 118507.
2. V. L'hospital *et al. New J. Chem.,* **2024**, *48*, 9656–9662.
3. V. L'Hospital *et al*. Catal. Today, **2025**, *submitted.*
4. R. Cherbański *et al. Chem. Eng. Process. - Process Intensif.* **2024**, *203*, 109878.

We thank the European Union for supporting TITAN program under GA N° 101069474. Views and opinions expressed are however those of the authors only and do not necessarily reflect those of the EU. Neither the EU nor the granting authority can be held responsible for them.

Innovative approach for highly contaminated PET recycling

Micaela Lorenzi[1], Lidia Castoldi[2]*
[1]*Greenchemicals S.R.L.*
[2]*Politecnico di Milano, Department of Energy, LCCP group, via La Masa 34, 20156 Milano, Italy*
*lidia.castoldi@polimi.it

Introduction

Plastic recycling is a critical process in managing one of the world's most abundant waste streams. With global plastic production reaching hundreds of millions of tons annually, recycling offers a way to reduce environmental impact, conserve resources, and curb pollution. Plastics are durable and versatile, making them indispensable in various industries but also challenging to dispose of sustainably[1,2].

Recycling plastic involves different approaches[3], each with unique benefits and limitations. Mechanical recycling, the most common method, reprocesses plastic waste through melting and re-extruding, making it a relatively low-cost and continuous solution, though it cannot handle all types of plastic contamination. Chemical recycling, on the other hand, breaks plastics down into their molecular components, allowing even heavily contaminated or complex plastics to be recycled. However, this process is more costly and energy-intensive, limiting its current application[4].

Emerging hybrid methods, such as chemical-mechanical recycling, combine the best of both approaches, offering a more adaptable and efficient system for a broader range of plastic types. This work explores the possibility of applying an innovative hybrid chemical-mechanical recycling to waste PET.

Materials and Methods

The chemical-mechanical innovative approach for plastic recycling combines chemical and mechanical methods by enabling partial chemical depolymerization during extrusion, which makes it a continuous process. While it cannot manage the full variety of plastic waste that chemical recycling can, it is compatible with a wider range of materials than pure mechanical recycling, at comparable costs.

The raw material is represented by highly contaminated PET, impossible to treat in a chemical process. Firstly, a cleaning step (i.e. metal removal) is necessary to achieve the desired quality in the final polyester polyol. Then, the waste is extruded in a continuous process under pressure during which volatiles are eliminated, and the melted PET is mixed with depolymerization reagents and catalyst. This method permits to raise processing temperatures and shorten reaction times. Additional cleaning steps can be integrated at the end.

Results and Discussion

The process described so far is represented in the scheme of Figure 1. At the end of the process, it is possible to obtain a polyester polyol with different molecular weights and viscosity. In particular, the molecular weight ranges from 250 to 3000 u.m.a; the presence of BHET (i.e. Bis (2- hydroxyethyl) terephthalate, formed during PET glycolysis) is estimated in the range of 2 - 15 units. The viscosity is in the range of 10÷2000 cps, so from liquid like water to viscous liquid, but always easy to pump and transport.

Color depends on starting PET and can be decolored in a downstream section.

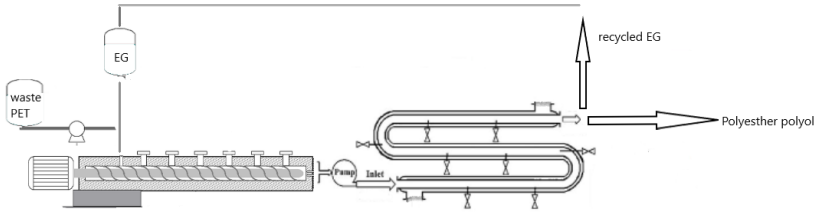

Figure 1. Scheme of the hybrid chemical-mechanical recycling of waste PET

Significance

The industrial and fundamental significance of advancements in plastic recycling lies in their potential to transform waste management and resource conservation on a global scale. Industrially, improved recycling methods reduce the demand for virgin plastic, lower production costs, and enable industries to meet stricter environmental regulations. Hybrid recycling methods, for instance, allow more complex or contaminated plastics to be reused, making recycling feasible for a wider range of materials.

Fundamentally, this work contributes to sustainability by advancing a circular economy model, where materials are continuously repurposed rather than disposed of. By closing the loop on plastic usage, these methods help mitigate pollution, reduce greenhouse gas emissions, and conserve finite resources, offering a pathway toward more responsible production and consumption practices worldwide.

References

1. K.P. Gopinath, V.M. Nagarajan, A. Krishnan, R. Malolan, *Journal of Cleaner Production*, **2020**, *274*, 123031
2. S. Chen, Y.H. Hu, *Chemical Engineering Journal*, **2024**, *493*, 152727
3. K. Ragaert, L. Delva, K. Van Geem, *Waste Management*, **2017**, *69*, 24
4. H. Jeswani, C. Krüger, M. Russ, M. Horlacher, F. Antony, S. Hann, A. Azapagic, *Science of The Total Environment*, **2021**, *769*, 144483

Plasma-catalytic hybrid process for CO_2 valorization into liquid fuels

Noelia Merino[1,3], Stéphanie Ognier[1]*, Xavier Duten[2], Maria Mikhail[3], Michael Tatoulian[1]
[1]*Institut de Recherche de Chimie Paris, UMR 8247 (CNRS – Chimie ParisTech), Équipe 2PM, 75005 Paris, France*
[2]*LSPM – CNRS UPR 3407 – Université Sorbonne Paris Nord, 93430 Villetaneuse, France*
[3]*ENERGO, 59120 Loos – Lille, France*
* stephanie.ognier@chimieparistech.psl.eu (corresponding author)

Abstract

Greenhouse gases such as CO_2 and CH_4 contribute significantly to climate change. Efforts are being made to reduce their emissions as well as to convert them into value-added products. As current thermal-catalysis processes used for the valorization of CO_2 require high temperatures and pressures, research is conducted to find a more direct approach to convert CO_2 and CH_4 into value-added liquid products under mild conditions. Non-thermal plasmas offer a promising alternative, as they carry highly energetic species that can cause excitation, ionization or even dissociation of gas molecules, while remaining at atmospheric pressure and relatively low temperatures. Adding the use of a catalyst enables to tune the selectivity of the reaction and to benefit from the synergy between plasma and catalysis. From an industrial standpoint, a plasma-catalysis process would be very valuable, as it would lower the energy demands for the valorization of CO_2 and CH_4.

Several studies have already been conducted with plasma-catalysis for the conversion of CO_2 and CH_4 into liquid products, most frequently using a dielectric barrier discharge (DBD) reactor[1,2,3,4]. They show promising results, with conversions up to 38% for CO_2 and 50% for CH_4 and a selectivity in liquid products, primary alcohols, ketones and carboxylic acids, up to 40%[1].

In this study, the experimental set-up consists in a dielectric barrier discharge (DBD) reactor inside which the catalyst is placed. The catalysts used are metal-oxide-based catalysts loaded on alumina-based supports. The reactor's external temperature is regulated by an oil circulation thermostat. At the reactor outlet, all products are heated through a transfer line at 180°C and analyzed on-line by GC-FID (gas chromatography with a flame ionization detector). Liquid products are then condensed using an ice bath, allowing light gaseous products to be analyzed on-line with a Micro GC. The catalysts are characterized by different techniques such as X-ray diffraction (XRD), scanning electron microscopy (SEM), hydrogen temperature-programmed reduction (H_2-TPR), CO_2 temperature-programmed desorption (CO_2-TPD), thermogravimetric analysis (TGA) and Fourier-transform infrared spectroscopy (FTIR). These characterization techniques provide insight into the catalyst properties and help understand its role in the plasma-catalytic process.

This work explores how CO_2 and CH_4 conversion and the selectivity in liquid products are influenced by experimental parameters such as temperature, electric power, frequency, ratio CO_2/CH_4 and gas hourly space velocity (GHSV) and by electric and physico-chemical properties of the catalyst. This will enable to find the optimal conditions to have the highest conversions and selectivity in liquid products and to identify the synergy between the plasma and the catalyst, thus laying the foundations for future industrial applications for the sustainable recovery of CO_2 and CH_4.

References

1. Li, D., Rohani, V., Fabry, F., Ramaswamy, A. P., Sennour, M., & Fulcheri, L. (2020). *Direct conversion of CO2 and CH4 into liquid chemicals by plasma-catalysis.* Applied Catalysis B: Environmental (ACBEE3), 261, 118228.
2. Li, J., Dou, L., Gao, Y., Hei, X., Yu, F., & Shao, T. (2021). Revealing the active sites of the structured Ni-based catalysts for one-step CO2/CH4 conversion into oxygenates by plasma-catalysis. Journal of CO2 Utilization (JCUOAJ), 52, 101675.
3. Dou, L., Liu, Y., Gao, Y., Li, J., Hu, X., Zhang, S., ... & Shao, T. (2022). Disentangling metallic cobalt sites and oxygen vacancy effects in synergistic plasma-catalytic CO2/CH4 conversion into oxygenates. Applied Catalysis B: Environmental (ACBEE3), 318, 121830.
4. Wang, Y., Fan, L., Xu, H., Du, X., Xiao, H., Qian, J., ... & Wang, L. (2022*). Insight into the synthesis of alcohols and acids in plasma-driven conversion of CO2 and CH4 over copper-based catalysts.* Applied Catalysis B: Environmental (ACBEE3), 315, 121583.

Shaping of Ni-Co catalyst for up-scale biogas dry reforming

Mahdi M.A.[1], Muriel C. [1], Lucette T. [1], Maya M. [2], Sébastien R. [1,3], Edmond A.B[1], Carmen C.[1], Cédric G.[1]*

[1] *Université du Littoral Côte d'Opale, UCEIV, 59140 Dunkerque, France*

[2]*Université de Lille, Institut Michel-Eugène Chevreul (IMEC), 59000 Lille, France*

[3]*Université de Lille, Unité de Catalyse et de Chimie du Solide (UCCS), 59000 Lille, France*

*cedric.gennequin@univ-littoral.fr

Introduction

Interest in carbon-free renewable energies has grown, as they offer solutions to the depletion of fossil fuel resources and the reduction of greenhouse gases. Biogas is considered a sustainable, renewable gaseous fuel, obtained by the inorganic methanization of organic waste[1]. Biogas is mainly composed of CO_2 and CH_4, and contains other impurities such as H_2S, N_2, VOCs, O_2, H_2O, etc. After purification, biogas can be used in a wide range of processes where CH_4 and/or CO_2 are converted to various fuels. Dry reforming process (DRM) ($CH_4 + CO_2 \rightarrow 2H_2 + 2CO$) is used to convert biogas into green H_2 or syngas (a mixture of H_2 and CO). The high bonding energies of the CH_4 and CO_2 molecules and the endothermic nature of the reaction require high temperatures (> 650 °C). This makes the reaction difficult to be highly challenging at an industrial scale. For this reason, catalytic materials are developed to increase the kinetics of the DRM at lower temperatures. Nickel-based catalysts have been used in the reaction, and can be promoted by other metals and/or various oxides, in order to resolve catalyst deactivation by carbon formation, sintering and poisoning[2]. In this study, we evaluate the influence of the Ni-Co mixed oxide ratio during DRM reaction. The catalyst with the best catalytic performance is synthesized in high quantities (100 g) and shaped (extruded) before being evaluated in large scale DRM setup.

Materials and Methods

In this study, mixed oxide catalysts are prepared by using co-precipitation method to synthesize layered double hydroxide (LDH) like materials ($Ni_xCo_{3-x}Mg_3Al_2$). Synthesis details are described elsewhere[2]. The Ni:Co ratio is (x = 0, 0.5, 1.5, 2.5, 3). After the precipitation process, LDH powder is calcined under air at 800 °C for 4h, then reduced in H_2 (10 vol.%) at 800 °C for 1h to obtain the metallic phases. Extrudates for 2.5Ni-0.5Co catalyst are prepared using a single-screw extruder (Caleva, Multi lab), then tested during DRM. Physico-chemical characterizations were performed on the dried, calcined, reduced and spent materials by XRD, N_2-physisorption, H_2-TPR, S/TEM-HAADF-EDSX, TGA.

Catalytic test and operating conditions

Catalytic DRM performances are evaluated in lab and pilot setup.

Lab-scale: DRM was carried out at 750 °C for 12 h with $CH_4/CO_2/Ar$=20/20/60 at a flow rate of 100 mL.min^{-1} and a GHSV of 30,000 mL.g_{cat}^{-1}.h^{-1}. Gas composition was analyzed via gas chromatography (Varian 3800). For DRM stability study the stream was maintained for 80 h.

Up-scale: Calcined 3 mm extruded of 2.5Ni-0.5Co (300 mg) was mixed with quartz spheres to ensure equal length of the fixed catalyst bed. DRM was performed on a pilot scale (reactor diameter of 10 mm) at 750 °C for 200 h with $CH_4/CO_2/Ar$=60/60/180 at 300 mL.min^{-1}, corresponding to a GHSV of 9000 mL.g_{cat}^{-1}.h^{-1}. Gas composition was analyzed using gas chromatography coupled to a mass spectrometer.

Results and Discussion

For dried powders, pure LDH structure is observed. After calcination, a mixture of single and mixed oxides and spinels are identified by XRD. Moreover, S_{BET} decreased from 167 to 76 m^2.g^{-1} with increasing Co content. S/TEM-HAADF shows a highly dispersed NPs (7-13 nm), and 800 °C is sufficient to obtain the Ni and Co metallic phases, which is in agreement with the TPR-H_2 reduction profiles. EDXS clearly shows a bimetallic formulation of NPs for 2.5Ni-0.5Co (figure 1-a). When shaped, LDH and mixed oxide phases are detected retaining the same structure obtained for the powder. Extruded 2.5Ni-0.5Co show an increase in S_{BET} from 162 to 223 m^2.g^{-1}, which relates to the extrusion phase which lead the increase in specific surface area.

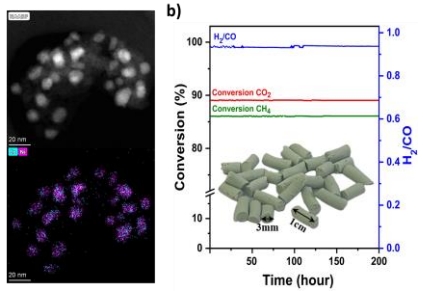

Figure 1. a) S/TEM-HAADF-EDXS (blue-Co, pink-Ni) for 2.5Ni-0.5Co R, b) Stability test using 3 mm extruded 2.5Ni-0.5Co for 200 h

Catalysts exhibited high reforming activity (≥78% conv.CH_4) for 12 h DRM, but sintering and carbon deposition caused deactivation of 0Ni-3Co catalyst after 4 h. However, 2.5Ni-0.5Co catalysts (powder) shows the best performance, 86 % conv. CH_4, and limited carbon deposition (≃ 10 wt.). These results are attributed to the synergistic effect between Ni and Co. In addition, an 80-h test confirms the high thermal stability. Up-scaling test for 200 h on 2.5Ni-0.5Co extrudates reveals excellent catalytic properties, of 87 % conv. CH_4 and 89 % conv. CO_2, with, high stability compared to the powder form (figure 1-b). Post-test characterization of spent extrudates indicates a reduction of carbon deposition from 23 wt.% (powder) to 14 wt.%, which is links with the mechanical strength and porosity of the extrudates. Based on these results, 2.5Ni-0.5Co extrudates should be tested in the presence of real biogas.

Acknowledgement

Mahdi Mohamad Ali acknowledges the Université du Littoral Côte d'Opale, Région Hauts de France, Séché Group and the project TI "Territoire d'Innovation" for their financial support.

References

1. Y.Gao, *Energy Convers Manag.**2018**;133-155; doi: 10.1016/j.enconman.2018.05.083*
2. M.Chaghouri, *Int J Hydrogen Energy.**2022**;415-429. doi:10.1016/j.ijhydene.2022.08.248*

Tailoring of the properties of sepiolite clays active in isopropanol dehydration to propylene

T.H. Nguyen.[1] *, J.-L. Dubois.[2], T. Caillot.[1], A. Auroux.[1], G. Postole.[1]
[1]*Université Claude Bernard Lyon 1, CNRS, IRCELYON, UMR 5256, Villeurbanne, F-69100*
[2]*Trinseo Netherlands B.V., Innovatieweg 14, 4542 NH Hoek, The Netherlands*
*tien-hoang.nguyen@ircelyon.univ-lyon1.fr

Introduction

Sepiolite is a fibrous hydrated magnesium silicate that features a unique sheet structure. This structure comprises tetrahedral silica sheets that sandwich discontinuous octahedral magnesia sheets, creating distinctive structural tunnels. As a result, sepiolite is well-suited for various applications, especially as an adsorbent [1]. The presence of a small percentage of Al^{3+} substituting Si^{4+} or Mg^{2+} could influence the acidity of sepiolite [2]. However, its potential use in acid-catalysed reactions has not been extensively investigated. In this study, sepiolite was employed as a catalyst for the dehydration of isopropanol (IPA) to yield propylene (PEN), which is an essential raw material. This process, an alternative to conventional petrochemical routes, requires fine tuning of acid/base properties of the catalyst to selectively produce PEN while minimizing by-products. The acidity of sepiolite by varying Al mass percentages was thoroughly characterized. Notably, it was observed that the presence of Al generates the co-existence of bridging silanol (Brønsted sites) and unsaturated Al^{V} (Lewis sites) acidity. This study highlights the potential of sepiolite as catalysts for producing high PEN yields and selectivity from IPA, owing to the combined influence of its physico-chemical characteristics, thermal stability, and proper acid-base properties.

Materials and Methods

Three sepiolite catalysts, named 0.9Al-Sep, 1.6Al-Sep, 2.0Al-Sep (the numbers indicate the mass percentage of Al in the catalyst), were studied. Their chemical composition, structure, textural properties, and thermal stability were characterized by XRF, XRD, N_2 adsorption isotherm, TGA-FTIR, ^{27}Al NMR, and ^{1}H NMR techniques. The nature, quantity, and strength of the acid/base active sites were assessed using NH_3/SO_2 adsorption microcalorimetry and NH_3 adsorption FTIR. A pulsed catalytic set-up was used to investigate the catalytic performances.

Results and Discussion

The specific surface area, total porous volume, mesoporous volume and mass percentage of Al, Si, Mg in the catalysts, as well as the density of acid sites obtained from adsorption microcalorimetry are shown in **Table 1**.

Table 1. Textural properties, chemical composition, and density of acid sites of the catalysts

Sample	S_{BET} (m^2/g)	V_{porous} (cm^3/g)	V_{meso} (cm^3/g)	Al (%)	Si (%)	Mg (%)	Density (acid sites/nm^2)
0.9Al-Sep	153	0.48	0.37	**0.9**	26.1	15.3	1.7
1.6Al-Sep	120	0.42	0.34	**1.6**	25.9	14.9	2.2
2.0Al-Sep	108	0.39	0.32	**2.0**	26.3	13.9	2.8

XRD patterns indicated that at temperatures above 150°C, the catalysts lost their crystallinity due to the characteristic structural folding of sepiolite (water loss). However, the basal planar spacing remained unchanged, determined as $d_{(110)}$ = 12.1 Å (characteristic sepiolite peak at 2θ = 7.29°). Among the three samples, 0.9Al-Sep exhibited the worst thermal stability. Additionally, the loss of coordinated water at the edges of the octahedral layers (above 200°C) generated coordinatively unsaturated Al^{V} sites, as evidenced by ^{27}Al NMR (chemical shift δ = 30 ppm), which may act as Lewis acid sites. Furthermore, the substitution of Si^{4+} by Al^{3+} at the tetrahedral layers led to the formation of bridging silanol Si-O(H^+)-Al sites, contributing to the Brønsted acidity in the catalysts, as demonstrated by their ^{1}H NMR spectra (chemical shift δ = 4 ppm). The co-existence of Brønsted and Lewis acid sites was demonstrated through NH_3 adsorption FTIR, as shown in **Figure 1**.

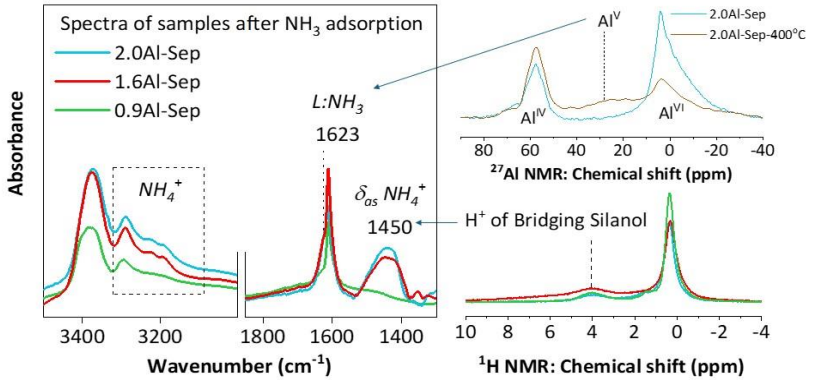

Figure 1: The presence of Brønsted and Lewis acid sites in the catalysts, as determined by NH_3 adsorption FTIR, ^{27}Al NMR and ^{1}H NMR.

Significance

High yields and selectivity for propylene were achieved due to the combined effects of specific pore distribution, thermal stability, and suitable acidity with low basicity of the sepiolite catalysts. The most acidic sample, presenting the highest amount of aluminium, exhibited the best activity. To our knowledge, this is the first study that proposes a deep characterisation of sepiolite-based materials for acid-catalysed reactions in order to define the catalyst properties required for an industrial scale application.

References

1. Tian, G.; Han, G. Sepiolite Nanomaterials: Structure, Properties and Functional Applications. In *Nanomaterials from Clay Minerals*; Elsevier, 2019; pp 135–201.
(2) De La Caillerie, J.-B. d'Espinose; Fripiat, J. J. Al Modified Sepiolite as Catalyst or Catalyst Support. *Catal. Today.* **1992**, *14* (2), 125–140.

This work is part of PYROCO2 project that has received funding from the European Union's Horizon 2020 research and innovation program under grant agreement No. 101037009.

Lab-Scale Evaluation of Functional Materials for Ammonia Production from Steel Industry Residual Gases

Santiago Palencia Ruiz[1], Liliana Lukashuk[1], H.A.J. van Dijk[2]*
[1] Johnson Matthey, Billingham, UK
[2] TNO, Petten, the Netherlands
** santiago.palenciaruiz@matthey.com*

Introduction

To reach EU climate targets, the steel and iron producing sectors are looking to decrease their CO_2 emissions by up to 90% by 2050. The residual carbon-rich gases from the steel-making process, such as basic oxygen furnace gas (BOFG, up to 68% CO), are considered a valuable feedstock for the chemical sector.[1] The INITIATE project focuses on the demonstration, at technology readiness level 7, of all the steps required to valorise this feedstock (Figure 1).[2] The demonstration includes the continuous production of $N_2 + H_2$ and CO_2 streams (i.e., a feedstock for the ammonia and urea industries), which would achieve a decrease of the primary energy use, the raw materials demand, and the direct CO_2 emissions. The pilot plant is currently being constructed at the partner SWERIM's site in Luleå, Sweden. The pilot plant will take BOFG from the adjacent SSAB steel plant and tune it into the H_2/N_2 ratio of the intermediate product and produce NH_3 (1.4 t/d NH_3).

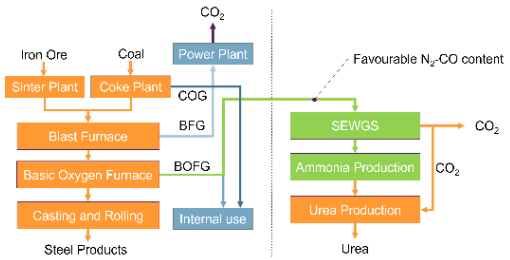

Figure 1. Schematic representation of the INITIATE industrial symbiosis.

Materials and Methods

One of the key aspects was the identification and quantification of the contaminants present in the BOFG stream, as it impacts the functional materials choice and the pilot plant lay-out.[1] In parallel to a literature review, extensive contaminants measurement campaigns were performed at SSAB steel plant for the BOFG stream. A detailed overview of the expected type and level of contaminants was conducted, facilitating the definition of the pilot plant clean-up section upstream the ammonia loop.

Based on the contaminants measurement campaigns results, the selected functional materials (i.e., water gas shift (WGS) catalyst to produce hydrogen from BOFG; materials for the removal of sulphur species and CO_x species to purify the hydrogen stream for ammonia production) were studied at lab-scale under simulated pilot plant conditions before their deployment in the pilot plant to determine the materials' operating envelopes. The lab-scale evaluation (pellets and sieve fractions) was carried out in fixed-bed reactors. The research was complemented by the materials characterization (e.g., by X-ray spectroscopy, Electron Probe Microanalysis, and X-ray diffraction) before and after tests to understand the impact of the operating conditions on the materials properties.

Results and Discussion

In this presentation, an overview of the INITIATE technology flowsheet will be discussed together with all the steps taken for the evaluation of the suitability of the functional materials (Figure 2).

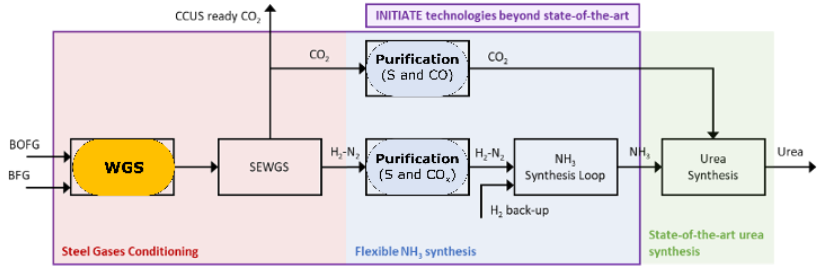

Figure 2. Block diagram of the INITIATE process technology for converting residual steel making industry gases to urea.

Lab-scale evaluation of the selected functional materials (i.e., WGS and purification materials) was conducted comparing their performance in varying impurities-containing feedstocks under different operating conditions. Results of the tests and samples' characterisation highlight the impact of the process gas composition onto the performance and physicochemical properties of the functional materials under the different evaluated operating conditions. The outcomes of the lab-scale evaluation demonstrate the suitability of the selected functional materials for the pilot plant operation and serve as a baseline to define testing programmes for the pilot plant testing.

Significance

The work carried out in this project, at technology readiness level 7, is a demonstration of the symbiosis between the chemical sector and the steel making industry. The anticipated outcomes from this symbiosis will be a reduction of the CO_2 emissions by 90% in the steel industry and up to 30% decrease in the energy consumption and the raw material used in the urea production sector.

Acknowledgments

This work is part of the INITIATE project that has received funding from the European Union's Horizon 2020 research and innovation programme under grant agreement N°958318.

References

1. de Kleijne, K., et al., Applied Energy. **2020**. 270.
2. https://www.initiate-project.eu/

Anode catalytic materials for the oxidative coupling of methane (OCM)

Morvan Guillon[1*], Ksenia Parkhomenko[1], Anne-Cécile Roger[1]
[1]ICPEES, University of Strasbourg, 67087 Strasbourg, France
parkhomenko@unistra.fr

Introduction

Power-to-methane processes, based on the use of electricity surpluses generated by green energies, aim to provide a sustainable production of methane (Eq. 1).

$4H_2 + CO_2 = CH_4 + 2H_2O$ (Eq.1)

$CH_4 + O^{2-}_{surface} \rightarrow C_2H_4 + C_2H_6 + H_2O$ (Eq. 2)

In this work, this sustainable methane is proposed to be admitted to the anode of a high-temperature electrolyser (HTE) where oxygen ions are generated as by-products of water electrolysis at the cathode to lead to the formation of ethylene and ethane through the reaction of oxidative coupling of methane (OCM) (Eq. 2). Such reaction might happen if the anode material exhibits mixed electro-ionic conductivity in order to act as a high-performance anode but also if it presents a good catalytic activity for OCM.

The choice of a catalytic anode has been directed on ceria-yttria-based materials. The work will present the study of ceria-yttria oxides of various compositions to establish a link between composition and activity in OCM/selectivity to C2. The effect of doping by alkaline earth metals will also be discussed. Eventually, with the final objective of being used as catalytic anode in a HTE device, the optimization of the reaction conditions on the ethylene yield was carried out: CH_4:O_2 ratio, GHSV, time of stream (TOS) and temperature.

Materials and Methods

Syntheses are carried out via the propionate route using metal acetates as starting salts. The prepared materials were fully characterized using XRD, N_2 adsorption-desorption, XPS, Raman, SEM, oxygen storage capacity, TPR and other techniques. The catalytic tests required methane (99.5%, Linde), oxygen (99.9%, Linde) and nitrogen (99.9%, Linde), the later acted as an internal standard for the gas chromatographic analyses (Micro GC M200H).

Results and Discussion

The catalytic results obtained over the different ceria-yttria catalysts (CeO_2/$Ce_{1.5}Y_{0.5}O_{2.85}$/ $Ce_1Y_1O_{3.5}$/$Ce_{0.5}Y_{1.5}O_{3.25}$/Y_2O_3) are shown in Figure 1. Among the series, Y_2O_3 showed the highest C_2 yield (8.9 %) and the highest ethylene/ethane ratio in the products. The addition of ceria tends to decrease both C_2 yield and ethylene/ethane ratio. A significant difference is observed for the activities of compounds with highest ceria contents (CeO_2 and $Ce_{1.5}Y_{0.5}O_{2.85}$). By calculating the lattice parameters of the mixed oxides synthesized, it was shown that Vegard's law was verified, accounting for the formation of solid solutions, for which improved oxygen mobility is expected and therefore that cerium was not totally detrimental to obtain a good catalytic activity when inserted in suitable proportions.

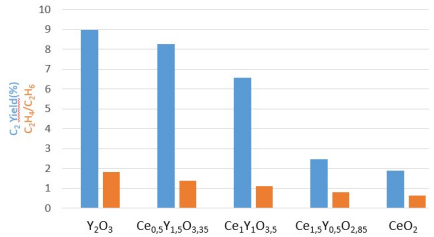

Figure 1. Yield C_2 (blue) and ethylene/ethane ratio (orange) of the selected compounds

As shown in Table 1, the addition of Ca and Sr increases both methane conversion and C_2 selectivity. These values are obtained at the reaction temperature of 700°C, a relatively low temperature for the OCM reaction[1], which is an advantage not only in terms of the temperature management for such exothermic reaction, but also for insertion into the HTE. Strontium as a dopant permitted to achieve better values of C_2 yield, but it was also evidenced that the addition of calcium as a dopant gave better stability when added to the cerium-yttrium mixed oxide or to yttrium alone (not shown here).

Table 1. Catalytic activity of the materials at 700°C (CH_4:O_2 = 2:1/ GHSV (STP) = 89000 h^{-1})

Code	CH_4 conversion (%)	C_2 selectivity (%)	C_2 yield (%)
$Ce_1Y_1O_{3.5}$	32.2	18.8	6.0
Y_2O_3	31.3	28.5	8.9
$Ce_1Y_{0.7}Ca_{0.3}O_{3.35}$	36.1	34.4	12.4
$Ce_1Y_{0.7}Sr_{0.3}O_{3.35}$	35.5	37.0	13.2
$Y_{1.7}Ca_{0.3}O_{2.85}$	37.9	37.1	14.1
$Y_{1.7}Sr_{0.3}O_{2.85}$	37.9	38.4	14.6

A compromise must therefore be reached to define an optimal anode composition, taking into account the role played by cerium in the reaction and in the ionic/electronic conductivity of the material.

These aspects, based on characterization using different techniques (XPS, TPD-CO_2 and isotope exchange) will be discussed.

Significance

The synergistic effect of cerium and yttrium oxides is rarely reported in the literature[2], particularly for the methane oxidative coupling reaction. The use of this type of compound in a high-temperature electrolyzer by valorizing co-produced oxygen seems promising. Proof of concept has yet to be provided for a new way of producing decarbonized ethylene, opening the way to decarbonize ethylene-based chemisty.

References

1. Liu, J. et al. Carbon Resources Conversion 5, 1–14 (2022).
2. Haneda, M., Katsuragawa, Y., Nakamura, Y. & Towata, A. Frontiers in Chemistry 6, (2018).

Greenhouse and acid gas conversion by electrothermal catalysis

H. Poelman[1], G. Veryasov[2], H. Retot[3], I. Shlyapnikov[4], J. Lauwaert[5], A. Delparish[6], Miha Grilc[7], V. Valtchev[8], H. Dura[9], B. Raa[10] and J. Thybaut[1]*

[1] *Laboratory for Chemical Technology, Technologiepark 125, 9052 Ghent, Belgium*
[2] *Total Energies One Tech Belgium, Zone industrielle C, 7181 Seneffe, Belgium*
[3] *Saint Gobain Research Provence and NORPRO, Cavaillon, France*
[4] *Center of Excellence Low Carbon Technologies, 1000 Ljubljana, Slovenia*
[5] *Industrial Catalysis and Adsorption Technology, V. Vaerwyckweg 1-C, 9000 Ghent, Belgium*
[6] *PDC Research Foundation, Paardeweide 7, NL-4824EH Breda, The Netherlands*
[7] *Catalysis and Chemical Reaction Engineering, NIC, Hajdrihova 19, 1000 Ljubljana, Slovenia*
[8] *Laboratory of Catalysis and Spectrochemistry, CNRS-ENSICaen-UniCaen, 14000 Caen, France*
[9] *DECHEMA Energie und Klima, Theodor-Heuss-Allee 25, 60486 Frankfurt, Germany*
[10] *Industrial Systems Engineering & Product Design, Technologiepark 46, 9052 Ghent, Belgium*
*corresponding author: joris.thybaut@UGent.be

Introduction

Mitigating CO_2 emissions becomes a continuously more pressing challenge. An important reason for the slow progress in this respect lies in the composition of CO_2 containing streams. Typical waste gases not only include CO_2, but also other acid gases, such as H_2S, a combination known as sour gas. Conventional removal technologies rely on separation and independent conversion of these components, which is inefficient, from the economical perspective as well as from the environmental one.

The Horizon Europe project e-CODUCT (https://e-coduct.eu/) tackles the environmental challenge of reducing both acid gases through a novel two-step technology (Figure 1a). The simultaneous presence of CO_2 and H_2S is turned into an opportunity by having them react into COS and water, followed by decomposition of COS into industrially valuable CO and elemental sulphur (S). For the latter conversion, an ElectroThermally Fluidized Bed reactor (ETFB), powered by renewable energy sources, is foreseen. The ultimate goal is to develop a breakthrough technology with a 50% reduced reactor size and energy demand, that enables the simultaneous reduction of CO_2 and H_2S for the production of marketable green end products in the form of fuels and useful chemicals (CO, S and CH_3OH).

Materials and Methods

Nine European partners team up to tackle the ambitious project goal, each taking on one or more of following objectives:

- Development of stable, sulphur-resistant catalysts for COS synthesis;
- Lab-scale investigation of thermal COS decomposition;
- Design and construction of an ETFB pilot plant, powered by renewable energy, for conversion of COS into CO and S; a technology readiness level (TRL) of 6 is aimed for with an annual production capacity amounting to 16 tonnes of CO;
- Multi-scale (micro)kinetic, reactor and process modelling to describe the interplay of all relevant elementary phenomena;
- Optimization of renewable energy supply for a chemical plant.

Results and Discussion

As alternative to the conventional Claus process for H_2S abatement, COS synthesis was realized at lab-scale over a 13X zeolite under a CO_2:H_2S feed ratio of 1:1, at 45°C and atmospheric pressure. The effects of temperature and water were assessed, showing slow deactivation of the zeolite by water poisoning.

COS thermal decomposition was examined at lab-scale in a tubular flow reactor with systematic variation of COS feed concentrations, residence times and catalysts. For an inlet COS concentration of 4.5 mol% and residence time of 5 s, the COS conversion in an empty Hastelloy X reactor exceeded 99% with CO as major component in the gas phase (> 99%) at temperatures above 950°C.

The ETFB reactor for COS decomposition to CO and S requires temperatures up to 800-1200°C. These will be achieved through Joule heating of the fluidized bed between two electrodes (Figure 1b). Currently, the ETFB pilot is under construction in a demonstration hall at the Institute Joseph-Stephan (IJS, Slovenia).

Parameter estimates for the COS synthesis kinetics, based on a Langmuir-Hinshelwood-Hougen-Watson (LHHW) mechanism, properly predict the experimental data from the transient fixed-bed reactor, including breakthrough, rollup and pseudo-steady state of the CO_2, H_2S and COS components. The ETFB reactor is also being modelled, based on co-axial and end-to-end resistors. In combination with microkinetic simulation of the reaction rates, the multi-scale modelling approach will eventually enable optimization of the catalytic materials, the reactor configuration, as well as the operating conditions.

In parallel, techno-economic assessment (TEA) and life-cycle analysis (LCA) modelling are performed to demonstrate the techno-economic and environmental performance of the developed e-CODUCT process. Given the use of renewable sources like solar and wind, intermittent by nature, energy fluctuations will be managed by means of a battery buffer connected to the grid as backup, in view of efficient e-CODUCT process operation.

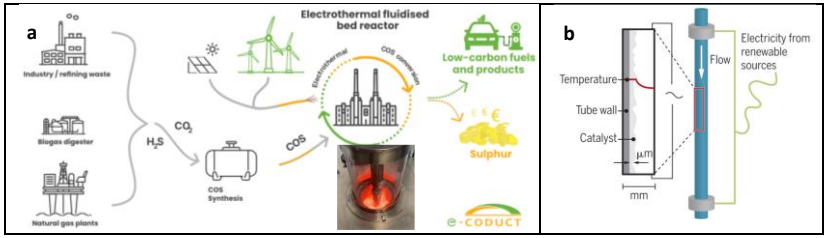

Figure 1. a: scheme of the e-CODUCT process and b: concept of the ETFB reactor.

Significance

The novel e-CODUCT technology contributes to simultaneous reduction of H_2S and CO_2, both produced as by-products in refineries and petrochemical industry. The mixture of gases is converted into COS, and further into platform molecule CO and marketable S. The entire technology relies on electrification as major driver to make chemical industry more sustainable.

Acknowledgment

The e–CODUCT project is funded under Horizon Europe Grant Agreement n°101058100.

Magnesium hydroxide fluorides as catalysts for the isomerization of glucose to fructose

Claudia Sa[1], Bakytzhan Yeskendir[1], Jonathan Sierra[2], Thomas Onfroy[1], Guillaume Laugel[1], Frédéric Richard[2], Stéphane Célérier[2], Hélène Lauron-Pernot[1]*

[1]*Laboratoire de Réactivité de Surface, Sorbonne Université, 75005 Paris, France*

[2]*IC2MP, 86000 Poitiers, France*

*helene.pernot@sorbonne-universite.fr

Introduction

Isomerization reactions play a crucial role in a wide range of applications related to the valorization of bio-based molecules, notably the isomerization of glucose to fructose (Figure 1(a)), which can then be converted into various high-value intermediates/products such as 5-hydroxymethylfurfural (5-HMF) and levulinic acid[1]. These platform molecules serve as key precursors for many essential compounds in chemistry, thus contributing to the transition towards a more sustainable economy with reduced dependence on fossil resources.

Currently, fructose is primarily produced via enzymatic catalysis, a method associated with several limitations, including high costs and restricted operating window[2]. In response to these challenges, extensive research has been conducted to explore the potential of solid catalysts in fructose production. Among these candidates, solid bases and Lewis acids are the most frequently proposed[3], but despite numerous studies, the relationship between the acid-base properties and the catalytic performance remains poorly understood. However, this relationship is essential for improving the activity and the selectivity of catalysts.

Interestingly, fluorine-based catalysts have not been examined in the context of glucose isomerization despite the potential interest of fluorine to tune acid-base properties[4,5]. Moreover, the sol-gel synthesis of fluorinated hydroxides offers a pathway to materials with variable fluorine content[4,6].

In this contribution, we will study the effect of incorporating fluorine into magnesium hydroxides on their activity and selectivity in the glucose isomerization reaction (Figure 1(a)). Their acid-base properties will be characterized using the 2-methyl-but-3-yn-2-ol (MBOH) conversion test (Figure 1(b)). The relationship between these properties and the reactivity in isomerization reaction will be finally discussed.

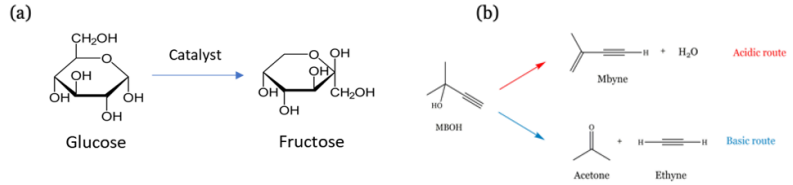

Figure 1. (a) Isomerization of glucose to fructose, (b) MBOH conversion reaction.

Materials and Methods

Magnesium hydroxide fluorides $MgF_x(OH)_{2-x}$, with x from 2.00 to 0, were prepared using a sol-gel method[4,6]. The MBOH test was carried out in the gas phase with N_2 as the carrier gas and a reaction temperature of 130 °C. The reactants and products were then analyzed by gas chromatography (GC). The isomerization of glucose to fructose was performed in aqueous phase at 80°C for 6 h. The reactants and products were then analyzed by high-performance liquid chromatography (HPLC).

Results and Discussion

The results obtained for the isomerization of glucose to fructose, on a set of $MgF_x(OH)_{2-x}$, show that fluorine influences both the glucose conversion and the fructose selectivity. According to Figure 2, fluorine introduction induces a decrease in the glucose conversion from 48 to 34 % accompanied by an increase in fructose selectivity from 73 to 86%. Further increase in the fluorine content induces a slow conversion decrease (from 34% to 24%) and fructose selectivity is maintained at high level (close to 80%). Finally, pure MgF_2 present the lowest activity with still high fructose selectivity. These results suggest that fluorine affects the strength and number of active sites.

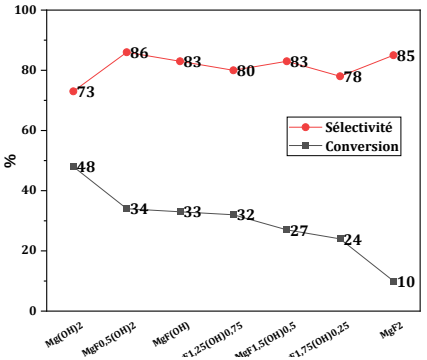

Figure 2. Conversion and selectivity of $MgF_x(OH)_{2-x}$ with x from 2.00 to 0 in the glucose to fructose isomerization reaction (T = 80°C; t = 6 h; m_{cata} = 50 mg).

Furthermore, through to the MBOH conversion model reaction, the introduction of fluorine appears to reduce the basicity of the catalyst, which could explain the observed improvement in isomerization selectivity. Indeed, the condensation of glucose on the catalyst surface, leading to the formation of humins, can be favored on the most basic sites.

It is also very interesting to note that the performance obtained in water at moderate temperature and under short reaction times with materials synthesized in soft an inexpensive conditions, are competitive with the results reported in the literature.[3] Moreover, no thermal activation treatment, often energy-intensive, is required to active them.

Significance

This study demonstrates that fluorine in magnesium hydroxides modifies the acid-base properties of the catalysts, improving selectivity for fructose during glucose isomerization, particularly in comparison with results from the literature.

References

1. L. T. Mika et al. *Chem.Rev.,* **2018**, *118* ,505-613
2. L. H. Lim et al. *Appl. Biochem. Biotechnol.*, **2007**, *137*, 115-130
3. I. Delidovich et al. *ChemSusChem*, **2016**, *9*, 547–561
4. M. Xu et al., *Catal.Sci.Technol*. **2019**, 9, 5793
5. S. Célérier et al. *Catal. Comm.* **2015**, 67, 26
6. G. Scholz et al. *Eur. J. Inorg. Chem.,* **2012**, *2012*, 2337

Cu and ZnO nanoparticles supported on MWCNTs as nanocatalysts for selective N-formylation using CO_2 and H_2

Ngoc-Anh Thai[1,2,3], Pierre Fau[3]*, David Mesguich[2]*, and Armelle Ouali[1]*

[1]*Institut Charles Gerhardt Montpellier, UMR 5253 Univ Montpellier, CNRS, ENSCM Pôle Chimie Balard Recherche - CC043 1919 route de Mende, 34293 Montpellier, France*

[2] *CIRIMAT, Université de Toulouse, CNRS, Université de Toulouse 3 - Paul Sabatier, 118 route de Narbonne, 31062 Toulouse, France*

[3]*LPCNO-INSA, 135 Avenue de Rangueil, 31077 Toulouse cedex 4, France*

*pfau@insa-toulouse.fr; *david.mesguich@univ-tlse3.fr; *armelle.ouali@enscm.fr

Introduction

Carbon dioxide (CO_2), a major greenhouse gas originating from human activities and natural processes, stands as a promising C1 feedstock for the synthesis of fuels and high-value chemicals. By utilizing molecular hydrogen (H_2), **C**O_2 can be reduced into various strategic molecules such as methanol[1], but also N-methylamines (R^1R^2N-**C**H_3)[2] or N-substituted formamides (R^1R^2N-**C**HO)[3] if amines are used as additional substrates. Among these reactions, the N-formylation reaction to form N-substituted formamides has been explored, but the heterogeneous catalytic systems employing non-noble metals for this transformation have not been studied extensively.[4] In this study, we present the copper (Cu) and zinc oxide (ZnO) nanoparticles (NPs) supported on multi-walled carbon nanotubes (Cu-ZnO@MWCNTs) as nanocatalysts for the selective N-formylation of amine using CO_2 and H_2. Efforts were devoted to better understand the influence of the catalyst properties (e. g. Cu/Zn ratio, order of metal deposition, metal dispersion on CNTs among other parameters) on its catalytic activity. It turned out that the close proximity of both metals on the supports revealed key for activity.

Materials and Methods

Functionalization of MWCNTs: The commercial MWCNTs (Nanocyl NC3100™) were functionalized with different oxygen-containing groups (OH, C=O, COOH) by double acidic treatment: first with 3M HNO_3, 130 °C, 24h; second with concentrated HNO_3/H_2SO_4 (1:3, v/v), 70 °C, 7h.

Preparation of ZnO@MWCNTs: The double-oxidized MWCNTs were decorated with ZnO NPs by simple hydrolysis of zinc (II) dicyclohexyl precursor with water vapor.

Preparation of Cu-ZnO@MWCNTs: The metallic Cu NPs were deposited onto ZnO@MWCNTs by hydrogenolysis of copper (I) mesityl precursor under a hydrogen atmosphere.

Results and Discussion

High-angle annular dark field scanning transmission electron microscopy (HAADF-STEM) combined with energy-dispersion X-ray spectroscopy (EDX) was used to study the morphology and chemical composition of as-synthesized Cu-ZnO@MWCNTs nanomaterial. While ZnO appears as small, homogeneously distributed nanoclusters on the MWCNTs, the Cu presents as both nanoparticles and nanoclusters distributing throughout the CNTs' surface. Moreover, the HAADF-STEM image and EDX mapping confirmed the close proximity between metallic Cu and ZnO, which is required to obtain catalytic activity in CO_2 hydrogenation reactions.[5] Indeed, the Cu-ZnO@MWCNTs demonstrated high catalytic activity for the N-formylation of various amines, producing N-formamide products with good-to-excellent yields and high selectivity. It's important to emphasize this high selectivity as N-methylamines may also be formed due to the over-reduction of the N-formamide products.

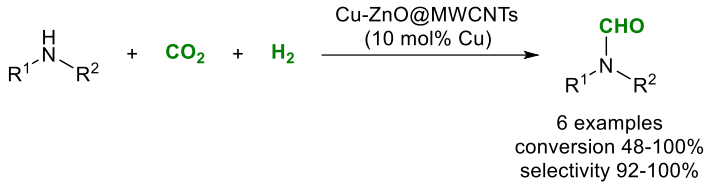

Figure 1. N-formylation of amines using CO_2 and H_2 catalyzed by Cu-ZnO@MWCNTs.

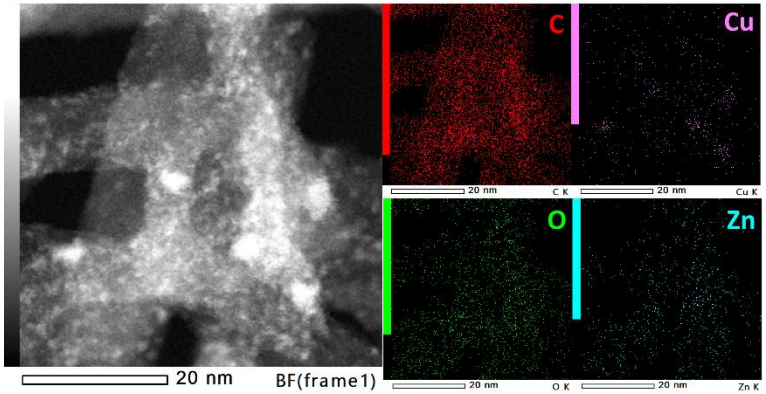

Figure 2. HAADF-STEM image and EDX elemental mapping of Cu-ZnO@MWCNTs.

Significance

This study highlights the role of CNTs as new and efficient support for achieving high dispersion of catalytic metals such as Cu and Zn for CO_2 hydrogenation towards N-substituted formamides.

References

1. S. Navarro-Jaén, M. Virginie, J. Bonin, M. Robert, R. Wojcieszak, and A. Y. Khodakov, *Nat. Rev. Chem.* **2021**, *5*, 564.
2. Y. Long, J. He, H. Zhang, Y. Chen, K. Liu, J. Fu, H. Li, L. Zhu, Z. Lin, A. Stefancu, E. Cortes, M. Zhu, M. Liu, *Chem. Eur. J.* **2023**, *29*, e202203152.
3. X. Dai, T. Li, B. Wang, C. Kreyenschulte, S. Bartling, S. Liu, D. He, H. Yuan, A. Brückner, F. Shi, J. Rabeah, X. Cui, *Angew. Chem. Int. Ed.* **2023**, *62*, e202217380.
4. Y. Uozumi, T. Takahashi, *Synfacts* **2023**, *19*, 0807.
5. A. Beck, M. A. Newton, L. G. A. van de Water, and J. A. van Bokhoven. *Chem. Rev.* **2024** *124*, 4543.

Integrated thermochemical CO_2 valorization to middle-range Olefins

J. Vachaud*[1], S. Jambur[2], A. Roussey[1], J. Boon[2], A.L. Alvarenga Marinho[1], A.C. Roger[3], S. Thomas[3], L. Lücking[2]

[1] *CEA, LITEN, DTNM, Univ. Grenoble Alpes, Grenoble, 38000, France*

[2] *TNO Energy Transition, Westerduinweg 3, 1755 LE Petten, the Netherlands*

[3] *Institute of Chemistry and Processes for Energy, Environment and Health (ICPEES), UMR 7515 CNRS-University of Strasbourg, Strasbourg 67087 Cedex 02, France*

*jose.vachaud@cea.fr

Introduction

Middle-range olefins (C_3-C_5) are a cornerstone of the chemical industry. From plastics to lubricants along with fuels, these molecules are essential in the fabrication of a large part of modern goods. The main issue concerning olefins is their fossil origin, turning them into significant contributors to greenhouse gas emissions[1]. Recently, several sustainable and cleaner methods to produce those olefins have emerged, among which Carbon Capture and Utilization (CCU) technologies offer opportunities to recover emitted carbon dioxide and integrate it into carbon value chains[2]. Avoiding the popular method of ethylene oligomerization by directly converting CO_2 into C_3-C_5 olefins (using renewable hydrogen) can also provide numerous benefits in terms of sustainability, energy requirements and economic feasibility[1,3]. The literature shows two main ways of CO_2 conversion to hydrocarbons, the methanol route and the modified Fischer-Tropsch way. Each of these routes can be performed in a two-steps or single step/integrated approach, thus offering multiple ways to get to the same C_3-C_5 olefins. In this study, an extensive review of the catalyst performance is presented. Secondly, both processes are simulated, highlighting advantages and drawbacks of each route.

Materials and Methods

Firstly, the study focuses on the development of the catalysts associated with the production of C_3-C_5 olefins. Their state of the art, limitations, and requirements for further developments in multifunctional catalysis are examined. Secondly, the different routes to obtain C_3-C_5 olefins from CO_2 and H_2 were analyzed using process modelling tool Aspen Plus V14. Material and energy balance method was used to compare and discuss the benefits, bottlenecks and optimal process conditions of the different routes. The reactor blocks were modelled using kinetics based models. Recycling of material streams and product upgrading are also considered in the process modelling. In order to have a first comparison with the literature and the simulation work, experimental tests of modified iron-based Fischer-Tropsch catalysts (NaFe, KFe) were made. The setup used is a fixed bed tubular reactor (~1g of catalyst) designed to operate at 320°C and 30 bars. The pre-treatment is done under pure H_2 at atmospheric pressure at 400°C. The reaction is operated using a 3:1 H_2/CO_2 mix with a WHSV of 2.5L.g^{-1}.h^{-1}.

Results and Discussion

The direct conversion of CO_2 into hydrocarbons is extensively studied and both routes show advantages and drawbacks. The "methanol route", which is usually carried out using metal oxides or noble metals (first step) combined with zeolites (second step), generally suffers from a large amount of unwanted CO produced, despite a high selectivity of C_3-C_5 olefins among hydrocarbons. On the other hand, the two-steps CO-mediated process is performed using Reverse Water-Gas Shift catalysts (copper oxide, iron oxide...) followed by Fischer-Tropsch ones (cobalt/iron-based catalysts). The integrated CO-mediated process is commonly done with modified iron-based Fischer-Tropsch catalysts. In any case, this route generally shows an interesting conversion, and despite a problematic selectivity due to the Anderson-Schulz-Flory (ASF) distribution, it usually gives a better yield in middle-range olefins (Fig.1). Experimental tests conducted with NaFe and KFe catalysts are consistent with this tendency.

The initial process simulation based on literature-based stoichiometric conversion came to the same conclusion concerning advantages and drawbacks of each route. As expected, it also suggests that in both routes the single step path is interesting to improve energy efficiency. Indeed, according to the first calculations, those energy savings compensate the slight decrease of H_2 utilization efficiency (Table 1). In any case, more detailed simulations must be performed to confirm those results.

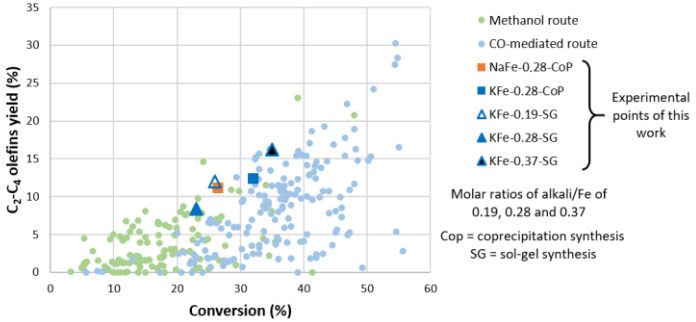

Figure 1. CO_2 conversion vs. C_2-C_4 olefins yield for catalysts from the literature performing the CO-mediated or the methanol route in CO_2 hydrogenation reaction, both integrated (1 step).

Table 1. Hydrogen utilization efficiency of each route according to the first process simulation

Route	Two-step or integrated	*Relative energy consumption (%)*	*Relative H_2 utilization efficiency (LHV basis, %)*
Methanol	Two-step	100	100
	Integrated	65	65
Modified Fischer-Tropsch	Two-step	100	100
	Integrated	45	79

Significance

This work is designed to give a clear overview of the CO_2 conversion routes to middle-range olefins by giving a detailed description of the existing process designs and catalysts, not forgetting the outlooks associated.

References

1. M. Ronda-Lloret, G. Rothenberg, N. R. Shiju, *ChemSusChem,* **2019**, *12 (17)*, 3896-3914
2. A. Reznichenko, A. Harlin, *SN Appl. Sci.*, **2022**, *4*, 108
3. Z; Liu, W. Wu, et al. *Nat. Commun.*, **2022**, *13 (1)*, 3896-3914

Stoichiometric selective carbonylation of methane to acetic acid by chemical looping

Yinghao Wang[1], Chunyang Dong[1,2]*, Mariya Shamzhy[3], Yury G. Kolyagin[1]*, Jeremie Zaffran[1]*, Andrei Y. Khodakov[1]* and Vitaly V. Ordomsky[1]*

[1]1 UCCS–Unité de Catalyse et Chimie du Solide, Université de Lille, CNRS, Centrale Lille, ENSCL, Université d'Artois, UMR 8181, Lille, France.

2 Department of Chemistry, The University of Hong Kong, Hong Kong, China.

3 Department of Physical and Macromolecular Chemistry, Faculty of Science, Charles University, Hlavova 2030/8, 12843 Prague, Czech Republic

*Corresponding authors: Chunyang Dong (dcyhk@hku.hk); Yury G. Kolyagin (Yury.Kolyagin@univ-lille.fr); Jeremie Zaffran (Jeremie.Zaffran@cnrs.fr); Chunyang Dong (snowflakelost@126.com); Andrei Y. Khodakov (Andrei.Khodakov@univ-lille.fr); Vitaly V. Ordomsky (Vitaly.Ordomsky@univ-lille.fr)

Introduction

Conversion of methane to valuable products is one of the main challenges of modern chemistry. Acetic acid (AcOH) is a key chemical reagent in industry[1], produced nowadays by the carbonylation of methanol over homogeneous Rh and Ir catalysts[2]. Here, we propose a stepwise chemical looping approach for highly selective stoichiometric synthesis of AcOH by carbonylation of methane with CO using single-site Pt over isolated phosphotungstic anions compensating positively charged titania (Pt-HPW-TiO_2). The reaction proceeds by methane activation, which coincides with reduction of platinum species in the presence of CO at 423 K and results in surface acetates attached to TiO_2. Subsequent hydrolysis by water at ambient temperature. Spent Pt-HPW-TiO_2 is regenerated to the initial state by subsequent calcination in air. This approach provides an opportunity for selective synthesis of AcOH (99 %) from methane and carbon monoxide. A high concentration of AcOH (1.1 wt %) in aqueous solution can be obtained at high conversion of methane (4.5 %)

Materials and Methods

The material for the carbonylation of methane to acetic acid was prepared by co-impregnation of an aqueous solution of tungstophosphoric heteropolyacid (HPW) together with metal salt to obtain 0.2 wt% of metal with subsequent calcination at 250 °C and removal of excess of HPW by washing of the catalyst and drying[3].

The reaction has been performed in multi-cycle mode. The first cycle involved treatment of 50 mg of dry material in batch reactor in the mixture of CH_4 and CO with ratio CH4/CO = 15 at the total pressure 15 bar and 175 °C for 2 h. After analysis of the gas phase products, the reactor was opened and 1 g of water has been added with further analysis of the liquid solution by NMR. The solid material was filtered out and calcined in the flow of air at 250 °C before the next cycle.

Results and Discussion

The characterization shows that the catalyst is composed of PtO_x anchored by polyoxometalate clusters to TiO_2. The atomic-resolved HAADF imaging showed that these highly dispersed species were isolated Keggin-type HPW clusters (**Figure a**).

The liquid phase after addition of water contained only single peak of acetic acid over Pt-HPW/TiO_2 with amount of $14.6 \bullet 10^{-7}$ mol. If using large amount of catalyst, high concentration acetic acid can be synthesized in water. (**Figure b-c**)

The importance of the presence of three components such as Pt, HPW and TiO_2 for the synthesis of AcOH from methane and CO can be assigned to the individual function of each of them. The oxidized PtO_x is required to activate of methane by dissociation of the C-H bond with simultaneous coupling with CO to form acetate. The role of heteropolyacid according to the mechanism of the reaction is in stabilization of single atom reduced Pt, providing oxygen transfer to TiO_2 for stabilization of acetate and hydrolysis of acetate. The role of TiO_2 is in capturing of acetate to form Ti-O-Ac species for subsequent hydrolysis.

The potential mechanism of the reaction can be explained by activation of methane by Pt oxidized species with dissociation of C-H bond with generation of CH_3 and H_2O with reduction of Pt0 (**Figure d**). The methyl group is transferred to CO which coordinates over O of heteropolyacid with generation of acetate compensating the charge of heteropolyacid. The hydrolysis of acetate should provide acetic acid and W-OH group and Pt can be reoxidized back by air with formation of cationic Pt species. . The recyclability of the material has been verified by several cycles with intermediate regeneration by air calcination.

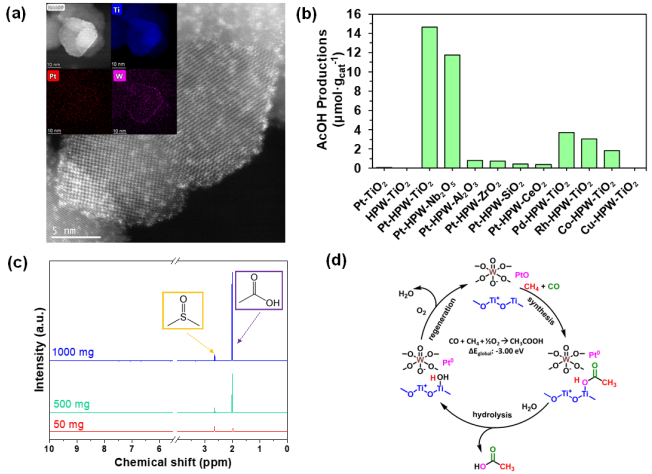

Figure. (a) Atomic-resolved HAADF-STEM image of Pt-HPW-TiO_2, (b) Amount of acetic acid which produced by per gram of different catalysts, (c) NMR of high concentration acetic acid synthesized in water (d) Scheme of the reaction.

Significance

The chemical looping strategy has been proposed in this work for direct acetic acid synthesis from methane over single-site Pt over isolated phosphotungstic anions, resulting in selective synthesis, with the potential to achieve high acetic acid concentrations at high selectivity.

References

1. Periana, et al. *Science* **2003**, *301* (5634), 814-818.
2. Q. Yuan, et al. *J. Catal.* **2005**, *233* (1), 221-233.
3. X. Yu, et al. *Nat. Energy* **2020**, 5, 511–519

Study of catalysts Ni-Ce-Mg-Al , Ni-Co-Mg-Al and Ni-Mg-Al obtained via hydrotalcites for the dry reforming of the methane

Ali Zazi[1,2*], V.M.Gonzalez-delaCruz [3],D Halliche[1], J.P.Holgado[3], A.Caballero [3], O.Cherifi[1]
[1]*Laboratoire de chimie du gaz naturel,Faculté de chimie ,USTHB ,Bp 32 El Alia Algerie*
[2]*Departement de chimie, Faculté des sciences,UMMTO,Tizi ouzou ,Algerie*
[3]*Instituto de Ciencia de Materiales de Sevilla (CSIC-University of Seville) and Departamento de Quimica Inorganica, University of Seville, Avda. Americo Vespucio, 49, 41092 Seville, Spain*
**aliz6dz@hotmail.com*

Introduction

The production of the synthesis gas and the hydrogen represents one major stake in the chemical industry in the world. These two gases are obtained via the reforming of the methane by one of the three proceeded:

-Dry reforming of methane: $CH_4 + CO_2 \longrightarrow 2CO + 2H_2$
-Steam reforming of methane: $CH_4 + H2O \longrightarrow CO + 3H_2$
-Partial oxidation of methane: $CH_4 + ½\ O2 \longrightarrow CO + 2H_2$

The reaction of the dry reforming drew a big attention by a wide public of researchers thanks to its contribution on the decrease of the atmospheric concentration of both greenhouse gases CO_2 and CH_4.

The majority of all works had for objective to improve the yield on this reaction and to increase the life cycle of catalyst which is poisoned by the deposit of coke which is until this day the major problem of this process.

Synthetic Mg–Al layered double hydroxide materials have found many applications due to their unique physicochemical properties; Catalysis is one of these applications (5).

This work consists in the preparation of materials catalysts, which can bring better performance.

Materials and Methods

The Catalysts materials were synthetized by classical method of coprecipeation at basic pH (pH=11), as reported by Miyata [3]. with molar ratio of $M^{2+} / M^{3+} = 2$.

Catalysts characterization has done with X-Ray powder diffraction, FTIR method, the surfaces area are measured by employing BET technique, Elemental analyses of metals of the samples was carried out by ICP. We have taken other technique like SEM image and TPR . The catalytic experiments Analysis is given by gas chromatograph with column Porapak Q.

Results and Discussion

The result of the ICP shows that the experimental composition is coherent with the nominal composition for each sample and the M^{2+}/M^{3+} ratio is around 2.

X-ray diffraction patterns of the samples before calcination shows that training hydrotalcites structures. X-ray diffraction patterns after calcination shows oxides mixtures of NiO and Al,Mg,Co,Ce oxides.

The results of BET surface areas show that BET areas increase after calcination, for NiMgAl and NiCoMgAl but decreases slightly for NiCeMgAl. The results of H_2-TPR measurements of the calcined samples showed a single reduction peak in the case of NiMgAl at higher temperature reduction (around 800°C), indicating the existence of species of NiO with strong interaction resulting from the formation of the NiO–MgO solid solution, characterized by its high stability. The NiMgAl catalyst shows a significant CH_4 conversions such as 87,0%, 92,0 %,88% respectively for NiMgAl , NiCoMgAl and NiCeMgAl. CO_2 conversionsfor NiMgAl , NiCoMgAl and NiCeMgAl are respectively86,0% and 90,0%, 88%.

The present study showed that the catalysts based on nickel and which are prepared by the Local hydrotalcite way gives a good activity for CH4 / CO2 reaction and that the addition of cobalt or Cerium improves the activity. A good stability is also observed for the catalysts of this study.

The importance of the study and improvement of the performance of dry reforming reaction, is its environmental contribution to the reduction of the two greenhouse gases $CO_2$and CH_4.

References

1. Victor M. Gonzalez-DelaCruz, Juan P. Holgado, Rosa Pereniguez, Alfonso Caballero, Journal of Catalysis 257 (2008) 307-314.
2. C.E. Daza , C.R. Cabrera ,S. Moreno , R. Molina , Applied Catalysis A: General 378 (2010) 125–133.
3. Miyata, Clays and Clay Miner.23 (1975) 369.
4. Umberto Costantino, Massimo Curini, Francesca Montanari, Morena Nocchetti, Ornelio Rosati, Journal of Molecular Catalysis195 (2003) 245-252.
5. Andrey I. Tsyganok, Tatsuo Tsunoda, Satoshi Hamakawa, Kunio Suzuki, Katsuomi Takehira, and Takashi Hayakawa, Journal of Catalysis 213 (2003) 191–20.

Synthesis and Comparison of Pt and Pt_3Sn Supported Catalysts for Transfer Hydrogenation from perhydro-dibenzyltoluene to acetone

Smitkriti[1,2], Xiaolong Ji[2,3], Laurent Veyre[1], Valérie Meille[2]*, Chloé Thieuleux[1]*
[1]*CP2M,* [2]*IRCELYON,* [3]*LAGEPP, Université Claude Bernard Lyon 1, 69100 Villeurbanne, France*
*chloe.thieuleux@univ-lyon1.fr; valerie.meille@ircelyon.univ-lyon1.fr

Introduction

Dibenzyltoluene (H0-DBT)/perhydro-dibenzyltoluene (H18-DBT) is a promising Liquid Organic Hydrogen Carrier (LOHC) system, which can be employed for safe storage and transportation of hydrogen. Currently, the industrial applications of LOHC are limited as the dehydrogenation step is endothermic, requiring high reaction temperature (300 °C), therefore decreasing the overall efficiency of the process. Although, this disadvantage can be mitigated by performing transfer hydrogenation between hydrogen-rich H18-DBT and an acceptor molecule such as acetone at mild temperatures, forming isopropanol, which can be, used as fuel in direct fuel cell concepts.[1] Pt-based catalysts have shown promising activity for transfer hydrogenation reaction in the literature but catalyst optimization has not been explored in details.[2,3] Beside monometallic NPs, Pt_xSn on alumina has been employed for the dehydrogenation of H18-DBT in a recent publication.[4] Hence, we propose to synthesize catalysts based on Pt nanoparticles (different methods on different oxide supports) and we aim to evaluate supported alloyed NPs (Pt_xSn) as catalysts for our targeted transfer hydrogenation reaction.

Materials and Methods

Pt NPs and Pt_3Sn NPs colloid were synthesized following a colloidal route developed in our team.[5, 6] Supported catalysts were prepared by impregnating the Pt and Pt_3Sn colloids onto two oxide supports (SBA-15 and SiO_2) to reach a metal loading of 1 wt.% or 5wt.%, using wetness impregnation. The impregnated catalysts were calcined at 500 °C under dry air and then hydrogenation and/or hydrogenolysis was carried out at 350 °C to reduce the metal oxides formed during calcination and eliminate any remaining alkyl chains. To study the effect of synthesis method, catalyst was also prepared using direct impregnation of $Pt(NH_3)_4(OH)_2$ complex on SiO_2 according to the literature. DRIFTS, STEM-HAADF Microscopy, HRTEM, EDX, H_2 chemisorption, PXRD and ICP-MS analysis were done to characterize the synthesized catalysts. Catalyst tests were carried out in a 100 mL stainless-steel batch reactor (Parr Instruments) at 200 °C with 1/3 as H18-DBT/Acetone molar ratio and compared to commercial catalysts (Pt/Al_2O_3, Pt/SiO_2 and Pt/C). The reaction was monitored by gas and liquid phase sampling, which were analyzed by two GC systems (Shimadzu) equipped with different columns (HeavyWax and RtQ), allowing the establishment of mass balances over all compounds.

Results and Discussion

We successfully prepared supported Pt and Pt_3Sn NPs catalyst, where no sintering was observed between colloidal nanoparticles even after impregnation. HRTEM and EDX analyses confirmed the presence of an alloyed Pt_3Sn phase (Figure 1). The complete removal of aliphatic chains of the stabilizing ligands after thermal treatments was observed by DRIFTS. The Pt_3Sn phase was maintained even after the post-treatments as confirmed by HRTEM and EDX analysis. Average particle size was calculated using both electron microscopy and H_2 chemisorption along with Pt loading from ICP-MS.

d	h k l	Angle(°)
0.231	1 1 1	0
0.200	2 0 0	54.5
0.234	-1 1 1	109.54

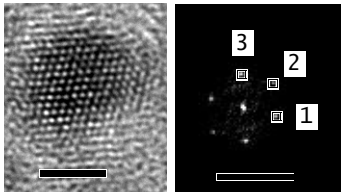

Figure 1. TEM micrograph (left) and TEM diffraction micrograph (right) for Pt_3Sn particle. The numbers 1, 2, 3 refer to 3 vectors used for crystallographic indexation (Miller indexes of the reticular plans and angles) in the table

The initial catalytic tests (Table 1) between Pt-based catalysts indicated no significant effect of mesoporous (SBA-15) and non-porous (SiO_2) support as well as indicated similar selectivity and activity for catalysts in the size range of 2-4 nm.

Table 1. Comparison of catalytic activities for transfer hydrogenation at 200 °C

Catalyst	Mean Size (nm)[a]	IPA Yield (%)	Selectivity (%)	TOF (h^{-1})
com. 1wt%Pt/SiO_2	3.6	12.3 ± 0.1	53 ± 1	242 ± 3
1wt%Pt/SiO_2	1.8	8.6 ± 0.5	47 ± 3	98 ± 6
1wt%Pt/SBA-15	2.8	10 ± 0.5	45 ± 2	120 ± 6

[a] *H_2-chemisorption*

Significance

Synthesizing and testing catalysts with different active metals, synthesis method and solid supports could provide a better understanding for the mechanism of transfer hydrogenation between H18-DBT and acetone, which will be beneficial for the catalyst optimization to achieve higher activity and selectivity knowing that the design and development of appropriate catalytic active phases are not explored in state-of-the-art publications.

References

1. G. Sievi, D. Geburtig, T. Skeledzic, A. Bösmann, P. Preuster, O. Brummel, F. Waidhas, M. A. Montero, P. Khanipour, I. Katsounaros, J. Libuda, K. J. J. Mayrhofer, P. Wasserscheid, *Energy Environ. Sci.*, **2019**, *12*, 2305-2314
2. D. Zakgeym, T. Engl, Y. Mahayni, K. Müller, M. Wolf, P. Wasserscheid, *Applied Catalysis A*, **2022**, *639,*118644
3. D. Geburtig, PhD Thesis, Friedrich-Alexander-Universität Erlangen-Nürnberg (FAU), **2019**
4. Z. Peng, H. Lu, S. Zhang, X. Cao, J. Chen, B. Wei, M. Sang, H. Wang, Y. Sun, *ACS Appl. Nano Mater*, **2023**, *6*, 16152−16160
5. M. Boualleg, J.-M. Basset, J.-P. Candy, P. Delichere, K. Pelzer, L. Veyre, C. Thieuleux, *Chem. Mater.*, **2009**, *21*, 775–777
6. M. Boualleg, D. Baudouin, J.-M. Basset, F. Bayard, J.-P. Candy, J.-C. Jumas, L. Veyre, C. Thieuleux, *Chem. Commun.*, **2010**, *46*, 4722–4724

Reduced cobalt oxide catalysts for catalytic ozonation of toluene

H. Zhang[1], V. Meille[1*], S. Gil[1*]
[1]*Institut de Recherches sur la Catalyse et l'Environnement de Lyon, CNRS, Université Claude Bernard Lyon 1, 2 avenue A. Einstein, 69626 Villeurbanne, France*
*valerie.meille@ircelyon.univ-lyon1.fr
*sonia.gil@ircelyon.univ-lyon1.fr

Introduction

Volatile organic compounds (VOCs) and ozone (O_3) are two major indoor and outdoor gaseous pollutants, which are a real problem for environment and human health. The abatement of these two air pollutants, which often co-exist in confined environments such as buildings and cabin aircrafts, is therefore crucial. Moreover, ozone is a powerful oxidant that has been widely used in many applications such as waste water and exhaust gas treatment, notably because its efficiency in oxidation reactions is higher than that of oxygen. It decomposes into oxygen, leaving no residue in the treatment process. Moreover, ozone is a pollutant in industrial exhaust gases and indoor air, so using ozone in elimination processes can help combat ozone pollution as well. Therefore, the idea of this study is to take advantage of the oxidizing capacity of ozone to remove VOCs by catalytic ozonation[1]. This catalytic process seems to reduce the reaction temperature, saving energy compared to conventional catalytic oxidation reaction, and will allow us to decompose simultaneously both pollutants[2].

Currently, supported noble metals and transition metal oxides are commonly employed as VOCs ozonation catalysts[3]. However, considering the price and susceptibility to poisoning of noble metals, cobalt oxides materials were chosen as the catalysts in this study. They are promising transition metal oxides because of their special spinel structure, which allows easy modification of their elemental composition, cobalt ion valence states and exposed crystal planes[4]. In previous reports, cobalt oxide catalysts showed some activity in toluene ozonation[5], but much lower than manganese oxide and noble metal catalysts. Therefore, this work aims to modify cobalt oxide catalysts to improve their catalytic activity and stability.

Materials and Methods

Co_3O_4 nanosheets were synthesized by a method reported by W. Lu et al.[6] and $NaBH_4$ was employed to mildly reduce some surface Co^{3+} to Co^{2+}, generating more active sites for ozone decomposition. $CoCl_2{\cdot}6H_2O$, hexamethylenetetramine and NaCl were used as precursors to synthesized layered α-$Co(OH)_2$. After calcination under flowing air at 400°C, Co_3O_4 nanosheet (RCo-b) were obtained. Lastly, Co_3O_4 nanosheets were reduced in varying concentrations of $NaBH_4$ (0.05 M, 0.1 M (RCo-0.1), 0.2 M, 1 M (RCo-1))[6]. The physicochemical properties of the different catalysts were characterized by X-ray diffraction (XRD), N_2 sorption, O_2 temperature programmed desorption (O_2-TPD), scanning electron microscopy (SEM), X-ray Photoelectron Spectroscopy (XPS), and Raman spectroscopy. The catalytic activity of the catalysts for O_3 decomposition and toluene ozonation were evaluated in a fixed-bed reactor. 5 mg catalyst (diluted in 95 mg SiC) are loaded in the reactor with the introduction of 350 mL.min^{-1} air feed containing 225 ppm ozone only, or 25 ppm of toluene and 250 ppm of ozone (10 vol.% oxygen and nitrogen as a balance), giving a weight hourly space velocity of 1200 L g^{-1} h^{-1}. In parallel, a study using in-situ infrared spectroscopy (DRIFTS) will be used to gain important insights into the pathway and intermediates involved in the reactions of interest.

Results and Discussion

Table 1 presents the physico-chemical and surface properties of our previous mentioned catalysts: RCo-b, RCo-0.1 and dRCo-1. The XRD results confirm that α-$Co(OH)_2$ precursor and Co_3O_4 spinel were successfully synthesized. After $NaBH_4$ reduction, the crystallinity of Co_3O_4 was decreased, but its crystalline phase was preserved, as corroborated by the Raman results. Additionally, Raman spectra reveal that $NaBH_4$ reduction significantly increased the abundance of oxygen vacancies on the Co_3O_4 surface, which affected the Co-O bond vibrations and consequently led to a shift in the Raman peaks. The results of O_2-TPD and XPS O1s further illustrate the changes in the oxygen species on the Co_3O_4 surface before and after $NaBH_4$ reduction. In particular, the proportion of chemisorbed oxygen species, which can participate in the catalytic oxidation of VOCs, significantly increased after $NaBH_4$ reduction (Table 1). Finally, the XPS Co 2p results demonstrate a significant increase in the amount of Co^{2+} on the catalyst surface after reduction. These species are considered to be the active sites for catalytic ozonation reaction of VOCs since they are the active sites for ozone decomposition, generating activated oxygen species for VOCs removal. Consequently, a higher concentration of Co^{2+} is associated with an enhanced catalytic ozonation reaction. Further research is needed to better elucidate the different properties (H_2-TPR, TEM, etc.) of these synthetized catalysts, namely in terms of catalytic efficiency for VOCs removal by catalytic ozonation. The catalytic tests and surface in-situ measurements are in progress.

Table 1. Textural and surface properties of synthetized catalysts.

Sample unit	S_{BET} [a] ($m^2{\cdot}g^{-1}$)	D_p [b] (nm)	V_p [b] ($mL{\cdot}g^{-1}$)	O_2 desorption [c] ($mmol{\cdot}g^{-1}$)	Co^{2+}/Co^{3+} [d]	O_v/O_{latt} [d]
RCo-b	30.2	23.2	0.12	0.12	0.53	0.34
RCo-0.1	42.0	22.6	0.12	1.88	1.15	1.90
RCo-1	43.5	19.0	0.14	2.27	1.50	3.63

[a] Determined by the BET method. / [b] Determined by the BJH method (adsorption branch).
[c] Determined by integration of O_2-TPD profiles. / [d] Determined by deconvolution of XPS spectra.

Significance

This study holds a great significance, it has the potential to improve air quality in building and aircraft cabins through development of noble metal-free catalysts, and should shed light on the reaction pathway of catalytic ozonation.

Acknowledgments

The authors Acknowledges the support of China Scholarship Council program (ID: 202308370181).

References

1. B. Liu, J. Jian, B. Zhang, W. Huang, Y. Gan, D. Leung, and H. Huang, *J. Hazard. Mater.* **2022**, vol. 422, p. 126847.
2. Y. Sui, X. Sun, J. Guan, Z. Chen, X. Zhu, X. Xiao, X. Li, J. Shen, X. Liu, X. Zhang, Y. Guo, G. Zhang, and R. Zhang, *RSC Adv.*, **2024**, vol. 14, no. 21, pp. 14784–14792.
3. M. Aghbolaghy, M. Ghavami, J. Soltan, and N. Chen, *J Ind Eng Chem*., **2019**, vol. 77, pp. 118–127.
4. Q. Ren, Z. Feng, S. Mo, C. and Huang, S. Li, *Catal. Today.*, **2019**, vol. 332, pp. 160–167.
5. M. Li, K. Hui, K. Hui, S. Lee, Y. Cho, H. Lee, W. Zhao, S. Cho, C. Chao, and Y. Li, *Appl. Catal. B Environ.*, **2011**, vol. 107, no. 3–4, pp. 245–252.
6. W. Lu, M. Yuan, J. Chen, J. Zhang, L. Kong, Z. Feng, X. Ma, J. Su, and J. Zhan, *Nano Res.*, **2021**, vol. 14, no. 10, pp. 3514–3522.

Ni-Based Cermets and High Entropy Alloys for Efficient Ammonia Decomposition

Dan Milas[1], Thomas Belin[1], Nicolas Bion[1]*, Fabien Can[1], Clément Comminges[1], Xavier Courtois[1], Antoine Meunier[1], Jeanne Boissadie[2], Gilles Taillades[2]

[1]*Institut de Chimie des Milieux et Matériaux de Poitiers (IC2MP), CNRS, Université de Poitiers, 86000 Poitiers, France*

[2]*Institut Charles Gerhardt Montpellier (ICGM, UMR 5253), CNRS, Université de Montpellier, 34293 Montpellier, France*

*nicolas.bion@univ-poitiers.fr

Introduction

Using hydrogen (H_2) as an energy vector in the transition to renewable energy is limited by the high energetic cost of storing and transportation.[1] Ammonia (NH_3) decomposition (cracking, $2NH_3 \rightarrow N_2 + 3H_2$) has the potential to solve this issue due to the favorable liquefaction conditions of NH_3 and high volumetric energy density (17.8 wt% hydrogen, 121 kg H_2/m^3 at 10 bar).[2] Currently, the endothermic decomposition of NH_3 ($\Delta H°$= +46 kJ/mol) reaches high conversion rates only at high temperatures (500–600 °C) or with catalysts based on scarce metals like ruthenium.

The Franco-German HADES project (Hydrogen through Ammonia Decomposition from Energy Storage), a collaboration of multiple research institutes from both countries, aims to develop a single proton-conducting ceramic reactor that integrates into a single step NH_3 decomposition, H_2 purification and compression, using non-critical materials such as BZCY perovskites ($BaZrCeYO_{3-\delta}$) electrolyte and Ni-based cermets anodes.[3] This work investigates the catalytic performance in ammonia cracking of Ni-BZCY and bimetallic M_1M_2-BZCY cermets as well as of novel high entropy alloys (HEAs) composed of earth-abundant transition metals for their use in proton conducting fuel cells (PCFC).

Materials and Methods

Ni cermets and BZCY perovskites (obtained by co-combustion method) were supplied by ICGM. Structural characterization is obtained by XRD analysis using an Empyrean, Malvern Panalytical diffractometer ($20° < 2\theta < 90°$; 0.06° and 5s per step). Reducibility of the cermet was determined by temperature-programmed reduction under 10% H_2 flow in Ar after oxidizing pre-treatment at 600°C. Oxygen mobility in electrolyte material was investigated with $^{18}O_2/^{16}O_2$ in a closed recycling set-up connected to a mass spectrometer (GDS200 Pfeiffer Vacuum) for continuous monitoring of the isotopologue distribution.

HEAs were synthesized using high purity metal precursors (Co, Mo, Fe, Ni, Cu from Sigma Aldrich) *via* the carbothermal shock method (Keithley SourceMeter) and tested in the same reaction conditions as the other catalysts. [4] Composition of HEA was determined by ICP-OES analysis after microwave-assisted mineralization in acid medium.

NH_3 cracking performance was measured in a fixed-bed quartz reactor after overnight reduction under a pure H_2 flow at 600 °C. NH_3 conversion was recorded after achieving steady-state conditions from 600°C to 300°C by step of 50 °C, using 25% NH_3 (Air Liquide GPM) at a fixed flow rate (6 $L/g_{cat}/h$, Brooks Instrument mass flow controller).The gas composition was analysed using a micro-GC (Agilent 990) equipped with two channels (Molecular Sieve 5Å for N_2 and H_2 and Volamine for NH_3) and a TCD sensor.

Results and Discussion

The Ni-BZCY sample achieved 99.3% ammonia decomposition at 500 °C and 50% of conversion (T_{50}) at ca. 440 °C while the support itself (BZCY181) displayed no activity below 600 °C (Figure 1a). Beyond the catalytic activity, cermet has to be good electronic and proton conductor. Electronic conductivity is guaranteed by the high Ni content. According to the Grotthuss mechanism of the H^+ conduction, the dynamics of the oxygen sub-lattice would play an important role in proton migration by facilitating the proton transfer step from an acceptor site to the adjacent site.[5] The $^{18}O_2/^{16}O_2$ isothermal isotopic exchange experiments confirmed the high oxygen mobility of the BZCY perovskite, which increases with temperature (Figure 1b). Bimetallic M_1M_2-BZCY were compared to the reference Ni-BZCY cermet in terms of activity and O mobility. The samples were characterized after catalytic cracking to check the potential modification of the surface under NH_3 flow at high temperature.

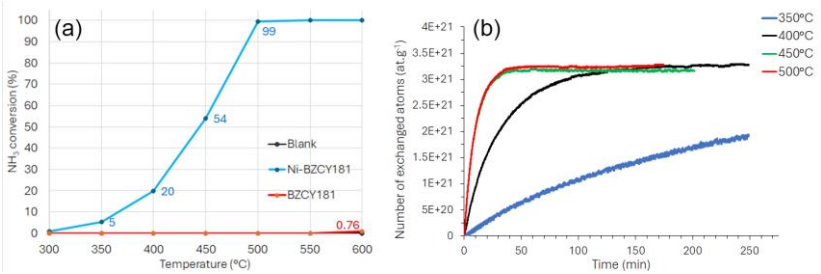

Figure 1. (a) NH_3 (25 $_{vol}$%) decomposition *vs*. temperature for Ni-BZCY (blue) and BZCY perovskite (red); (b) Number of exchanged O atoms *vs*. time for the BZCY perovskite during the $^{18}O_2/^{16}O_2$ isothermal isotopic exchange experiments at various temperatures.

Significance

Achieving cheap and efficient ammonia cracking technology has the potential to accelerate the development of the European hydrogen economy.

References

1. J.O.M. Bockris, *Int. J. Hydrogen Energy* **2013**, *38*, 2579–2588
2. J.W. Makepeace; T.J. Wood; H.M.A. Hunter; M.O. Jones; W.I.F. David, *Chem. Sci.* ***2015****, 6,* 3805-3815.
3. P. Pers, V. Mao, M. Taillades, G. Taillades, *Int. J. Hydrogen Energy* **2018**, *43, 4*, 2402-2409
4. A. Abdelhafiz, B. Wang, A.R. Harutyunyan, J. Li, *Adv. Energy Mater.* **2022**, *12*, 2200742
5. H. Iwahara, *Solid State Ionics* **1996**, *86-88*, 9

Proving photoactive Polyoxometalates as potent prosthetic groups for a novel class of artificial metalloenzymes.

Alisa Ranscht, Daniel Murillo Ilbay, Nada Savic, Tatjana N. Parac-Vogt*

Laboratory of Bioninorganic Chemistry, KU Leuven, 3001 Leuven, Belgium
*tatjana.vogt@kuleuven.be

Introduction

Boosting the catalytic activity of natural enzymes under conditions relevant to fine chemical synthesis remains an ongoing challenge.[1,2] Introducing non-natural metal **cofactors** into proteins has already proven to be a powerful strategy to overcome the limitations in reactivity typically associated with natural enzymes.[3] The resulting biohybrid catalysts, also known as **artificial metalloenzymes (ArMs)**, enable many new-to-nature reactions to be carried out under the strict control of the protein environment, including C-H activation, C-C bond formation, and hydration reactions, among others.

ArMs active under visible light, like their fully biological counterparts, remain extremely rare; however, they offer an exciting prospect for achieving mild and selective reaction conditions.[4] **Polyoxometalates (POMs)**, which are anionic cluster molecules, hold great promise as **cofactors** in the design of such photoactive **ArMs** because they (a) bind regioselectively to proteins[5,6] and (b) exhibit good photoactivity in some cases, though mostly under UV light.[7] To date, no **POM@protein** complexes have been reported as active hybrid photocatalysts.

Materials and Methods

Two transition metal-substituted POMs known in the literature, **M-Kg** and **M-WD**, along with their non-substituted counterparts, were synthesized and evaluated for their ability to catalyze the selective C–C cleavage of diastereomers and enantiomers of hydrobenzoin (**meso-1, R,R-1, S,S-1)** to benzaldehyde under irradiation with LED light sources (360-525 nm). The reactions were conducted in the presence and absence of commercially proteins from different mammalian sources. Yields were quantified via HPLC, and the regiospecific binding of the POM to the protein was investigated using spectroscopic methods (NMR, UV-vis, fluorescence spectroscopy, circular dichroism).

Results and Discussion

The photoactivity of the specific **M-POMs M-Kg** and **M-WD** has never been reported for purely inorganic cluster species. Our results indicate that **M-POMs** can catalyze oxidative cleavage of C-C bonds in the presence of light, even in the absence of photosensitizers, while control experiments with simple **M**-salts showed no catalytic activity. Similarly, the inorganic ligands alone- the mono-lacunary Wells-Dawson and Keggin **POM** salts- also exhibited no activity. This clearly demonstrates that the synergistic combination of **M** and the **POM** (as an inorganic ligand bound to it) is essential for the observed photocatalytic activity. We further found that the activity of **M-Kg** improves by a factor of 3 in the presence of specific albumin proteins (**SAs**), while other proteins, such as **Myoglobin**, **Cytochrome C** and Hen egg white lysozyme (**HEWL**), were diminishing the yield significantly. Additionally, higher reactivity was observed for specific diastereomers and, in some cases, enantiomers, which is only achievable in the presence of specific albumin proteins. **M-WD** does not show this reaction behavior, indicating differences in its interaction with the proteins. ^{1}H NMR investigations confirmed a strong interaction between **M-Kg** and the diol substrate exclusively in the presence of protein, supporting the in situ formation of the reactive **M-Kg@SA** complex, where **M-Kg** binds to the protein via coordination forces.

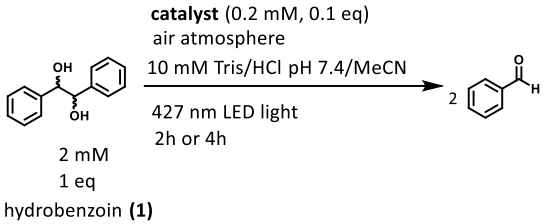

Scheme 1. Optimized reaction conditions for the visible light activated photooxidative C-C cleavage of hydro benzoin using M-Kg and proteins.

Tab 1. Yield of Benzaldehyde obtained in presence of photoactive POM (M-Kg) and proteins in presence of different diastereomers of the substrate hydrobenzoin (1) under visible light irradiation (427 nm).

entry	Catalyst	Substrate	t/ h	Yield/ %
1	**MKg**	meso-**(1)**	4	37 (0.6)
2	**Kg**	meso-**(1)**	4	4.1 (0.9)
3	**MKg @Myoglobin (2:1)**	meso-**(1)**	4	9 (1)
4	**MKg @Cytochrom C (2:1)**	meso-**(1)**	4	3
5	**MKg @SA-A (2:1)**	meso-**(1)**	4	46 (2)
6	**MKg @SA-A (1:1)**	meso-**(1)**	4	92 (0.5)
7	**MKg @SA-A (1:1)**	meso-**(1)**	2	63 (1)
8	**MKg @SA-A (1:1)**	R,R-**(1)**; S,S-**(1)**	2	92 (1)

Significance

We herein demonstrate, for the first time, (i) the photoredox activity of specific **M-Kg** and **M-WD POMs**, and (ii) provide compelling evidence that **M-Kg** acts as a highly active artificial photoredox cofactor within the chiral reaction environment of the serum albumin protein. To the authors' knowledge, this represents the first example of a photoactive **ArM** constructed from a **POM** and a protein.

References

[1] Renata, H. et al. *Angew. Chem. Int. Ed.* **2015**, *54* (11), 3351–3367.
[2] Zhou, L., et al., *Biotechnol. Adv.* **2024**, *73*, 108376.
[3] Schwizer, F. et al., *Chem. Rev.* 2018, *118* (1), 142–231.
[4] Emmanuel, M. A., et al. *Chem. Rev.* **2023**, *123* (9), 5459–5520.
[5] Salazar Marcano, D. E. et al. (Parac-Vogt, T.N.) *JACS Au* **2023**, *3* (4), 978–990.
[6] Goovaerts, V. et al (Parac-Vogt, T. N) *Phys. Chem. Chem. Phys.* **2013**, *15* (42),
[7] Suzuki, K. et al. *ACS Catal.* **2018**, *8* (11), 10809–10825.

BIOCHAR-BASED CATALYSTS FOR DRY METHANE REFORMING

K.PARKHOMENKO [1], A.BEUCHAT[1], M.MALIKZADE[1], M.GUILLMONT[2], B.RETY[2], Z.NADIF[2], C.COURSON[1], D.BEGIN[1], R.GADIOU[2], N.THEVENIN[3], L.RUIDAVETS[3]

[1] *Institut de Chimie et Procédés pour l'Energie, l'Environnement et la Santé (ICPEES), CNRS, Université de Strasbourg, Strasbourg, France.*

[2] *Institut de Science des Matériaux de Mulhouse (IS2M), CNRS, Université Haute-Alsace, Mulhouse, France.*

[3] [2]*RITTMO Agroenvironnement®, Colmar, France.*

1. Keywords

Biochars, methane reforming, sewage sludge, grape pomace, hydrogen

2. Highlights

- Composite biochars from waste – grape pomace and sewage sludge – prepared by slow and fast pyrolysis, activated by steam and fully characterized.
- High potential of as-prepared biochars in heterogeneous catalysis due to the high metal content induced by the original waste biomass.
- Comparison of the pyrolysis methods, influence of the ratio between grape pomace and sewage sludge for biochars preparation, comparison of methane reforming methods will be presented.

3. Purpose

This project is focused on the preparation and activation of composite biochars from biomass of two different types - lignocellulose (grape pomace) and sewage sludge. Biomass from a sewage treatment plant contains large quantities of inorganic compounds (ash), including high quantity of Fe (1,6 mass%), mainly from the flocculant widely used in wastewater treatment, other present elements – Si, Al, Ca, K, Mg, P, Na. The waste from wine production is valorized in the biochars preparation via mixing with sewage sludge in different ratios before pyrolysis step. Mixed biochars were prepared by copyrolysis using the "slow" and "fast" routes. The aim of this study is the preparation of two families of biosourced catalytic materials naturally loaded with metals, with improved physico-chemical and morphological properties compared to the oxide surfaces alone. Thus a novel route for valorization of different types of waste is proposed for the preparation of composite biochars. The composite biochars are physically (steam) activated to make up the micro-mesoporous structure and higher specific surface areas for further application. In this work the catalytic activity of composite biochars was tested in two reactions – dry methane reforming and steam methane reforming. Through methane dry reforming, greenhouse gases of CH_4 and CO_2 can be converted into syngas that has a wide application for hydrogen production or synthesis of a variety of valuable chemicals. The use of biochars as catalytic materials in this reaction is helpful to overcome the mane problematics – heavy coking and active metal sintering. [1, 2] The integration of steam reforming of methane is still limited due to the same problems. [3]

4. Materials and methods

The slow pyrolysis conditions for composite biochars preparation were as follows - drying of biomass at 110°C for 12 hours, followed by "slow" pyrolysis at 800°C (heating rate 10°C/min) under an inert atmosphere. The fast pyrolysis conditions for composite biochars preparation were as follows - drying of biomass at 110°C for 12

hours, followed by "fast" pyrolysis at 800°C under an inert atmosphere (oven was heated using heating rate 10°C/min, then biomass was introduced for 10 min, after this time the biochar was removed from the oven into the ambient atmosphere). Activating of all biochars with steam (800°C, 10°C/min, 2h) was carried out post-synthesis. The properties of composite biochars before and after activation were compared. TGA (composition and oxidation kinetics), XRD, elemental analysis, TEM and SEM microscopies, TPD-MS, Raman, BET-N_2, BET-CO_2 and IR techniques were applied in order to fully characterize the composite biochars.

5. Results and discussion

The pyrolysis yields of grape pomace/sludge composite biochars were determined slightly smaller for fast pyrolysis (29,5-30,5%) comparing to yields in slow pyrolysis (30,5-34,6%). The single biochars were also prepared and analysed. The comparison of nitrogen adsorption isotherms for single grape pomace biochar, composite biochar, activated composite biochar (family of slow pyrolysis) is shown in Figure 1, the consequent rise in the specific surface area is noticeable. The elemental analysis revealed the content of iron (by XRF) equal to 4,2mass% in the composite grape pomace/sludge biochar, the amount that exhibit catalytic properties. The detailed analysis of the structure, morphology, and chemical composition of the biochars before and after activation will be presented, some parameters are shown in Table 1. The activation by steam had a positive effect increasing surface area and porosity making up the meso-microporous character of the materials. The composite biochars were tested in the mentioned reactions and their activity will be discussed in details and compared to two industrial catalysts: Ni/Al_2O_3 basic catalyst for methane conversion as well as Fe/support that is closer to the studied materials with high content of iron.

Table 1. Comparison of CO_2 sorption capacity of biochars.

Sample	SSA, m^2/g	Ashes, %	Pore volume, cm^3/g
Grape pomace slow	14	13,7	0,01
Grape pomace slow activated	455		0,19
Grape pomace + sludge slow	46	40,9	0,07
Grape pomace + sludge s activated	261		0,21
Grape pomace + sludge fast	229	43,1	0,15
Grape pomace + sludge f activated	303		0,17

Figure 1. N_2 adsorption-desorption isotherms (family of slow pyrolysis)

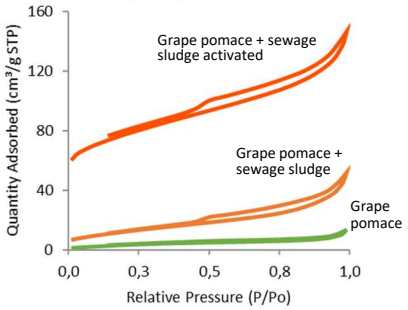

6. Conclusions and perspectives

Two families of composite biochars (grape pomace mixed with sewage sludge) were prepared: “slow pyrolysis” and “fast pyrolysis”. The single biochars were also prepared for understanding of the intimate interactions of composite components. All biochars were activated by steam and were fully characterized before and after activation. The application of the composite biochars in the CO_2 and steam methane reforming reactions revealed their high potential as carbon-based catalysts for hydrogen production. The catalytic activity was compared to industrial Ni and Fe containing catalysts. Novel engineered composite biochars prepared only from waste flows (grape pomace as waste from wine production; sewage sludge – common waste) are proposed as heterogeneous catalysts.

7. References

[1] Longzhi Li, Jian Chen, Sheng Wang, Yongdong Tan, Bo Meng, Guifu Zou, Fumao Wang, Zhanlong Song, Chunyuan Ma, Utilization of biochar for a process of methane dry reforming coupled with steam gasification under microwave heating, Journal of Cleaner Production, 237, 2019, 117838

[2] Qing-ming CHEN, Da-wei LIU, Sui-ming LÜ, Wei-xiang ZHANG, Qing-peng ZHAO, Ning ZHANG, Long XU, Xiao-xun MA, Research progress on the preparation process of biochar-based catalyst support for dry reforming of methane, Journal of Fuel Chemistry and Technology, 51, 2023, 273-293

[3] Jie Ren, Yi-Ling Liu. Direct Conversion of Syngas Produced from Steam Reforming of Toluene into Methane over a Ni/Biochar Catalyst. ACS Sustainable Chem. Eng. 2021, 9, 33, 11212–11222

[4]

One-pot Lignin Catalytic Depolymerization and Demethylation

Hugo Lilti, *Christophe Geantet, Dorothée Laurenti**
Institut de Recherches sur la Catalyse et l'Environnement de Lyon, UMR 5256 – CNRS / Université Lyon 1
*dorothee.laurenti@ircelyon.univ-lyon1.fr

Introduction

Lignin as the most abundant renewable aromatics feedstock, can be a promising resource of biobased chemicals. One way to valorize technical lignins from pulp industries or cellulosic biorefinery, is in polymers applications , as a polyol for the production of polyurethane-like polymers[1]. However, its low reactivity linked to low hydroxyl content, condensed units and high versatility in structure hinders its intensive utilization. Increasing the hydroxyl content by cleavage of ether inter-units bonds and abundant methoxy groups can increase lignin reactivity and decrease its polydispersity index (PDI)[2]. Both reactions being based on the cleavage of an aryl alkyl ether bond, the development of a one-step process to demethylate and partially depolymerize lignin might be an interesting approach. Lignin is usually depolymerized to monomers in hydrogen donor solvents (mainly alcohols) under reductive atmosphere with the help of hydrogenolysis catalysts (Ru/C , Pd/C, CoMo/Al_2O_3 …)[3,4]. The ether inter-units bond can be easily cleaved, whereas C-C inter-units bonds are partially preserved so that oligomers can be produced. Demethylation of the methoxy groups on the ortho position of the phenolic groups, would proceed thanks to the action of Lewis acid catalysts[5]. Methods using homogeneous catalysis and inorganic acids were successfully employed. However, none of those catalysts are heterogeneous nor sustainable. The use of water as solvent and reactant in a hydrothermal liquefaction (HTL) of lignin was also reported to yield high amount of demethylated compounds by hydrolysis[6]. In this work we compared both hydrogenolysis and hydrolysis pathways, and we investigated the effect of various catalysts on demethylation and partial depolymerization to get lignin-oligomers having a high concentration of phenolic OH to be further used after chemical functionalization as macromers in polymer production.

Materials and Methods

Experiments are performed in a 100 mL Parr batch reactor after mixing the lignin (2.5 g), catalysts (10 wt%) and the solvent (40 mL DI water for HTL and isobutanol for hydrogenolysis). Hydrogenolysis reaction were performed under H_2 with a total pressure of 90 bar. For HTL reactions autogeneous pressure of around 120 bar was reached. After reaction, the liquid fraction is recovered, while for hydrogenolysis lignin oligomers were recovered in the isobutanol soluble phase. For both reactions the solid are washed with THF to recover the remaining oligomers and called THF-soluble. ^{31}P NMR after phosphitylation is performed on the depolymerized lignin in order to qualify and quantify hydroxyls groups. Size Exclusion Chromatography (SEC) gavemolecular masses distribution to assess the depolymerization state. Hetero Single Quantum Coherence spectroscopy (HSQC) is also used to differentiate and semi-quantify Interunit Bond (IUB).

Results and Discussion

The conversion of lignin in the presence of both alumina supported CoMoS catalyst under hydrogenolyzing conditions and with sodium doped manganese oxide in HTL showed a significant increase in hydroxyls content (table 1). The catechol moieties of depolymerized lignin show a great increase especially for the HTL reaction showing that demethylation is achieved. The depolymerized lignin does not present β-O-4 IUB, C-C bonds (β-5, β- β, β-1 and 5-5) however are partially preserved for both depolymerized fractions. The overall decrease of IUB should result in a decrease of the molecular mass, indeed observed in GPC analysis.

Table 1. Quantification of aromatic OH (mmol/g), IUB (per 100 G units) and molecular mass (PS eq.) of lignin prior and after depolymerization

^{31}P NMR	β-5	Syr 4-O-5	5-5	Gua	Catechol	H-PHE	Total Phenolics
Kraft lignin	0,44	0,54	0,72	1,69	0,41	0,17	3,96
CoMoS/$Al_2O_3$$^{(I)}$	0,51	0,52	0,61	2,76	1,03	0,37	5,80
$Na_xMnO_2$$^{(II)}$	0,29	0,53	0,44	1,81	1,83	0,91	5,82

HSQC and SEC	β-O-4	β-5	β-β	β-1	5-5	OMe	Mn	Mw
Kraft lignin	5,7	16,4	5,8	3,8	2,6	112,2	788$^{(1)}$	3240$^{(1)}$
CoMoS/$Al_2O_3$$^{(I)}$	**0,0**	6,5	2,2	4,9	1,2	65,2	690	942
$Na_xMnO_2$$^{(II)}$	**0,0**	8,6	2,3	3,9	0,9	71.3	565$^{(1)}$	1482$^{(1)}$

Conditions: (I) 2h; 280 °C; total pressure: 90 bar; P_{H2} = 15 bar; catalyst: CoMoS/Al_2O_3 (II) 1h; 320°C; Initial pressure: 1 atm N_2.

Depolymerized lignin with HTL shows less IUB than the lignin depolymerized with hydrogenolysis, probably due to the higher temperature of the HTL. While both fraction shows an increase in phenolics moieties, HTL is much more selective toward demethylation than hydrogenolysis. This could be explained by the mechanism of hydrolysis of the methoxy bond occurring during HTL, regardless of where the methoxy group is cleaved, a hydroxyl group will be created. Another possibility would be the potential HydroDeOxygenation (HDO) occurring during hydrogenolysis of lignin leading to less hydroxyl moieties. However, it is important to note that the THF soluble fraction of the HTL is rather low (15%) compared to the hydrogenolysis one (39%). The reason may be the repolymerization reactions happening during HTL and the presence of oligomers still in the aqueous fraction. These repolymerization reactions may also explain the higher mass average molar mass of the THF soluble produce by HTL. The results show that the demethylation and depolymerization has been successfully achieved in both reactions.

Significance

Control of the lignin depolymerization to provide new appropriate bio-materials for polymer industry is a challenging task that can be achieved by heterogeneous catalysis. The resulted depolymerized, OH-enriched lignin derived oligomers will be used in polymerization to produce biobased non-isocyanates polyhydroxyurethane foams in collaboration with ICPEES and Soprema company.

Aknowledgments ANR is thanks for the funding of BIOPOLIOL project (ANR-21-CE43-0026).

References

1. S. Luo, *J Wood Sci* **2020**, *66* (1), 23
2. C. Zhang, *Acc. Chem. Res.* **2020**, *53* (2), 470–484.
3. T. Ročnik, *Chemical Engineering Journal* **2022**, *448*, 137309.
4. X. Erdocia, *ACS Sustainable Chem. Eng.* **2016**, *4* (3), 1373–1380.
5. J. Podschun, *Reactive and Functional Polymers* **2017**, *119*, 82–86.
6. M. Islam, *Ind. Eng. Chem. Res.* **2018**, *57* (14), 4779–4784.